Exercise strategies to improve vascular health and exercise tolerance. Implications for rehabilitation.

Molly May Baldwin

Submitted in accordance with the requirements for the degree of
Doctor of Philosophy

The University of Leeds
Faculty of Biological Sciences
School of Biomedical Sciences

March 2021

The candidate confirms that the work submitted is her own and that appropriate credit has been given where reference has been made to the work of others.

Professional Activities

Abstracts arising from this thesis

- Feasibility and Effectiveness of High-intensity Interval Training with Blood Flow Restriction in Heart Failure. *American College of Sports Medicine Annual Meeting*. San Francisco, CA, USA (cancelled due to COVID-19). 2020. Published in: *Med Sci Sports Exerc*, 2020, 52: S890. (Chapter 4).

Oral presentations

- Characterisation of the decline in maximal voluntary isokinetic power during ramp-incremental cycle ergometry exercise, in "Fatigue as a limitation to exercise performance" satellite symposium. *Physiological Society Annual Meeting*. Aberdeen, UK. 2019. (Chapter 3).
- Exercise Training with Blood Flow Restriction in Heart Failure – Feasibility and Effect on Cellular Markers of Vascular Health. *Multidisciplinary Cardiovascular Research Centre Retreat*. Lake district, UK. 2019. (Chapter 4).

Poster presentations

- The Acute Effect of High-intensity Exercise with Blood Flow Restriction on Circulating Progenitor Cell Number in Chronic Heart Failure. *American Physiological Society Intersociety Meeting: Integrative Physiology of Exercise*. Online. 2020. (Chapter 4).
- Characterisation of the decline in maximal voluntary isokinetic power during ramp-incremental cycle ergometry exercise. *Physiological Society Annual Meeting.* Aberdeen, UK. 2019. (Chapter 3).
- The effect of high-intensity interval exercise with blood flow restriction on markers of vascular repair in chronic heart failure: study proposal. *Multidisciplinary Cardiovascular Research Centre Retreat*. Lake district, UK. 2018. (Chapter 4).

Other professional activities during PhD study

- Ferguson C, Chadwick MR, **Baldwin MM**. 2019. Does the relationship between exercise intensity and tolerance preclude an answer? Comment on CrossTalk 43: Exercise intensity is/is not more important than volume to promote increases in human skeletal muscle mitochondria content. *J Physiol*. Online.
- Lyall GK, **Baldwin MM**, Birch KM. 2021. Commentaries on Viewpoint: Differential impact of shear rate in the cerebral and systemic circulation: Implications for endothelial function. *J Appl Physiol*. **130**(4), pp.1155-1160.

Acknowledgements

First and foremost, I would like to thank my primary supervisor Dr Carrie Ferguson for her unrivalled support, guidance and knowledge throughout this process. Your enthusiasm and commitment to both myself and this research project has made this thesis possible. I would also like to thank my secondary supervisor Prof. Karen Birch for her support and guidance throughout this process.

To Drs Bryan Taylor, Matt Davies and Gemma Lyall, thank you for always keeping your door, and now your phones and inboxes, open and for making time for me. I will always be grateful for the support, advice and the self-belief that you gave me throughout this process.

I would also like to thank the fantastic team in the Clinical Research Facility; Klaus Witte, John Gierula, Maria Paton, Judith Lowry, Aaron Koshy, Roo Byrom-Goulthorp, Hermant Kumar and Julie Corrigan. The clinical research in this thesis would not have been possible without you all.

I wish to extend this gratitude to Dr Sally Boxall for her time, expertise and guidance with the flow cytometry work in this thesis. I could not have done this aspect of my thesis without your help.

Thank you to all of the participants who volunteered and sacrificed their time to take part in these studies. None of this research would have been possible without you, and spending time with you all made data collection a thoroughly enjoyable process.

To everyone in the PhD office (past and present), thank you for all the good times that we have shared together. In particular, I would like to thank Tim Hardy and Matt Chadwick for providing me with round the clock support and entertainment; I am really glad that we went through this experience together.

A special thank you to all of my family for their unconditional love and support. Together with my closest friends, you are the world's best cheerleaders! Mum and Dad, I am incredible lucky to have you, the opportunities and experiences that you have given me have made this journey possible.

Finally, I would like to thank Cormac for his endless support, patience and encouragement throughout this process, and for telling me that 'everything is going to be ok' a million times - it only works when you say it!

This thesis is dedicated to the memory of Robert 'Bob' Baldwin.

Abstract

Exercise tolerance strongly predicts morbidity and mortality, and correlates with health-related quality of life. The mechanisms underpinning exercise intolerance were investigated in Chapter 3. Peripheral vascular dysfunction occurs when there is an imbalance between endothelial damage and endogenous repair mechanisms, and can contribute to exercise intolerance. Vascular dysfunction typically precedes a diagnosis of cardiovascular disease and is related to disease severity in cardiovascular disease patients (e.g. chronic heart failure; CHF). Exercise training increases vascular function and exercise tolerance in health and CHF, with high-intensity interval training (HIIT) often inducing greater improvements than continuous 'control' protocols. However, it is unknown whether the effectiveness of HIIT can be improved.

Therefore, Chapter 4 investigated the acute and chronic effect of HIIT with and without blood flow restriction (BFR) on vascular endogenous repair capacity, ramp-incremental exercise tolerance and $\dot{V}O_{2peak}$ in CHF. Four weeks of HIIT did not induce acute or chronic vascular adaptations; however, chronic HIIT increased ramp-incremental exercise tolerance and $\dot{V}O_{2peak}$. BFR did not increase training efficacy.

Chapter 5 determined whether 6 weeks of HIIT at a high work rate with short work:recovery bouts (intended to maximise the volume of shear rate accumulated) increased vascular endogenous repair capacity, endothelial function, exercise tolerance and $\dot{V}O_{2peak}$ more than intensity-matched continuous exercise training in healthy adults. No acute or chronic vascular adaptations were seen with HIIT. This type of HIIT increased post-training exercise tolerance and $\dot{V}O_{2peak}$ but was no more effective than intensity-matched constant work rate exercise training.

Overall, increases in exercise tolerance and $\dot{V}O_{2peak}$ in both training studies were not underpinned by improvements in peripheral vascular endothelial function and/or increases in vascular endogenous repair capacity. Therefore, despite the efficacy of training to increase exercise tolerance, further work is needed to develop exercise strategies that effectively and specifically target improvements in vascular endogenous repair capacity and peripheral vascular function.

Table of Contents

List of Tables

List of Figures

Abbreviations

Akt – protein kinase B

AMP – adenosine monophosphate

ATP – adenosine triphosphate

AUC – area under curve

BFR – blood flow restriction

BH_4 – tetrahydrobiopterin

BMI – body mass index

cGMP – cyclic guanosine monophosphate

CHF – chronic heart failure

CXCR4 – C-X-C chemokine receptor 4

ECG – electrocardiogram

EMG – electromyography

eNOS – endothelial nitric oxide synthase

FMD – flow-mediated dilation

FMO – florescence minus one

FSC – forward scatter

GTP – guanosine triphosphate

Hb – haemoglobin

HFpEF – heart failure with preserved ejection fraction

HFrEF – heart failure with reduced ejection fraction

HIF-1α – hypoxia-inducible factor 1-alpha

HIIT – high-intensity interval training

HR – heart rate

HR_{peak} – peak heart rate

HRR – hear rate reserve

ICAM-1 – intracellular adhesion molecule-1

KDR – kinase insert domain receptor

LoT – limit of tolerance

LT – lactate threshold

LVEF – left ventricular ejection fraction

mKitL – membrane bound Kit ligand

MLHFQ – Minnesota Living with Heart Failure Questionnaire

MMP – matrix metalloproteinase

MVIP – maximum voluntary isokinetic power

NAD – nicotinamide adenine dinucleotide

Nfr2 - nuclear factor erythroid 2-related factor 2

NIRS – near-infrared spectroscopy

NO – nitric oxide

NYHA – New York Heart Association

O_2 – oxygen

PCr – phosphocreatine

$P_{ET}CO_2$ – end-tidal partial pressure of CO_2

$P_{ET}O_2$ – end-tidal partial pressure of O_2

PGC-1α - peroxisome proliferator-activated receptor-γ coactivator-1 alpha

PI3K – phosphoinositide 3-kinase

PKG – protein kinase G

PO_2 – partial pressure of oxygen

PSGL-1 – P-selectin glycoprotein ligand-1

$\dot{Q}$ – blood flow

RI – ramp-incremental

RI-MVIP – ramp-incremental exercise with integrated measures of maximal voluntary isokinetic power

RMS – root mean square

ROS – reactive oxygen species

SaO_2 – arterial oxygen saturation

SDF-1α – stromal derived factor-1 alpha

Ser^{1177} – serine 1177

sGC – soluble guanylyl cyclase

sKitL – soluble Kit ligand

SSC – side scatter

SvO_2 – venous oxygen saturation

TNF-α – tumour necrosis factor-alpha

TSI – tissue saturation index

VCAM-1 – vascular cell adhesion molecule-1

$\dot{V}CO_2$ – peak carbon dioxide output

$\dot{V}_E$ – minute ventilation

$\dot{V}_E/\dot{V}CO_2$ – ventilatory equivalent of oxygen

$\dot{V}_E/\dot{V}O_2$ – ventilatory equivalent of carbon dioxide

VEGF – vascular endothelial growth factor

VEGFR2 – vascular endothelial growth factor receptor-2

$\dot{V}_{Epeak}$ – peak ventilation

$\dot{V}O_2$ – rate of oxygen uptake

$\dot{V}O_{2max}$ – maximal oxygen uptake

$\dot{V}O_{2peak}$ – peak oxygen uptake

WR – work rate

WR_{peak} – peak work rate

Chapter 1 Literature review

1.1 General introduction

To undertake any physical task, an individual requires the necessary exercise tolerance to perform the task successfully. Practically, achieving extreme tasks, such as running a marathon, therefore requires a much greater exercise tolerance than performing activities of daily living. Peak oxygen uptake ($\dot{V}O_{2peak}$) measured during maximal dynamic whole-body exercise, such as running or cycling, is the gold-standard measure used to quantify an individual's capacity to exercise and is a measure of the upper integrated limits for oxygen (O_2) delivery *and* utilisation. Individuals can only sustain tasks that have an O_2 uptake requirement that is less than or equal to their $\dot{V}O_{2peak}$, with tolerance to that task then determined by the magnitude of the metabolic perturbation (i.e. the exercise intensity). Inactivity, detraining, ageing and the onset and progression of chronic disease are all known to reduce $\dot{V}O_{2peak}$ which has been shown to be the strongest independent predictor of morbidity and mortality (Myers et al., 2002). Moreover, $\dot{V}O_{2peak}$ strongly correlates with quality of life as it determines the ability to perform tasks of daily living; for independent living it has been proposed that a minimum $\dot{V}O_{2peak}$ of 18 and 15 $ml \cdot min^{-1} \cdot kg^{-1}$ for men and women, respectively is required (Paterson et al., 1999). Thus, if $\dot{V}O_{2peak}$ is maintained or even increased, the risk of death and likelihood of requiring clinical support or intervention is reduced. Currently, the mechanisms that limit exercise tolerance and $\dot{V}O_{2peak}$ remain poorly understood. However, identifying specific mechanisms and how to target these through intervention is critical for designing effective disease prevention and rehabilitation strategies. Thus, exercise strategies that successfully overcome exercise limitations and improve $\dot{V}O_{2peak}$ are likely to improve health-related quality of life and provide morbidity and mortality

protection to ageing individuals and those with chronic disease, with this aim at the heart of this thesis.

1.2 Exercise tolerance

A wide variety of tests are available to assess exercise tolerance (e.g. time-trials, time-to-intolerance trials, 6-minute walk test, incremental shuttle walk test and endurance shuttle walk test) with the specific measures derived dependent on the test used. A ramp-incremental (RI) exercise test to the limit of tolerance or symptom limitation, combined with comprehensive breath-by-breath monitoring of cardiopulmonary gas exchange variables (e.g. O_2 uptake [$\dot{V}O_2$], carbon dioxide output [$\dot{V}CO_2$] and minute ventilation [$\dot{V}_E$]) is typically considered to be the gold standard for measuring exercise tolerance in health and disease. A number of parameters of aerobic function can be derived from this test including, mean response time, lactate threshold, functional gain ($\Delta\dot{V}O_2$ / ΔWR) and $\dot{V}O_{2peak}$ (Whipp et al., 1981). In addition, other variables shown to be prognostic can be measured from this exercise test, such as the ventilatory equivalent for carbon dioxide ($\dot{V}_E/\dot{V}CO_2$; Arena et al., 2004) and the O_2 pulse ($\dot{V}O_{2peak}/HR_{peak}$; Oliveira et al., 2009). Subsequently, RI exercise tests with concomitant measures of cardiopulmonary gas exchange are extremely valuable in performance and clinical settings. Identifying the mechanisms that limit RI exercise, and how these develop throughout the test is critical for understanding limitations to exercise tolerance and developing more effective exercise strategies that improve exercise tolerance in health and disease. The mechanisms underpinning RI exercise intolerance are investigated in Chapter 3.

1.3 Determinants of $\dot{V}O_{2peak}$

The 'Wagner' model (Wagner, 1996) describes the relationship between the convective and diffusive components of O_2 transport and the interaction of these to

determine $\dot{V}O_{2peak}$ (Figure 1.1). Convective O_2 transport describes the rate of O_2 delivery from the atmosphere to the microcirculation and includes diffusive O_2 transport at the lung. Convective O_2 delivery is determined by the Fick principle, such that O_2 delivery is the product of blood flow ($\dot{Q}$) multiplied by arterial O_2 content. However, arterial O_2 content itself, is the product of arterial O_2 saturation (SaO_2) and haemoglobin concentration ([Hb]; ignoring the typically minor contribution of physically dissolved O_2; Wagner, 1996). Theoretically, the O_2 carrying capacity of a gram of haemoglobin is 1.39 ml; however, the measured capacity is closer to ~1.34 ml. Therefore, convective O_2 delivery is equal to 1.34 x [Hb] x SaO_2 x $\dot{Q}$. This explains why the convective O_2 delivery line in Figure 1.1 is curvilinear because this is directly reflective of the haemoglobin dissociation curve. Nevertheless, this equation for convective O_2 delivery (i.e. 1.34 x [Hb] x SaO_2 x $\dot{Q}$) does not take into account that not all O_2 is extracted from the arterial blood, therefore the equation for convective O_2 delivery must be modified to: convective O_2 delivery = 1.34 x [$\dot{Q}$] x [Hb] x [SaO_2 – SvO_2].

In contrast, diffusive O_2 transport describes the delivery of O_2 from the microcirculation to the mitochondria where it is utilised in the process of oxidative phosphorylation. This component of O_2 transport is dictated by Fick's law of diffusion, meaning that O_2 extraction from the microcirculation is determined by the O_2 partial pressure (PO_2) difference between the capillary (microvascular PO_2) and the intramuscular milieu (intracellular PO_2) working against a known O_2 diffusing capacity. Often, this diffusion capacity is described as fixed; however, it can be influenced by variables, such as capillary surface area and temperature. The O_2 pressure difference (i.e. the PO_2 gradient) between the microvascular and intramuscular milieu is dependent on the O_2 delivery to O_2 utilisation ratio. The PO_2 gradient relies on the rate of O_2 utilisation by the mitochondria to maintain the pressure difference. Therefore, to increase $\dot{V}O_{2peak}$, convective (bulk O_2 delivery)

and/or diffusive (movement of O_2 from haemoglobin to mitochondria and O_2 utilisation) O_2 transport must be improved. The contributions of both convective and diffusive O_2 delivery in determining $\dot{V}O_{2peak}$ are not fixed and will change in response to interventions that impact the uptake, transport and utilisation of O_2, including altitude, disease or exercise training (Wagner, 1996).

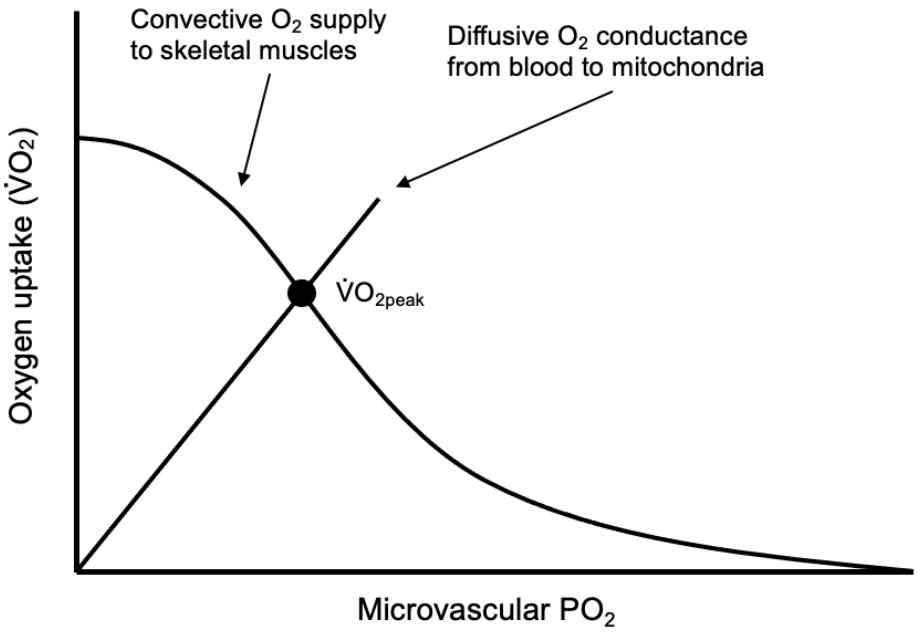

Figure 1.1 Convective (curved lines, Fick principle, $\dot{V}O_2$ = blood flow [$\dot{Q}$] x [arterial O_2 content – venous O_2 content]) and diffusive (straight lines from origin, Fick's law, $\dot{V}O_2$ = O_2 diffusing capacity x [microvascular PO_2 – intracellular PO_2]) components of O_2 transfer that interact to determine $\dot{V}O_{2peak}$ (black circle). Adapted from Wagner (1996).

The implication of these interdependent relationships is interventions that increase convective and/or diffusive O_2 transport can increase $\dot{V}O_{2peak}$ by different magnitudes, depending on the limitations to exercise (Figure 1.2). For example, if a scenario is considered where an intervention increases convective O_2 transport only, then $\dot{V}O_{2peak}$ would improve from point A to B in Figure 1.2. However, if an intervention increased diffusive O_2 transport only, the increase in $\dot{V}O_{2peak}$ would be greater,

increasing from point A to C. Nevertheless, therapeutic strategies that increase both components of O_2 transport will be the most efficient in increasing $\dot{V}O_{2peak}$ (A to D).

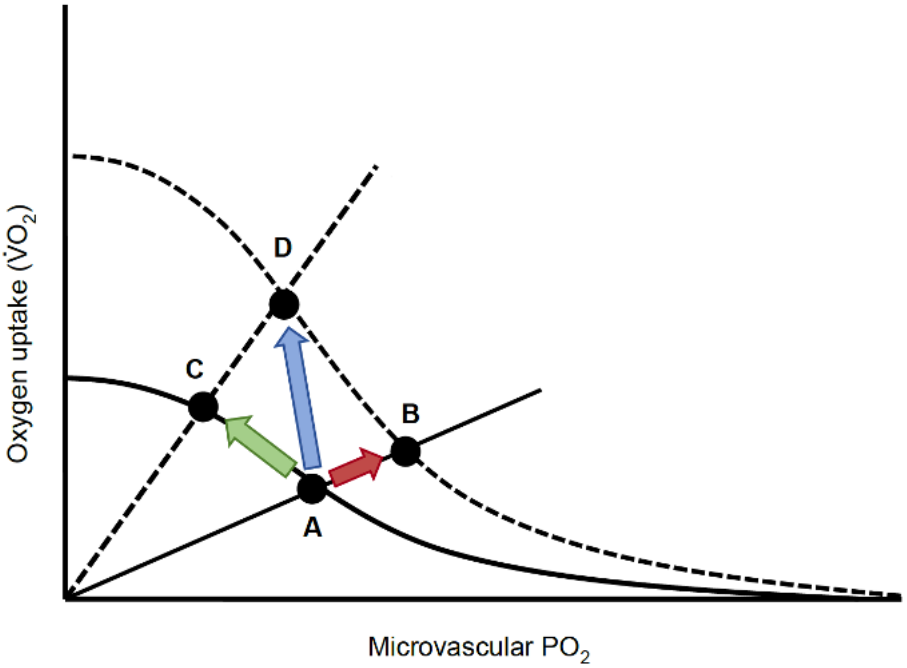

Figure 1.2 Illustration of how changes in convective (curved lines) and/or diffusive (straight lines from origin) O_2 transport impact $\dot{V}O_{2peak}$ (solid black circles). Solid lines represent pre-intervention components of O_2 transport; dashed lines represent post-intervention components of O_2 transport. The red arrow indicates the increment in $\dot{V}O_{2peak}$ that would occur if an intervention improved convective O_2 transport only (A to B). The green arrow indicates the increment in $\dot{V}O_{2peak}$ that would occur if an intervention increased diffusive O_2 transport only (A to C). The blue arrow represents the rise in $\dot{V}O_{2peak}$ that would occur if an intervention improved both convective and diffusive components of O_2 transport (A to D). Adapted from Wagner (1996).

1.4 Peripheral arterial tree and vessel structure

The peripheral arterial tree plays a crucial role in convective O_2 transport, determining blood flow (i.e. O_2 delivery) to the skeletal muscle. The peripheral arterial network consists of conduit, resistance and exchange vessels. Conduit arteries include the anatomically named arteries, such as the brachial and femoral artery, and are ~1-10 mm in diameter (Thijssen et al., 2008). The primary function of these vessels is to distribute large volumes of blood from larger elastic arteries to smaller arteries that

descend into resistance vessels. Subsequently, resistance vessels are smaller than conduit arteries and include feed arteries (also known as terminal arteries; ~100-400 μm in diameter) and arterioles (~5-100 μm in diameter; Johnson, 2008). The principal role of resistance vessels is to regulate tissue perfusion. In accordance with their name, resistance vessels are the chief site of vascular resistance in the arterial network. Finally, exchange vessels consist of capillaries (~5-10 μm in diameter; Johnson, 2008). These small vessels are connected to the most distal elements of the arteriolar tree and are responsible for the exchange of gases (e.g. O_2 and CO_2), nutrients and waste products between blood and tissue, primarily by diffusion (Johnson, 2008).

Conduit and resistance vessels are all made of three layers: the tunica intima, tunica media and adventitia (Figure 1.3). A dynamic interaction between these layers is required to maintain vascular health and function. The tunica intima is the layer which is closest to the artery lumen and consists of the endothelium on the luminal side and internal elastic lamina on the outer side (Lusis, 2000). The endothelium is a single monolayer of cells lining the inner surface of blood vessels and is the first barrier encountered by circulating cells in the cardiovascular system. Endothelial cells play a pivotal role in maintaining vascular homeostasis. The endothelium is responsible for the release of biochemical mediators, such as nitric oxide, prostacyclin, and endothelin-1 that influence vascular tone, platelet activity and coagulation factors, as well as mediating vascular inflammation and smooth muscle cell migration and proliferation (Bonetti et al., 2003). Located between endothelium and the internal elastic lamina is a subendothelial extracellular matrix containing collagen and elastin (Lusis, 2000). The tunica media is the middle layer of an artery and primarily consists of vascular smooth muscle cells, collagen and elastin fibres (Lusis, 2000). Vascular smooth muscle cells contract and relax to induce vasoconstriction and vasodilation in response to autonomic nerve activity and vasoactive stimuli. Therefore, this

muscular layer is responsible for maintaining vascular tone. Lastly, the adventitia is the outer layer of the artery. This layer is comprised of connective tissues, such as collagen and elastic fibres, interspersed with cellular elements (e.g. fibroblasts, macrophages and mast cells), lymphatic vessels and autonomic nerves (Majesky et al., 2011). In addition to providing structural support and shape to the vessel, this layer has an array of functions that include immune surveillance, cell trafficking and vessel growth and repair (Majesky et al., 2011). The adventitia regulates the development and regression of the vasa vasorum, a network of micro vessels that penetrate the adventitia to nourish the tunica media and intima (Majesky et al., 2011). The adventitia is separated from the tunica media by the external elastic lamina (Figure 1.3). In contrast, capillaries are only composed of a single endothelial layer to permit the rapid exchange of gases, substrates and waste products (Johnson, 2008).

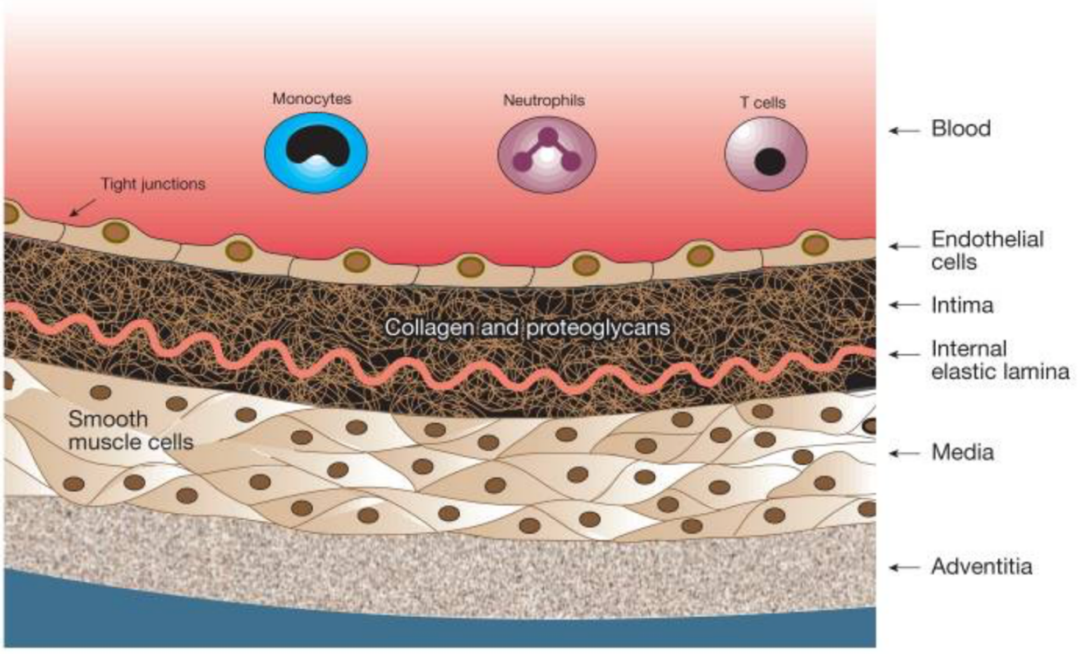

Figure 1.3. Schematic of the three layers of the artery: the tunica intima, tunica media and adventitia. The tunica intima consists of the endothelium on the luminal side and the internal elastic lamina on the outer side. Taken from Lusis (2000).

1.5 Peripheral vasculature and $\dot{V}O_{2peak}$ in health

Skeletal muscle blood flow (i.e. O_2 delivery) must match the 'metabolic demand' of the skeletal muscle to prevent convective O_2 transport limiting $\dot{V}O_{2peak}$ during dynamic whole-body exercise. Figure 1.4 demonstrates the tight coupling that occurs between O_2 demand and increases in blood flow in skeletal muscle during different types of exercise (Mortensen et al., 2008). Cardiac output can increase from ~5 $L \cdot min^{-1}$ at rest to ~20 $L \cdot min^{-1}$ during exercise in untrained individuals (Joyner and Casey, 2015). During small muscle mass exercise, such as single-leg knee-extension, even when performed maximally, maximal cardiac output exceeds the cardiac output required to meet the O_2 demand of the contracting muscles (Esposito et al., 2010b). Thus, a 'cardiac output reserve' is present and convective O_2 transport does not limit $\dot{V}O_{2peak}$. However, during large muscle mass exercise (e.g. whole-body dynamic exercise, such as running or cycling) a cardiac output of ~20 $L \cdot min^{-1}$ is only enough to supply a proportion of the working skeletal muscles with maximum blood flow. Therefore, whole-body dynamic exercise, necessitates the redistribution of blood flow during exercise away from less active skeletal muscle and other body organs, such as the liver and kidneys, so that the vast majority of cardiac output is directed to the working skeletal muscle, whilst maintaining blood pressure. This redistribution of blood flow and increased delivery of blood flow to the working muscles, in concert with an increase in O_2 extraction, increases O_2 delivery to the mitochondria of the contracting muscles during dynamic whole-body exercise. In healthy individuals, O_2 delivery tends to exceed oxidative capacity (i.e. capacity for O_2 utilisation) during whole-body exercise; however, in cardiovascular disease, it is not uncommon for oxidative capacity to exceed O_2 delivery during whole-body exercise, meaning convective O_2 transport can limit $\dot{V}O_{2peak}$ (Cardús et al., 1998, Esposito et al., 2010b). The redistribution of blood flow and increased delivery of blood flow to the working muscles during exercise relies on vasomotor control.

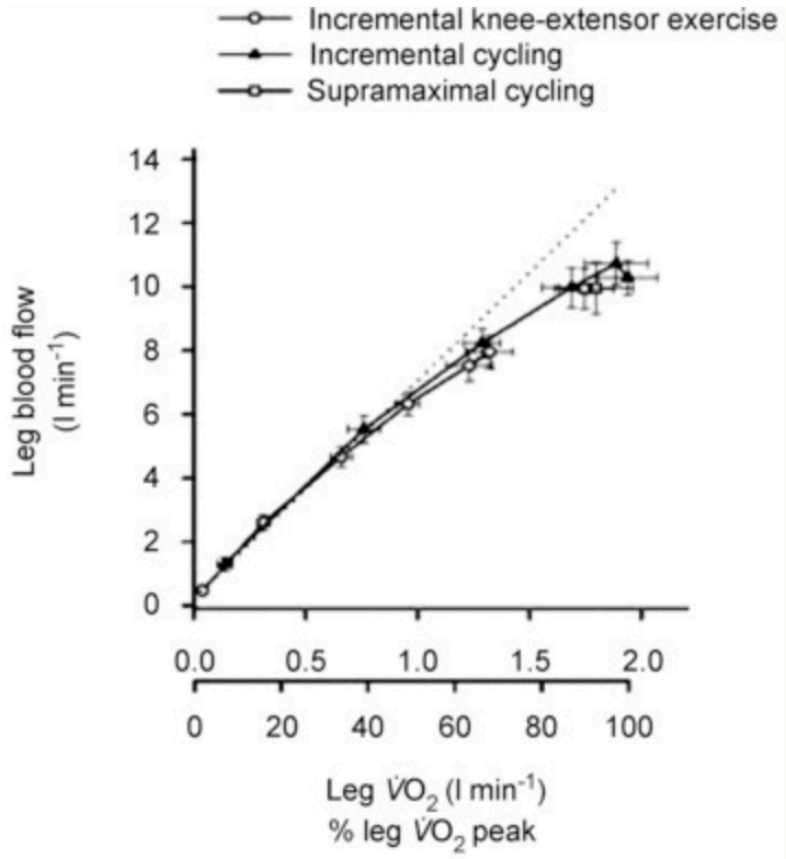

Figure 1.4. Tight coupling between leg blood flow and O_2 demand during knee-extensor exercise and maximal and submaximal cycling. Taken from Casey and Joyner (2012) adapted from Mortensen et al. (2008).

1.6 Haemodynamics

Blood flow ($\dot{Q}$) to the working skeletal muscle is determined by Darcy's law of flow, whereby: flow = pressure gradient / resistance. The pressure gradient in the vasculature system is the difference between arterial and venous blood pressure. Mean arterial pressure is tightly regulated and maintained within small margins by multiple mechanisms (e.g. baroreceptor reflex, antidiuretic hormone and renin-angiotensin-aldosterone system) at rest and during exercise. Indeed, mean arterial pressure typically remains at ~100 mmHg during dynamic whole-body aerobic exercise, a value that is not dissimilar to rest in healthy males (Clausen, 1976). Thus, control of blood flow to skeletal muscle is largely dependent on changes in vascular resistance, a parameter that is determined by the viscosity of blood, vascularisation

of the tissue (i.e. the size and number of vessels) and the calibre of resistance vessels (i.e. the degree of vasodilation; Korthuis, 2011).

Blood viscosity remains fairly constant at rest within short periods of time but can be influenced by exercise. Indeed, blood viscosity increased by ~20% following 10 min of treadmill running at >95 and 60-65% $\dot{V}O_{2peak}$ in healthy sedentary males (Hitosugi et al., 2004). Exercise-induced haemoconcentration, caused by dehydration and an increase in fluid moving from the peripheral vasculature into the interstitial space due to an increase in intramuscular metabolite concentration, in unison with increased plasma viscosity and blood aggregation increase blood viscosity pre- to post-exercise (Buono et al., 2016). However, proportionally, blood viscosity plays a relatively small role in determining vascular resistance in comparison to vessel diameter. This is apparent from Poiseuille's law, an equation that can be applied to individual arteries to determine flow resistance, assuming laminar flow and a constant pressure:

$$Flow\ resistance = \frac{8\,\eta\,L}{\pi\,r^4}$$

Where, η is the viscosity of the blood, L: the length of vessel, and r: the radius of the vessel lumen. Small changes in the radius of an artery (which is raised to the fourth power) result in large changes in flow resistance. Therefore, skeletal muscle blood flow largely depends on vasomotor tone, determined by the delicate balance between vasoconstriction and vasodilation, to ensure O_2 reaches the 'end user'.

1.7 Vascular tone

1.7.1 Vascular tone at rest in health

Under resting conditions, the primary purpose of vascular tone is to maintain blood pressure and ensure blood flow (i.e. O_2 delivery) meets the basal metabolic rate of the body's organs and tissues. Vascular tone is dependent on the interaction between several mechanisms and vasoactive compounds (Figure 1.5). The

magnitude of effect that each of these mechanisms have in determining overall vascular tone varies across the peripheral artery tree (Figure 1.5). Broadly, these influences can be separated into extrinsic and intrinsic factors depending on whether they originate from inside the vessel and surrounding tissue or outside of the vessel and surrounding tissue.

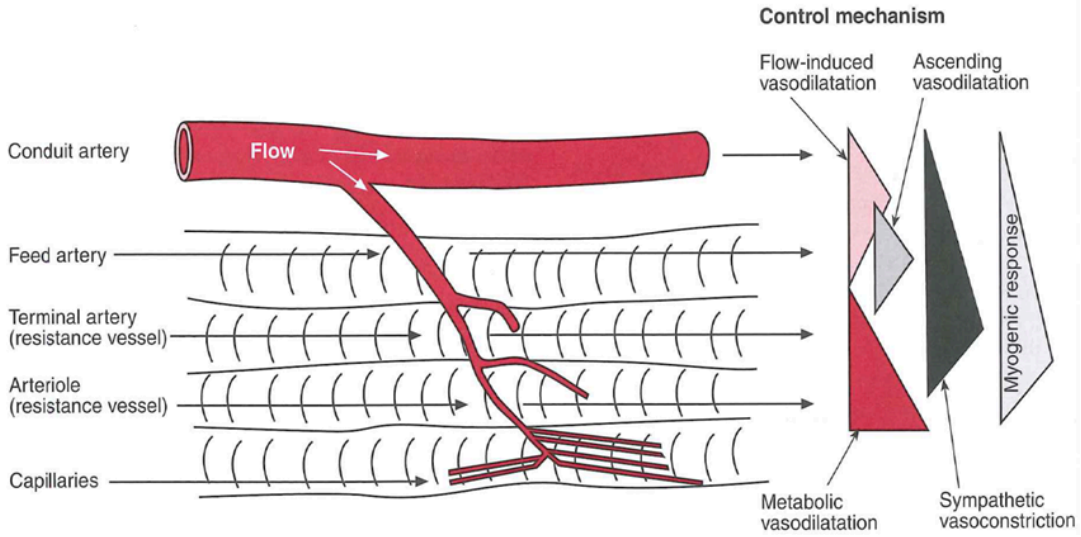

Figure 1.5. Mechanisms controlling vascular tone and the relative role that each mechanism plays in determining vascular tone throughout the different levels of the peripheral artery tree. Taken from Levick (2012).

The primary extrinsic factor is sympathetic activation; this factor regulates arterial pressure by altering systemic vascular resistance. At rest, basal sympathetic activity means that vessels are in a partially constricted state to maintain blood pressure. This vasoconstriction is consequent to noradrenaline, released from sympathetic nerve endings in the adventitia, binding to adrenergic receptors located on vascular smooth muscle cells and inducing vasoconstriction (Bruno et al., 2012).

Intrinsic mechanisms that control vascular tone at rest include the myogenic response: a reflex response characterised by an increase in vasoconstriction and vasodilation in response to an increase and decrease in intraluminal pressure,

respectively. The magnitude of the myogenic response varies in different vascular beds; the greatest response occurs in the resistance vessels, whilst larger (e.g. conduit arteries) and very small vessels (e.g. capillaries) retain a weak myogenic response (Figure 1.5). The myogenic response contributes to basal vascular tone but in concert with sympathetic activation, permits increases and decreases in vasoconstriction and vasodilation in response to other stimuli, such as vasoactive substances released from endothelial cells.

Endothelial cells release various vasoactive substances that maintain vascular tone. These substances include vasoconstrictor factors, such as thromboxane and endothelin 1, and vasodilator factors, such as endothelium-derived hyperpolarising factor and prostacyclin. At rest, basal levels of all of these vasoactive substances contribute towards maintaining vascular tone. However, nitric oxide (NO) is considered to be the major vasodilator produced by endothelial cells. Endothelium-derived NO is synthesised by endothelial nitric oxide synthase (eNOS). Numerous chemical and mechanical stimuli activate eNOS, including vascular endothelial growth factor (VEGF), adenosine triphosphate (ATP), adenosine, acetylcholine, insulin, bradykinin, histamine, thrombin, oestrogen, stretch and shear stress (da Silva et al., 2009, Haynes et al., 2000, Dimmeler et al., 1999, Nyberg et al., 2010, Michell et al., 1999, Vanhoutte et al., 2017).

The latter, shear stress, induces vasodilation via a mechanism known as flow-mediated dilation. Shear stress is the frictional force applied to the endothelium by blood flow as it passes through the vessel wall. At rest, the vasculature is exposed to relatively low levels of shear stress consequent to basal blood flow. Most humoral ligands (e.g. ATP, acetylcholine and bradykinin) increase NO production from eNOS by increasing the level of intracellular calcium, with calcium required for the activation

of calmodulin that subsequently activates eNOS (Förstermann and Münzel, 2006). However, shear stress stimulates NO production via eNOS by a calcium-independent mechanism (Ayajiki et al., 1996; Figure 1.6). Shear stress is detected by several mechanosensors on the surface of endothelial cells, leading to the activation of the phosphatidylinositol 3-kinase (PI3K)/protein kinase B (Akt) pathway which phosphorylates Akt (Alderton et al., 2001). In turn, Akt phosphorylates eNOS at its serine 1177 (Ser^{1177}) site. This results in the oxidation of L-arginine and generation of L-citrulline and NO as products (Alderton et al., 2001).

Following synthesis, NO diffuses out of the endothelial cell into the adjacent vascular smooth muscle cells where it binds to the enzyme soluble guanylyl cyclase (Figure 1.6). This now activated enzyme is responsible for the conversion of guanosine triphosphate to cyclic guanosine monophosphate; a secondary messenger in vascular smooth muscle cells that directly activates protein kinase G. Protein kinase G modulates calcium activated potassium channels on the membrane of vascular smooth muscle cells, increasing the probability that the potassium channels will open (Burgoyne and Eaton, 2010). Increased export of potassium results in hyperpolarisation and the closure of voltage-dependent calcium channels, thus, reducing calcium influx (Burgoyne and Eaton, 2010). This evokes vasodilation by inhibiting myosin light chain kinase activity and activating myosin light chain phosphatase, leading to the conversion of the myosin light chain from its phosphorylated contractile state to dephosphorylated relaxed state (Burgoyne and Eaton, 2010). As vascular smooth muscle cells relax, artery diameter increases, increasing blood flow through the vessel (Figure 1.6). At rest, flow-mediated dilation, facilitates a constant production of NO, evoking a sustained ‘steady-state’ vasodilation that maintains vascular tone and the delivery of blood (i.e. O_2) to the body’s tissues and organs.

Together, all of the mechanisms described above work in concert to maintain vascular tone at rest and ensure the bodies tissues and organs receive adequate blood flow. However, the ability of these mechanisms to respond to an increase in metabolic demand is essential to ensure O_2 delivery meets O_2 demand during dynamic whole-body exercise.

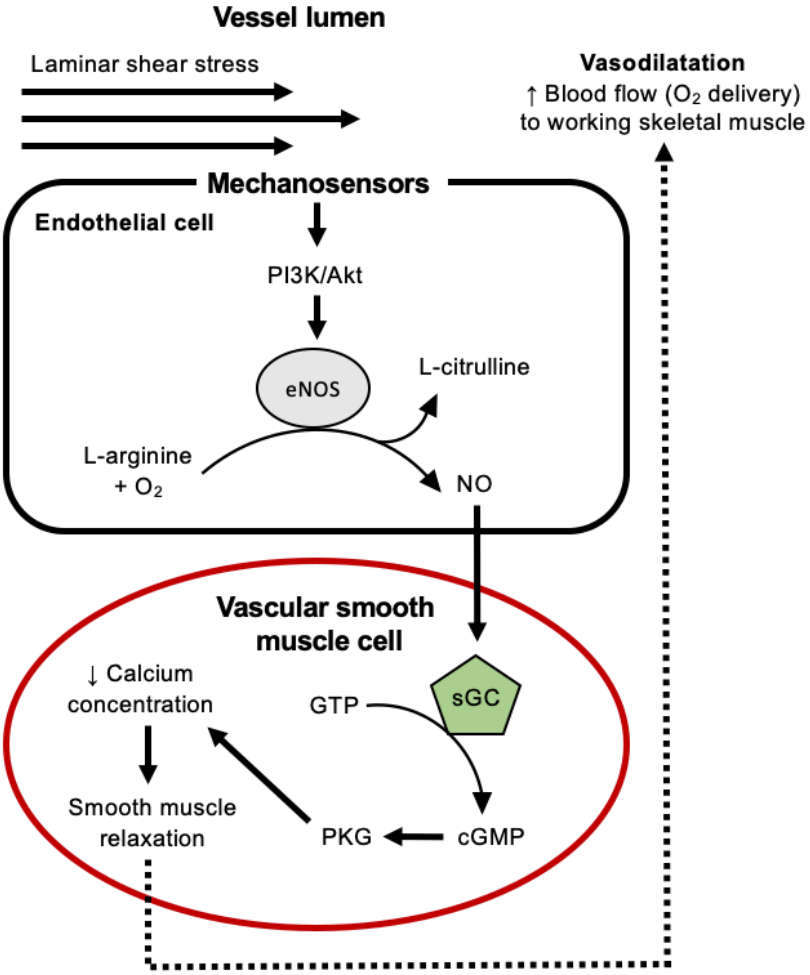

Figure 1.6. Shear stress-induced nitric oxide synthesis and vasodilation pathway. Mechanosensors on endothelial cell surface detect shear stress and trigger the phosphatidylinositol 3-kinase (PI3K)/Akt pathway, leading to the phosphorylation of endothelial nitric oxide synthase (eNOS) and production of nitric oxide (NO). NO diffuses into the adjacent vascular smooth muscle cell and increases the rate of conversion of guanosine triphosphate (GTP) to cyclic guanosine monophosphate (cGMP) by activating soluble guanylyl cyclase (sGC). cGMP stimulates protein kinase G (PKG) causing a reduction in intracellular calcium concentration that evokes relaxation of smooth muscle.

1.7.2 Vascular tone during exercise in health

At the onset of exercise, several mechanisms facilitate a rapid increase in blood flow (O_2 delivery) to the contracting skeletal muscles (Joyner and Casey, 2015). This includes an increase in sympathetic activity that affects nearly all of the vascular beds in the peripheral artery tree. However, whilst this increase in sympathetic activity induces an increase in sympathetic vasoconstriction in inactive tissues, this effect is attenuated or even abolished in vessels in the active skeletal muscle due to functional sympatholysis (Gliemann et al., 2019, Remensnyder et al., 1962). Together, these actions redistribute blood flow away from inactive tissues and facilitate an increase in blood flow (i.e. O_2 delivery) to the contracting skeletal muscle.

In addition, conducted (ascending) vasodilation facilitates an increase in blood flow to the contracting muscles at exercise onset. Conducted vasodilation is when vasodilation ascends from intramuscular arterioles into the feed arteries outside of the skeletal muscle, increasing blood flow (O_2 delivery) to the skeletal muscle (Bagher and Segal, 2011). This mechanism of vasodilation is consequent to the propagation of endothelial hyperpolarisation between endothelial cells in both directions via gap junctions (Gliemann et al., 2019). Conducted vasodilation is triggered by compounds such as acetylcholine and by muscle contraction, with the latter shown to be dependent on NO and ATP-sensitive potassium channels (Bagher and Segal, 2011). Studies showing conducted vasodilation in response to muscle contraction supports the role of this mechanism in exercise vasodilation. In a recent investigation, tetanic muscle contraction led to the rapid onset of endothelial hyperpolarisation, whereas, rhythmic muscle contraction resulted in a delayed vasodilatory response that was underpinned by flow-mediated dilation and metabolic vasodilation (Sinkler and Segal, 2017). Thus, indicating conducted vasodilation supports the rapid vasodilation that occurs immediately following exercise onset.

Cardiac output (i.e. blood flow) also increases at the onset of exercise, causing a large increase in shear stress in the peripheral vasculature. In turn, this increase in shear stress induces a large vasodilation in the arterioles and feed arteries, followed by a smaller vasodilation in larger upstream vessels, via flow-mediated dilation (see section 1.7.1), leading to a large increase in blood flow (i.e. O_2 delivery) to the working skeletal muscle to meet the muscles increased metabolic demand. As the exercise continues, cardiac output remains high, continuing the vessels exposure to high shear stress. This continued exposure to high shear stress maintains the vessels dilatated state, maintaining increased blood flow to the working skeletal muscles throughout exercise to meet the increased O_2 demand.

Substances released by the contracting skeletal muscle also contribute toward the rapid and prolonged increase in blood flow that occurs at the onset of exercise and during continued exercise, respectively. Increased muscle metabolism during exercise increases the interstitial concentration of metabolic products that are vasodilator mediators including CO_2, lactate, potassium and adenosine (Sarelius and Pohl, 2010). All of these signalling molecules can reach the vascular smooth muscle of adjacent arterioles via diffusion and activate ATP-sensitive potassium channels. When activated, these channels open and an outward flux of potassium follows, creating a more negative membrane potential. In turn, this hyperpolarisation leads to the closure of voltage-dependent calcium channels and thus, the relaxation of vascular smooth muscle cells. It is unclear whether these metabolic products can reach larger vessels, such as small feed arteries by diffusion to allow for a more coordinated response among daughter and parent vessels.

All of mechanisms described above work together to increase blood flow to the working skeletal muscle during exercise to ensure O_2 delivery meets the increased O_2 demand. The majority of these mechanisms rely on the interaction between the vascular endothelium and smooth muscle cells. When endothelial-dependent mechanisms of vasodilation are blocked, such as the double blockage of NO and prostaglandins, skeletal muscle blood flow is reduced by ~20% during exercise (Mortensen et al., 2007, Schrage et al., 2004). Therefore, vascular endothelial health and function is critical to skeletal muscle blood flow (i.e. convective O_2 transport).

1.8 Endothelial dysfunction

Endothelial dysfunction is characterised by a reduction in endothelial-dependent vasodilation which can be measured non-invasively using the flow-mediated dilation technique (FMD; described in section 2.10). Reported values for mean brachial artery FMD in young men range between 5-7.5% (Doshi et al., 2001, Dyson et al., 2006, Franzoni et al., 2005, Gates et al., 2007, Dawson et al., 2008); however, lower values (2.2-3.4%; Betik et al., 2004, Clarkson et al., 1999, Wray et al., 2006) have also been reported. In healthy individuals, a progressive decline in brachial artery endothelial function, as assessed using FMD, occurs as a consequence of the normal ageing process. In healthy males this decline (0.21% per year) begins after 40 years of age (Celermajer et al., 1994). The onset of this decline is delayed in females until menopause, but the rate of functional degeneration is accelerated (0.49% per year) with then a consistent impairment observed in males and females by 65 years of age (Celermajer et al., 1994). In line with this decline, Black et al. (2009) reported a 38% and 26% reduction in brachial artery FMD in older sedentary females (60 ± 2 y) and males (59 ± 2 y) respectively, compared to their younger counterparts (26 ± 1 y).

This endothelial dysfunction is a consequence of an imbalance between endothelial damage and repair, favouring the former. The structure and function of the

endothelium may be compromised by several types of insult; these include physical and biochemical injuries and immune-mediated damage. Information on the mechanisms involved in age-dependent endothelial dysfunction is limited and primarily comes from animal models. This is due to the difficulty in assessing mechanisms in humans as it necessitates isolated vessels and numerous samples (Brandes et al., 2005). However, a reduction in the bioavailability of NO has been proposed as the primary mechanism for age-related vascular endothelial dysfunction (Seals et al., 2011). This is supported by studies demonstrating a reduction in the vasoconstrictor response to NG-monomethyl-L-arginine (eNOS inhibitor) administration in resistance arteries (Taddei et al., 2000, Singh et al., 2002).

Reduced NO bioavailability with ageing appears to result from a reduction in NO production and/or increased NO removal by reactive oxygen species (ROS). Conflicting results have been reported concerning alterations in eNOS expression with ageing. Studies in rodents have shown both a decrease and increase in eNOS expression with ageing (van der Loo et al., 2000, Barton et al., 1997). Whilst a human study reported no difference in eNOS expression in endothelial cells taken from the brachial artery of young (21 ± 1 y) and older (62 ± 1 y) men (Donato et al., 2009). Thus, supporting the notion that eNOS expression and NO production is maintained in older humans.

Overproduction of ROS is associated with oxidative stress and endothelial dysfunction (Cai and Harrison, 2000). Several changes occur with ageing that increase oxidative stress. For example, ageing is linked with a reduction in the expression and/or activity of antioxidant enzymes, including superoxide dismutase, glutathione and catalase, which are the first line of defence against excessive ROS production (Hagen, 2003). Ageing is also associated with eNOS uncoupling which

leads to ROS production (Cau et al., 2012). During NO production by eNOS, NADPH donates electrons to tetrahydrobiopterin (BH_4) to facilitate the conversion of L-arginine to L-citrulline and NO. However, reduced availability of L-arginine and/or BH_4 that can occur with ageing results in eNOS uncoupling (Delp et al., 2008, Cai and Harrison, 2000); a state whereby eNOS favours the production of superoxide over NO. In addition to directly decreasing NO production, NO bioavailability is reduced because superoxide produced by uncoupled eNOS interacts with NO, leading to the generation of peroxynitrite a harmful nitrogen species that contributes to endothelial dysfunction.

Other mechanisms that may contribute to vascular ageing and the development of endothelial dysfunction include increased arterial stiffness (Donato et al., 2018), endothelial cell senescence owing to decreased telomerase activity and telomere shortening (De Meyer et al., 2011), endothelial cell apoptosis, attenuated vascular smooth muscle cell function (Montero et al., 2015), a reduction in circulating endothelial progenitor cell number and function (Vasa et al., 2001, Heiss et al., 2005), decreased vascular expression of sirtuin 1 (Donato et al., 2011, Cencioni et al., 2015), and an increase in vasoconstrictor tone due to endothelin-1 release (Donato et al., 2009).

All of these mechanisms increase endothelial damage and/or reduce endogenous repair mechanisms, promoting a state of endothelial dysfunction. The significance of endothelial dysfunction is that it impairs the ability of the endothelium to vasodilate, causing an increase in peripheral vascular resistance. At rest, this increase in peripheral vascular resistance may induce hypertension, leading to additional vascular damage and an increase in cardiovascular disease risk (discussed in section 1.9). Nevertheless, blood flow through the peripheral vasculature at rest

remains sufficient to meet the basal metabolic rate of the bodies organs and tissues. However, during exercise, when the metabolic demand of the contracting skeletal muscle is increased, this increase in vascular resistance may impair blood flow distribution, reducing convective O_2 transport and thus, O_2 delivery to the working skeletal muscle. In turn, adverse changes in the peripheral vasculature may contribute to the reduction in $\dot{V}O_{2peak}$ and exercise tolerance that occurs with ageing.

1.9 Endothelial dysfunction and cardiovascular disease risk

In addition to the adverse effect on convective O_2 transport, age-related endothelial dysfunction is a hallmark for the development of cardiovascular disease and strong predictor of future cardiovascular events (Green et al., 2011, Lerman and Zeiher, 2005). A meta-analysis of observational studies (*n* = 5547) reported that a 1% decrease in FMD is associated with an approximate 13% increase in risk of future cardiovascular events (Inaba et al., 2010). Currently, the primary risk factors for cardiovascular disease as identified by the Framingham heart study are high blood pressure, high cholesterol, smoking, obesity, diabetes, and physical activity, as well as, related factors such as age, gender and psychosocial issues (Hajar, 2016). However, these risk factors only explain ~60% of cardiovascular disease risk, the remaining 40% is thought to be due to adverse changes in the peripheral vasculature (Mora et al., 2007, Joyner and Green, 2009, Green et al., 2008, Thijssen et al., 2010).

In cases of endothelial dysfunction, where the vasodilatory capacity of the vasculature is decreased due to a reduction in the bioavailability of NO, a pro-atherogenic, pro-inflammatory and pro-thrombotic environment is created (Vanhoutte et al., 2009). This is because in addition to mediating vascular tone, NO maintains vascular homeostasis through its actions as an anti-inflammatory, anti-thrombotic and anti-hypertrophic molecule (Vanhoutte et al., 2009). NO liberated from endothelial cells into the vascular lumen prevents platelet aggregation and adhesion

to the endothelium (Radomski et al., 1990). NO also inhibits leukocyte adhesion and subsequent migration into the vessel wall by preventing an adhesive bond forming between leukocyte adhesion molecule CD11/CD18 and the endothelial cell surface and suppressing CD11/CD18 expression on leukocytes (Förstermann and Münzel, 2006). Moreover, NO has been shown to inhibit vascular smooth muscle cell proliferation and migration (Rudic et al., 1998). Collectively, these actions prevent the development of atherosclerosis, the underlying cause of most cardiovascular diseases.

Atherosclerosis is characterised by the incorporation and oxidisation of low-density lipoprotein, the invasion of monocytes and macrophages and the migration and proliferation of smooth muscle cells in the vascular wall (Hansson and Libby, 2006). These atherogenic processes result in the formation of atherosclerotic lesions that narrow the vessel lumen. Moreover, if unstable or obstructive, these lesions can lead to acute ischemic events, such as myocardial infarction, that can impair cardiac function, leading to development of chronic heart failure (CHF; discussed in detail in section 1.13).

1.10 Role of hematopoietic and endothelial progenitor cells in vascular repair

Endothelial dysfunction occurs when endothelial repair is unable to keep up with endothelial damage. Over a decade ago, it became evident that endothelial repair does not depend solely upon the proliferation of mature endothelial cells, but also on the mobilisation of bone-marrow derived hematopoietic and endothelial progenitor cells. In the original paper by Asahara et al. (1997), $CD34^+$ cells isolated from human peripheral blood and cultured in the presence of growth factors were positive for endothelial cell markers, including VEGF receptor 2 (VEGFR2), CD45 (leukocyte common antigen) and eNOS, and produced NO in response to acetylcholine and

VEGF. These cells also formed cellular networks and tube-like structures when plated on fibronectin *in vitro* and incorporated into capillaries in the ischaemic hindlimb of mice and rabbits after intravenous administration *in vivo* (Asahara et al., 1997). Subsequently, it was postulated that these cells, described as 'putative progenitor endothelial cells', contribute to neovascularisation and vascular repair in adults. Shortly after this initial study, Shi et al. (1998) demonstrated that after canines received a bone-marrow transplant, $CD34^+$ cells with endothelial morphology and donor DNA were present on grafts implanted in the descending thoracic aorta (Shi et al., 1998). This led to the suggestion that $CD34^+$ cells originate from the bone marrow and are mobilised in response to vascular injury to aid vascular repair. In support of this notion, after mice had a bone-marrow transplant, bone-marrow cells from the donor were identified in the ischaemic hindlimb of the mice, whilst no cells were detected in non-ischaemic tissues (Tepper et al., 2005). Moreover, the degree of cell recruitment was directly proportional to the degree of ischaemia (Tepper et al., 2005). The mechanisms by which hematopoietic and endothelial progenitor cells elicit endothelial repair are still not fully understood. Progenitor cells may differentiate into mature endothelial cells and incorporate into the vascular wall or secrete proangiogenic factors which stimulate neovascularisation (Rehman et al., 2003, Leone et al., 2009, Urbich and Dimmeler, 2004). Irrespective of the mechanism, the maintenance of an intact endothelial monolayer, either by progenitor cells or mature endothelial cells, prevents the development of endothelial dysfunction in healthy individuals and the associated reductions in exercise tolerance.

1.10.1 Characterisation of hematopoietic and endothelial progenitor cells

Hematopoietic progenitor cells are consistently defined as $CD34^+$-expressing mononuclear cells and have the potential to differentiate into multiple phenotypes, such as hematopoietic and endothelial lineages, and participate in vascular repair. In

contrast to hematopoietic progenitor cells, there has been controversy within the field regarding the characterisation of endothelial progenitor cells as no single marker or pattern of DNA has been established to unambiguously identify endothelial progenitor cells. Subsequently, disparity continues regarding their definition and researchers have labelled a variety of cell types as 'endothelial progenitor cells'. Two primary approaches are used to study endothelial progenitor cells both involve peripheral blood samples: 1. Flow cytometry-based assays and 2. *In vitro* cell culture techniques (Medina et al., 2017).

Using flow cytometry, endothelial progenitor cells are identified and quantified based on the specific cell surface antigens that they express. Commonly, endothelial progenitor cells are regarded as cells expressing CD34 and kinase insert domain receptor (KDR; also known as VEGFR2 and CD309) or cells expressing CD34, KDR and CD45 (i.e. $CD34^{+}/KDR^{+}$ or $CD45^{dim}/CD34^{+}/KDR^{+}$ cells). Often, the absence of specific markers that other haematopoietic and vascular endothelial subsets display, such as CD3 and CD14, contribute towards endothelial progenitor cell identification using this approach. Circulating hematopoietic and endothelial progenitor cell number were assessed using flow cytometry throughout this thesis.

In the second approach, endothelial progenitor cells are identified *in vitro* using cell culture techniques, leading to the identification of two distinguished populations named after their time-dependent appearance in culture: early and late endothelial progenitor cells. Early progenitor cells, also referred to as 'circulating angiogenic cells', are thought to be from haematopoietic lineage, have a low proliferative capacity and are not able to incorporate in the vasculature or differentiate into endothelial cells *in vivo* (Richardson and Yoder, 2011). Instead, these cells aid vascular repair in a paracrine fashion by secreting an array of angiogenic cytokines,

including VEGF, hepatocyte growth factor, granulocyte colony-stimulating factor and granulocyte-macrophage colony stimulating factor (Rehman et al., 2003).

In contrast to early endothelial progenitor cells, late endothelial progenitor cells, now more commonly referred to as endothelial colony forming cells, represent an endothelial cell type (Medina et al., 2017). These cells hold a potent intrinsic angiogenic capacity demonstrated by their ability to proliferate and differentiate into endothelial cells, and to form capillary like structures *in vitro* and integrate into, or form, functional blood vessels *in vivo* (Tasev et al., 2016). In addition, human endothelial colony forming cells support vascular repair by releasing angiocrine factors (Lin et al., 2014).

1.10.2 Hematopoietic and endothelial progenitor cell mobilisation, homing and adhesion in health

To participate in endothelial repair, progenitor cells must be mobilised from the bone marrow microenvironment into the circulation, migrate to sites of vascular damage and adhere to the vascular wall. The precise mechanism(s) that underpin progenitor cell mobilisation are still under investigation. However, exercise, ischaemia, hematopoietic growth factors (granulocyte monocyte colony-stimulating factor and granulocyte colony-stimulating factor), oestrogen, erythropoietin, VEGF and cytokines, such as stromal derived factor-1 alpha (SDF-1α), are all known to stimulate the release of progenitor cells from the bone marrow into the circulation (Urbich and Dimmeler, 2004; Figure 1.7). In their quiescent state, progenitor cells are tethered by adhesion molecules, such as VCAM-1, to stromal cells in the bone marrow microenvironment (Lapidot and Petit, 2002). Stromal cells play an important role in regulating progenitor cell release; they secrete SDF-1α to ensure progenitor cells remain in the bone marrow due to the interaction with the SDF-1α receptor C-X-C chemokine receptor 4 (CXCR4) on progenitor cells (Lapidot and Petit, 2002). Mobilisation of progenitor cells is mediated by several proteinases, including

elastase, cathepsin G and matrix metalloproteinases (MMPs; Lapidot and Petit, 2002). Following activation, these proteinases cleave the adhesive bonds between stromal cells and progenitor cells, releasing progenitor cells in the proliferative bone marrow niche.

One of the primary mobilisation pathways involves MMP-9. Once activated, bone marrow MMP-9 cleaves membrane bound Kit ligand (mKitL) in the bone marrow, leading to the release of soluble Kit ligand (sKitL) that interacts with adhesion molecules, enhancing the mobility of progenitor cells (Heissig et al., 2002). This affords the transfer of hematopoietic stem and endothelial progenitor cells from the osteoblastic to the vascular niche in the bone marrow. In addition, sKitL degrades SDF-1α to a non-functional chemokine, and thus, prevents its interaction with CXCR4 (Lapidot and Petit, 2002). This is a key step in progenitor cell mobilisation as it reduces the concentration of functional SDF-1α in the bone marrow, reversing the gradient that prevents progenitor cells from leaving the bone marrow. Together, these actions favour the movement of progenitor cells out of the bone marrow through the sinusoidal endothelium and into the blood stream. Support for MMP-9 as a major mediator of progenitor cell mobilisation comes from murine investigations demonstrating progenitor cell mobilisation is impaired in MMP-$9^{-/-}$ mice and during MMP-9 inhibition (Heissig et al., 2002).

NO production, and thus, eNOS expression and activity are critical for progenitor cell mobilisation. Indeed, progenitor cell mobilisation in response to VEGF, statin, exercise, and oestrogen is NO-dependent (Aicher et al., 2003, Landmesser et al., 2004, Iwakura et al., 2003, Laufs et al., 2004). In part, this is because NO stimulates MMP-9, triggering the aforementioned mobilisation pathway (Figure 1.8). As such, mice deficient in eNOS ($Nos3^{-/-}$ mice) demonstrate significantly lower levels of MMP-9 in the bone marrow and impaired progenitor cell mobilisation in response to VEGF

(Heissig et al., 2002). Furthermore, recovery from hind limb ischaemia is defective in Nos3$^{-/-}$ mice but is improved following intravenous infusion of progenitor cells from wild-type mice but not bone marrow transplantation, reaffirming progenitor cell mobilisation is impaired in Nos3$^{-/-}$ mice (Aicher et al., 2003).

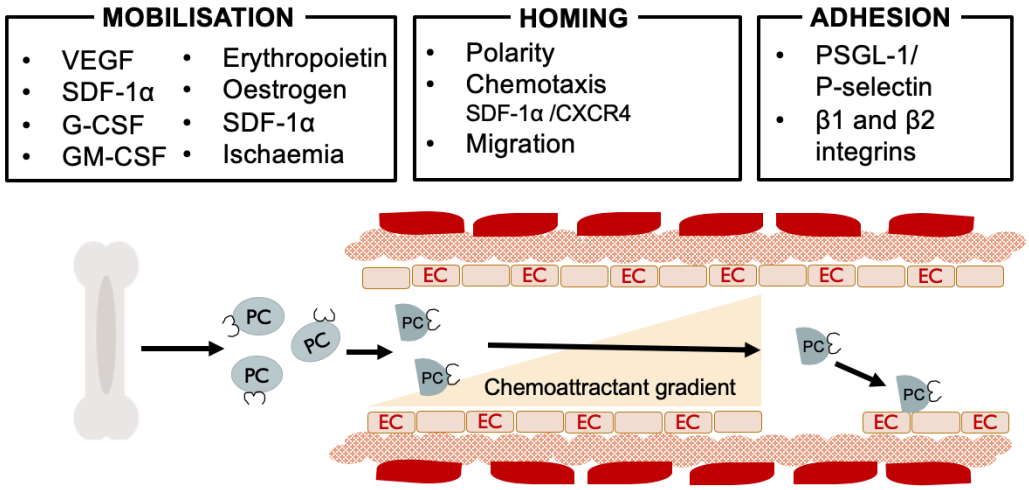

Figure 1.7 Progenitor cell (PC) mobilisation, homing and adhesion pathways. PCs are mobilised from the bone marrow niche into the peripheral blood in response to several cytokines and mobilisation factors. After establishing cell polarity, PCs migrate down a chemoattractant gradient to the site of vascular damage and adhere to the activated vasculature. PCs then participate in vascular repair either by differentiating into mature endothelial cells or by secreting growth factors that stimulate the proliferation and migration of existing endothelial cells near the site of damage. CXCR4 = C-X-C chemokine receptor 4; EC = endothelial cell; G-CSF = granulocyte colony-stimulating factor; GM-CSF = granulocyte-macrophage colony stimulating factor; PSGL-1 = P-selectin glycoprotein ligand-1; SDF-1α = stromal derived factor-1 alpha; VEGF = vascular endothelial growth factor.

Following release from the bone marrow, hematopoietic and progenitor cells in the peripheral circulation must be attracted to the site of vascular damage. In addition to the role it plays in progenitor cell mobilisation, SDF-1α has been consistently reported to be involved in progenitor cell migration (Zheng et al., 2007). In response to vascular damage, the endothelial monolayer is activated, and endothelial cells

release SDF-1α. In addition, platelets that have rapidly aggregated to the exposed subendothelial layer secrete high-levels of SDF-1α and VEGF (Zampetaki et al., 2008). Together, these factors create a chemokine gradient that attracts hematopoietic and progenitor cells to the site of injury (Figure 1.7). Progenitor cells are attracted to SDF-1α and VEGF due to the expression of CXCR4 and VEGFR2 on progenitor cells, respectively.

Before progenitor cells can migrate down chemokine gradients to sites of vascular injury, cell polarity must be established for directional locomotion. Polarisation in progenitor cells is regulated by Rho family GTPases, specifically Rac GTPases that are also known as compass proteins, and results in the formation of a front leading edge and a back edge of the cell (Shen et al., 2011). Chemokine receptors, such as CXCR4, are redistributed to the leading edge of the cell, facilitating migration (Giebel et al., 2004).

To exert their pro-angiogenic affect or differentiate into endothelial cells and incorporate into the vascular wall, hematopoietic and progenitor cells must adhere to the vascular wall. The mechanisms involved in progenitor cell adherence are not fully understood and vary between progenitor cell subsets. Early endothelial progenitor cells rely on the interaction between P-selectin glycoprotein ligand-1 (PSGL-1) on progenitor cells and P-selectin expressed on platelets (Cao et al., 2010). When the vascular wall is damaged, platelets adhere to the endothelium and express P-selectin and SDF-1α. In turn, SDF-1α interacts with CXCR4 on progenitor cells, increasing the expression of PSGL-1 (Lapidot and Petit, 2002). In contrast, late outgrowth progenitor cells can adhere to sites of vascular damage in the absence of platelets. PSGL-1 expressed by late outgrowth endothelial cells can bind to L-selectin on neutrophils present at the site of vascular injury (Hubert et al., 2014). The adhesion of progenitor cells to the vascular wall may also be supported by the interaction β2

integrins on progenitor cells and adhesion cells (e.g. intracellular adhesion molecule 1; ICAM-1) on endothelial cells or on fibronectin (Chavakis et al., 2005). This is supported by the observation that progenitor cells derived from β2 integrin deficient mice are less capable of homing to the site of ischaemia and aiding neovascularisation compared to progenitor cells obtained from wild-type mice when inserted into athymic mice 24 h after induction of hind-limb ischaemia (Chavakis et al., 2005). Collectively, the processes involved in mobilisation, migration and adhesion are crucial for hematopoietic and progenitor cells to participate in vascular repair. These processes are continually ongoing in health to ensure that normal endothelial damage is repaired, and vascular function is maintained.

1.10.3 Hematopoietic and endothelial progenitor cell number and ageing

Ageing is associated with a reduction in the number of circulating hematopoietic and endothelial progenitor cells (Thijssen et al., 2006, Xia et al., 2012). Thijssen et al. (2006) reported a 71 and 77% reduction in $CD34^+$ and $CD34^+/KDR^+$ cell number, respectively, in older sedentary men (67-76 y) compared to younger sedentary men (19-28 y). In agreement with these results, Yang et al. (2013) demonstrated a ~50% reduction in $CD34^+/KDR^+$ number in older sedentary men (59-72 y) compared to younger men (21-33 y). Further, Ross et al. (2018) concluded that age is inversely associated with $CD34^+/CD45^{dim}/KDR^+$ number after processing blood samples from 107 males aged between 18-75 years. Nevertheless, Heiss et al. (2005) found no difference in $CD34^+/KDR^+$ number between older (61 ± 2 y) and younger (25 ± 1 y) subjects. This may be a consequence of the experimental procedure that was used to enumerate $CD34^+/KDR^+$ cells.

Although the mechanisms responsible for the age-related decline in circulating hematopoietic and endothelial progenitor cell number remain unclear, the reduction in endogenous repair capacity that occurs with advancing age increases the risk of

endothelial dysfunction as it adversely influences the balance between endothelial damage and repair mechanisms, favouring the former. Thus, interventions that attenuate or prevent age-related declines in hematopoietic and endothelial progenitor cell number are likely to help prevent endothelial dysfunction and the associated consequences that it can have on cardiovascular disease risk and exercise tolerance.

1.10.4 Hematopoietic and endothelial progenitor cell response to exercise in health

1.10.4.1 Hematopoietic and endothelial progenitor cell response to a single session of exercise in health

Exercise can have a potent effect on progenitor cell mobilisation in healthy individuals (Möbius-Winkler et al., 2009, Ribeiro et al., 2017, Van Craenenbroeck et al., 2008b, Krüger et al., 2015). Several studies have demonstrated an increase in the number of progenitor cells after a single bout of aerobic exercise. On two occasions the progenitor cell response to a maximal exercise test has been investigated in healthy adults, with both studies reporting a large (66-76%) increase in $CD34^+/KDR^+$ number pre- to post-exercise when cells were assessed 10-30 min post-exercise (Yang et al., 2007, Van Craenenbroeck et al., 2008b). Laufs et al. (2005) also reported an increase in $CD34^+/KDR^+$ cells following 10 min of intensive running (~82% $\dot{V}O_{2max}$) and 30 min of moderate running (~68% $\dot{V}O_{2max}$). However, no changes were observed following 10 min of moderate running, suggesting exercise-induced progenitor cell mobilisation is dependent on exercise intensity and duration (Laufs et al., 2005).

In support of the role of exercise intensity in progenitor cell mobilisation, $CD34^+/CD45^{dim}$ number was higher following sprint interval exercise (6 x 20 s sprints) on a cycle ergometer but remained unchanged in the same participants following 45 min of continuous exercise at 70% $\dot{V}O_{2peak}$ (O'Carroll et al., 2019). However, the number of $CD45^{dim}/CD34^+/KDR^+$ cells increased pre- to post-exercise in both groups,

with no difference in the magnitude of change between groups, indicating heterogeneity in exercise-induced mobilisation exists between progenitor cell subsets. In support of this heterogeneity, the number of $CD45^+/CD34^+$ cells increased after healthy males cycled at 80% $\dot{V}O_{2peak}$ until exhaustion (average cycling time: 43 ± 5 min), with no change in $CD45^{dim}/CD34^+/KDR^+$ observed (Krüger et al., 2015).

In regard to the role of exercise duration in exercise-induced progenitor cell mobilisation, Möbius-Winkler et al. (2009) investigated the kinetics of $CD34^+$ and $CD34^+/KDR^+$ mobilisation during a 4 h cycling protocol at 70% anaerobic threshold in healthy men. The highest concentrations of $CD34^+$ and $CD34^+/KDR^+$ cells were both recorded at 210 min, with $CD34^+$ and $CD34^+/KDR^+$ number rising 3.1 and 5.5-fold, respectively. However, in contrast to these findings, Niemiro et al. (2017) reported a peak in $CD34^+$ number within the first 20 min of treadmill exercise at 70% $\dot{V}O_{2peak}$ in young men, despite participants running for 1 h. Although these studies follow a different time course, both demonstrate a significant increase in $CD34^+$ concentration that was sustained until exercise cessation.

Indeed, the majority of studies demonstrate a rise in circulating $CD34^+$ cells following acute exercise in healthy individuals (Bonsignore et al., 2010, Morici et al., 2005). After an ‘‘all-out’ 1000m row, the number of $CD34^+$ cells doubled (+114%) in young competitive rowers ($\dot{V}O_{2peak}$: 56.5 ± 11.4 $ml \cdot min^{-1} \cdot kg^{-1}$; Morici et al., 2005). Similarly, an elevation in $CD34^+$ number was observed after a 1.5 km running time-trial (mean time: 335 ± 35 s) in 10 healthy amateur runners (Bonsignore et al., 2010). However, the effect of more strenuous exercise (e.g. marathons and ultramarathons) on $CD34^+$ mobilisation appears less favourable. Bonsignore et al. (2002) recorded no change in $CD34^+$ number after amateur runners completed a marathon or half-marathon. Whereas, Adams et al. (2008) reported an inflammatory response and consequent

reduction in $CD34^+$ cells (~35%) but no change in $CD34^+/KDR^+$ cell number immediately after older runners (57 ± 6 y) completed a marathon race. The lack of an increase in $CD34^+$ number after strenuous exercise may be consequent to a lack of progenitor cell mobilisation or greater progenitor cell utilisation due to the endothelial damage elicited by the strenuous exercise. This purports further evidence that a balance between exercise intensity and duration is required to increase circulating progenitor cell number.

Other authors have observed no increase in circulating progenitor cells ($CD34^+/KDR^+$ number) following acute exercise (Lansford et al., 2016, Lockard et al., 2010, Thijssen et al., 2006, Adams et al., 2008). The lack of $CD34^+/KDR^+$ mobilisation in these studies may be due to variations in the duration and intensity of the exercise and the age of the participants. The majority of these studies (Lockard et al., 2010, Thijssen et al., 2006, Adams et al., 2008) involved older men with authors concluding that ageing lowers circulating progenitor cell number and attenuates the acute exercise-induced increase in progenitor cells. Whilst Lansford et al. (2016) employed a constant work rate cycling protocol with a shorter duration (43-63 min) and lower exercise intensity (60-70% $\dot{V}O_{2peak}$) than most studies reporting a rise in $CD34^+/KDR^+$ number pre- to post-exercise (Möbius-Winkler et al., 2009, Bonsignore et al., 2010, Yang et al., 2007, Van Craenenbroeck et al., 2008b). Thus, highlighting the effect of age and reiterating the pivotal role of exercise intensity and duration on progenitor cell mobilisation.

1.10.4.2 Hematopoietic and endothelial progenitor cell response to exercise training in health

Whilst acute exercise induces a transient increase in progenitor cell number in health, chronic exposure to exercise (i.e. exercise training) can increase the baseline number of progenitor cells. This increase in vascular endogenous repair capacity is likely to positively influence the balance between endothelial damage and repair,

reducing the risk of endothelial dysfunction. Evidence of the effect exercise training has on baseline progenitor cell number in health is summarised in Table 1.1.

Several different training strategies have been employed that have successfully induced an increase in progenitor cell number in healthy individuals, including sprint interval training and high-intensity interval training (HIIT; Tsai et al., 2016, Harris et al., 2014). Currently, no studies have examined the time-course for changes in baseline progenitor cell number with exercise training; however, these studies have shown increases in progenitor cell number after 4-12 weeks of exercise training. In contrast to these studies, other investigations using constant work rate exercise training and HIIT have reported either no change in progenitor cell counts or a reduction in endogenous repair capacity pre- to post-training (Thijssen et al., 2006, Rakobowchuk et al., 2012; Table 1.1). These results may be due to the different cell populations that were studied or that a young healthy population was investigated who already possess an ideal endogenous repair capacity.

Collectively, the studies summarised in section 1.10.4.1 and Table 1.1, demonstrate that there are both short- and long-term benefits of exercise on endogenous repair capacity in health. A single session of aerobic exercise induces a transient increase in circulating hematopoietic and endothelial progenitor cell number, and exercise training leads to a sustained increase in baseline hematopoietic and endothelial progenitor cell number. However, the optimal exercise strategy to induce these short- and long-term increases in hematopoietic and endothelial progenitor cell number to improve vascular repair capacity in health remains unknown.

Table 1.1 Hematopoietic and endothelial progenitor cell responses to exercise training in health

Study	*n*	Participants	Duration/frequency	Training Protocol	Results	
Thijssen et al. (2006)	8	Sedentary older adults (67-76 y)	8 weeks/ 3 times per week	- Supervised cycle exercise - 10 min at 65% HRR - 20 min at 65-85% HRR	- $CD45^{dim}/CD34^{+}/KDR^{+}$ decreased by 46% - $CD45^{dim}/CD34^{+}$ did not change	↓ =
Xia et al. (2012)	25	Older adults (68 ± 3)	12 weeks/ 3 times per week	- Treadmill training - 30 min	- $CD34^{+}/KDR^{+}$ increased - KDR+/CD133+ increased	↑
Rakobowchuk et al. (2012)	20	Healthy adults (23 ± 3 y)	6 weeks/3 times per week	- 30-40 min cycle exercise - 2 groups: moderate and heavy work matched interval training - Work:recovery duration = moderate: 10:20 s; heavy: 30:60 s - Work:recovery work rate = 120% WR_{peak}: 20 W	- $CD34^{+}$, $CD34^{+}/KDR^{+}$ and $CD34^{+}/CD133^{+}/KDR^{+}$ number did not change	=
Harris et al. (2014)	12	Healthy females (22 ± 2 y)	4 weeks/ 3 times per week	- Cycle exercise - 2 groups: sprint interval and continuous - Interval: 4 x Wingate test separated by 4.5 min - Continuous: work matched continuous sprint	- $CD34^{+}$ increased in both groups (Int: +44%; Con: +28%) - $CD34^{+}/CD45^{dim}$ did not change in either group	↑ =

Tsai et al. (2016)	40	Sedentary young males (22 ± 2 y)	6 weeks/5 times per week	- Cycle exercise - 3 groups: HIIT; MCT; Control - HIIT: 5 x 3 min at 80% $\dot{V}O_{2peak}$ followed by 3 min recovery at 40% $\dot{V}O_{2peak}$ - MCT: 30 min at 60% $\dot{V}O_{2peak}$	- $CD34^+$ did not change - $CD34^+/KDR^+$ increased in HIIT (+34%) and MCT (+47%) - $CD34^+/KDR^+/CD133^+$ increased in HIIT (+52%) and MCT (+50%) - $CD34^+/KDR^+/CD31^+$ and $CD34^+/KDR^+/CD117^+$ increased in HIIT only by +100% - No changes in control group	= ↑
Niemiro et al. (2018)	17 10	Lean adults (24 ± 5 y) Obese adults (29 ± 8 y)	6 weeks/3 times a week	- Cycle or treadmill exercise - 30-60 min at 60-75% HRR	- $CD34^+$ decreased in lean adults (-67%), with no change in obese adults - $CD34^+/CD45^{dim}$ reduced in lean (-78%) and obese (-77%) adults - $CD45^-/CD34^+/CD31^+$ did not change	↓ = ↓ =

↑ = increase pre- to post-training; ↓ = decrease pre- to post-training; = = no change pre- to post-training. HIIT = high-intensity interval training; HRR = heart rate reserve; MCT = moderate intensity continuous training; $\dot{V}O_{2peak}$ = peak oxygen uptake; WR_{peak} = peak work rate from ramp-incremental exercise test.

1.10.5 Mechanisms underpinning exercise-induced hematopoietic and endothelial progenitor cell mobilisation

Although exercise has consistently been identified as a stimulus for hematopoietic and endothelial progenitor cell mobilisation, the mechanisms underpinning exercise-induced progenitor cell mobilisation remain poorly understood. However, experimental studies suggest that NO plays an essential role in exercise-induced progenitor cell mobilisation.

When NO production is blocked in humans using L-NMMA, $CD34^+/KDR^+$ and $CD133^+/CD34^+/KDR^+$ progenitor cell mobilisation in response to an acute bout of moderate intensity cycling exercise is completely abolished (Cubbon et al., 2010). Likewise, progenitor cell mobilisation in response to 28 days of physical activity (access to a running wheel) is significantly attenuated in $eNOS^{-/-}$ mice and mice treated with a nitric oxide synthase inhibitor when compared to control mice (Laufs et al., 2004). Moreover, progenitor cell mobilisation correlates with surrogates of NO bioavailability (Steiner et al., 2005, Paul et al., 2007). Coronary artery disease patients who showed an increase in progenitor cell number after a 36-session cardiac rehabilitation programme also showed a significant increase in blood nitrate compared to those whose progenitor cell level remained unchanged after completing the exercise intervention (Paul et al., 2007). The increase in NO production reported in patients with coronary artery disease following 12 weeks of supervised running training also positively correlated with the increase in $CD34^+/KDR^+/CD133^+$ progenitor cell number seen pre- to post-training (Steiner et al., 2005).

During acute exercise, increases in shear stress in the bone marrow vasculature, caused by increases in cardiac output, activate eNOS and increase NO production

(refer to section 1.7). This shear-stress-induced increase in NO, in concert with an exercise-induced increase in adenosine, also increases outflow of VEGF from the skeletal muscle, which activates eNOS, leading to an increase in NO bioavailability (Adair, 2005, Høier et al., 2010). Repeated exposure to exercise-induced shear stress through exercise training may also increase NO bioavailability via an increase in eNOS; Hambrecht et al. (2003) demonstrated a two-fold increase in the expression of eNOS and a four-fold increase in eNOS Ser^{1177} phosphorylation levels in the left internal mammary artery of coronary artery disease patients following 4 weeks of supervised in-hospital exercise training (10 min on the cycle ergometer and 10 min on the row ergometer 3 times a day) compared to non-exercising control patients.

Exercise training also increases the expression of antioxidant enzymes, including superoxide dismutase, glutathione peroxidase, glutathione levels and catalase (Powers and Jackson, 2008). Increased expression of these enzymes increases NO bioavailability by limiting the rapid inactivation of NO by ROS. Further, exercise training decreases the expression of inflammatory mediators (e.g. TNF-1α, interleukin-6, interleukin-1β and inducible NOS) and increases the expression of anti-inflammatory mediators (e.g. interleukin-10; Gielen et al., 2003, Zheng et al., 2019), reducing inflammatory-induced vascular damage and increasing NO bioavailability.

The exercise-induced elevation in NO consequent to the mechanisms described above may increase progenitor cell mobilisation via the pathway outlined in section 1.10.2, involving MMP-9 (Figure 1.18). In support of this mechanism, Gatta et al. (2012) reported an increase in the ratio of MMP-9 to tissue inhibitor of metalloproteinase 1 in concert with an increase in $CD34^{+}/KDR^{+}$ progenitor cell number in individuals with chronic heart failure after 3 weeks of cycle exercise training.

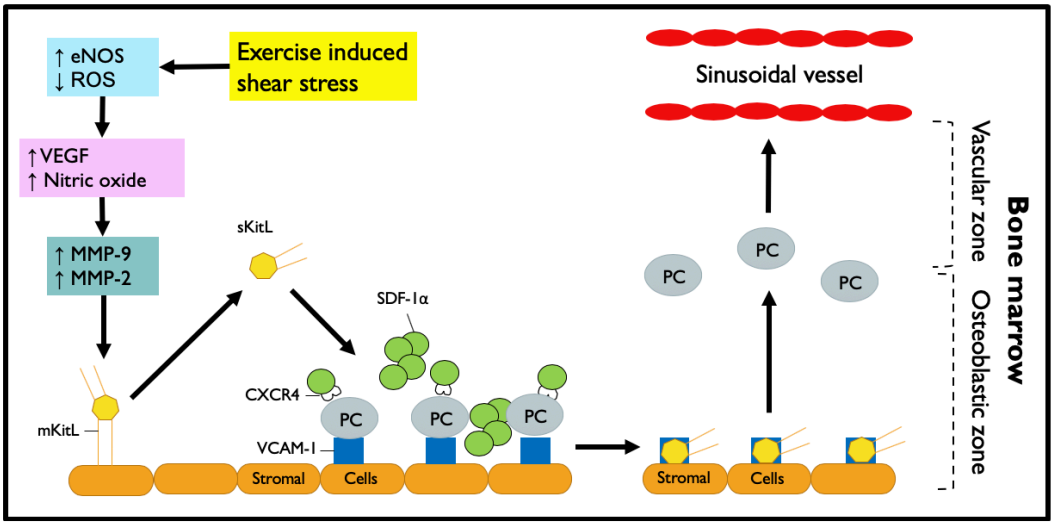

Figure 1.8 Exercise-induced progenitor cell (PC) mobilisation. Elevations in nitric oxide (NO) and vascular endothelial growth factor (VEGF), consequent to an exercise-induced increase in shear stress in the bone marrow vasculature, activate matrix metalloproteinases (MMPs). MMPs cleaves membrane bound Kit ligand (mKitL), leading to the release of soluble Kit ligand (sKitL) that interacts with adhesion molecules and degrades stromal derived factor-1 alpha (SD1F-1α). Together these steps enable progenitor cells to leave the osteoblastic niche and travel out of the bone marrow down a chemoattractant gradient via the vascular niche. eNOS = endothelial nitric oxide synthase; ROS = reactive oxygen species; VCAM-1 = vascular cell adhesion molecule-1.

1.11 High-intensity interval training

High-intensity interval training (HIIT) is characterised by short periods of work at a high exercise work rate, interspersed by periods of recovery exercising at a low rate or rest. This form of exercise training increases vascular function (assessed by FMD) and $\dot{V}O_{2peak}$ in health and disease at least as well as traditional constant work rate protocols (Rakobowchuk et al., 2008, Harris et al., 2014, Boff et al., 2019, Sawyer et al., 2016, Conraads et al., 2015, Moholdt et al., 2009, Wisløff et al., 2007). Moreover, it is perceived to be more enjoyable than continuous exercise training (Bartlett et al., 2011). The specific physiological adaptations induced by HIIT are likely influenced by a multitude of factors, including the exact exercise protocol that is employed (e.g. intensity and duration of work:recovery bouts; MacInnis and Gibala, 2017, Gibala and Little, 2020). Subsequently, it may be possible to augment the improvement in

vascular health and $\dot{V}O_{2peak}$ gained from HIIT by altering the precise HIIT protocol that is used. Alternatively, combining HIIT with another training technique, such as blood flow restriction (BFR), may increase stimulus for adaptation in the peripheral vasculature, leading to greater improvements in vascular health and $\dot{V}O_{2peak}$ than HIIT alone.

1.12 Exercise with blood flow restriction

During BFR an external pressure, usually achieved using a tourniquet, elastic band or inflated cuff, is applied to the proximal portion of the exercising limb, causing a reduction in arterial inflow and fully restricting venous outflow in the musculature. As a result, the local metabolic milieu is altered (or maintained at the level induced by the exercise), leading to an upregulation of multiple downstream pathways and augmentation of the adaptive response to exercise (Manini and Clark, 2009). The majority of previous investigations have focussed on the adaptive potential of resistance exercise training with BFR to increase muscle mass and strength in health (Pearson and Hussain, 2015). However, more recently, the adaptive potential of aerobic exercise with BFR to enhance $\dot{V}O_{2peak}$ and exercise tolerance has been explored. Protocols have been employed that expose participants to either continuous or intermittent BFR during exercise. The pressure prescribed to restrict blood flow varies between studies depending on whether the pressure is intended to cause partial (~90-160 mmHg) or complete (~240-300 mmHg) occlusion. Furthermore, in some studies a blanket approach is taken whereby all participants are exposed to the same external pressure, whereas, in other studies an individual pressure is prescribed. This is because several factors influence the magnitude of blood flow that is restricted in response to a set external pressure including: blood pressure, cuff width and limb circumference (Hunt et al., 2016, Leonneke et al., 2011).

Early studies investigating the effect of BFR on $\dot{V}O_{2peak}$ and exercise tolerance used pressure chambers to continuously restrict blood flow during single-leg cycling (Sundberg, 1994, Kaijser et al., 1990, Sundberg et al., 1993). These studies demonstrated a greater increase in $\dot{V}O_{2peak}$ (~10%; Sundberg et al., 1993) and time to intolerance (~15%; Kaijser et al., 1990) after 4 weeks of exercise training in the leg exposed to BFR compared to the control leg without BFR.

More recent studies that have restricted blood flow via the application of inflatable cuffs also indicate that BFR may enhance the physiological adaptations derived from aerobic exercise training. Indeed, several studies (summarised in Table 1.2) have reported greater increases in $\dot{V}O_{2peak}$ and exercise tolerance following aerobic exercise training with BFR compared to aerobic exercise alone. For example, Abe et al. (2010) investigated the effects of 8 weeks of low-intensity cycle exercise (40% $\dot{V}O_{2peak}$) with continuous BFR (160-210 mmHg) in young men on $\dot{V}O_{2peak}$ and exercise tolerance. Post-training, there was a significant increase in $\dot{V}O_{2peak}$ (6.4%) and exercise tolerance (15.4%) in the BFR cohort only, despite the control group performing a greater volume of exercise (45 vs. 15 min per session; Abe et al., 2010). Nevertheless, in contrast to these studies, Kim et al. (2016) reported no significant increase in $\dot{V}O_{2peak}$ after 6 weeks of low-intensity cycle training (30% of heart rate reserve) with continuous BFR (160-180 mmHg). However, exercise intensity was lower in this study than in Abe et al. (2010; ~59% of heart rate reserve). Thus, it is possible that the exercise protocol utilised by Kim et al. (2016) imposed less stress (supported by a low/moderate rate of perceived exertion: 11.5 ± 0.5 using 6-20 scale) than other BFR training protocols, resulting in an insufficient stimulus for physiological adaptation.

Although continuous BFR (i.e. cuffs applied during the exercise) increases $\dot{V}O_{2peak}$ and exercise tolerance, it results in significantly greater ratings of perceived exertion and pain than intermittent BFR (Fitschen et al., 2014). Subsequently, several authors have explored the effect of intermittent BFR on $\dot{V}O_{2peak}$ and exercise tolerance (see Table 1.2), typically in the form of low- or high-intensity interval training whereby BFR is applied during exercise bouts but not during recovery. For example, de Oliveira et al. (2016) reported that the addition of BFR (140-200 mmHg) to low-intensity interval training (30% WR_{peak}) resulted in a superior increase in $\dot{V}O_{2peak}$ and maximal power output than the same training without BFR. Moreover, the adaptations triggered by this training strategy were similar to those induced by the same interval protocol performed at a much higher intensity with normal blood flow (95-110% WR_{peak}). Taken together, the studies summarised in Table 1.2 demonstrate the additive effect of combining aerobic exercise training with continuous or intermittent BFR on $\dot{V}O_{2peak}$ and exercise tolerance.

Table 1.2 Aerobic exercise with blood flow restriction in health

Study	*n*	Participants	Duration/frequency	Training Protocol	Results	
Park et al. (2010)	12	Collegiate basketball players	2 weeks/ 2 sessions a day, 6 days a week	- Walk training - 5 x 3 min walk at 4-6 km/h with 5% incline) either with or without continuous BFR (160-220 mmHg)	- $\dot{V}O_{2peak}$ increased by 11.6% in the BFR group with no change in the control	↑
Ursprung and Smith (2017)	10	Trained males (34 ± 7 y)	3 weeks/ 5 days a week	- Walk training - 20 min walk at 45% $\dot{V}O_2$ reserve with continuous BFR to restrict venous return	- $\dot{V}O_{2peak}$ increased by 3.4% - No control group	↑
Abe et al. (2010)	19	Physically active young men (20-26 y)	8 weeks/ 3 days a week	- Cycle exercise at 40% $\dot{V}O_{2peak}$ - Control group: 40 min cycling - BFR group (160-210 mmHg): 15 min cycling with continuous BFR	- $\dot{V}O_{2peak}$ increased by 6.4% in BFR group only - Exercise tolerance increased by 15.4% in BFR group only	↑
Kim et al. (2016)	31	Physically active males (22 ± 3 y)	6 weeks/ 3 days a week	- Cycle exercise, 3 groups: - Vigorous intensity group: 20 min at 60-70% HRR - Low-intensity BFR group: 20 min at 30% HHR with continuous BFR (160-180 mmHg) - Control: no exercise	- $\dot{V}O_{2peak}$ remained unchanged pre- to post-training training in all groups	=
Paton et al. (2017)	16	Healthy adults (24 ± 7 y)	4 weeks/ 2 days a week	- Treadmill exercise, 2 groups: - BFR: 2-3 sets of 30 s work (80% of peak running velocity), separated by 30 s recovery with continuous BFR - Control: same exercise without BFR	- $\dot{V}O_{2peak}$ increased in BFR and control groups, with no difference in the magnitude of change between groups	↑

de Oliveira et al. (2016)	37	Healthy adults (24 ± 4 y)	4 weeks/ 3 days a week	- Cycle interval exercise - 2 sets of 5-8 reps of 2 min work then 1 min passive rest, 4 groups: - BFR: WR = 30% WR_{peak} with BFR during each work bout (140-200 mmHg) - HIIT: WR = 95-110% WR_{peak} no BFR - HIIT+BFR: 1 set performed as BFR and the other as HIIT - LIIT: WR = 30% WR_{peak} no BFR	- $\dot{V}O_{2peak}$ and WR_{peak} increased in BFR (6, 12%), HIIT (9, 15%) and HIIT+BFR (6, 11%) with no difference in the magnitude of change between groups	↑
Christiansen et al. (2019b)	13	Healthy males (25 ± 4 y)	6 weeks/ 3 days a week	- Cycle interval exercise - Each leg performed 3 x 2 min cycling at 60-80% WR_{peak} - One leg was trained without BFR and the other leg was trained with BFR (180 mmHg)	- Exercise tolerance, assessed by single leg knee-extensor peak power increased in BFR leg more than non-BFR leg	↑
Keramidas et al. (2012)		Untrained healthy adults (23 ± 5 y)	6 weeks/ 3 days a week	- Cycle exercise, 2 groups: - BFR: interval exercise consisting of 2 min work at 90% $\dot{V}O_{2peak}$ followed by 2 min recovery at 50% of $\dot{V}O_{2peak}$ with continuous BFR (90 mmHg) - Control: same exercise without BFR	- $\dot{V}O_{2peak}$ remained unchanged in both groups pre- to post-training	=

↑ = increase pre- to post-training; ↓ = decrease pre- to post-training; = = no change pre- to post-training. BFR = blood flow restriction; HIIT = high-intensity interval training; HRR = heart rate reserve; LIIT = low-intensity interval training; $\dot{V}O_{2peak}$ = peak oxygen uptake; WR = work rate; WR_{peak} = peak work rate from exercise test.

1.12.1 Post-exercise blood flow restriction

An alternative approach to incorporating BFR into aerobic exercise training is to restrict blood flow post-exercise (i.e. during recovery periods). This allows the muscles to perform normally during the exercise bouts but introduces an additional stimulus during recovery periods that may lead to greater training adaptions than exercise alone. Two studies have previously investigated the effect of post-exercise BFR during sprint interval training on $\dot{V}O_{2peak}$ (Taylor et al., 2016, Mitchell et al., 2019). A 4-week training period was utilised in both studies, whereby trained individuals ($\dot{V}O_{2peak}$ >60 $ml \cdot min^{-1} \cdot kg^{-1}$) performed 2 sprint interval sessions each week, involving 4-7 maximal 30 s sprints separated by 4.5 min recovery either alone or with BFR during the recovery (cuff pressure: ~120-130 mmHg). The latter cohort immediately dismounted the ergometer after each sprint and laid in a semi-supine position before BFR was applied. Both studies reported a significant improvement in $\dot{V}O_{2peak}$ following sprint interval training with BFR only (Taylor et al., 2016: 4.5%; Mitchell et al., 2019: 5.9%). Thus, demonstrating the potency of post-exercise BFR to improve the effectiveness of training and induce greater increases in $\dot{V}O_{2peak}$ without increasing training volume in well-trained individuals; a population where inducing further adaptations is notoriously difficult due to the already well adapted physiology of these individuals' consequent to years of high volumes of training. Further studies are needed to determine whether superior adaptations can be derived using post-exercise BFR in conjunction with other exercise training strategies, such as HIIT, and in other populations who are unable to perform sprint interval training or increase training volume but would particularly benefit from increasing the effectiveness of exercise training (e.g. clinical populations).

1.12.2 Blood flow restriction and vascular adaptations

The increases in $\dot{V}O_{2peak}$ reported following aerobic exercise with BFR may in part be attributed to improved convective O_2 delivery consequent to adaptations in the peripheral vasculature (Christiansen et al., 2020). Several studies indicate that

exercise training in tandem with BFR can lead to superior vascular adaptations at all levels of the peripheral artery tree compared to the same exercise training without BFR. For example, Hunt et al. (2013) investigated the effect of 6 weeks of unilateral plantar flexion training (30% 1RM) with BFR (cuff pressure: 110 mmHg) on conduit, resistance and capillary vessel function by assessing popliteal artery maximum diameter, peak reactive hyperaemia and calf filtration capacity, respectively. Post-training, all parameters increased, whilst no changes occurred following the same exercise without BFR.

In addition to the aforementioned study, superior increases in femoral and brachial artery structure have been observed following knee-extensor exercise training and handgrip exercise training, respectively, when performed with BFR compared to normal blood flow (Christiansen et al., 2020, Hunt et al., 2012). Whilst superior adaptations in resistance vessel structure, assessed via changes in peak reactive hyperaemia, have been observed following low-intensity lower limb resistance training and unilateral plantar-flexion training both with BFR in older and young participants, respectively, compared to matched exercise training without BFR (Shimizu et al., 2016, Patterson and Ferguson, 2010). Finally, calf filtration capacity (an indirect measure of capillarisation) increased by 26% in the leg exposed to BFR (150 mmHg) during 4 weeks of low-intensity resistance exercise, whilst no changes were reported in the non-BFR leg (Evans et al., 2010).

However, it is important to note that other authors have suggested that acute and chronic exercise combined with BFR may have an adverse effect on vascular health, reflected by a decrease in conduit artery FMD (Credeur et al., 2010, Renzi et al., 2010, Paiva et al., 2016). Nevertheless, all of these studies implemented exercise protocols involving a 20-30 min period of ischaemia that is likely to reduce NO

bioavailability and impair vascular function due to significant ROS generation following reperfusion. These protocols are vastly different to the BFR protocols that are commonly employed involving a short period of continuous or intermittent BFR. Thus, the ecological validity of these studies must be considered before the findings are applied to commonly used BFR protocols.

1.12.3 Blood flow restriction and hematopoietic and endothelial progenitor cell mobilisation

In addition to exercise with BFR inducing superior changes in structure and function compared to exercise without BFR, this training technique may also increase baseline progenitor cell number. Kimura et al. (2007) investigated the effect of ischemic preconditioning training, a stimulus very similar to BFR, on endothelial function and endothelial progenitor cell number ($CD34^{+}ACC133^{+}CD45^{low}$ cells) in young men. After exposure to upper limb ischaemia (cuff pressure: 200 mmHg) for 5 min, 6 times a day, for 4 weeks, endothelial progenitor cell number increased in the ischemic group with no change in the control. In addition, forearm blood flow response to acetylcholine increased pre- to post-training in the ischemic group only. The administration of N(G)-monomethyl-L-arginine, a nitric oxide synthase inhibitor, completely abolished this response to acetylcholine, indicating BFR increases the bioavailability of NO which plays an essential role in endothelial progenitor cell mobilisation. Although this study suggests BFR may augment progenitor cell number, investigations are required to determine whether combining this stimulus with exercise training leads to greater improvements in progenitor cell number than exercise training alone.

Although chronic exposure to BFR may improve endogenous repair capacity, the effect of acute exercise with BFR on progenitor cell number remains unclear. Joshi et al. (2020) demonstrated an increase in progenitor cell number ($Lin^{-}CD45^{low}CD34^{+}$)

30 min after 4 sets of unilateral knee-extensor exercise at 10% 1RM with BFR (80% limb occlusion pressure applied via inflation cuff) compared to 30 min of seated rest. However, Montgomery et al. (2019) reported no change in progenitor cell ($CD34^+/CD45^{dim}$, $CD34^+/KDR^+$ and $CD34^+/CD45^{dim}/KDR^+$) number immediately after 4 sets of single leg knee-extensor exercise with BFR (60% occlusion pressure applied via inflation cuff), despite an elevation in $CD34^+/KDR^+$ and $CD34^+/CD45^{dim}/KDR^+$ cells after the same protocol without BFR. Thus, suggesting that the addition of BFR to a single session of resistance exercise may impair exercise-induced progenitor cell mobilisation. The discrepancies between these studies may relate to the different progenitor cell phenotypes that were investigated and/or difference in pressure applied altering the hypoxic stimulus that drives progenitor cell mobilisation. Subsequently, further investigation is required to determine the acute effect of exercise with BFR on progenitor cell number.

1.12.4 Physiological stimuli induced by blood flow restriction

The mechanisms that underpin adaptive responses to aerobic exercise training with BFR are not yet fully understood. However, the reduction in O_2 tension and alterations in shear stress and ROS induced by BFR may mobilise hematopoietic and endothelial progenitor cells and stimulate vascular repair in areas of endothelial damage (Figure 1.10).

1.12.5.1 Haemodynamic response

The external pressure applied to the limb during BFR, mechanically compresses the vasculature underneath, altering the dynamics of blood flow in the limb. Directly underneath the cuff, there is an increase in intramuscular pressure that is exacerbated during muscular contractions (Kacin et al., 2015). This pressure causes the artery to either partially or completely collapse, particularly during diastole, reducing vessel diameter (Mouser et al., 2018). As artery diameter decreases, according to Poiseuille's law (section 1.6), this region of the artery will experience an

increase in shear stress as a greater proportion of blood flow is in contact with the vessel wall, increasing eNOS activation and NO production. In line with this notion, *in vitro*, placement of a cast around a murine carotid artery created a region of high-shear stress that was associated with increased eNOS mRNA expression (Cheng et al., 2005). Elevations in NO production consequent to increased shear-stress during BFR may increase circulating hematopoietic and endothelial progenitor cell levels.

Proximal to the inflated cuff during BFR, the impeded blood flow downstream, causes a reduction laminar shear stress and an increase in retrograde shear stress (Credeur et al., 2010, Thijssen et al., 2009). This consequence of BFR has been demonstrated in the brachial and superior femoral artery of healthy individuals subjected to BFR at rest, with higher cuff pressures leading to greater increases in retrograde shear rate (Schreuder et al., 2014, Thijssen et al., 2009). Acute exposure to an increased volume of retrograde shear stress has been seen to decrease endothelial function and downregulate eNOS expression, indicating endothelial damage (Thijssen et al., 2009, Ziegler et al., 1998). However, these studies increased the volume of retrograde shear stress for ≥30 min. BFR tends to be applied for shorter periods of time (<20 min; Table 1.2), especially when BFR is combined with interval exercise (2-3 min; Table 1.2), likely dampening or even eliminating this response.

Distal to the inflated cuff, there is a region of disturbed blood flow characterised by low and oscillatory shear stress (Chiu and Chien, 2011). The reduction in shear stress and the magnitude of oscillatory shear stress that is experienced by the vessel endothelium underneath the cuff during BFR is pressure-dependent (Mouser et al., 2017, Paiva et al., 2016). Chronic exposure to oscillatory shear stress (>20-30 min) augments the production of ROS, endothelin-1 and adhesion molecules (e.g. VCAM-1), and decreases eNOS expression, inducing endothelial damage and impaired

endothelial function (Jenkins et al., 2013, Laughlin et al., 2008, Rakobowchuk et al., 2013). However, acute exposure to oscillatory shear stress, such as that experienced during exercise with intermittent BFR, may increase shear-stress-mediated release of NO from the endothelium (Green et al., 2005), and therefore, increase hematopoietic and endothelial progenitor cell mobilisation from the bone marrow into the circulation.

Upon release of the cuff, the artery is exposed to a transient increase in shear stress consequent to reactive hyperaemia. Although this response is pressure-dependent, reactive hyperaemia has been reported in the brachial artery following short term exposure (5 min) to cuff pressures as low as 100 mmHg (Takarada et al., 2000). Following exercise with BFR, femoral artery blood flow (area under the curve) remained significantly elevated for at least 1 h post-exercise, highlighting the protracted nature of this shear stress stimulus (Gundermann et al., 2012). Repeated exposure to this increase in shear stress via exercise training is likely to induce an increase in eNOS activity and NO bioavailability, and therefore, induce an increase in baseline hematopoietic and endothelial progenitor cell counts.

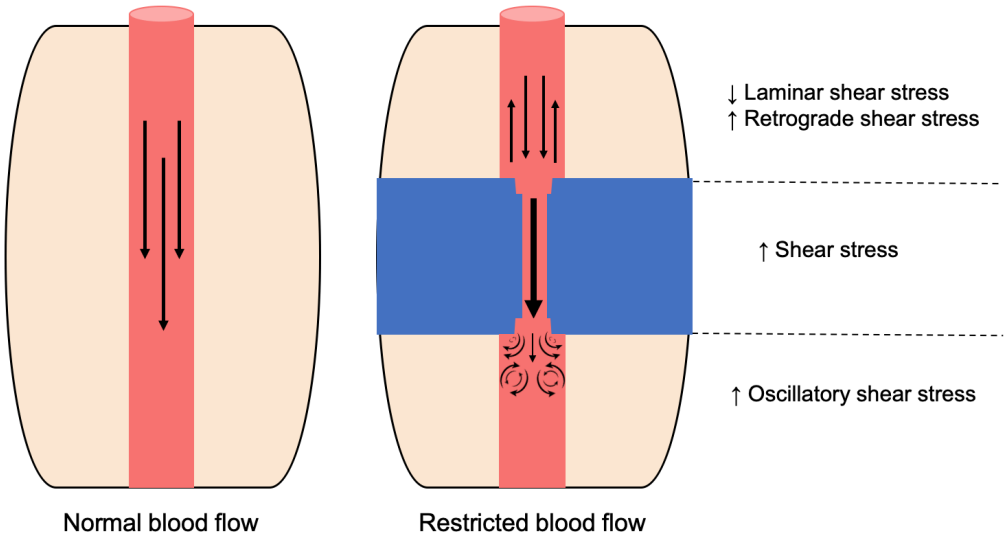

Figure 1.9 Schematic representation of altered haemodynamics during blood flow restriction. On the left, blood flows in a single direction and is parallel to the vessel walls, exposing the endothelium to laminar shear stress. On the right, cuff inflation restricts blood flow, causing a reduction in laminar shear stress and an increase in retrograde shear stress proximal to the cuff. Underneath the cuff, vessel diameter is reduced due to the compression caused by the cuff, creating a region of high shear stress. Distal to the cuff there is an area of low and oscillatory shear stress. Adapted from Cheng et al. (2006).

1.12.5.2 Chemical signalling

Restricted O_2 delivery during BFR induces local muscle hypoxia, represented by a reduction in muscle tissue O_2 saturation when measured using near-infrared spectroscopy (Corvino et al., 2017). This relative deoxygenation inhibits prolyl hydroxylase, leading to an increase in the concentration of hypoxia-inducible factor 1-alpha (HIF-1α) and subsequent transcription of VEGF (Hudlicka and Brown, 2009, Ameln et al., 2005, Egginton, 2008; Figure 1.10). Independent to this pathway, it is possible that the increase in ATP breakdown during exercise with BFR (i.e. increase in adenosine monophosphate [AMP]/ATP ratio) stimulates AMP-activated protein kinase that can promote VEGF transcription through the activation of peroxisome proliferator-activated receptor-γ coactivator 1α (PGC-1α; Figure 1.10; Leick et al., 2009). Mechanisms aside, several studies have reported a greater increase in VEGF

following exercise with BFR compared to the same exercise without BFR (Ferguson et al., 2018, Larkin et al., 2012). Following knee-extensor exercise with BFR (cuff pressure: 80% limb occlusion pressure; ~30% reduction in vastus lateralis muscle O_2 saturation), plasma VEGF concentration increased three-fold compared to resting values (Joshi et al., 2020). This study also demonstrated a four-fold increase in SDF-1α compared to baseline values (Joshi et al., 2020). As previously described (section 1.10.2), VEGF and SDF-1α play an important role in the mobilisation of hematopoietic and endothelial progenitor cells from the bone marrow into the peripheral circulation. As such, greater concentrations of these angiogenic factors are associated with progenitor cell mobilisation (Yamaguchi et al., 2003, Hattori et al., 2001). Thus, it is tempting to speculate that exercise with BFR may increase hematopoietic and endothelial progenitor cell mobilisation compared to exercise without BFR.

1.12.5.3 Reactive oxygen species

In order for ROS to be generated, in addition to a high reductive capacity (high $NADH/NAD^+$), sufficient O_2 is required (Clanton, 2007). Subsequently, ROS formation peaks during the transition to hypoxia, when NADH is rising and O_2 delivery is falling (Clanton, 2007). BFR creates intermittent periods of hypoxia followed by reperfusion, thus, exercise with BFR is likely to facilitate the formation of ROS. In line with this notion, several authors have reported an increase in ROS following acute exercise with BFR compared to the same exercise without BFR (Barili et al., 2018, Centner et al., 2018, Christiansen et al., 2018). The level of ROS detected after exercise with BFR is unlikely to cause cellular damage but may induce the expression of antioxidant enzymes with repeated exposure to this stimulus (i.e. exercise training) resulting in an augmented antioxidant capacity (Gomez-Cabrera et al., 2008, Kojda and Hambrecht, 2005, Centner et al., 2018; Figure 1.10). Indeed, elevated oxidative stress caused by exercise has been demonstrated to upregulate the expression of nuclear factor erythroid 2-related factor 2 (Nfr2); a transcription factor that regulates the transcription of several antioxidant genes, such as, peroxidase-1, superoxide

dismutase and catalase (Gounder et al., 2012, Muthusamy et al., 2012). The upstream signals that regulate Nfr2 include PGC-1α (Wright et al., 2007; Figure 1.10). In support of this mechanism, 6 weeks of cycle interval training, only increased the abundance of antioxidant enzymes, including Cu/Zn-superoxide dismutase (~39%) and glutathione peroxidase-1 (~29%), in the leg trained with BFR (cuff pressure ~180 mmHg), with no changes seen in the non-BFR leg (Christiansen et al., 2019a). This increase in antioxidant capacity helps to maintain vascular homeostasis, the continual balance between vascular damage and repair, by stabilising or deactivating free radicals, preventing oxidative stress induced cellular damage and the rapid inactivation of NO by ROS. The latter, promotes an increase in NO bioavailability that is critical for hematopoietic and endothelial progenitor cell mobilisation (Powers and Jackson, 2008).

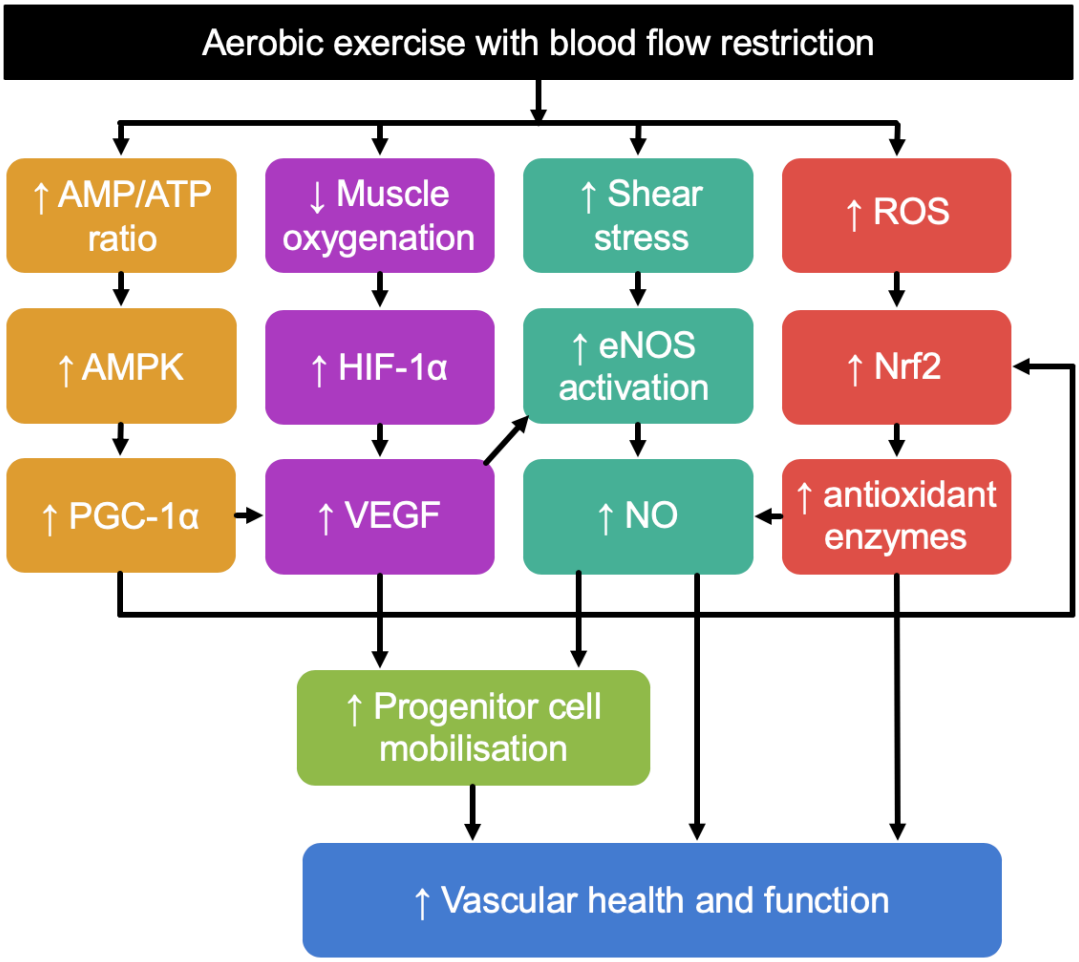

Figure 1.10 The hypothesised effect of aerobic exercise with blood flow restriction on hematopoietic and endothelial progenitor cell mobilisation and vascular health and function. AMPK = adenosine monophosphate activated protein kinase; AMPK = adenosine monophosphate activated protein kinase; ATP = adenosine triphosphate; eNOS = endothelial nitric oxide synthase; HIF-1α = hypoxia-inducible factor 1-alpha; NO = nitric oxide; Nrf2 = nuclear factor erythroid 2-related factor 2; PGC-1α = peroxisome proliferator-activated receptor-γ coactivator 1-alpha; ROS = reactive oxygen species; VEGF = vascular endothelial growth factor.

1.13 Chronic heart failure

As previously discussed in section 1.9, endothelial dysfunction precedes the development of cardiovascular disease; a condition that commonly terminates with CHF. Indeed, CHF represents the final common endpoint of the majority of cardiac conditions; for example, within 5 years of a myocardial infarction ~28% of patients develop CHF (Gerber et al., 2013).

CHF is a complex clinical syndrome, characterised by reduced exercise tolerance in the presence of cardiac dysfunction. Approximately half of CHF patients have heart failure with reduced ejection fraction (HFrEF; left ventricular ejection fraction [LVEF] <40%), whilst the remainder of patients have heart failure with preserved ejection fraction (HFpEF; Bursi et al., 2006). At present, CHF affects approximately 900,000 people in the UK (Rayner et al., 2001) and more than 23 million people worldwide (McMurray and Stewart, 2000). Mortality rates associated with CHF have improved but remain high at 20-30% three years after diagnosis (Meta-analysis Global Group in Chronic Heart Failure, 2012). The treatment cost of CHF in the UK is more than 900 million per annum, of which over 60% is spent on hospital inpatient care (Stewart et al., 2002). CHF accounts for ~2% of all National Health Service inpatient bed days and ~5% of all emergency admissions to hospital (Stewart et al., 2002). Along with the ageing population, improvements in myocardial infarction survival rates are anticipated to cause the number of hospital admissions due to CHF to rise by 50% over the next 25 years (Gale et al., 2011). Thus, CHF remains a national health problem and effective prevention and treatment strategies are of vital importance (Braunwald, 2015). Although the central tenet of HFrEF and HFpEF is a reduction in cardiac output, they are distinct disease phenotypes that are underpinned by different pathophysiological mechanisms and exercise limitations (Poole et al., 2018). The focus of this thesis is on HFrEF only.

1.13.1 Exercise intolerance in HFrEF

Over the last 30 years, the first line treatment for HFrEF patients has shifted from digoxin and diuretics to a battery of therapies (angiotensin-converting enzyme inhibitors, beta-blockers, aldosterone antagonists and cardiac devices) capable of delaying disease progression and prolonging survival (Sacks et al., 2014, Packer et al., 2001, Goldenberg et al., 2014). However, despite these new therapies, disease symptoms still persist and exercise tolerance, a key determinant of quality of life, remains reduced.

$\dot{V}O_{2peak}$ is reduced in HFrEF and forms the basis of the Weber classification of CHF severity. The reduction in $\dot{V}O_{2peak}$ is the strongest predictor of morbidity, mortality and health related quality of life in HFrEF (Kodama et al., 2009, Myers et al., 2002). Indeed, a decrease of 1 $ml \cdot min^{-1} \cdot kg^{-1}$ in $\dot{V}O_{2peak}$ is associated with an approximate 16% increase in the risk of all-cause mortality in HFrEF (Keteyian et al., 2016). Although the Weber classification provides a single set of cut off values, it is important to note that the prognosis associated with a given $\dot{V}O_{2peak}$ is sex dependent: a 10% 1-year mortality rate corresponds to a $\dot{V}O_{2peak}$ of 10.9 and 5.3 $ml \cdot min^{-1} \cdot kg^{-1}$ in men and women, respectively (Keteyian et al., 2016).

$\dot{V}O_{2peak}$ is also strongly predictive of cardiac-related hospitalisations in HFrEF (Arena and Humphrey, 2002, Sarullo et al., 2010). HF-ACTION, a large multicentre clinical trial of exercise training compared to standard care in HFrEF patients, reported that a 6% increase in $\dot{V}O_{2peak}$ was associated with an 8% lower risk of heart failure related hospitalisation (Swank et al., 2012). This study demonstrates the potency of aerobic exercise training to increase $\dot{V}O_{2peak}$ in HFrEF and prevent the downward decline in functional capacity associated with the progression of HFrEF. Understanding the

mechanisms that reduce $\dot{V}O_{2peak}$ in HFrEF is critical to developing exercise strategies that successfully overcome exercise limitations and improve $\dot{V}O_{2peak}$.

1.13.2 Determinants of $\dot{V}O_{2peak}$ in HFrEF

Historically, the reduction in $\dot{V}O_{2peak}$ observed in HFrEF was attributed to central cardiac abnormalities that combine to reduce maximum cardiac output, including chronotropic incompetence and reduced LVEF, reducing convective O_2 transport (Esposito et al., 2010b). However, it is now well established that cardiac function, assessed by LVEF, is poorly related to $\dot{V}O_{2peak}$ in HFrEF (Figure 1.11), and is not the sole reason for the reduced $\dot{V}O_{2peak}$ (Witte et al., 2004, Franciosa et al., 1981).

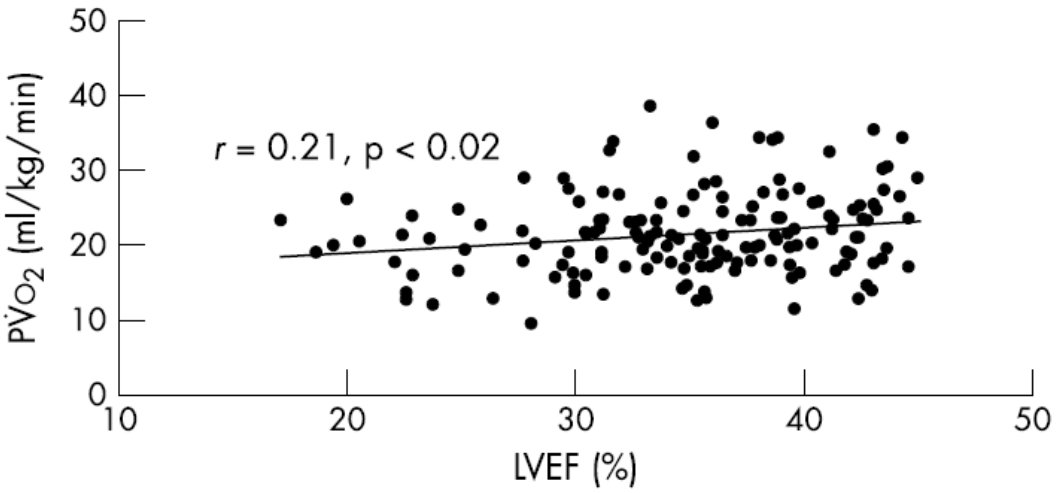

Figure 1.11 Relationship between $\dot{V}O_{2peak}$ and LVEF in HFrEF patients. Taken from Witte et al. (2004).

The lack of an immediate clinical improvement after transplant and/or therapies that increase cardiac output and/or decrease capillary wedge pressure support the hypothesis that other systems contribute to reduced $\dot{V}O_{2peak}$ in HFrEF (Rubin et al., 1979, Pickworth, 1992, Mettauer et al., 1996, Williams and McKenna, 2012). Indeed, although HFrEF is triggered by a failing cardiac pump (whether due to coronary artery disease causing a myocardial infarction or other aetiology, i.e. cardiomyopathy), it is characterised by the activation of several compensatory mechanisms that affect all

levels of the O_2 transport and utilisation cascade (Piepoli et al., 2010, Poole et al., 2012). These compensatory mechanisms attempt to preserve cardiac output, blood pressure and organ perfusion when the capacity to generate cardiac output is reduced due to the failing heart (Piepoli et al., 2010, Poole et al., 2012). These adaptations, that are stimulated by reduced blood pressure, include increased activation of the renin-angiotensin-aldosterone pathway (leading to increased water and salt retention) to maintain cardiac output and increased sympathetically-mediated vasoconstriction to maintain blood pressure and tissue perfusion (Piepoli et al., 2010, Poole et al., 2012).

However, chronic stimulation of these compensatory mechanisms drives a negative chain of events that leads to peripheral maladaptations (Conraads et al., 2013, Piepoli et al., 2010, Poole et al., 2012). These effects are despite optimal HFrEF management which includes contemporary therapies to modulate the activation of neurohormonal pathways (e.g. beta-blockers and angiotensin converting enzyme inhibitors).

Vascular dysfunction has emerged as a common pathophysiological pathway that contributes to the development and propagation of HFrEF (Bauersachs and Widder, 2008). Specifically, with regards to the heart, via the basic mechanisms discussed above that increase vascular damage and decrease vascular repair (section 1.8), vascular dysfunction reduces the vasodilatory capacity of the coronary arteries, thus contributing towards reduced myocardial perfusion (Bauersachs and Widder, 2008). This induces altered cardiomyocyte metabolism, apoptosis, and mitochondrial damage, leading in impaired cardiac function as a consequence of the reduction in peak cardiac output (Braunwald and Bristow, 2000, Benjamin and Schneider, 2005). In addition, increased peripheral resistance elevates ventricular afterload

(Bauersachs and Widder, 2008). This increases cardiac workload (i.e. the failing heart must work harder to generate the same cardiac output), setting the stage for further reductions in cardiac function that reduce peak convective O_2 delivery.

In addition to central cardiac vascular dysfunction there is also peripheral vascular dysfunction, which is both a precursor and consequence of HFrEF and is involved in propagating disease severity (Marti et al., 2012, Vita, 2005, Bank et al., 2000, Drexler, 1998). At the proximal end of the O_2 transport and utilisation cascade, pulmonary hypertension, consequent to increased sympathetic nervous activity, can lead to alveolar-capillary injury (Piepoli et al., 2010). This reduces the anatomical integrity and functional property of the lung capillaries and alveolar spaces, resulting in impaired gas exchange and a decrease in diffusive O_2 transport at the lung (i.e. hypoxaemia), reducing convective O_2 transport (Piepoli et al., 2010). In addition, patients with HFrEF often develop mild ventilation/perfusion abnormalities, caused by increased pressure in the vasculature increasing blood flow to the top of the lung where ventilation is poor (Clark et al., 1995). Together with increased lung stiffness caused by emphysema and chronic hyperventilation driven by increased stimulation of peripheral chemoreceptors (carotid bodies), the ventilation/perfusion abnormalities in HFrEF, increase the work of breathing (Cross et al., 2020, Stickland et al., 2007, Olson et al., 2010). This is supported by an increase in ventilation with respect to CO_2 output (high $\dot{V}_E/\dot{V}CO_2$) in HFrEF (Clark et al., 1992, Wasserman et al., 1997), with $\dot{V}_E/\dot{V}CO_2$ also shown to be strongly and independently prognostic (Guazzi et al., 2005). The increased ventilatory requirement observed in HFrEF (high $\dot{V}_E/\dot{V}CO_2$) may lead to the respiratory muscles requiring a greater proportion of the already reduced available cardiac output, thereby further comprising convective skeletal muscle O_2 delivery during exercise (Harms et al., 1997). In the peripheral vascular system, increased activation of the sympathetic nervous system and pro-inflammatory changes, such as increased oxidative stress, reduce NO bioavailability, causing

vasoconstriction (Bauersachs and Widder, 2008, Zelis et al., 1981, Vanhoutte, 1983). In addition, humoral mediators, including elevations in circulating angiotensin, norepinephrine, endothelin-1, and vasopressin (Teerlink, 2005), as well as, increased intravascular sodium and water retention (Zelis et al., 1988a), increase peripheral resistance in HFrEF (Poole et al., 2012). Although these mechanisms are active at rest, the impact of these mechanisms is seen during exercise: increased peripheral vascular resistance impairs blood flow distribution during exercise, limiting convective O_2 transport. The presence of vascular dysfunction in HFrEF is supported by studies documenting reduced FMD in response to reactive hyperaemia in individuals with HFrEF compared to healthy controls (Patel et al., 2001, Giannattasio et al., 2001, Gori et al., 2010). Due to the pathophysiological consequences of HFrEF (described in detail in section 1.13.3), the degree of vascular dysfunction measured in HFrEF is greater than the magnitude of endothelial dysfunction that occurs with ageing alone (Drexler et al., 1992a, Landmesser et al., 2002, Kubo et al., 1991). In addition, a reduction in capillarisation and the percentage of flowing capillaries in HFrEF decreases O_2 delivery to the capillary-myocyte interface (Hirai et al., 2015, Kindig et al., 1999, Poole et al., 2012). This reduces the microvascular PO_2 gradient that drives O_2 into the mitochondria for use in oxidative metabolism. Collectively, these impairments caused by peripherical vascular dysfunction adversely affect both convective and diffusive O_2 delivery.

Maladaptations in the skeletal muscle, such as, reductions in mitochondrial volume density and enzyme activity, as well as mitochondrial dysfunction also reduce oxidative metabolism in HFrEF, increasing the generation of ROS and impairing diffusive O_2 transport (Mancini et al., 1992, Drexler et al., 1992b, Esposito et al., 2010b). Indeed, rapid depletion of muscle phosphocreatine during exercise and slow replenishment after exercise in HFrEF was reported in a study conducted by Mancini et al. (1992) using ^{31}P magnetic resonance spectroscopy. Due to the reduced

oxidative metabolism, blood lactate, a marker of metabolic acidosis, exceeds a critical limit (i.e. lactate threshold) at a low work rate in HFrEF. After the lactate threshold has been surpassed, $\dot{V}_E$ for a given work rate is increased, increasing the ventilatory demand of the exercise and the blood flow (i.e. O_2 delivery) needed by the respiratory muscles. This causes an additional reduction in the blood flow available to the contracting muscles, thus, reducing convective O_2 transport. The impairments caused by peripheral vascular dysfunction and skeletal muscle dysfunction in HFrEF compromise both convective and diffusive O_2 delivery to differing degrees depending on disease severity with these interacting to determine the reduction in $\dot{V}O_{2peak}$ in HFrEF (Figure 1.12). Thus, vascular dysfunction represents a unifying feature that drives reductions in $\dot{V}O_{2peak}$, with these reductions manifesting as symptoms of exercise intolerance in individuals with HFrEF and increasing morbidity and mortality risk.

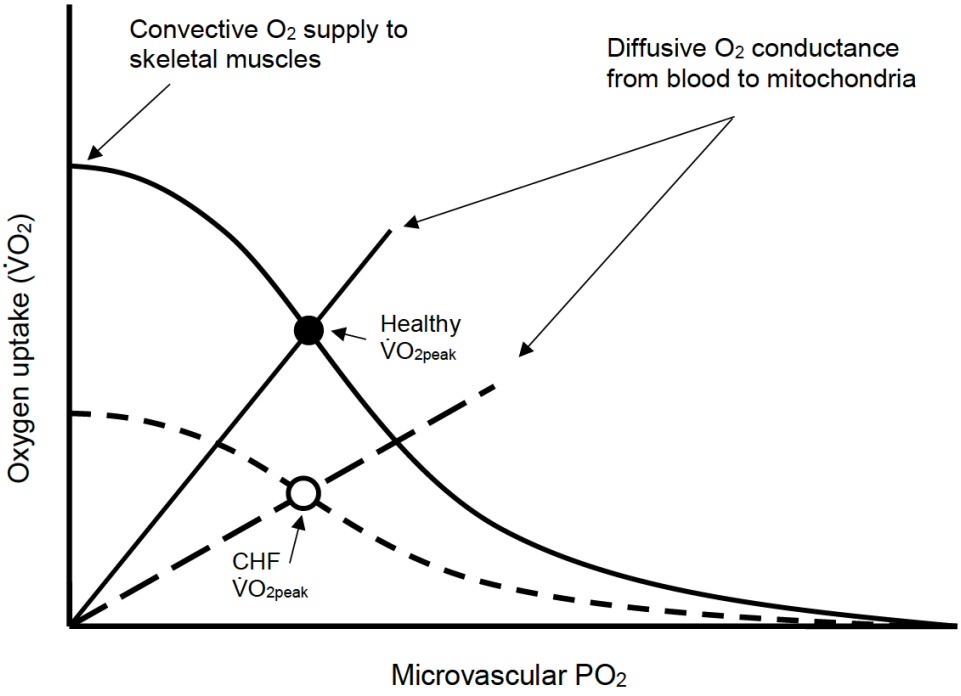

Figure 1.12 Convective (curved lines) and diffusive (straight lines from origin) components of O_2 transport that interact to determine $\dot{V}O_{2peak}$ in health (solid lines) and in HFrEF (dashed lines). Black circle represents $\dot{V}O_{2peak}$ of healthy individuals. Open circle represents $\dot{V}O_{2peak}$ in HFrEF. Note how both convective and diffusive components combine to reduce $\dot{V}O_{2peak}$ in HFrEF. Adapted from (Wagner, 1996).

1.13.3 Endothelial dysfunction in HFrEF

In addition to the neuro-hormonal mechanisms of vascular dysfunction discussed above, the balance between endothelial damage and endogenous repair mechanisms is also compromised in HFrEF (Ross, 1993). As previously discussed (section 1.8 and 1.9), NO is central to maintaining vascular homeostasis. Although it remains unclear whether the basal release of NO is decreased, preserved, or even increased, in HFrEF during resting conditions, NO production in response to stimulation is reduced in HFrEF (Mohri et al., 1997, Drexler et al., 1993). This includes NO production in response to hormonal agonists (e.g. acetylcholine) and shear-stress, with the latter resulting in reduced vasodilation during exercise (Drexler et al., 1993, Katz et al., 1999). In line with this, impaired NO-mediated vasodilation during

submaximal exercise (handgrip exercise) has been reported in the forearm circulation of patients with HFrEF (Katz et al., 1996). In part, this reduction in NO production may be consequent to lower production of eNOS which has been reported in two different experimental models of HFrEF (Smith et al., 1996, Comini et al., 1996).

The shear stress stimulus during exercise is also reduced in HFrEF, further attenuating NO production. This is because impaired cardiac function reduces maximum $\dot{Q}$ during exercise, reducing blood flow through the peripheral arteries as the body balances the competing demands between the working skeletal muscle for more blood flow with the need to preserve organ perfusion and maintain blood pressure (Bauersachs and Widder, 2008). This reduces the shear exerted on the luminal surface of the endothelium in the peripheral arteries during exercise, resulting in a decrease in eNOS activation and NO production compared to healthy individuals (Bauersachs and Widder, 2008).

Elevated levels of ROS also increase endothelial damage in HFrEF, promoting a state of endothelial dysfunction (Bauersachs and Widder, 2008). The primary sources of ROS in HFrEF include uncoupled eNOS (refer to section 1.8), xanthine oxidase, NADPH oxidase and the electron transport chain (Dixon et al., 2003, Bauersachs and Widder, 2008). ROS, particularly superoxide anions, decrease the bioavailability of NO by decreasing the activity eNOS and by rapidly reacting with NO to form the strong oxidant peroxynitrite (section 1.8; Bauersachs and Widder, 2008). Excess ROS has also been documented to increase mitochondrial DNA damage, reduce mitochondrial RNA transcription, inhibit mitochondrial protein synthesis, reduce cellular adenosine triphosphate and alter redox function in *in vitro* experiments involving human aortic smooth muscle cells (Ballinger et al., 2000).

These maladaptations impair mitochondrial function, affecting smooth muscle cell function (Ballinger et al., 2000). Thus, in addition to causing impaired endothelial function, increases in ROS induce vascular smooth muscle dysfunction causing further reductions in vascular function that are likely to reduce convective O_2 transport, with negative consequences for exercise tolerance.

For many HFrEF patients, vascular dysfunction is present prior to HFrEF diagnosis and leads to the development of this complex multi-organ syndrome (section 1.13.2). Thus, in many HFrEF patients, vascular dysfunction is not only the unifying feature that drives reductions in exercise tolerance, but it is the common origin for impairments in O_2 delivery. Indeed, vascular dysfunction initiates a sequence of events that affects the O_2 delivery cascade at all levels, from cellular signalling pathways to whole-body systems. Therefore, if the balance between endothelial damage and repair can be maintained and endothelial dysfunction limited, convective O_2 transport, and therefore exercise tolerance may be preserved and HFrEF disease progression attenuated.

1.13.4 Hematopoietic and endothelial progenitor cell number in HFrEF

In various disease states, including HFrEF, the number of circulating $CD34^+$ and $CD34^+/KDR^+$ progenitor cells is reduced (Samman Tahhan et al., 2017). Compared to referent controls, the number of circulating $CD34^+/KDR^+$ cells in younger (>55 y) and older (>65 y) HFrEF patients was reduced by 40 and 45%, respectively (Sandri et al., 2016). The magnitude of reduction in circulating $CD34^+/KDR^+$ number also correlates with HFrEF disease severity (assessed by New York Heart Association [NYHA] classification), with more than a three-fold reduction in circulating $CD34^+/KDR^+$ cells in patients with advanced symptoms (Samman Tahhan et al., 2017). Valgimigli et al. (2004) reported a similar model of circulating $CD34^+$ cell behaviour, with higher levels of circulating $CD34^+$ cells documented in early stages

of HFrEF and lower levels in more advanced HFrEF. It is tempting to speculate that the increase in $CD34^+$ cells during early HFrEF represents a 'repair response' to the diffuse endothelial damage in HFrEF. However, in contrast to these results, Van Craenenbroeck et al. (2010a) reported a ~60% reduction in circulating $CD34^+$ cells in patients with both mild and severe HFrEF compared to healthy controls, suggesting $CD34^+$ number is equally impaired during all stages of the disease. Interestingly, the aetiology of CHF does not appear to influence the number of circulating progenitor cells, indicating that the clinical state of the patient may be the dominant factor that influences progenitor cells (Michowitz et al., 2007, Valgimigli et al., 2004). Reduced hematopoietic and endothelial progenitor cell number in HFrEF indicates an impaired endogenous repair capacity in this patient population that is likely to affect endothelium function by negatively impacting the balance between endothelial damage and repair mechanisms.

The functional capacity, including the migratory capacity and proliferative potential, of cultured endothelial progenitor cells is also impaired in HFrEF compared to controls (Sandri et al., 2016, Heeschen et al., 2004). This dysfunction conflates with low circulating progenitor levels to reduce endogenous repair capacity in individuals with HFrEF. However, whilst efforts should be made to understand progenitor cell dysfunction in HFrEF in order to enhance endogenous repair capacity and maintain vascular health in this patient population, the focus of this thesis is on hematopoietic and endothelial progenitor cell number due to their use as disease biomarkers.

The quantitative deficit in circulating progenitor cells in HFrEF is an independent predictor of morbidity and mortality. Prior to a cardiovascular disease diagnosis, reduced $CD34^+/KDR^+$ progenitor cell number is an independent predictor of early subclinical atherosclerosis in healthy individuals (Fadini et al., 2006). Following

disease progression, circulating $CD34^+/KDR^+$ cell number inversely correlates with the risk of adverse cardiovascular events and is an independent predictor of poor prognosis in coronary artery disease patients, even after traditional cardiovascular disease risk factors and disease severity have been taken into account (Werner et al., 2005, Schmidt-Lucke et al., 2005). Moreover, $CD34^+$ number independently predicts all-cause mortality in HFrEF. Individuals with CHF with a low $CD34^+$ count have a 1.8-fold increased risk of mortality compared to those with a higher $CD34^+$ count (Samman Tahhan et al., 2017). The link between progenitor cell counts and clinical outcomes supports the role of progenitor cells as disease biomarkers. Further, it supports therapeutic efforts to increase progenitor cell number to maintain vascular health and improve patient prognosis.

1.13.5 Mechanisms for reduced circulating hematopoietic and endothelial progenitor cell number in HFrEF

The reduction in the number of hematopoietic and endothelial progenitor cells quantified in the peripheral blood of HFrEF patients may be due to several different causes: exhaustion of the pool of progenitor cells in the bone marrow, impaired progenitor cell mobilisation, early progenitor cell death in the circulation and/or a high rate of progenitor cell utilisation.

HFrEF is associated with bone marrow dysfunction (Westenbrink et al., 2010). Iversen et al. (2002) reported a reduction of up to 60% of $CD34^+$ cells in the bone marrow of mice with HFrEF. Whereas, bone marrow taken from the sternum of HFrEF patients during cardiac surgery contained ~50% less $CD34^+$ cells compared to controls (Westenbrink et al., 2010). Therefore, the reduction in circulating hematopoietic and endothelial progenitor cells in HFrEF may be a proportional reflection of the bone marrow content.

Defective mobilisation also contributes to the low numbers of circulating progenitor cells in HFrEF. As previously mentioned (section 1.10.2), for progenitor cell mobilisation to occur, the activation of eNOS is required to activate MMP-9 in the bone marrow niche. However, uncoupled eNOS and reduced eNOS expression and phosphorylation are key features of HFrEF. In line with this, it is conceivable that the number of circulating hematopoietic and endothelial progenitor cells in HFrEF may be reduced due to impaired NO-mediated progenitor cell mobilisation.

Impaired progenitor cell mobilisation in HFrEF has also been linked to increased serum concentrations of TNF-α exerting a suppressive effect on haemopoiesis. Indeed, *in vitro* experiments suggest that TNF-α markedly inhibits the growth of bone marrow $CD34^+$ haemopoietic stem cells and down-regulates CXCR4 expression on endothelial cells (Feil and Augustin, 1998, Hu et al., 1999). However, there is no correlation between TNF-α concentration and the number or function of progenitor cells in HFrEF, suggesting TNF-α is unlikely to play a major role in progenitor cell dysfunction in this clinical population (Nollet et al., 2016).

Increased sympathetic activity in HFrEF has also been postulated to impair the mobilisation of various progenitor cell populations (Berezin and Kremzer, 2014). Murine models have demonstrated that the sympathetic nervous system regulates progenitor cell mobilisation in response to granulocyte colony-stimulating factor and ischaemia, with norepinephrine treatments inducing progenitor cell mobilisation in norepinephrine deficit mice (Katayama et al., 2006, Récalde et al., 2012). The mobilisation of progenitor cells in response to catecholamines also appears to be dependent on eNOS-related pathways (Récalde et al., 2012). However, a mechanistic link between increased sympathetic activity and impaired progenitor cell mobilisation in HFrEF is yet to be established.

1.13.6 Hematopoietic and endothelial progenitor cell response to a single session of exercise in HFrEF

In contrast to healthy individuals (discussed in section 1.10.4.1), exercise-induced progenitor cell mobilisation appears to be severely attenuated in individuals with HFrEF. Van Craenenbroeck and co-workers have consistently showed no significant increase in $CD34^+/KDR^+$ number immediately after a symptom-limited cardiopulmonary exercise test in HFrEF, despite elevations occurring in younger and older healthy controls (Van Craenenbroeck et al., 2011, Van Craenenbroeck et al., 2010a, Van Craenenbroeck et al., 2010b). The majority of these investigations also reported no significant increase in $CD34^+$ number pre- to post-exercise (Van Craenenbroeck et al., 2010a, Van Craenenbroeck et al., 2010b). In line with these results, Carvalho et al. (2009) collected a blood sample from HFrEF patients during a cardiopulmonary exercise test at peak effort and reported no increase in $CD34^+$ number compared to resting pre-exercise levels. To rule out the possibility that exercise-induced progenitor cell mobilisation is delayed in HFrEF rather than severely reduced, Van Craenenbroeck et al. (2011) collected multiple blood samples between 30 min and 48 h after a cardiopulmonary exercise test. A small but insignificant increase in $CD34^+/KDR^+$ number was reported immediately post-exercise; however, no significant increases were observed within 48 h time period, leading the authors to conclude that progenitor cell mobilisation is not delayed in HFrEF but severely attenuated. However, in contrast to these results, Kourek et al. (2020) reported an increase in $CD34^+/CD45^-/CD133^+$, $CD34^+/CD45^+/CD133^+/KDR^+$ and $CD34^+/CD133^+/KDR^+$ cells, immediately after a cardiopulmonary exercise test in 49 HFrEF patients. Given that an identical exercise stimulus was provided, the discrepancy between these results likely results from the different progenitor cell subpopulations that were investigated.

Together, these studies suggest that a single session of aerobic exercise does not induce a transient increase in progenitor cell number in HFrEF, and therefore, does not positively impact endogenous repair capacity as seen in healthy individuals. Nevertheless, it is unknown whether this acute response to exercise can be restored in HFrEF by employing a more effective exercise strategy that provides a greater stimulus for exercise-induced progenitor cell mobilisation or by exercise training.

1.13.7 Hematopoietic and endothelial progenitor cell response to exercise training in HFrEF

In contrast to acute exercise, repeated exposure to exercise appears to increase the number of baseline progenitor cells in HFrEF. Thus, exercise training represents an opportunity to enhance vascular endogenous repair capacity in this patient population, resulting in improved vascular health and thus, improved convective O_2 delivery to the working skeletal muscle. Evidence of the effect exercise training has on baseline progenitor cell number in HFrEF is summarised in Table 1.3.

Increases in $CD34^+/KDR^+$ progenitor cell number ranging between 66-86% have been identified after 3 weeks to 6 months of high-intensity continuous exercise training in HFrEF (Sandri et al., 2016, Gatta et al., 2012, Van Craenenbroeck et al., 2010b). A significant rise in $CD45^{dim}/CD34^+/KDR^+$ number (98-115%) was also observed following 3 months of light-to-moderate aerobic exercise training in HFrEF (Eleuteri et al., 2013, Mezzani et al., 2013), indicating that interval and continuous exercise strategies can be employed to increase circulating progenitor cell number in HFrEF. However, the majority of the effective exercise strategies in Table 1.3 require patients to exercise >3 times per week, potentially compromising the feasibility of these interventions in real-world rehabilitation settings. For example, at present, funding for cardiac rehabilitation in England allows for only 2 exercise sessions per week.

The difference in the magnitude of the progenitor cell responses in Table 1.3 is likely due to the heterogeneity in exercise protocols, specific cell populations that were investigated and the experimental procedures used to enumerate the cell populations. Comparisons between study results are often inappropriate, due to variations in the experimental procedures and the gating strategies used to interpret the flow cytometric events (Van Craenenbroeck et al., 2008a). Nevertheless, the studies summarised in Table 1.3 demonstrate that circulating hematopoietic and endothelial progenitor cell number is not fixed and can be modified using exercise training in HFrEF.

Table 1.3 Hematopoietic and endothelial progenitor cell responses to exercise training in HFrEF

Study	*n*	Participants	Duration/frequency	Training Protocol	Results	
Sarto et al. (2007)	22	HFrEF patients (LVEF:31%; 61 ± 2 y)	8 weeks/ 3 times per week	- Supervised cycle exercise - 55 min at 60% HRR	- $CD34^+/KDR^+$ increased (+251%)	↑
Erbs et al. (2010)	18	HFrEF patients (LVEF: 24%; 61 ± 8y)	12 weeks: week 1-3: 3-6 times a day in hospital. week 4-12: daily, home-based.	- Cycle exercise - Week 1-3: 5-20 min at 50% $\dot{V}O_{2peak}$ - Week 4-12: 20-30 min at 60% $\dot{V}O_{2peak,}$ with 1 x 60 min supervised group session	- $CD34^+$ increased (+33%) - $CD34^+/KDR^+$ increased (+83%)	↑
Van Craenenbroeck et al. (2010b)	21	HFrEF patients (LVEF: 27%; 61 ± 2y)	6 months/3 times per week	- Aerobic exercise - 60 min at 90% of HR at RC - Dynamic resistance exercises	- $CD34^+/KDR^+$ increased but change was not significant compared to untrained control - $CD34^+$ remained unchanged	↑ =
Gatta et al. (2012)	14	HFrEF patients (LVEF: 34%; 72 ± 11y)	3 weeks/2 times a day on 6 days/week	- Cycle exercise - 30 min at 75-85% of HR_{max} - Plus calisthenics	- $CD34^+/KDR^+$ increased (+80%)	↑
Eleuteri et al. (2013)	11	HFrEF patients (LVEF: 28%; 66 ± 2 y)	3 months/5 times per week	- Cycle exercise - 30 min at ventilatory threshold	- $CD45^{dim}/CD34^+/KDR^+$ increased (+115%) - No change in control group	↑

Mezzani et al. (2013)	15	HFrEF patients (LVEF: 28%; 65±7 7y)	3 months/5 times a week	- Cycle exercise - 30 min at ventilatory threshold	- $CD45^{dim}/CD34^{+}/KDR^{+}$ increased (+98%) - No change in control group	↑
Sandri et al. (2016)	30 30	HFrEF young (LVEF: <40%; ≤55 y) HFrEF older (LVEF: <40%; ≥65 y)	4 weeks/4 times a day on 5 days a week	- Cycle exercise -15-20 min at 70% $\dot{V}O_{2peak}$ - Plus 1 x 60 min aerobic group session per week	- $CD34^{+}/KDR^{+}$ increased (young: +127%; older: +129%) - $CD133^{+}/KDR^{+}$ increased (young: +135%; older: +133%) - No change in control group	↑

↑ = increase pre- to post-training; ↓ = decrease pre- to post-training; = = no change pre- to post-training. CAD = coronary artery disease; HFrEF = heart failure with reduced ejection fraction; HR = heart rate; HR_{max} = maximum heart rate; HRR = heart rate reserve; LVEF = left ventricular ejection fraction; RC = respiratory compensation; $\dot{V}O_{2peak}$ = peak oxygen uptake; WR_{peak} = peak work rate from ramp-incremental exercise test.

1.13.8 Blood flow restriction training in HFrEF

Aerobic exercise training combined with BFR may augment training adaptations and lead to superior improvements in vascular health, exercise tolerance and $\dot{V}O_{2peak}$ than the same exercise without BFR in health (previously described in section 1.12). Several studies have demonstrated that HIIT is well tolerated in HFrEF and can increase vascular function and exercise tolerance (Ramos et al., 2015, Wisløff et al., 2007, Ellingsen et al., 2017). Combining HIIT with BFR may increase the stimulus for adaptation, increasing the benefits of exercise training in HFrEF. A single session of HIIT with BFR may evoke a short-term increase in progenitor cell number, whilst HIIT exercise training with BFR may increase baseline progenitor cell number and lead to a greater improvement in $\dot{V}O_{2peak}$ through additional increases in peripheral vascular shear stress, decreases in muscle oxygenation and increases in the release of angiogenic factors (section 1.12.4). However, HIIT with BFR is yet to be investigated in HFrEF; therefore, it remains unknown whether this mode of training is feasible and effective in this clinical population.

1.14 Thesis aims

An important step in developing effective interventions to improve $\dot{V}O_{2peak}$ in both health and disease is understanding the mechanisms that limit dynamic whole-body exercise in which $\dot{V}O_{2peak}$ is attained. Therefore, the first aim of this thesis was:

- To investigate the mechanisms that induce exercise intolerance during ramp-incremental exercise in health (Chapter 3).

From the information in the preceding literature review, it is clear that the addition of BFR to aerobic exercise training can induce greater adaptations in the peripheral vasculature and increases in $\dot{V}O_{2peak}$ in health than matched exercise without BFR. Further, a single session of aerobic exercise can induce a transient increase in progenitor cell number in health, with exercise training increasing baseline progenitor cell number. In HFrEF, although exercise training can increase baseline progenitor cell number, the normal transient response to a single session of aerobic exercise seen in healthy participants is absent. However, it is unknown whether a single session of HIIT with or without BFR can evoke a transient increase in hematopoietic and endothelial progenitor cell number pre- to post-exercise in HFrEF, or whether BFR can increase the adaptive responses derived from HIIT in HFrEF, leading to a greater increase in baseline hematopoietic and endothelial progenitor cell number. Therefore, the second aim of this thesis was:

- To investigate whether HIIT with BFR is feasible in HFrEF and determine whether 4 weeks of HIIT with BFR leads to greater improvements in vascular endogenous repair capacity (hematopoietic and endothelial progenitor cell number), exercise tolerance and $\dot{V}O_{2peak}$ than HIIT alone. Further, to determine whether a single bout of HIIT with or without BFR increases hematopoietic and endothelial progenitor cell number in HFrEF in an untrained and/or trained state (Chapter 4).

As discussed, a single session of aerobic exercise can induce a transient increase in hematopoietic and endothelial progenitor cell counts, and exercise training can lead to a sustained increase in baseline progenitor cell numbers in health. However, the optimal exercise strategy for inducing these increases is unknown. HIIT increases vascular function and $\dot{V}O_{2peak}$ at least as well as traditional constant work rate exercise; however, it is unknown how the specific characteristics of HIIT (e.g. work rate, work:recovery ratio and exercise intensity) interact to influence acute and chronic vascular adaptations, limiting our understanding of how to personalise exercise therapy to maximise impact. Therefore, the final aim of this thesis was:

- To determine if 6 weeks of HIIT with a high-work rate that maximises the volume of shear stress that is accumulated, and time at peak shear, leads to a greater increase in vascular function (FMD), endogenous repair capacity (hematopoietic and endothelial progenitor cell number) and $\dot{V}O_{2peak}$ than intensity-matched constant work rate exercise in young healthy individuals. To investigate hematopoietic and endothelial progenitor cell responses to a single session of HIIT with a high work rate and intensity-matched constant work rate exercise pre- and post-training to determine if these exercise strategies increase circulating progenitor cell numbers in health, or if this response is absence, whether repeated exposure to the exercise strategies (i.e. exercise training), can induce this response (Chapter 5).

Chapter 2 General Methods

2.1 Recruitment

2.1.1 Healthy participants

Participants were recruited through word of mouth, study posters and recruitment emails that were distributed across the University. Each study was ethical approved by the Faculty of Biological Sciences ethics Committee, in line with the declaration of Helsinki. Healthy participant status and suitability was confirmed using a medical questionnaire, and all participants provided written informed consent. Specific study inclusion and exclusion criteria can be found in each experimental chapter.

2.1.2 Chronic heart failure participants

Participants with HFrEF were recruited for the Blood Flow Restriction training study (Chapter 4). This study was ethically approved by the Yorkshire and the Humber Leeds East Research NHS Ethics Committee. All HFrEF participants were recruited from Leeds Teaching Hospitals NHS Trust, specifically Leeds General Infirmary Heart Failure Clinic. All potential participants were identified by a member of the study team and given a patient information sheet. Potential participants were given the opportunity to ask questions before they decided whether or not they would like to take part in the study. Study eligibility criteria can be viewed in full in Chapter 4, along with inclusion/ exclusion criteria and participant characteristics. All HFrEF participants provided written informed consent. After study completion or following study exclusion or withdrawal, all HFrEF participants returned to standard of care treatment.

2.2 Cycle ergometry

All exercise tests were performed on an upright electromagnetically braked computer-controlled cycle ergometer (Excalibur Sport PFM, Lode BV, Groningen, NL). The minimum and maximum continuous work rate (W; also referred to as power

output) on this ergometer is 8 and 1500 W, respectively. The accuracy of work rates on this ergometer is 2% when work rates are 100-1500 W and cadence is 25-180 revolutions per minute (rpm) according to the manufacturer's specifications. The ergometer was calibrated typically once every 2 years, including a dynamic calibration, by Cranlea Human Performance Ltd to ensure that these specifications were maintained. The last calibration (July 2017) reported an actual measurement error well within the manufacturer's specifications (2%) of 0.74% and 0.17% for power and cadence, respectively. Occasionally, training sessions without concomitant measures (e.g. pulmonary gas exchange) in Chapter 4 and 5 were performed on a different electromagnetically braked cycle ergometer (Corival cpet, Lode BV, Groningen, NL). This ergometer was also calibrated typically annually to ensure that it was working within the manufacturer's specifications (work rate accuracy of 3% when work rate is between 100-500 W and cadence is 30-150 rpm). Both cycle ergometers were interfaced with Lode Ergometer Manager that was used to pre-programme and control the exercise protocols. The saddle (height, angle and horizontal position) and handlebar (height and horizontal position) of both ergometers was adjusted and optimised for each participant; this information was digitally recorded, and settings were used for all subsequent visits.

2.2.1 Ergometer cycling modes

Two cycling modes were used in all study chapters: a hyperbolic mode (cadence-independent) and an isokinetic mode (cadence-dependent).

2.2.1.1 Hyperbolic cycling

When operating in the hyperbolic mode, a specific (programmed) work rate is maintained independently of the participant's cadence. The programmed power is achieved, and then maintained in this mode via a feedback loop that exists in the ergometer; the ergometer continuously measures cadence on a pedal-by-pedal stroke basis and appropriate adjustments are made in electromagnetic brake force to maintain the required power (e.g. electromagnetic brake force increases when

cadence decreases, and electromagnetic brake force decreases when cadence increases to maintain a constant power). Although this feedback loop ensures that the mean power generated by the participant is equal to the programmed power, the small changes in power and cadence produced by the participant creates a natural fluctuation in pedal-by-pedal stroke power. The natural fluctuation in power that occurs during hyperbolic cycling is discussed in detail in section 2.7.1.3. The hyperbolic cycling mode was used during all ramp-incremental exercise tests, constant work rate exercise tests and during interval and constant work rate exercise training protocols.

2.2.1.2 Isokinetic cycling

The Lode Excalibur ergometer used in this thesis was capable of transitioning from hyperbolic cycling (cadence-independent) to isokinetic cycling (cadence-dependent) modes almost instantaneously (<1 s), permitting the measurement of maximum voluntary isokinetic power (MVIP). During the isokinetic cycling mode, electromagnetic braking force is used to fix cadence at a predetermined number of revolutions per minute. To ensure cadence is controlled correctly (i.e. electromagnetic brake force is applied appropriately) in this mode, a continuous feedback loop is employed.

During isokinetic cycling, torque (Nm) was measured by strain gauge force transducers in the bottom bracket spindle. Left and right torque were measured independently. The strain gauges in this system were capable of measuring 2000 N, with a <0.5 N resolution and measurement uncertainty of <3% (manufacturers specifications). Before every study visit involving the ergometer, a zero-force adjustment was performed to calibrate the strain gauges. To eliminate the effect of gravity on the strain gauges during this calibration the left and right pedal were positioned at 0° and 180°, respectively. Concurrent to the strain gauge

measurements, angular velocity (rad.s^{-1}) was measured by three independent optical sensors sampling in succession. Housed in the bottom bracket assembly, these sensors have a measurement uncertainty of <1% (manufacturers specifications). Torque and angular velocity measurements were mutually sampled every 2° of angular rotation to permit the calculation of left and right crank power (crank power = torque [Nm] x angular velocity [rad.s^{-1}]). Torque and angular velocity measurements were converted into a digital form and stored on Lode Ergometer Manager (software provided by the ergometer manufacturer) ready to export for later analyses.

2.3 Pulmonary gas exchange

The following gas exchange analysis system was used to obtain pulmonary gas exchange data: Ultima Cardio$_2$, Medgraphics, Medical Graphics Corporation, St Paul, MN, USA. Healthy participants were fitted with a mouthpiece and nose clip, whilst individuals with HFrEF were given a face mask that covered their nose and mouth for breath-by-breath gas exchange measurements (PreVent® face mask, Medgraphics, Medical Graphics Corporation, St Paul, MN, USA). Face masks were used in HFrEF participants because unlike mouthpieces they allow the individual to swallow, increasing comfort. To minimise the risk of exhaled air leaking out the sides of the masks, several different mask sizes were available to participants and the fit of each mask was checked before exercise. A pneumotach featuring a bidirectional pitot tube (preVent® flow sensor, Medgraphics, Medical Graphics Corporation, St Paul, MN, USA) was connected to the mouthpiece or mask. Pneumotach specifications: length 7.26 cm; outside diameter 3.5 cm; dead space 39 ml; range ± 18 L/s; accuracy ± 3% or 50 ml, whichever is greater; resistance <1.5 cm H_2O at 14 L/s. An umbilical, containing the flow sensor, was then inserted into the pneumotach, enabling the measurement of flow and transfer of respiratory gases to O_2 and CO_2 analysers. The gas analysers run in parallel, rather than in series, and consisted of an electrochemical galvanic fuel cell (range 0-100%; response [10-90%] <180 ms;

accuracy ± 1%) for measurement of O_2 and a non-dispersive infrared CO_2 analyser (range 0-15%; response [10-90%] <180 ms; accuracy ± 0.1 [0-10% CO_2]). Flow measurement and gas concentrations are measured at a slightly different time because the former takes less time to measure than the latter. Two components are responsible for this delay: transit time and gas analyser time. However, the analysis software corrects for this delay in real time by detecting the start and end of each breath and time aligning gas concentrations.

2.3.1 Gas exchange calibration

Prior to each use, the flow and gas sensors were calibrated. First, ambient conditions that influence gas concentration were entered into the system: temperature, ambient pressure and humidity. Second, a 3 L syringe (Medgraphics, Medical Graphics Corporation, St Paul, MN, USA) was used to deliver 10 pump strokes of varying flow rates (i.e. covered the physiological spectrum of flows) across the flow sensor. This step was repeated to verify the calibration and measurements were only recorded after the system reported an actual measured volume (10 stroke mean) of 2.99-3.01 L with an SD of ≤ 0.02 L. A flow meter (FMA-A2305, Omega, Stamford, CT, USA) was used before each test to ensure flow through the umbilical was ≥100 cm^3/min^{-1} (i.e. there were no blockages in the system and the umbilical was fit for use). Gases of known concentrations that span the physiological range of inspired and expired O_2 and CO_2 values were used to calibrate the O_2 and CO_2 analysers (5% CO_2, 12% O_2, Bal N_2 and 0% CO_2, 21% O_2, Bal N_2). Before and after each test, these gases were sampled to verify the stability of the calibration.

2.4 Heart rate and ECG monitoring during exercise tests

All participants were attached to a 12-lead ECG (Mortara X12+, Mortara Instrument, Milwaukee, WI, USA) during all maximal exercise tests. In healthy participants this was monitored by the researcher for obvious irregularities (e.g. ST elevation/depression). In individuals with HFrEF, a cardiac specialist (cardiac

registrar or cardiac physiologist) was present for all maximal exercise tests to monitor the ECG for irregularities. In the event that an irregularity was detected the response (i.e. decision to continue or abort the exercise test) was dictated by the cardiac specialist. The following tests were aborted: healthy n = 0; HFrEF n = 2. The ECG of all participants was monitored for at least 6 min after exercise cessation and in HFrEF the ECG was only terminated with the consent of the cardiac specialist. The 12-lead ECG was also used to collect heart rate data in all study chapters during exercise tests. During exercise training sessions in Chapter 5, participants wore a heart rate sensing chest belt (Polar H10; Polar Electro, Kempele, Finland). This wireless device was linked to a heart rate watch that displayed and recorded heart rate.

2.5 Electromyography

Surface electromyography (EMG) was used in Chapter 3 to measure the electrical activity of locomotor muscles during MVIP measurements. A surface EMG system (Noraxon TeleMyo 2400T G2, Noraxon USA Inc, Scottsdale, AZ, USA) recorded EMG signals at 1500 Hz. These signals were transferred wirelessly from the transmitter worn by participants on a waist belt to the receiver (Noraxon TeleMyo 2400R G2, Noraxon USA Inc, Scottsdale, AZ, USA) using a radio system. A connection between the receiver and computer then allowed signals to be displayed and recorded in real-time on software provided by the manufacturer (Noraxon MyoResearch XP, Noraxon USA Inc, Scottsdale, AZ, USA) for later analysis.

2.5.1 Electrode placement sites

Electrodes were placed on the following five muscles of the right leg: gastrocnemius lateralis, biceps femoris, vastus lateralis, rectus femoris and vastus medialis. These muscles were selected because they play a primary role in power generation during cycle ergometry (Ericson et al., 1986). Further, previous studies investigating MVIP and changes in muscle activation before and at the limit of ramp-incremental exercise have used these muscle sites (Ferguson et al., 2016; Coelho et al., 2015). Electrode

placement sites and skin preparation procedures followed Surface ElectroMyoGraphy for the Non-Invasive Assessment of Muscles (SENIAM) guidelines. Electrodes were placed over the gastrocnemius lateralis 1/3rd the distance between the head of the fibula and the calcaneus, over the biceps femoris positioned halfway between the ischial tuberosity and the lateral epicondyle of the tibia, over the vastus lateralis 2/3rd of the distance from the anterior superior iliac spine to the lateral border of the patella, over the rectus femoris midway between the anterior superior iliac spine and the superior part of the patella and over the vastus medialis 8/10^{ths} of the distance between the anterior superior iliac spine to the joint space in front of the anterior border of the medial ligament. Electrode placement sites can be seen in Figure 2.1.

2.5.2 Skin preparation and electrode placement

After electrode sites were selected and marked using a permeant marker, skin was prepared to ensure good skin-electrode contact; this is important to minimise electrical interference, ensure electrodes are balanced and reduce noise. In line with SENIAM guidelines, a razor was used to remove hair from electrode sites. All sites were rubbed with an abrasive gel to remove dead skin cells and reduce skin impedance (Nuprep, Weaver and company, Aurora, CO, USA). To finish, all sites were cleaned with alcohol wipes (70% Isopropyl alcohol) and left to dry before electrodes were attached.

For ease and to prevent discomfort, electrodes were snapped onto lead wires before placement on the skin. Two electrodes (Kendall H93SG electrodes, Covidien, Minneapolis, MN, USA) were placed on the muscle belly of each site (previously stated in section 2.5.1) with an inter electrode distance of ~20 mm. All electrodes were orientated parallel to the muscle fibres to increase signal strength. Participants were asked to perform a series of lower limb contractions before sitting on the cycle

ergometer to assess the signal quality of each placement site. If the signal of a site was deemed to be suboptimal, electrodes were removed, and fresh electrodes were applied in a preferred position. To minimise movement artefacts, all electrode lead wires were secured to the participant before exercise using surgical tape (3M, Bracknell, Berkshire, UK). The final surface EMG system set up can be seen in Figure 2.1.

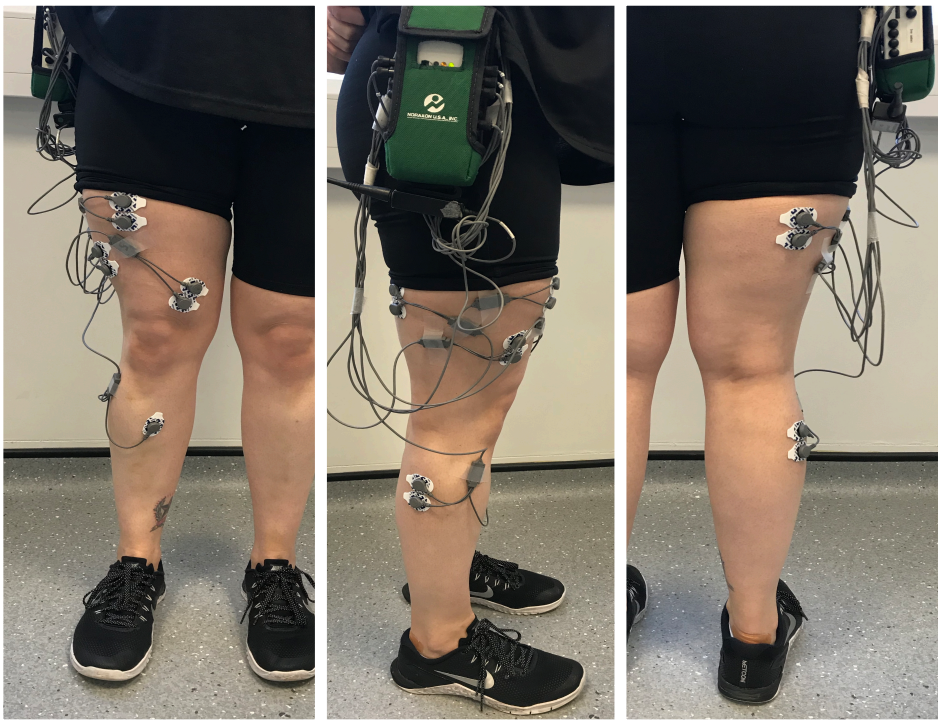

Figure 2.1 Participant wearing surface EMG system. Electrode placement sites and skin preparation procedures adhered to Surface ElectroMyoGraphy for the Non-Invasive Assessment of Muscles guidelines. Electrode wires were secured using surgical tape to minimise signal artefacts.

2.6 Exercise protocols

2.6.1 Experimental procedures

All study visits involving healthy participants (Chapter 3 and 5) took place in an exercise physiology or vasculature laboratory at the University of Leeds. All study visits with HFrEF participants (Chapter 4) took place in the exercise physiology laboratory in the Clinical Research Facility at Leeds General Infirmary. Both laboratories were temperature controlled (19-20°). Exact procedures for each study are outlined in specific experimental chapters. All study visits for healthy participants and those with HFrEF were separated by at least 24 h. Before visits involving a maximal exercise test (e.g. ramp-incremental or constant-load exercise test) all participants were instructed to avoid strenuous exercise in the previous 24 h and to abstain from ingesting food or caffeine in the previous 3 h. Prior to characterisation visits, when hematopoietic and endothelial progenitor cell numbers were enumerated (Chapter 4 and 5) and endothelial function was assessed (Chapter 5 only), healthy participants and those with HFrEF were asked to avoid strenuous exercise in the previous 24 h and refrain from consuming caffeine 12 h beforehand. Healthy participants were also asked to arrive in a fasted state (>12 h). All of these actions were taken due to the effect that exercise, caffeine and food can have on the vasculature (Harris et al., 2010). All characterisation visits (Chapter 4 and 5) were performed at a similar time of day to account for diurnal variations in the number of circulating progenitor cells, previously characterised by a significant peak in the evening (Mheid et al., 2014).

2.6.2 Maximal voluntary isokinetic power

Maximal voluntary isokinetic power (MVIP) was measured in Chapter 3 and 4 by rapidly switching (<1 s) from hyperbolic to isokinetic cycling modes on the cycle ergometer and asking participants to provide a short (~6 s) maximal effort. This measurement was employed at different time points (exact details are described in each chapter) to measure MVIP and assess exercise-induced fatigue.

Due to the velocity-dependent nature of power output (Beelen and Sargeant, 1991), the predetermined (i.e. pre-programmed) cadence that is used during isokinetic cycling bouts influences maximal power output. Subsequently, it is crucial that the cadence during MVIP measurements is controlled. Prior research suggests that a parabolic relationship exists between maximal power generation and cadence, with maximal power achieved in a non-fatigued state between 100-110 rpm (Sargeant et al., 1981). However, this relationship appears to flatten in a fatigued state, leading to maximal power generation at 80-120 rpm (Elmer et al., 2013, Beelen and Sargeant, 1991). To limit the time between the attainment of the limit of tolerance at 50 rpm and the measurement of MVIP, a cadence of 80 rpm was selected for all MVIP measurements in healthy individuals in Chapter 3. This cadence was also selected because participants tend to cycle around this cadence during exercise in the laboratory.

In contrast to the MVIP measurements made in healthy individuals, a cadence of 70 rpm was selected for all MVIP measurements performed by HFrEF patients in Chapter 4. Although the optimal cadence for maximal power generation is yet to be determined in HFrEF, this cadence was selected to account for the functional limitation of these patients. Many patients may have struggled to achieve a target cadence of 80 rpm at the limit of tolerance. A target of 70 rpm also minimises the time taken for individuals with HFrEF to achieve the target cadence at the limit of tolerance, limiting the opportunity for recovery. This cadence was also selected to align with previous literature investigating maximal isokinetic power in a chronic disease state (chronic obstructive pulmonary disease; Cannon et al., 2016).

2.6.3 Familiarisation to MVIP measurements

After being introduced to the concept of isokinetic cycling and the measurement of MVIP, participants were asked to perform sub-maximal isokinetic efforts until they were comfortable with the technique and capable of producing reproducible sub-maximal power outputs. This also provided each participant with the opportunity to adjust the position of ergometer (e.g. seat height and handlebar position) before data collection and become familiar with the ergometer.

2.6.4 Baseline MVIP

Participants completed a set of isokinetic bouts (~ 6 s) for measurement of baseline MVIP. Healthy individuals were asked to provide an isokinetic effort that was 25, 50 and 75% of what they perceived to be their maximum, as well as two maximal (i.e. 100%) efforts. In contrast, individuals with HFrEF performed a single isokinetic effort that they deemed to be equivalent to 25% of their maximal effort followed by two maximal efforts. Each submaximal isokinetic effort was separated by ≥30 s, whereas maximal efforts were separated by ≥2 min. Participants were instructed to maintain a cadence that was 5-10 rpm below the target isokinetic cadence during the 5 s countdown to each isokinetic effort. This minimised the time taken to achieve the target cadence whilst ensuring participants initiated each isokinetic effort below the target cadence. The latter is important because if cadence exceeds the target cadence at start of the isokinetic effort, a harsh braking force is applied by the ergometer. In turn, this braking force jolts the participant and causes an immediate reduction in cadence that can potentially impact the remainder of the effort.

2.6.5 Ramp-incremental exercise test

Ramp-incremental (RI) exercise tests are the gold standard assessment of aerobic function as they permit the determination of peak oxygen uptake ($\dot{V}O_{2peak}$), lactate threshold (LT), work efficiency ($\Delta\dot{V}O_2$ / ΔWR) and the mean response time of the oxygen uptake response. In addition, this single exercise test provides prognostic

parameters, such as ventilatory efficiency ($\dot{V}_E/\dot{V}CO_2$). Subsequently, it is the most widely used assessment in health and clinical settings.

At the start of the test, individuals were instructed to sit on the cycle ergometer and rest for 2 min to allow resting gas exchange values to be measured (Figure 2.2). Participants then entered a ~4-6 min period of unloaded cycling (healthy: 20 W; HFrEF: 10 W) at 50-70 rpm; the duration of this period depended on the time taken for pulmonary gas exchange indices to attain a steady state (e.g. respiratory exchange ratio = 0.7-0.9). This is important because hyperventilation at the onset of exercise can affect the estimation of LT using gas exchange criteria (refer to section 2.7.2.3). Hyperventilation increases CO_2 output, reducing body CO_2 stores. However, when body CO_2 production increases during exercise stores are subsequently replenished. When replenishment ceases this increases $\dot{V}CO_2$ and the $\dot{V}CO_2$ vs. $\dot{V}O_2$ slope, but at a point that is not indicative of LT (termed a 'pseudo-threshold') due to the unstable initial baseline in CO_2 stores (Ozcelik et al., 1999).

After a steady state was achieved, work rate on the ergometer increased linearly as a function of time (Figure 2.2). RI exercise tests should be ~8-12 min in duration (Buchfuhrer et al., 1983). RI exercise tests that are too short (i.e. the rate at which work is incremented [ramp rate] is too high) can result in insufficient data being collected, whilst RI exercise tests that are too long (i.e. the ramp rate is too low) may result in participant boredom and subsequent premature termination of the test, with both scenarios potentially resulting in an underestimation of $\dot{V}O_{2peak}$ (Wasserman et al., 2011). Therefore, the rate at which work is incremented is selected based on the predicted performance of the participant. In healthy participants this tends to be 20 and 25 W min^{-1} for males and females, respectively. However, in individuals with HFrEF this varied between ~5 and 20 W min^{-1}. To ensure an appropriate ramp rate

was selected in HFrEF, information pertaining the patient's exercise tolerance (previous test history and clinical status) was reviewed prior to the test. All pre- and post-training RI ramp incremental rates were matched to permit appropriate comparisons. Participants were instructed to self-select a cadence that was comfortable to them throughout the test (60-100 rpm). However, participants were advised to increase their cadence gradually during the test as work rate increased and received verbal instructions when needed.

Work rate continued to increase until participants became symptom limited or attained the limit of tolerance (Figure 2.2). This was defined as an inability to maintain a cadence >50 rpm, despite strong verbal encouragement. Immediately after the limit of tolerance in Chapter 3, the ergometry was switched from the hyperbolic to isokinetic cycling mode, and the participant was instructed to provide a maximal effort for 6 s at 80 rpm (Figure 2.2). This measurement of MVIP was subtracted from baseline MVIP to quantify the degree of exercise-induced fatigue (termed performance fatigue). All participants completed ~6 min at their unloaded work rate at a self-selected cadence after RI exercise as recovery.

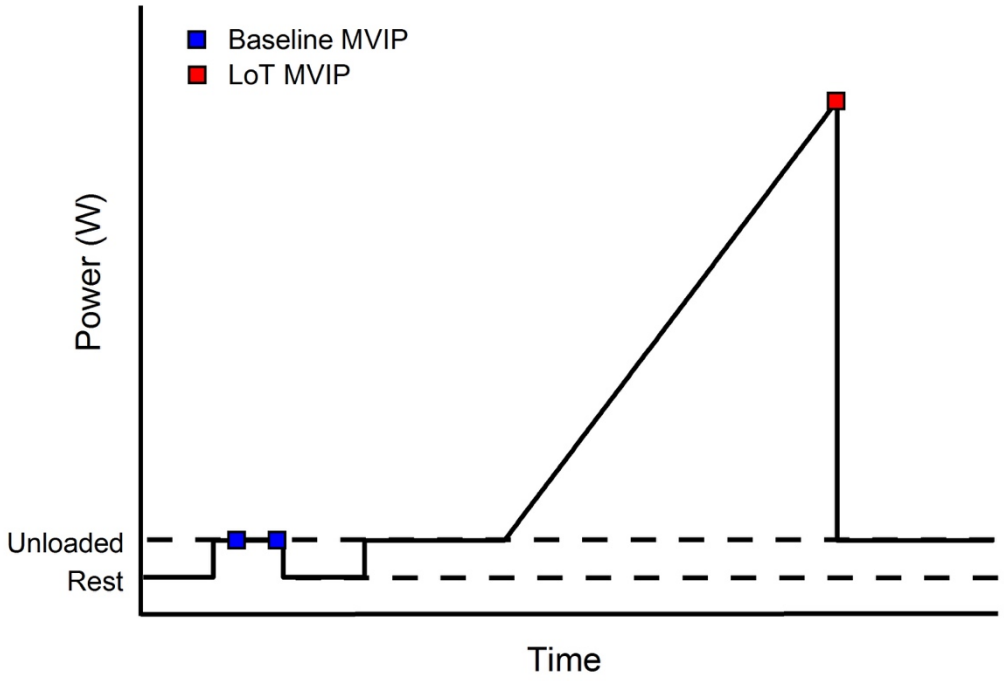

Figure 2.2 Schematic of ramp-incremental exercise test. Following a period of rest, participants then completed at least 4 min of unloaded cycling before work rate increased linearly as a function of time. Work rate continued to increase until the limit of tolerance (LoT) was attained. Maximal voluntary isokinetic power was measured at baseline (baseline MVIP) in Chapter 3 and 4, and at the limit of tolerance (LoT MVIP) in Chapter 3. The test ended with at least 6 min of unloaded cycling.

2.6.6 Constant work rate exercise test

In contrast to RI exercise, where work rate gradually increases, work rate in constant work rate exercise tests is applied as a step function and remains unchanged until the limit of tolerance is attained (Figure 2.3). Often, interventions that harbour small increases in $\dot{V}O_{2peak}$ that fall below the 'minimum clinically important difference' threshold, demonstrate appreciably larger increases in time to intolerance during high-intensity constant work rate exercise tests (Whipp and Ward, 2009, Costes et al., 2003, Emtner et al., 2003). Subsequently, high-intensity constant work rate exercise tests are commonly used to evaluate the effect of interventions on exercise

capacity because they have a greater sensitivity to discriminate change than RI exercise tests (Palange et al., 2007).

After completing the same rest and warm-up phases as the RI exercise test, work rate was applied instantaneously (rate of 1000 $W.s^{-1}$). This work rate was individualised for each participant using the following equation:

$$Constant\ power\ work\ rate = WRpeak - (2\ x\ ramp\ rate)$$

This supra-critical power work rate was designed to produce an exercise duration of ~4-8 min (mean ± SD in Chapter 5; 309 ± 24 s; van der Vaart et al., 2014). All participants received a 30 s warning before work rate was applied and were advised to increase cadence to 80-100 rpm to overcome the initial increase in flywheel resistance. Participants were then instructed to settle at their preferred cadence and continue cycling until the limit of tolerance (Figure 2.3). In line with the RI exercise test, this was defined as an inability to maintain a cadence >50 rpm, despite strong verbal encouragement. After the limit of tolerance was attained, participants completed >6 min of unloaded cycling at ~50-60 rpm.

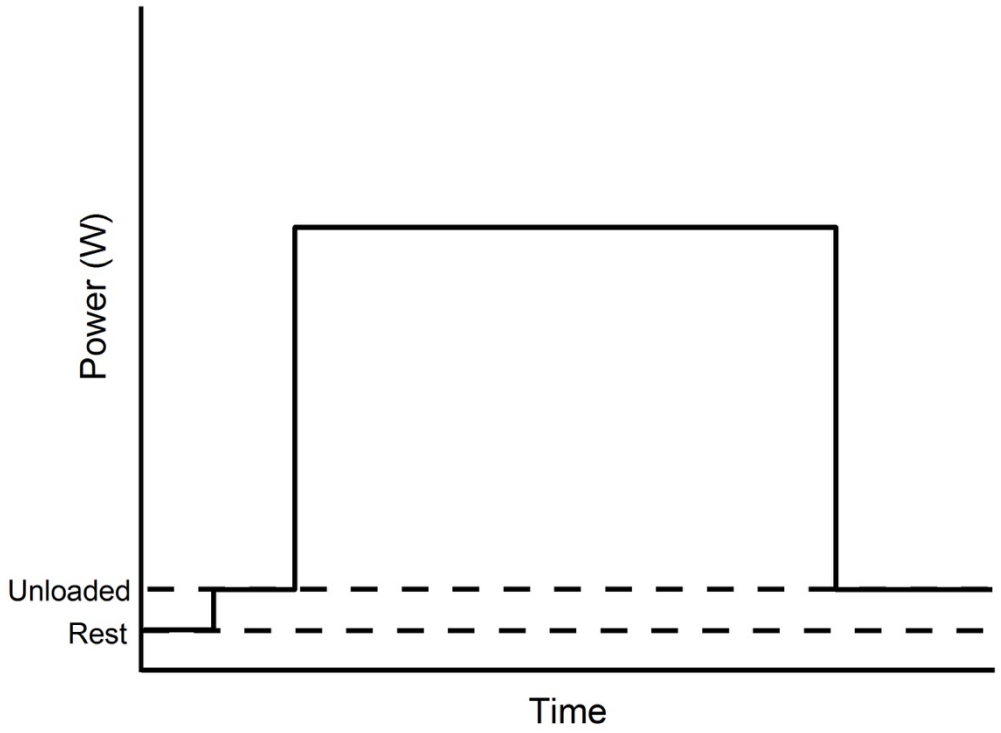

Figure 2.3 Schematic of constant work rate exercise test. Following a period of rest, participants completed at least 4 min of unloaded cycling before work rate was increased instantaneously as a step function. Participants continued to cycle until the limit of tolerance was attained. The test ended with at least 6 min of unloaded cycling.

2.7 Data analysis

2.7.1 Power measurements

Power measurements were analysed using a combination of OriginPro 2019b and Excel (Microsoft Corporation, Redmond, WA, USA).

2.7.1.1 Peak work rate

Peak work rate (WR_{peak}) refers to the peak power output achieved during the ramp-incremental exercise test (i.e. work rate at the limit of tolerance). WR_{peak} was measured at the flywheel whilst the ergometer was in the hyperbolic cycling mode. Therefore, WR_{peak} reflects the task requirement (i.e. the work rate that has been programmed) rather than the 'actual' power generated (i.e. power measured at the crank). The following equation was used to calculate WR_{peak}:

$$WRpeak = \frac{RI\ duration\ (s)}{60}\ x\ ramp\ rate\ (W.min^{-1}) + unloaded\ work\ rate$$

2.7.1.2 Maximum voluntary isokinetic power

Throughout each isokinetic effort power was measured every 2° of angular rotation at the left and right crank. Subsequently, for each pedal stroke 180 power measurements were recorded at the left and right crank, respectively. A mean was calculated from the 180 power output measurements recorded at the left crank to determine 'left crank power'. This process was repeated with the 180 measurements made at the right crank to determine 'right crank power'. There was no difference between left and right crank power ($p > 0.05$). Therefore, left and right crank power were summed to derive a single power output measurement for each pedal stroke. This permitted comparisons to be made between power measured during isokinetic efforts and flywheel power because the latter also reflects the combined output of the left and right crank. The first three pedal strokes that were constrained at the desired isokinetic cadence (80 rpm for healthy; 70 rpm for HFrEF) during each maximal voluntary isokinetic effort were selected; these tended to be the 2nd, 3rd and 4th pedal strokes (Figure 2.4). A mean of the three pedal strokes was taken to provide a final MVIP value.

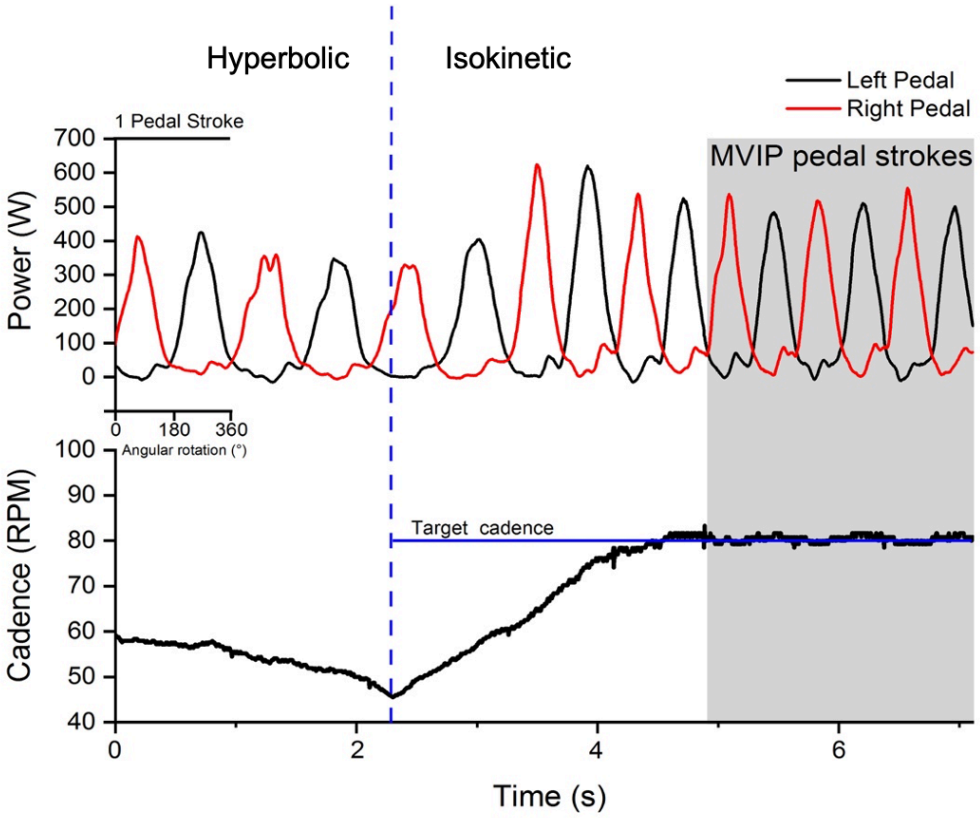

Figure 2.4 Maximal voluntary isokinetic power (MVIP) measured at the limit of ramp-incremental exercise. Right and left crank power were measured independently. The first three pedal strokes constrained at 80 rpm were used to calculate MVIP (pedal strokes in grey box). Blue dashed line represents switch from hyperbolic to isokinetic cycling mode. Blue solid line represents target isokinetic cadence.

2.7.1.3 Natural fluctuation in power output

Whilst the mean power output during hyperbolic cycling equals the desired task requirement (i.e. the work rate that has been programmed) variation exists in the power generated between individual pedal strokes. The natural fluctuation in pedal-by-pedal stroke power output was calculated during ramp-incremental exercise in Chapter 3. First, the power output of each individual pedal stroke was determined using the same method that was used to derive pedal-by-pedal stroke power output during maximal isokinetic efforts (section 2.7.1.2). Second, the percentage difference between actual power and required task power of each pedal stroke for the entire ramp-incremental exercise test was plotted against required task power and 95%

prediction limits were applied (Figure 2.5; individual example). It should be noted that a power equivalent to two ramp rates (e.g. 50 W for 25 W min^{-1} ramp-incremental exercise test) was excluded at the start of each test and not included in the 95% prediction limits. This was due to the high variability in actual power output when the required power output is low. The application of 95% prediction limits derived an upper and lower limit of natural fluctuation in power output for each participant. A group mean was also calculated in Chapter 3. For this, pedal strokes from each participant's ramp-incremental exercise test were amalgamated and time aligned before the same process that was used to calculate individual natural fluctuations in pedal power output was repeated. The mean fluctuation was 27 ± 6 and 28 ± 6% above and below task requirement, respectively.

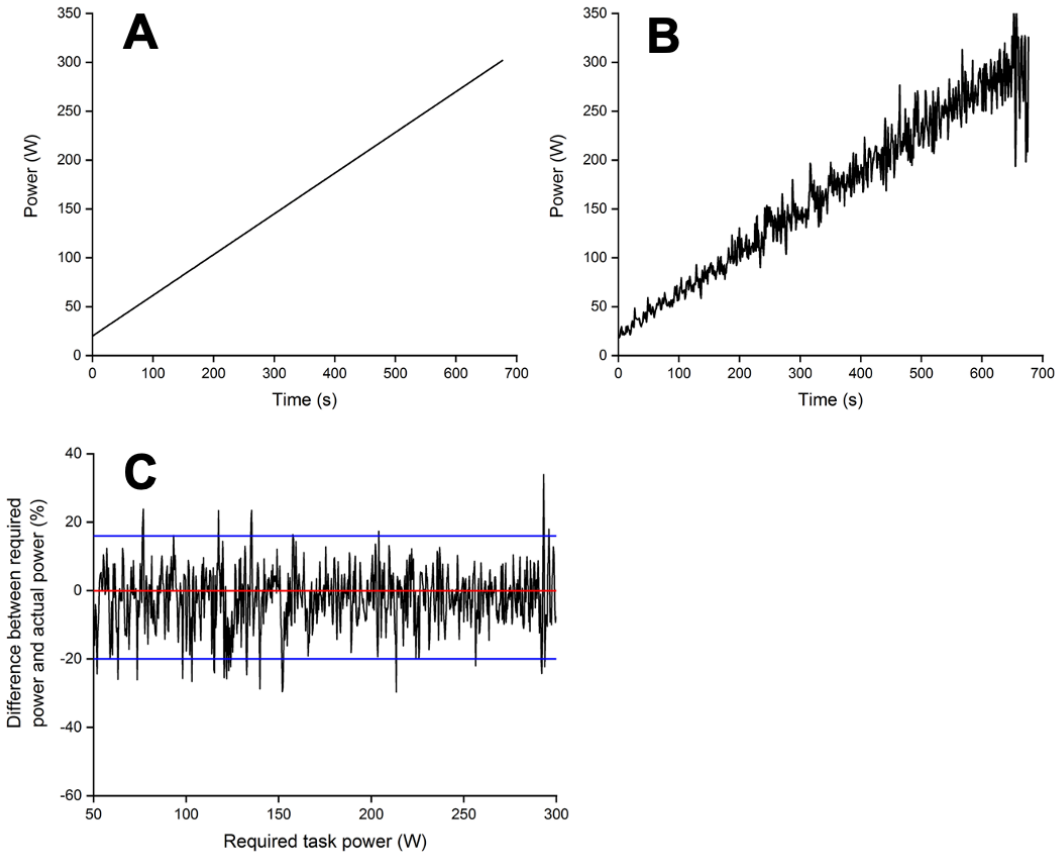

Figure 2.5 Example of individual natural fluctuation in crank power output during a ramp-incremental (RI) exercise test. A: Required power output during RI exercise. B: Actual pedal-by-pedal stroke power output measured at the crank during RI exercise. C: Natural fluctuation in crank power output during RI exercise. Red line represents adherence to the required power output (i.e. 0% fluctuation). Blue lines denote upper and lower limits in fluctuation (95% prediction limits).

2.7.1.4 Power reserve

The following calculation was used to determine if a power reserve was present or absent:

$$\text{Power reserve [W]} = (\text{MVIP at LoT} - \text{Task requirement at LoT})$$

In this equation MVIP is maximal voluntary isokinetic power and LoT is the limit of tolerance. If a power reserve was present (i.e. the equation above resulted in a positive number), the power reserve was considered physiologically significant if it was greater than the individual's natural fluctuation in pedal-by-pedal stroke power.

2.7.2 Gas exchange

Data analyses of pulmonary gas exchange data were performed using OriginPro 2019b (OriginLab Corporation, Northampton, MA, USA) and Microsoft Excel (Microsoft Corporation, Redmond, WA, USA).

2.7.2.1 Data editing

All breath-by-breath data was collected whilst the participant was wearing either a mouthpiece or mask. Both of these apparatuses can increase the likelihood of the participant coughing or spluttering during rest or exercise. If the participant coughs, splutters or talks during breath-by-breath data collection, data points splay and do not represent the true $\dot{V}O_2$ response (Lamarra et al., 1987). Subsequently, the breath-by-breath $\dot{V}O_2$ data was plotted against time and 99% prediction limits were applied around the mean fit of the $\dot{V}O_2$ data (Lamarra et al., 1987). Outlying breaths were deleted to ensure that the $\dot{V}O_2$ response reflected the true underlying physiological response (Whipp and Rossiter, 2005; Figure 2.6).

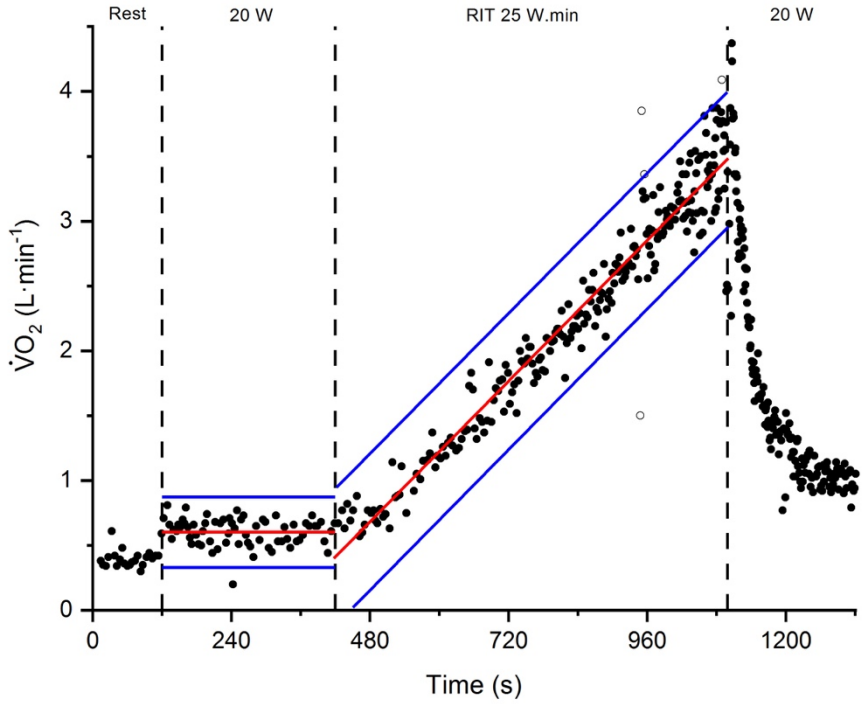

Figure 2.6 A representative example of $\dot{V}O_2$ response to ramp-incremental exercise test with data editing processes applied. A line of best fit (red line) with 99% prediction bands (blue lines) was applied. Any data points falling outside of these bands were deleted (open circles). Dashed lines separate different stages of the ramp-incremental exercise test.

2.7.2.2 Peak oxygen uptake

Peak oxygen uptake ($\dot{V}O_{2peak}$) refers to the highest $\dot{V}O_2$ achieved during a presumed maximal effort exercise test. $\dot{V}O_{2peak}$ was calculated in all chapters via the application of a 12-breath rolling mean. Working backwards from the final breath of the ramp-incremental exercise test, a 12-breath rolling mean was applied 8 times to breath-by-breath $\dot{V}O_2$ data. The highest 12-breath $\dot{V}O_2$ ascertained from this process was then determined as $\dot{V}O_{2peak}$. The same 12-breath mean was also used to determine HR_{peak} and peak oxygen pulse.

2.7.2.3 Lactate threshold

The lactate threshold is the $\dot{V}O_2$ that if exceeded results in a sustained elevation in blood lactate and a metabolic acidosis due to an imbalance between the rate of lactate production and lactate clearance. Above LT, lactate acid dissociates into

lactate and H^+; the latter is buffered by bicarbonate via the following equation, causing an increase in CO_2 production (Beaver et al., 1986a):

$$CO_2 + H_2O \leftrightarrow H_2CO_3 \leftrightarrow HCO_3^- + H^+$$

This increase in CO_2 production can be detected in the breath, providing a non-invasive assessment of LT. Using this approach, LT was determined from gas exchange data collected during ramp-incremental exercise tests in all experimental chapters. After pulmonary gas exchange data was edited (section 2.7.2.1), the following variables were plotted against oxygen uptake ($\dot{V}O_2$): the rate of carbon dioxide output ($\dot{V}CO_2$), end-tidal partial pressure of O_2 ($P_{ET}O_2$) and CO_2 ($P_{ET}CO_2$), the ventilatory equivalents for O_2 ($\dot{V}_E/\dot{V}O_2$) and CO_2 ($\dot{V}_E/\dot{V}CO_2$) and the respiratory exchange ratio ($\dot{V}CO_2$ vs. $\dot{V}O2$; Figure 2.7). All of these plots were used to estimate LT (Figure 2.7). First, the slope of the $\dot{V}CO_2$ vs. $\dot{V}O_2$ relationship was examined because a breakpoint in this slope can represent the LT. This is because the relationship between $\dot{V}CO_2$ and $\dot{V}O_2$ becomes steeper when the metabolically produced CO_2 is supplemented by additional CO_2 from the bicarbonate buffering of lactate. During exercise $\dot{V}_E$ tracks CO_2 status more closely than O_2 status; therefore, $\dot{V}_E$ is also associated with a hyperventilation relative to O_2 but not relative to CO_2 at the point of LT. Thus, LT was confirmed by identifying an increase in $\dot{V}_E/\dot{V}O_2$ and $P_{ET}O_2$ but no change in $\dot{V}_E/\dot{V}CO_2$ and $P_{ET}CO_2$ when plotted against $\dot{V}O_2$ (Figure 2.7). Initially above the lactate threshold there is a period of isocapnic buffering (approximately 2 min in duration) where $\dot{V}_E$ and $\dot{V}CO_2$ increase in a proportional linear relationship. After this period of time, as work rate continues to increase during the ramp-incremental exercise test, the carotid bodies respond to the metabolic acidosis and increase ventilation further. This is known as the respiratory compensation point and is reflected in an increase in $\dot{V}_E/\dot{V}CO_2$ and reduction in $P_{ET}CO_2$, due to the hyperventilation in relation to $\dot{V}CO_2$. The respiratory compensation point was identified to support the estimation of the LT (Figure 2.7). Finally, RER was used to

confirm that a pseudo-threshold had not been detected; RER should be stable and then increase during RI exercise but if a pseudo-threshold is present RER will decrease before it increases.

Three researchers independently estimated LT and if the 3 values were within 200 ml of each other a mean was taken as the LT. If values differed by more than 200 ml, additional researchers were asked to provide an estimation of LT and the data was discussed until the LT was agreed.

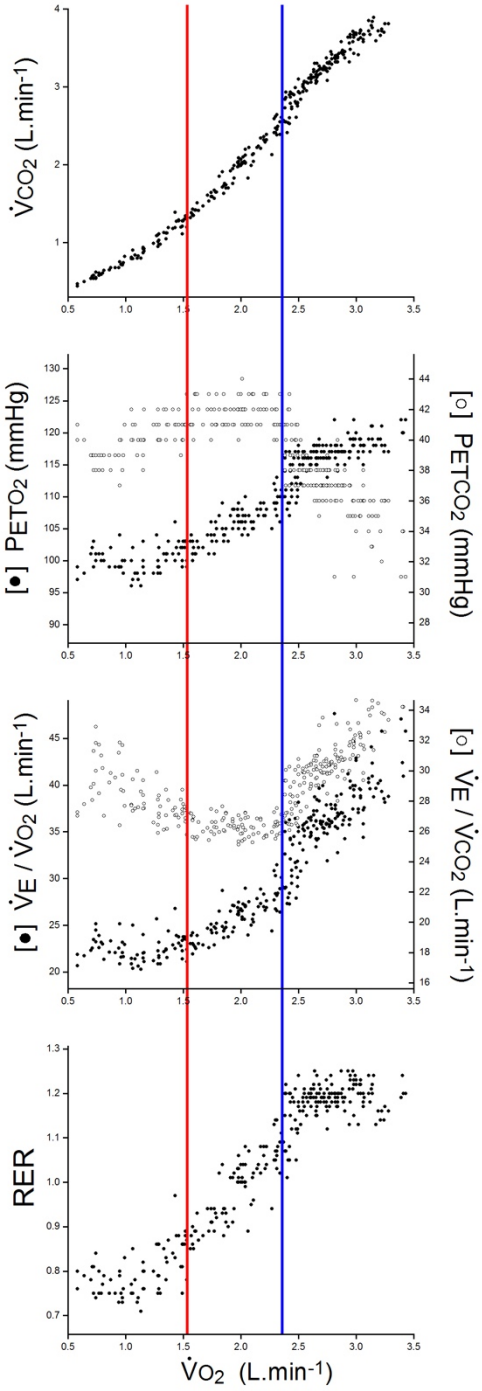

Figure 2.7 Non-invasive estimation of the lactate threshold using the V-slope method. Plots display a representative example of pulmonary gas exchange data from the incremental phase of a ramp-incremental exercise test on a cycle ergometer. The red line represents the estimated lactate threshold for this test. The respiratory compensation point (blue line) occurs after the lactate threshold and is confirmed by an increase in $\dot{V}_E/\dot{V}CO_2$ and reduction in $P_{ET}CO_2$.

2.7.2.4 Ventilatory efficiency ($\dot{V}_E/\dot{V}CO_2$)

Ventilation (V_E) is more closely linked to carbon dioxide output ($\dot{V}CO_2$) than oxygen uptake ($\dot{V}O_2$), therefore the relationship between $\dot{V}_E$ and $\dot{V}CO_2$ is used to assess ventilatory efficiency. The relationship between V_E and $\dot{V}CO_2$ can be expressed as a ratio ($\dot{V}_E/\dot{V}CO_2$ minimum) or as a slope ($\dot{V}_E/\dot{V}CO_2$ slope). A higher value reflects a more inefficient gas exchange. In HFrEF, $\dot{V}_E/\dot{V}CO_2$ is an important cardiopulmonary exercise test parameter because it is highly predictive of cardiac-related hospitalisation and mortality (Arena et al., 2004, Myers et al., 2009). Due to the prognostic power of $\dot{V}_E/\dot{V}CO_2$ it can also be used to classify disease severity (Arena et al., 2007). The ventilatory class system uses $\dot{V}_E/\dot{V}CO_2$ to categorise patients with HFrEF into one of four groups: ventilatory class I (≤ 29), ventilatory class II (30.0-35.9), ventilatory class III (36.0-44.9) and ventilatory class IV (≥ 45.0). The risk of event free survival reduces from ventilatory class I to IV (Arena et al., 2007).

$\dot{V}_E/\dot{V}CO_2$ minimum: $\dot{V}_E/\dot{V}CO_2$ was calculated for each breath during the ramp-incremental exercise test. An 8-breath $\dot{V}_E/\dot{V}CO_2$ mean was calculated and plotted against $\dot{V}O_2$. The nadir of the curve was taken as $\dot{V}_E/\dot{V}CO_2$ minimum.

$\dot{V}_E/\dot{V}CO_2$ slope: $\dot{V}_E$ was plotted against $\dot{V}CO_2$. The $\dot{V}_E/\dot{V}CO_2$ slope was then calculated (via linear regression in OriginPro 2019b) using data from the initiation of exercise to the respiratory compensation point.

2.7.2.5 Work efficiency

Work efficiency is measured from the slope of $\dot{V}O_2$-work rate relationship ($\Delta\dot{V}O_2/\Delta WR$). In healthy individuals, irrespective of their age, gender and training status $\Delta\dot{V}O_2/\Delta WR$ is typically equal to ~10 ml O_2/min/W (Hansen et al., 1987). However, in HFrEF, although the steady-state relationship is similar, the slope *may* be shallower (~7-10 ml O_2/min/W) during ramp-incremental exercise (Solal et al.,

1990, Hansen et al., 1987). Work efficiency was calculated pre- and post-training from ramp-incremental exercise test data in Chapter 4. Only data below the LT was used to calculate work efficiency because the $\Delta\dot{V}O_2/\Delta WR$ slope *can* become more complex after the LT has been exceeded, although this is influenced by both ramp rate and test duration (Hansen et al., 1988, Wasserman et al., 2011).

2.7.2.6 Peak oxygen pulse

Oxygen pulse is a measure of the oxygen uptake per heartbeat ($\dot{V}O_2$/heart rate ratio) and is an indicator of stroke volume and arteriovenous O_2 difference during exercise. Peak oxygen pulse was calculated pre- and post-training in HFrEF participants in Chapter 4 by dividing $\dot{V}O_{2peak}$ by HR_{peak} and was expressed as ml/beat. HR_{peak} was calculated by averaging the 12 heart beats that corresponded to the 12 breaths that determined $\dot{V}O_{2peak}$ (section 2.7.2.2).

2.7.3 EMG analysis

EMG data was analysed using the software provided by the system manufacturer; Noraxon MyoResearch XP software (Noraxon USA Inc, Scottsdale, AZ, USA). Raw EMG signals were bandpass filtered between 10 and 500 Hz to reduce noise and artefact contamination. Raw EMG signals were then rectified and smoothed by computing the root mean square (RMS) value of the signal using a 100 ms time window. The three contractions corresponding to the three pedal strokes used to calculate each MVIP measurement were identified. For each pedal stroke, the peak RMS-EMG of each of the five muscles was calculated and summed, resulting in an RMS-EMG value for each of the three pedal strokes. A mean of these values was then calculated to generate a single RMS-EMG value to pair with each MVIP measurement. The analysis process performed on raw EMG signals is outlined in Figure 2.8. All RMS-EMG values were normalised to baseline MVIP (i.e. the visit maximum). All participants performed two baseline MVIP efforts in Chapter 3. There was no difference in RMS-EMG between these efforts, therefore, a mean was taken, and all subsequent RMS-EMG measurements were reported relative to this value.

Normalisation was performed to attenuate the effect of day-to-day variations in skin preparation, conductance and temperature at electrode placement sites (Coelho et al., 2015).

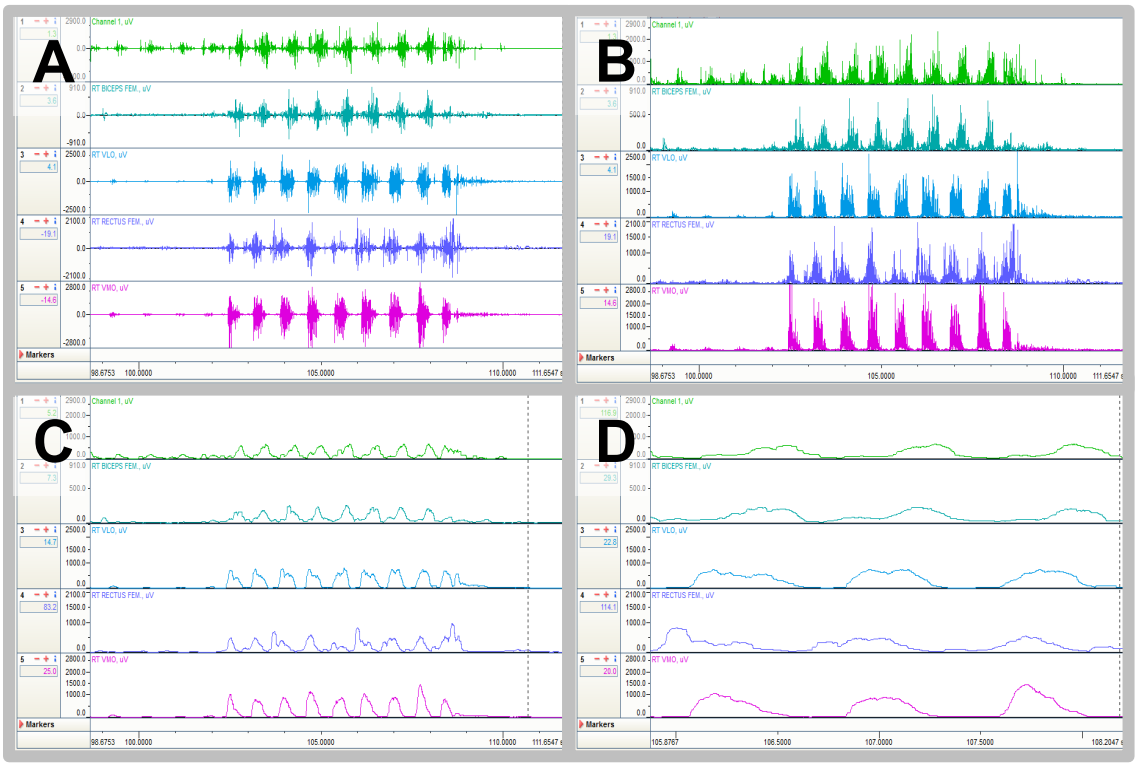

Figure 2.8 A representative example of raw EMG signals during a baseline maximal voluntary isokinetic power (MVIP) effort and the analysis steps that were performed. Raw EMG signals (A) during MVIP are rectified (B) and smoothed via a root-mean-square with a moving window of 100 ms (C) before the three pedal strokes that were used to calculate MVIP are identified (D). The peak RMS-EMG of each of the five muscle for each contraction were calculated and summed to determine a single RMS-EMG value for each pedal stroke.

2.7.4 Assessment of body mass index (BMI)

Height and weight were measured using a stadiometer and manual scales. Measurements were recorded to the nearest 0.1 cm and 0.1 kg for height and weight, respectively. The following calculation was used to determine BMI:

$$\text{BMI (kg / m}^2\text{)} = \text{Body weight (kg)} \,/\, \text{Height}^2\text{ (m)}$$

2.8 Venepuncture protocol

Venous blood was collected from the antecubital fossa into EDTA tubes for enumeration of hematopoietic and endothelial progenitor cells using flow cytometry (section 2.9). The first 3 ml of blood collected was discarded to prevent contamination with circulating endothelial cells which could be released during the venepuncture.

2.9 Quantification of hematopoietic and endothelial progenitor cells

2.9.1 Flow cytometry

Flow cytometers utilise light to rapidly generate information about the properties and characteristics of individual cells in a heterogeneous cell sample (e.g. cell size, cell surface receptors and cell cycle). This information can then be used to identify, count and separate different cell populations. The basic operation of a flow cytometer can be seen in Figure 2.9. After the sample tube is loaded onto the flow cytometer, the sample is taken up into the instrument to the flow cell. The majority of flow cytometers then use hydrodynamic focusing to achieve the desired flow rate through the flow-cell. This technique involves enclosing the sample stream in a more rapidly flowing stream sheath to reduce the diameter of the sample stream to that of a single cell. Each cell then passes through the interrogation point of the laser beam. Cells that are illuminated by the laser cause the light to scatter. Typically, two scatter parameters are measured: forward scatter (FSC) and side scatter (SSC). FSC is detected by a lens that is located along the path of the laser beam and is a measure of cell size (e.g. lymphocytes are smaller than monocytes and granulocytes). Across the front of this forward lens is an obscuration bar that prevents the laser beam from striking the forward lens. Subsequently, only light that has been scattered far enough away from its original direction, to the extent that it avoids the obscuration bar, is detected as FCS. Cells with large-cross sectional areas refract more light onto the lens than smaller cells, creating a relationship between the amount of light refracted

and cell size. However, the refractive index of the cell (a parameter that describes how well light propagates a medium) also influences FSC. For example, a large intact cell will refract more light than an equally large dead cell with a permeable membrane. SSC is measured by a lens that is perpendicular to the laser beam and is a measure of cellular granularity. Light that is scattered to this wide lens is refracted by irregularities on the cell surface or in the cytoplasm of the cell, helping to identify cell groups. Collectively, all of this information is used to help identify individual cell populations.

More information about cells within the sample stream can be derived by labelling the cells utilising the application of fluorescently labelled antibodies, fluorescent proteins or fluorescent dyes. Several detectors within the cytometer are used to sense the presence of fluorescing antibodies that are conjugated to antigens of cells of interest in the sample stream. Fluorescent light occurs when a molecule that has been excited by absorbing a higher energy photon from one wavelength, falls back to its ground (unexcited) state by emitting light of a lower energy photon that is therefore of a longer wavelength than the exciting light. The excitation wavelengths (generated by the flow cytometer's lasers) and the wavelengths emitted by excited molecules can be separated from each other using optical filters. Together with optical mirrors, these filters direct the light of a specified wavelength to photodetectors that convert the light signals into voltages. These voltages are then converted from analogue to digitised data and displayed on the computer screen.

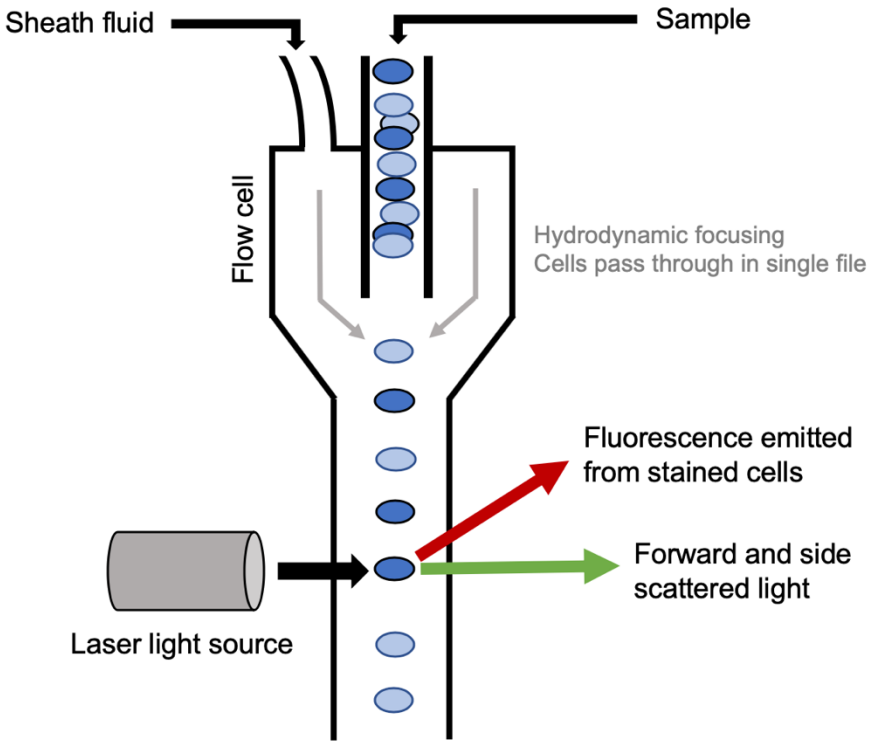

Figure 2.9 Basic operations of a flow cytometer. A sample containing suspended cells is taken up into the flow cell. Cells pass through the beam of laser light (point of interrogation) in single file, causing the light to scatter. Forward scatter and side scatter are measured to provide information on cell size and granularity. The laser light also excites fluorochromes on stained cells. The intensity of fluorescence emitted from fluorochromes is detected by the flow cytometer and displayed on the computer screen, permitting the identification of specific cell populations.

2.9.2 Protocol for quantification of $CD34^+$ and $CD34^+/KDR^+$ progenitor cells (Chapter 4)

A 4 ml blood sample was diluted with 40 ml of red blood cell lysis solution and vortexed for 5 seconds before it was incubated at room temperature for 10 min. 20 µL of lysed blood was removed for a white blood cell count using trypan blue and a haemocytometer for calculation of the total number of white blood cells in the 44 ml lysed blood sample. 10 million cells were then removed from the lysed blood sample and centrifuged at 300 x g for 10 min at room temperature. The supernatant was aspirated, and the cell pellet was re-suspended in 500 µL of FACS buffer (PBS, 0.5%

BSA). 50 µL of cell suspension was placed into the sample, isotype control, single control (CD3, CD34, KDR, KDR isotype, unstained and DAPI tubes) and florescence minus one (FMO) control Eppendorf tubes. In line with the manufacturer's guidelines, 20 µL of Fc-Receptor Blocking Reagent (Miltenyi Biotec, Bergisch Gladbach, Germany) was added to all tubes, except for DAPI and unstained control; tubes were then mixed and incubated for 10 min in the refrigerator. Conjugated antibodies were then added to tubes (see Table 2.1). All tubes requiring KDR-APC were incubated with 10 µL KDR-APC (R&D Systems, Minneapolis, MN, USA) for 15 min before additional conjugated antibodies were added. The exact antibodies and quantities used are detailed in Table 2.2. All tubes were then topped up to a final volume of 100 µL with PBS and incubated in the fridge for 15 min (2-8°C).

Table 2.1 Conjugated antibodies used in Chapter 4 to quantify $CD34^+$ and $CD34^+/KDR^+$ progenitor cells

	Antibodies				Dye
Tube	**KDR-APC**	**CD34-PE**	**CD3-FITC**	**Mouse IgG1-APC**	**DAPI**
Sample	**X**	**X**	**X**		**X**
Isotype control		**X**	**X**	**X**	**X**
Single controls					
KDR	**X**				
CD34		**X**			
CD3			**X**		
KDR Isotype				**X**	
DAPI					**X**
Unstained					
FMO controls					
FMO-1		**X**	**X**		**X**
FMO-2	**X**		**X**		**X**
FMO-3	**X**	**X**			**X**
FMO-4	**X**	**X**	**X**		

FMO = Fluorescence minus one.

Table 2.2 Conjugated antibodies used in Chapter 4

Antibody	Clone	Manufacturer	Quantity used
CD34-PE	AC136	Miltenyi Biotec, Bergisch Gladbach, Germany	2 µL
KDR-APC	89106	R&D Systems, Minneapolis, MN, USA	10 µL
CD3-FITC	REA613	Miltenyi Biotec, Bergisch Gladbach, Germany	2 µL
Mouse IgG_1 APC	11711	R&D Systems, Minneapolis, MN, USA	10 µL

After the incubation period, the cell suspension in each tube was washed with 1 ml of FACS buffer before final centrifugation at 300 x g for 10 min at room temperature. The remaining pellet was re-suspended in 1 ml of FACS buffer and 10 µL of DAPI was added to appropriate tubes (Table 2.1). All tubes were then taken to the flow cytometer (CytoFLEX S, Beckman Coulter, Indianapolis, IN, USA) on ice for analysis. This flow cytometer contains a Violet laser (405 nm), Blue laser (488 nm), Yellow-Green laser (561 nm) and a Red laser (640 nm). Prior to analysis, the flow cytometer was cleaned to remove any residual cells. A minimum of one million total events were collected per sample. The number of $CD34^+$ and $CD34^+/KDR^+$ cells were analysed using CytExpert software (Beckman Coulter). Gates were set using single controls, fluorescence minus one and isotype control tubes. The sequential gating strategy that was used to detect $CD34^+$ and $CD34^+/KDR^+$ progenitor cells in Chapter 4 is shown in Figure 2.10. Live cells were gated in a DAPI vs. FSC-A density plot before a gate was set on a SSC-A vs. FSC-A density plot to contain all lymphocytes. Single cells in this population were then gated in a SSC-A vs. SSC-H density plot. Next, a dump channel was created on a CD3-FITC vs. SSC-A dot plot to exclude $CD3^+$ cells from further analysis. $CD3^-$ cells that were $CD34^+$ (i.e. $CD34^+/CD3^-$ cells) were gated on a CD34-PE vs. SSC-A dot plot and quantified. $CD34^+/CD3^-$ cells that co-express

KDR (i.e. $CD34^+/KDR^+/CD3^-$ cells) were then identified and gated on a KDR-APC vs. SSC-A dot plot.

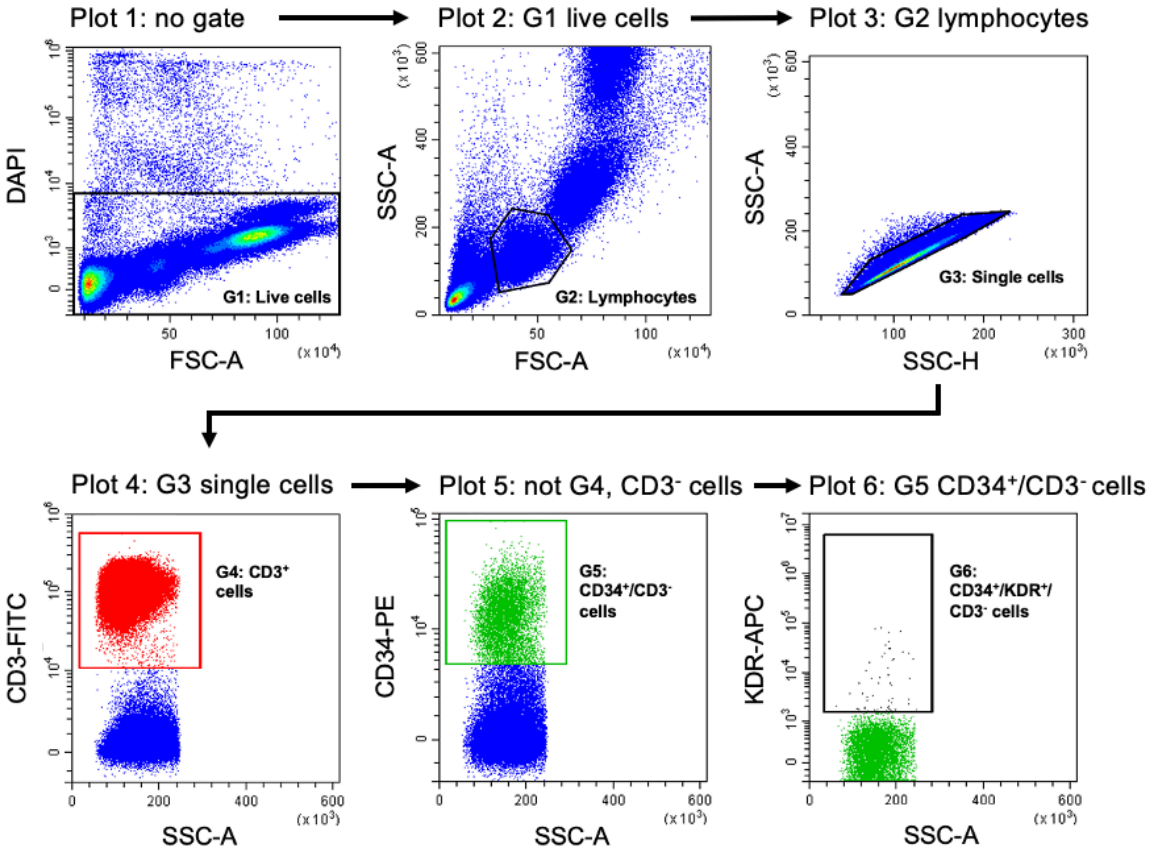

Figure 2.10 Sequential gating strategy used in Chapter 4 to quantify hematopoietic ($CD34^+/CD3^-$) and endothelial ($CD34^+/KDR^+/CD3^-$) progenitor cells. Live cells were gated (G1) on a DAPI vs. FSC-A density plot (Plot 1). Next, a gate was set on a SSC-A vs FSC-A density plot to contain all lymphocytes (G2; Plot 2) before single cells in this population were gated on an SSC-A vs. SSC-H density plot (G3; Plot 3). A dump channel was then created on a CD3-FITC vs. SSC-A dot plot to exclude $CD3^+$ cells from further analysis (G4; Plot 4). $CD3^-$ negative cells that were $CD34^+$ were gated in a CD34-PE vs. SSC-A dot plot and quantified (G5; Plot 5). Finally, a KDR-APC vs. SSC-A dot plot was used to gate endothelial progenitor cells ($CD34^+/KDR^+/CD3^-$ cells; G6; Plot 6).

2.9.3 Protocol for quantification of $CD45^{dim}/CD34^{+}$ and $CD45^{dim}/CD34^{+}/KDR^{+}$ progenitor cells (Chapter 5)

In Chapter 5, the effect of acute and chronic exercise on circulating $CD45^{dim}/CD34^{+}$ and $CD45^{dim}/CD34^{+}/KDR^{+}$ cell number was assessed. $CD45^{dim}$ was introduced as a hematopoietic and endothelial progenitor cell marker in Chapter 5 to move towards a more standardised method of quantifying circulating progenitor cells (Schmidt-Lucke et al., 2010). Blood (4 ml) was lysed, and white blood cells were counted as previously described (section 2.9.2). 10 million cells were then removed from the lysed blood sample and centrifuged at 300 x g for 10 min at room temperature. The supernatant was aspirated, and the cell pellet was re-suspended in 500 µL of FACS buffer. 50 µL of cell suspension was placed into all Eppendorf tubes (see Table 2.3). Next, 20 µL of Fc-Receptor Blocking Reagent (Miltenyi Biotec, Bergisch Gladbach, Germany) was mixed into all tubes, except the unstained and DAPI control tubes, and tubes were incubated for 10 min in the refrigerator. Conjugated antibodies were then added to tubes (see Table 2.3). All of the tubes requiring KDR-APC were incubated with 10 µL KDR-APC (R&D Systems, Minneapolis, MN, USA) for 15 min before other conjugated antibodies were added. The exact antibodies and quantities used are detailed in Table 2.4. All tubes were then topped up to a final volume of 100 µL with PBS and incubated in the fridge for 15 min (2-8°C). The cell suspension in each tube was then washed with 1 ml of FACS buffer before final centrifugation at 300 x g for 10 min at room temperature. The remaining pellet was re-suspended in 1 ml of FACS buffer and 10 µL of DAPI was added to appropriate tubes (Table 2.3). Samples were then taken on ice to the flow cytometer (CytoFLEX S, Beckman Coulter, Indianapolis, IN, USA) which was cleaned before each use.

Table 2.3 Conjugated antibodies used in Chapter 5 to quantify $CD45^{dim}/CD34^{+}$ and $CD45^{dim}/CD34^{+}/KDR^{+}$ progenitor cells

	Antibodies				Dye
Tube	**KDR-APC**	**CD34-PE**	**CD45-PE-Cy7**	**Mouse IgG1-APC**	**DAPI**
Sample	**X**	**X**	**X**		**X**
Isotype control		**X**	**X**	**X**	**X**
Single controls					
KDR	**X**				
CD34		**X**			
CD45			**X**		
KDR Isotype				**X**	
DAPI					**X**
Unstained					
FMO controls					
FMO-1		**X**	**X**		**X**
FMO-2	**X**		**X**		**X**
FMO-3	**X**	**X**			**X**
FMO-4	**X**	**X**	**X**		

FMO = Fluorescence minus one.

Table 2.4 Conjugated antibodies used in Chapter 5

Antibody	Clone	Manufacturer	Quantity used
CD34-PE	AC136	Miltenyi Biotec, Bergisch Gladbach, Germany	2 µL
KDR-APC	89106	R&D systems, Minneapolis, MN, USA	10 µL
CD45-PE-Cy7	HI30	BD Biosciences, San Jose, CA, USA	5 µL
Mouse IgG_1 APC	11711	R&D systems, Minneapolis, MN, USA	10 µL

At least 1 million total events per sample were acquired and data were analysed using CytExpert software (Beckman Coulter). Appropriate compensation for fluorescence spill over was applied; the greatest compensation used was 11% to correct for the spill over of CD45-PE-Cy7 into KDR-APC. Gates were set using single controls, fluorescence minus one and isotype control tubes. The sequential gating strategy was used to quantify the number of $CD45^{dim}/CD34^{+}$ and $CD45^{dim}/CD34^{+}/KDR^{+}$ progenitor cells is shown in Figure 2.11. After nonnucleated cells, debris and cell doublets were excluded, a gate was set on a SSC-A vs. FSC-A density plot to contain all mononuclear cells. Next, $CD45^{dim}$ events were gated on a SSC-A vs. CD45-PE-Cy7 dot plot. $CD45^{dim}$ events that were $CD34^{+}$ positive (i.e. $CD45^{dim}/CD34^{+}$ cells) were then gated on a SSC-A vs. CD34-PE dot plot and counted. To enumerate $CD45^{dim}/CD34^{+}/KDR^{+}$ cells a KDR-APC vs. CD34-PE dot plot was used (Figure 2.11).

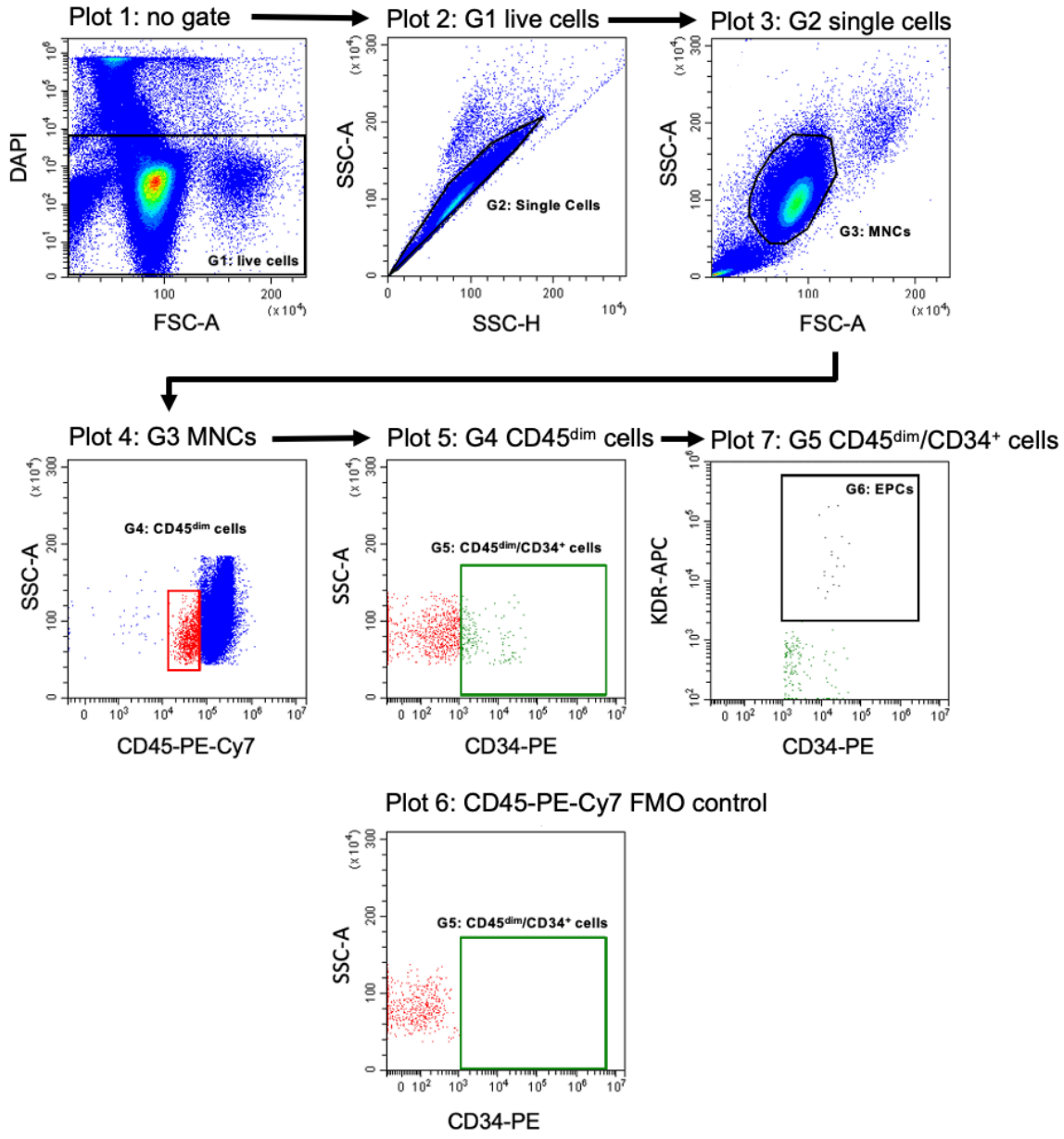

Figure 2.11 Sequential gating strategy used in Chapter 5 to enumerate $CD45^{dim}/CD34^{+}$ and $CD45^{dim}/CD34^{+}/KDR^{+}$ progenitor cells. Only nucleated cells (Plot 1; G1) that were single events (Plot 2; G2) were included in this analysis. A gate was set on a SSC-A vs. FSC-A density plot to contain all mononuclear cells (MNCs; G3; Plot 3). Next, G3 events were displayed on a SSC-A vs. CD45-PE-Cy7 dot plot and a gate (G4) was set on $CD45^{dim}$ events (Plot 4). $CD45^{dim}$ events that were $CD34^{+}$ were then gated (G5) in on a SSC-A vs. CD34-PE dot plot (Plot 5) and quantified; G5 placement was determined from a CD45-PE-Cy7 fluorescence minus one (FMO) control (Plot 6). Finally, endothelial progenitor cells (EPCs), defined as $CD45^{dim}/CD34^{+}/KDR^{+}$ events, were identified by a gate (G6) set on a KDR-APC vs. CD34-PE dot plot and counted (Plot 7).

2.9.4 Hematopoietic and endothelial Progenitor cell reproducibility

Within and between day reproducibility for circulating hematopoietic and endothelial progenitor cell numbers was performed (Table 2.5). For within day reproducibility, blood was drawn from 3 participants before and after a 30 min resting period. A blood sample was then drawn from the same participants a day later to determine between day reproducibility. All blood samples were drawn from individuals who had abstained from strenuous exercise for 24 h and fasted for >12 h.

Table 2.5 Within and between day reproducibility for hematopoietic and endothelial progenitor cell numbers.

	Test re-test variability (%)	Absolute difference*
Within day		
$CD34^+/CD3^-$	12.7	599
$CD34^+/KDR^+/CD3^-$	4.7	12
$CD45^{dim}/CD34^+$	10.1	48
$CD45^{dim}/CD34^+/KDR^+$	17.0	13
Between day		
$CD34^+/CD3^-$	11.4	290
$CD34^+/KDR^+/CD3^-$	10.6	9
$CD45^{dim}/CD34^+$	10.2	60
$CD45^{dim}/CD34^+/KDR^+$	40.5	29

*Absolute difference for $CD34^+/CD3^-$ and $CD34^+/KDR^+/CD3^-$ cells expressed as cells/ (10^6/total events). Absolute difference for $CD45^{dim}/CD34^+$ and $CD45^{dim}/CD34^+/KDR^+$ expressed as cells/ (10^6/mononuclear cells).

2.10 Assessment of brachial artery endothelial function

2.10.1 Flow-mediated dilation

Flow mediated dilation (FMD) is considered to be the gold standard technique for non-invasively assessing endothelial function. First used in 1992, flow-mediated dilation can be used to predict cardiovascular disease risk in asymptomatic

individuals and those with diagnosed cardiovascular disease (Celermajer et al., 1992, Yeboah et al., 2007, Ras et al., 2013). The acute and chronic effect of HIIT with a high work rate and intensity-matched constant work rate exercise training on brachial artery endothelial function was assessed in Chapter 5. The methodological approach that was applied to obtain FMD measurements followed the guidelines set by Thijssen et al. (2019).

Participants rested in a supine position for 10-15 min before measurements were recorded. The brachial artery of the left arm was imaged longitudinally at a depth of 3-4 cm (depending on participant characteristics) using a 10 MHz linear probe (9L) attached to a high-resolution ultrasound machine (Vivid E9, GE Healthcare, Milwaukee, WI, USA). The angle of insonation was set to 60° to ensure that the ultrasound beam was aligned with the direction of blood flow, allowing higher frequency doppler signals to be obtained (improving ultrasound image quality).

After depth and gain settings were altered to optimise the image in B-mode, duplex mode was entered, and a baseline scan (30 s) was recorded. An ischemic stimulus was then created using pneumatic cuff inflation (TMC7^{TM} straight segmental cuff, Hokanson, WA, USA). The cuff was placed distal to the ultrasound probe on the left forearm and inflated to a supra-systolic pressure (>200 mmHg) to occlude arterial flow for a period of 5 min before rapid cuff deflation. Imaging of the brachial artery was recorded continuously 30 s before cuff deflation until 150 s post-deflation to capture transient changes in brachial artery diameter and blood flow. Images were obtained at a rate of 15 frames per second. A probe-holding device was used to support the weight of the probe and minimise movement during recordings. The set up used for this technique can be seen in Figure 2.12. Ultrasound probe position (measured as the distance between the probe and the medial epicondyle) was

recorded after the participant's first FMD to ensure that the same section of the artery was assessed before and after exercise, both pre- and post-training. Pre- and post-training FMD examinations were performed at the same time of day to avoid diurnal variations (typically between 7 and 11 am to permit overnight fasting). During post-training assessments the researcher also viewed baseline images to confirm identical positioning of the probe based on anatomical landmarks, such as artery branch points, collateral vessels, connective tissue and muscle striation markings.

Figure 2.12 Assessment of brachial artery flow-mediated dilation. An ultrasound scan of the brachial artery was obtained before and after an increase in blood flow was induced by the inflation of a cuff placed around the forearm at a pressure of >200 mmHg for 5 min, followed by release.

2.10.2 Analysis of brachial artery diameter

Analysis was performed using Brachial Analyzer for Research® Software (Medical Imaging Applications LLC, Coralville, Iowa, USA). First, a square region of interest (i.e. segment of artery chosen for analysis) encompassing both sides of the endothelial lumen with clear vascular boundaries was selected (Figure 2.13). The

edge detection software was then used to measure tunica media to tunica media diameter within the region of interest. Image frames were excluded if the confidence interval was below 70% or the tunica media was not clearly visible.

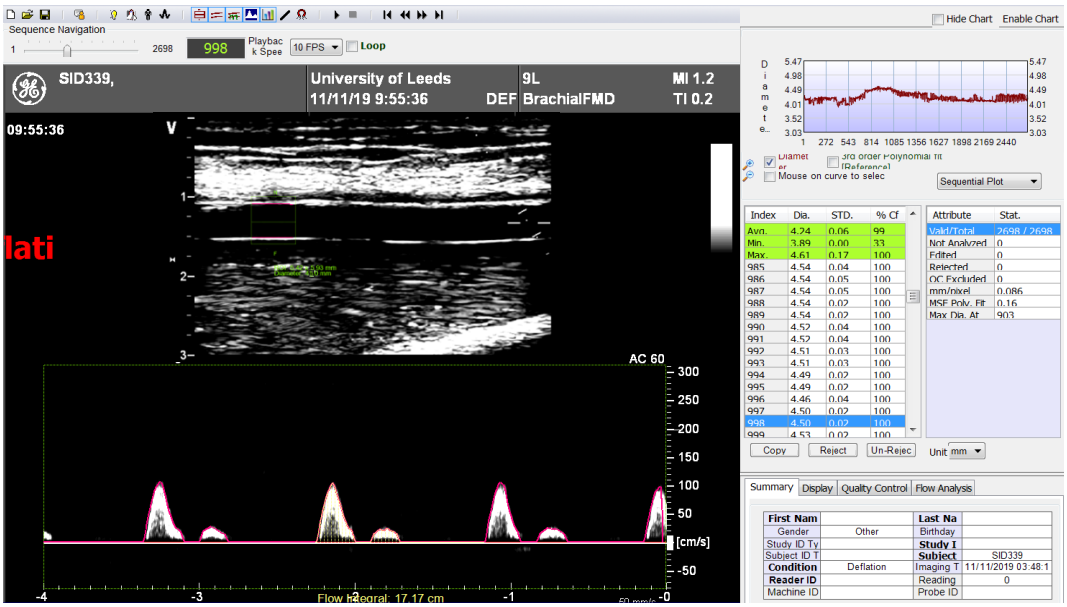

Figure 2.13 Analysis of brachial artery diameter and blood velocity using Brachial Analyzer for Research® Software. A region of interest (green box) was highlighted with clear vascular boundaries (tunica media visible on both sides of artery lumen). Semi-automated edge detection software was used to identify vessel walls (pink lines) and measure brachial artery diameter at rest and following a 5 min period of ischemia. A region of interest was also placed on the Doppler blood velocity trace to detect and measure anterograde waveforms.

A mean of all frames across the 30 s baseline diameter recording was taken to calculate 'baseline diameter'. A three-point rolling mean of arterial diameter post cuff inflation was performed to smooth data; the highest three-point mean was then determined as 'peak diameter'. Absolute and relative FMD were then calculated using the following equations:

$$Absolute\ FMD\ (mm) = Peak\ diameter - baseline\ diameter$$

$$Relative\ FMD\ (\%) = \frac{Peak\ diameter - baseline\ diameter}{baseline\ diameter} \times 100$$

Time to peak diameter was also calculated from the point of cuff deflation to the time of peak diameter.

2.10.3 Doppler blood flow velocity analysis

Blood velocity after cuff release was measured using Brachial Analyzer for Research® Software (Medical Imaging Applications LLC, Coralville, Iowa, USA). The doppler blood velocity profile was selected, and the X (time) and Y (velocity) axes were calibrated. The programme then automatically analysed the doppler trace of all cardiac cycles and mean blood velocity was calculated using the doppler shift equation:

$$Mean\ blood\ velocity\ (m/s) = \frac{doppler\ frequency\ x\ 1540}{(2\ x\ 5000)\ x\ cos\ \theta}$$

Where, 1540 m/s is the average velocity of sound in a tissue, 5000 is the transmitted frequency and θ is the angle of insonation. Peak hyperaemia was also calculated. This parameter was determined as the highest mean blood flow velocity after cuff release. Mean blood velocity was also used to calculate peak shear rate using the following equation:

$$Peak\ shear\ rate\ (s^{-1}) = \frac{Peak\ hyperaemia\ (\mathrm{cm}/s)}{Baseline\ diameter\ (mm)}\ x\ 8$$

In addition, the velocity-time integral (VTI) was calculated by Brachial Analyzer using the trapezium rule:

$$VTI = \frac{(V1 + V2)}{2}\ x\ t$$

In this equation V1 and V2 are net velocities and t is the time difference between the two velocities. VTI was determined for 60 and 90 s post-cuff deflation, enabling the area under the shear rate curve (AUC) to be calculated for these periods (i.e. AUC_{60} and AUC_{90}) as:

$$AUC = \frac{8\ x\ VTI}{Mean\ baseline\ diameter\ (mm)}$$

The between day reproducibility for brachial artery FMD and concomitant blood flow measurements from 8 participants are reported in Table 2.6.

Table 2.6 Between day reproducibility for FMD and concomitant blood flow measurements

	Test re-test variability (%)	Absolute difference
Baseline diameter (mm)	0.36	0.01
Peak diameter (mm)	0.46	0.02
Absolute FMD (mm)	3.45	0.02
Relative FMD (%)	3.36	0.64
Peak reactive hyperaemia (s^{-1})	10.52	7.1
Peak shear rate (s^{-1})	10.27	148
Shear rate AUC_{60}	3.65	5555
Shear rate AUC_{90}	3.45	6207

AUC = area under shear rate curve; FMD = flow-mediated dilation.

2.11 Statistics

Prior to each investigation, a Shapiro-Wilk test was used to confirm normal distribution and a Mauchly's test of sphericity to verify homogeneity of variance. The statistical operations performed following these initial assessments are detailed in the methods section of each study chapter. All data are presented mean ± SD, unless stated otherwise. The level of significance for all statistical analysis was accepted at $p \leq 0.05$. All statistical analysis was performed using IBM SPSS Statistics 24 (SPSS Inc., Chicago, IL, USA).

Chapter 3 Characterising the decline of maximal voluntary isokinetic power during ramp-incremental cycle exercise to intolerance

3.1 Introduction

Ramp-incremental exercise is the gold-standard test performed to assess parameters of aerobic function (e.g. lactate threshold and $\dot{V}O_{2peak}$), which are related to the ability to tolerate exercise. Understanding the physiological determinants of the performance limits identified during this test are important, as to perform activities of daily living and remain independent a minimum threshold of exercise tolerance is required. Furthermore, reductions in exercise tolerance that occur with ageing and the onset and progression of chronic disease are associated with reduced quality of life and increased risk of morbidity and mortality (Keteyian et al., 2016, Newman et al., 2006, Myers et al., 2002). Subsequently, understanding the mechanisms of exercise tolerance is critical for developing effective prevention and rehabilitation strategies.

Exercise-induced fatigue is a reduction in the force or power-generating capacity of the working muscle that is reversible with rest, and plays a key role in determining exercise tolerance (Bigland-Ritchie and Woods, 1984). This transient decrease in muscle performance is a consequence of central and peripheral factors. Central fatigue refers to processes that originate proximal to the neuromuscular junction, causing a reduction in the degree to which the central nervous system can activate skeletal muscle (Gandevia, 2001). Whereas, peripheral fatigue refers to processes that occur at or distal to the neuromuscular junction (i.e. within the skeletal muscle), resulting in impaired contractile function that reduces the capacity of the muscle to generate force/power when maximally activated (Bigland-Ritchie and Woods, 1984, Allen et al., 2008). Exercise-induced fatigue can be assessed by measuring the decline in force generated during maximal voluntary contractions. However, to

determine the peripheral and central components of exercise-induced fatigue use of non-volitional stimulated contractions are required. Common approaches include stimulating the surface of the muscle, peripheral nerve (electrical or magnetic) or the motor cortex (transcranial magnetic stimulation). Often, these stimulations are performed in isolation or combined with maximal voluntary contractions (i.e. interpolated twitch technique; Cairns et al., 2005, Gandevia, 2001, Gruet et al., 2014, Polkey et al., 1996, Millet et al., 2011).

However, due to the nature of external non-volitional stimulation techniques, they can only be performed using isometric or dynamic isokinetic single-joint exercise (e.g. knee extension exercise). These actions are vastly different to the complex, multi-muscle coordinated, and dynamic contractions used during whole-body exercise, such as running or cycling; actions that are relevant because they represent the reality of real-life locomotion, rehabilitation and exercise training (Coelho et al., 2015). Indeed, compared to whole-body exercise where maximum rates of ventilation, oxygen uptake and cardiac output can be achieved, single-joint exercise is associated with reduced cardiopulmonary strain at the limits of the task. Rossman et al. (2012) documented that heart rate and minute ventilation were ~20 and ~30% lower, respectively, at the point of task failure after knee-extensor exercise compared to whole-body cycle exercise. The contributions of peripheral and central fatigue at intolerance are also different following single-joint and whole-body exercise (Rossman et al., 2012). Despite equal changes in voluntary muscle activation and therefore similar levels of central fatigue after both exercise modalities, knee-extensor exercise resulted in a ~19% greater reduction in potentiated quadriceps twitch force (i.e. peripheral fatigue) than whole-body cycling exercise at task failure (Rossman et al., 2012). Thus, disparity exists between the integrated limitations to exercise in single-joint and whole-body exercise.

An alternative approach is to perform whole-body exercise and then assess exercise-induced fatigue using external stimulation techniques. However, this requires the participant to dismount the ergometer or treadmill prior to assessment, introducing a critical delay of ~2 min (Amann and Dempsey, 2008). The recovery of locomotor power is rapid, with the majority occurring within the first 2 min of exercise termination (Froyd et al., 2013, Coelho et al., 2015, Sargeant and Dolan, 1987). A new approach involving a modified ergometer circumvents this delay as it permits electrical stimulation whilst participants are seated on the ergometer. Nevertheless, fatigue is task specific, and this approach assesses isometric contractions of the quadriceps only, while whole-body exercise is dynamic and involves multiple muscle groups during the cycling motion (Temesi et al., 2017, Doyle-Baker et al., 2018, Kruger et al., 2019).

Ideally, exercise-induced fatigue would be measured *during* dynamic whole-body exercise (i.e. the task that evokes exercise limitation), without a delay between exercise cessation and fatigue assessment, to provide an insight into the mechanisms of exercise-induced fatigue. One approach that meets these criteria is to assess exercise-induced fatigue during whole-body exercise on a cycle ergometer via the reduction in maximal voluntary isokinetic power (MVIP; Coelho et al., 2015). This measurement can be made almost instantaneously (< 3 s) at any point during an exercise protocol, including at the limit of tolerance, by rapidly switching from standard hyperbolic cadence-independent to isokinetic cycling on the ergometer from which MVIP can then be measured (Coelho et al., 2015). This method of fatigue assessment provides a measurement of the velocity specific reduction in task-specific power, addressing two important factors associated with fatigue assessment in ergometry: 1) locomotor power output during ergometry is velocity dependent due

to the power-velocity relationship and 2) exercise-induced fatigue is task specific (Sargeant et al., 1981, Elmer et al., 2013, Beelen and Sargeant, 1991). Together, these characteristics of the MVIP assessment permit appropriate comparisons to be made before, during and after exercise to assess the magnitude of exercise-induced fatigue. Further, the rapid application of this technique, minimises the opportunity for recovery, resulting in an ideal assessment of exercise-induced fatigue (Coelho et al., 2015).

Concomitant electromyography (EMG) measurements of the lower limb during MVIP assessments can provide additional insight into the mechanism of exercise-induced fatigue (Coelho et al., 2015). Specifically, allowing insight into the proportion of exercise-induced that can be attributed to 'muscle fatigue' and 'activation fatigue', surrogate markers of peripheral fatigue and central fatigue, respectively. This is due to the strong linear relationship that exists between muscle activity (i.e. EMG) and power production (i.e. MVIP; Coelho et al., 2015). Changes in this relationship can infer the contributions of muscle activation and muscle fatigue to overall exercise-induced fatigue (Figure 3.1). For example, if muscle activation is reduced to 70% (i.e. EMG 70% of baseline maximum [$\%_{max}$]) during a maximal isokinetic effort but this still results in 70% of maximal power output (i.e. MVIP 70%$_{max}$), exercise-induced fatigue is solely attributed to activation fatigue (Figure 3.1: A to B). However, if during a maximal isokinetic effort, muscle activation remains at 100% (i.e. EMG 100%$_{max}$) but there is a 70% reduction in maximal power output (i.e. MVIP 30%$_{max}$), exercise-induced fatigue is attributed to muscle fatigue (Figure 3.1: A to C). Exercise-induced fatigue can also result from a combination of both activation and muscle fatigue, the contributions of which can then be identified through this relationship from identifying

the reduction in MVIP relative to that expected for the measured EMG (Figure 3.1: A to D).

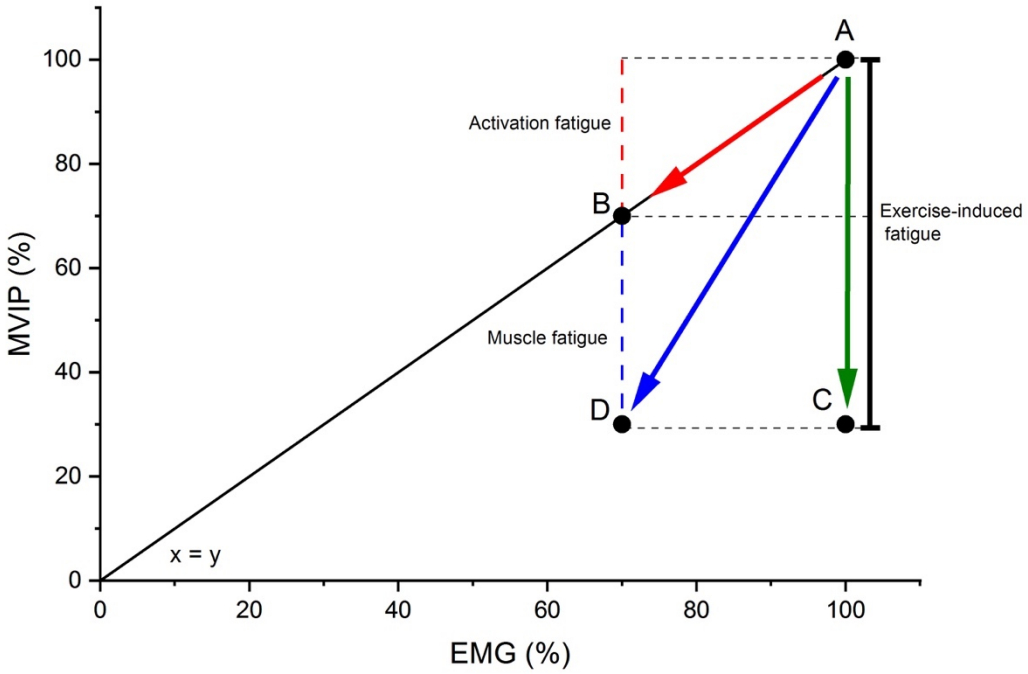

Figure 3.1 The linear relationship between electromyography (EMG) and maximal voluntary isokinetic power (MVIP) can be used to determine the proportions of exercise-induced fatigue due to muscle activation and muscle fatigue. Solid black line represents the line of identity. Black circles (●) represent MVIP measurements. MVIP measurements located on the line of identity indicate that an appropriate power has been generated for a given level of muscle activation. In the non-fatigued state, 100% EMG (i.e. muscle activation) results in 100% MVIP (A). If the MVIP measurement slides down the line of identity towards the origin (red arrow) exercise-induced fatigue is consequent to a reduction in muscle activation (B). If the MVIP measurement falls below the line of identity it represents a reduction in power for the given level of muscle activation, indicating muscle fatigue. Thus, the green arrow represents a reduction in MVIP due only to muscle fatigue (C). The blue arrow represents a reduction in MVIP due to muscle activation and muscle fatigue (D). The red and blue dashed line show the proportions of D attributed to activation and muscle fatigue, respectively.

Exercise-induced fatigue has previously been assessed using MVIP measurements in constant work rate exercise (Cannon et al., 2011). During moderate-intensity constant work rate exercise, below the lactate threshold where there is no

accumulation of fatigue-related metabolites (Wasserman et al., 1986, Black et al., 2017), there is no reduction in MVIP, consistent with the absence of exercise-induced fatigue (Cannon et al., 2011). However, during heavy-intensity constant work rate exercise, above the lactate threshold where there is an accumulation of fatigue-related metabolites, exercise-induced fatigue is present. Indeed, a 10 ± 5% reduction in MVIP was measured 3 min into heavy-intensity constant work rate exercise that was maintained until exercise termination at 8 min (Cannon et al., 2011). A greater reduction in MVIP (18 ± 14% reduction) was then reported after 3 min of very-heavy intensity exercise (supra-critical power) that was maintained until exercise cessation at 8 min (Cannon et al., 2011). The temporal characteristics of exercise-induced fatigue during heavy and very-heavy constant work rate exercise (early onset followed by no further reduction in MVIP) follow a similar time course to that of fatigue-related intramuscular metabolites (Rossiter et al., 2002). For example, there is a progressive increase in blood lactate, a marker for the metabolic acidosis, immediately after the onset of heavy-intensity constant work rate exercise that peaks within ~10 min of exercise before decreasing and stabilising at a lower magnitude (Wasserman et al., 1986), indicating a mechanistic link between disruption in intramuscular homeostasis and exercise-induced fatigue (Korzeniewski and Rossiter, 2020).

The limit of ramp-incremental exercise is associated with a significant reduction in MVIP of ~45-50%, indicating the presence of exercise-induced fatigue (Ferguson et al., 2016, Swisher et al., 2019, Coelho et al., 2015). This reduction in MVIP is consequent to a decline in muscle activation (EMG ~73% baseline value) and a reduction in power produced in response to this muscle activation at intolerance, suggesting muscle activation and muscle fatigue are contributory to the intolerance (Coelho et al., 2015, Ferguson et al., 2016, Davies et al., 2021). However, the temporal characteristics of exercise-induced fatigue, including the time course of

muscle activation and muscle fatigue contributions, during ramp-incremental exercise are unknown.

At intolerance in ramp-incremental exercise, MVIP is equal to the task demand (required flywheel power) in young individuals who are recreationally active, or endurance trained, as well as, older individuals, suggesting that task failure occurs because individuals are unable to meet the task demand (Ferguson et al., 2016, Davies et al., 2021). However, individuals with chronic disease may be able to briefly exceed task power at the point of intolerance in ramp-incremental exercise. Indeed, patients with chronic obstructive pulmonary disease are capable of producing a power that is ~2.6 times peak work rate (WR_{peak}) at the limit of ramp-incremental exercise (Cannon et al., 2016). In addition to identifying that a reserve in power output exists at intolerance in these individuals, these studies suggest that the mechanisms of fatigue that underpin intolerance in ramp-incremental exercise may vary depending on age, training and health status.

Characterising the time course of exercise-induced fatigue, including the proportions of fatigue that are attributable to activation and muscle fatigue, is likely to provide insight into the mechanisms of exercise intolerance and how these develop with time throughout the ramp-incremental test. An accurate understanding of the fatigue mechanisms that underpin intolerance is an important first step in developing effective interventions to improve exercise tolerance in both health and disease. Therefore, the primary aim of this study was to characterise the development of exercise-induced fatigue via the reduction in MVIP during maximal ramp-incremental exercise to intolerance. EMG was also measured during MVIP measurements to determine the proportions of exercise-induced fatigue consequent to muscle activation and muscle fatigue during the ramp-incremental test. In contrast to

constant work rate exercise, ramp-incremental exercise spans all intensity domains. Therefore, it was hypothesised that there would be no reduction in MVIP below the lactate threshold, but a progressive decline in MVIP above the lactate threshold to the limit of ramp-incremental exercise tolerance (Ferguson et al., 2016).

3.2 Methods

3.2.1 Participants and ethical approval

Ten healthy recreationally active males volunteered and provided written informed consent to participate in this study (24 ± 3 y; 179 ± 7 cm; 74 ± 8 kg). Participants were screened using a Health and Physical Activity Status Questionnaire and confirmed fit to exercise before beginning the study. For study inclusion and exclusion criteria see section 2.1.1. This study was approved by The Faculty of Biological Sciences Research Ethics Committee and all procedures conformed with the principles set out in the latest version of the declaration of Helsinki.

3.2.2 Exercise protocols

Participants completed two exercise protocols: 1) a ramp-incremental test (RI) and 2) a RI test with integrated measures of maximal voluntary isokinetic power (RI-MVIP). Each exercise protocol was performed on a separate visit to the laboratory in a randomised order, with visits separated by at least 24 hr. Participants were instructed to abstain from strenuous exercise (24 h) and food and caffeine consumption (3 h) before each testing session. All participants were familiarised with the testing environment and laboratory procedures at their first laboratory visit. At the start of both visits, participants performed two short (~6 s) bouts of maximal effort isokinetic cycling at 80 rpm to determine MVIP at baseline. Breath-by-breath pulmonary gas exchange was measured throughout both exercise protocols. Muscle activation (EMG) was assessed during all maximal voluntary isokinetic efforts.

3.2.2.1 Ramp-incremental exercise test (RI)

Following the completion of baseline MVIP measures, participants completed 2 min of seated rest on the cycle ergometer and a 4 min warm-up (20 W) before work rate on the cycle ergometer increased at a rate of 25 $W.min^{-1}$ until intolerance, determined as the point at which participants could not maintain a cadence above 50 rpm despite strong verbal encouragement. At the limit of tolerance, the cycle ergometer was rapidly switched from the hyperbolic to isokinetic cycling mode and participants performed a final maximal isokinetic effort at 80 rpm for ~6 s (Figure 3.2A). Participants cycled at ~80 rpm throughout this exercise test to match the cadence required in RI-MVIP. This exercise protocol permitted estimation of lactate threshold (LT) and $\dot{V}O_{2peak}$.

3.2.2.2 Ramp-incremental exercise test with measurement of maximal voluntary isokinetic power (RI-MVIP)

In line with the standard RI, following completion of the baseline MVIP measures, and after 2 min of seated rest on the cycle ergometer and a 4 min warm-up (20 W), the work rate on the cycle ergometer increased at 25 $W.min^{-1}$ until the point of intolerance. However, during this RI test, participants performed ~6 s of maximal effort isokinetic cycling at 80 rpm every 90 s. All participants received a 30 s and 10 s warning followed by a 5 s countdown to each maximal isokinetic effort. Participants were instructed to cycle at 80 rpm until 10 s before each maximal isokinetic effort when cadence was reduced to 75 rpm. This permitted a smooth transition between hyperbolic and isokinetic cycling modes when participants returned to 80 rpm because no electromagnetic braking resistance is applied below the target velocity. Due to the smooth transitions power during the RI-tests was indistinguishable between protocols (Figure 3.3). After each 6 s maximal isokinetic effort, participants re-commenced hyperbolic cycling and ramp-incremental exercise. At the limit of tolerance participants performed a final maximal isokinetic effort at 80 rpm for ~6 s (Figure 3.2B).

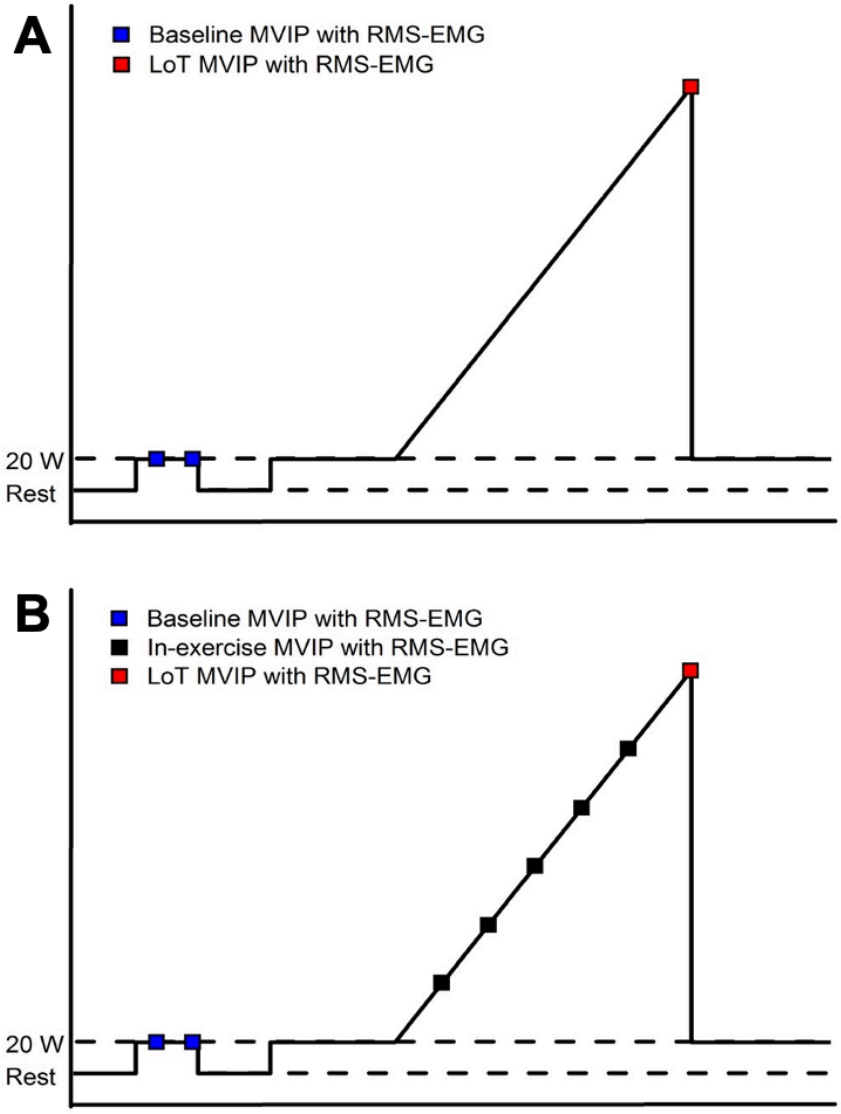

Figure 3.2 Schematic of exercise protocols. A: Ramp-incremental exercise test (RI), B: Ramp-incremental exercise test with integrated measures of maximal voluntary isokinetic power (RI-MVIP). MVIP was measured at baseline and at the limit of tolerance (LoT) in both protocols. In RI-MVIP, MVIP was also measured every 90 s in exercise. Root mean square EMG (RMS-EMG) was measured throughout all MVIP measurements.

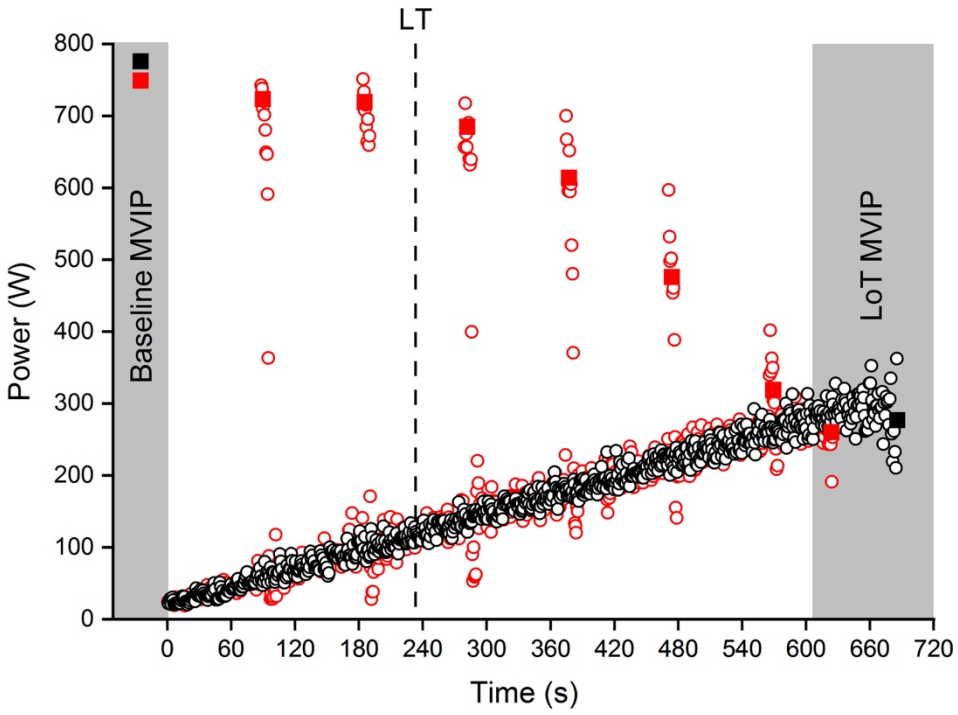

Figure 3.3 Representative participants pedal-by-pedal stroke power output (W) response during RI (○) and RI-MVIP (○) with MVIP measurements shown (RI: ■;RI-MVIP: ■). MVIP measurements represent the average power output for the first 3 pedal strokes constrained at the target cadence (80 rpm) during maximal isokinetic efforts. The lactate threshold (LT; dashed black line) is also identified.

3.2.3 Equipment and measures

3.2.3.1 Ergometry

Both exercise protocols were performed on a computer-controlled electromagnetically braked cycle ergometer (Excalibur Sport PFM, Lode, Groningen, The Netherlands) with the capacity to rapidly switch between hyperbolic and isokinetic cycling modes for measurement of MVIP (Cannon et al., 2011). Each MVIP measurement was calculated from the product of force (N m) and angular velocity (rad·s^{-1}). Force was measured every 2° of angular rotation by strain gauges in the crank axis, and angular velocity was calculated from three independent sensors sampling in succession in the bottom bracket assembly (Cannon et al., 2011). For additional details on the cycle ergometer and MVIP calculations see section 2.2 and 2.7.1.2.

3.2.3.2 Pulmonary gas exchange

Breath-by-breath pulmonary gas exchange was measured throughout both ramp-incremental exercise protocols using a gas analysis system (Cardio2, Medgraphics, Medical Graphics Corporation, St Paul, MN, USA; for details on this system see section 2.3). The system was calibrated immediately prior to each test; briefly, a 3 L syringe was used to calibrate the flow sensor over a range of physiological possible values expected at rest or during exercise. Gases of known concentrations (O_2: 12 and 21%; CO_2: 0 and 5%) were used to calibrate O_2 and CO_2 analysers. These gases were independently checked pre- and post-exercise to confirm no excessive drift. Participants were attached to a 12-lead ECG (Mortara X12+, Mortara Instrument, Milwaukee, WI, USA) throughout both exercise protocols to measure heart rate and monitor the electrical activity of the heart for any obvious abnormalities that would have resulted in the immediate termination of the test (e.g. ST segment elevation or depression).

3.2.3.3 Electromyography

Surface EMG was measured in five muscles of the right leg: gastrocnemius lateralis, biceps femoris, vastus lateralis, rectus femoris and vastus medialis (for precise anatomical positions see section 2.5.1). EMG signals were recorded at 1500 Hz. Prior to electrode placement, sites were shaved, abraded and cleaned using 70% isopropyl alcohol to minimise skin impedance. The leads connected to the electrodes were secured using surgical tape (3M, Bracknell, Berkshire, UK) to reduce signal artefacts caused by lead movement.

3.2.4 Data analysis

3.2.4.1 Pulmonary gas exchange

Breath-by-breath $\dot{V}O_2$ data collected during both exercise protocols was plotted against time and 99% prediction limits were fitted. Individual breaths located outside of the prediction limits were removed; these sporadic breaths typically result from the participant coughing/spluttering and are therefore unlikely to represent true $\dot{V}O_2$

(Lamarra et al., 1987). Working backwards from the last breath of ramp-incremental exercise, a 12-breath breath rolling average was applied 8 times to breath-by-breath $\dot{V}O_2$ data. $\dot{V}O_{2peak}$ was determined as the highest 12-breath mean derived from this process. LT was estimated from the RI test using the V-slope method and supporting ventilatory and pulmonary gas exchange criteria (Beaver et al., 1986b). Due to the continual oscillations in $\dot{V}O_2$ and $\dot{V}CO_2$ in the RI-MVIP test, consequent to integrated MVIP measurements, the LT could not be estimated from this protocol (Figure 3.4). For further details on $\dot{V}O_2$ data editing, estimation of LT and calculation of $\dot{V}O_{2peak}$ and other gas exchange variables see section 2.7.2.

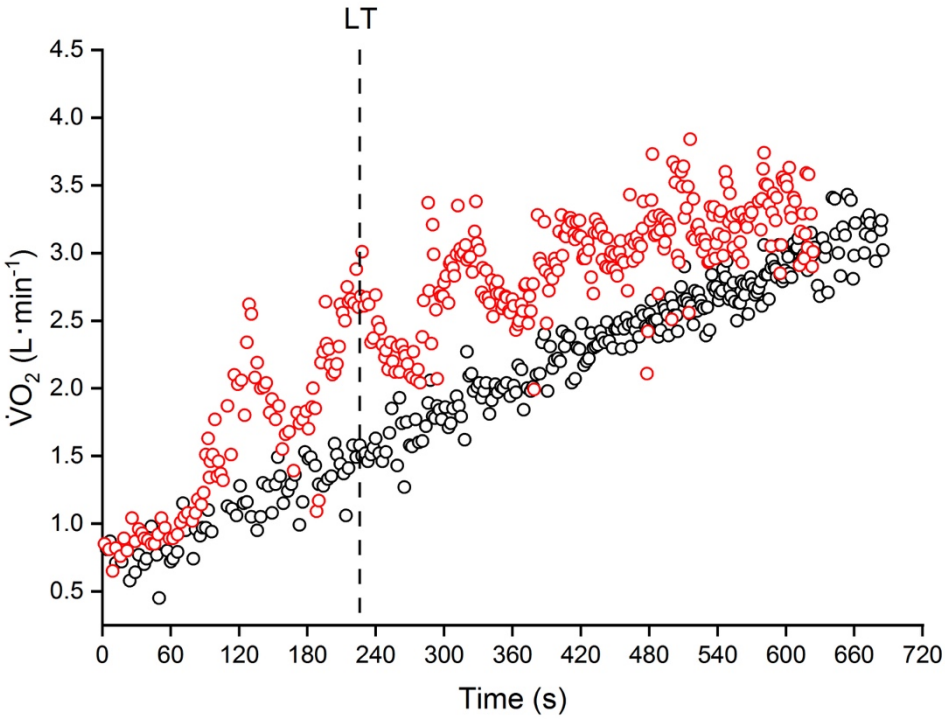

Figure 3.4 Representative participants oxygen uptake ($\dot{V}O_2$) response during RI (○) and RI-MVIP (○) exercise. The lactate threshold (LT; dashed black line) is also identified.

3.2.4.2 Maximal voluntary isokinetic power

The first three pedal strokes that were constrained at 80 ± 1 rpm during each maximal voluntary isokinetic effort were selected; these tended to be the 2nd, 3rd and 4th pedal strokes. The time between the last hyperbolic pedal stroke and first pedal stroke used

to measure MVIP was 2.7 ± 1.1 s. Isokinetic power was measured independently at the left and right crank axis every 2° of angular rotation. Left and right crank power for each pedal stroke was then summed to give a value for isokinetic power for each pedal stroke. A mean of the three pedal strokes was then taken to provide a final MVIP value. This value was then paired with the root mean square (RMS) EMG datum (described below).

There was no difference between the first and second MVIP measurements performed at baseline before each protocol (RI: 861 ± 109 vs. 857 ± 118, p = 0.78, test re-test variability = 3.6%; RI-MVIP: 852 ± 141 vs. 849 ± 131 W; p = 0.89, test re-test variability = 5.1%). Therefore, baseline MVIP was taken as the mean of the two measurements. Participants performed between 6 and 7 maximal isokinetic efforts during RI-MVIP (depending on RI-MVIP duration). All MVIP measurements were expressed as a % of the LT. Only MVIP measurements below and above LT that were common to all participants were included in the final analysis (n = 5), these were termed: Pre-LT 1, Pre-LT 2, Post-LT 1, Post-LT 2 and Post-LT 3. The magnitude of exercise-induced fatigue was calculated by subtracting MVIP at the limit of tolerance from MVIP at baseline.

When cycling in the hyperbolic (cadence independent) mode changes in cadence occur during RI exercise. These variations in cadence are detected almost instantaneously by the ergometer via a feedback loop and in response flywheel resistance is adjusted to maintain target power (i.e. programmed work rate). This results in fluctuations in crank power above and below the target flywheel power (see section 2.7.1.3; Figure 2.5). These fluctuations were measured throughout RI exercise in each participant to characterise the mean and 95% prediction limits of the pedal force measurements during the ramp-incremental task.

If maximal evocable power (i.e. MVIP) can be increased and is greater than the task demand (i.e. RI WR_{peak}) at the limit of tolerance, a 'power reserve' exists. Therefore, MVIP at the limit of tolerance was compared to RI WR_{peak} to determine if a power reserve was present or absent, with the 95% prediction limits of the fluctuation data used to determine the meaningfulness of this power reserve in a physiological context. In other words, a power reserve was considered to be present if the following conditions were met: 1. MVIP at the limit of tolerance was statistically greater than WR_{peak}, 2. The difference between MVIP at the limit of tolerance and WR_{peak} was greater than the natural fluctuation in pedal-by-pedal stroke power (deviation above or below the required task power) that occurs during hyperbolic cycling. For additional information on MVIP, WR_{peak}, and power reserve calculations see section 2.7.1.

3.2.4.3 Electromyography

A bandpass filter of 10-500 Hz was applied to raw EMG signals to reduce noise and artefact contamination. Raw EMG signals were then rectified, and RMS smoothed with a 100 ms time window. The three contractions corresponding to the three pedal strokes used to calculate each MVIP measurement were identified. For each pedal stroke, the peak RMS-EMG of each of the five muscle groups was determined and all values were summed. This derived a single RMS-EMG value for each of the three pedal strokes from which a mean was taken to derive an appropriate RMS-EMG datum to pair with the MVIP measurement. All RMS-EMG values were normalised to baseline MVIP (i.e. the visit maximum). Participants performed two baseline MVIP efforts before each protocol, however, there was no difference in RMS-EMG between these efforts (RI: 3810 ± 495 vs. 3885 ± 352 mV; $p = 0.75$; RI-MVIP: 3242 ± 892 vs. 3232 ± 682 mV; $p = 0.91$). Therefore, an average was calculated, and all RMS-EMG measurements were reported relative to this value (expressed as $\%_{max}$).

3.2.4.4 Work done

Pedal-by-pedal stroke power from RI and RI-MVIP exercise tests were plotted against time and integrated to calculate work done (work done [kJ] = (Power*Time power performed for [s]) / 1000; Figure 3.5). Work done during the MVIP measurements in RI-MVIP was also calculated and subtracted from the work done during the same time period in the RI protocol to determine the additional work done during maximal isokinetic efforts in RI-MVIP. Finally, RI duration was greater than RI-MVIP duration; therefore, the additional work done during ramp-incremental exercise in RI was calculated and compared to work done during MVIP in RI-MVIP.

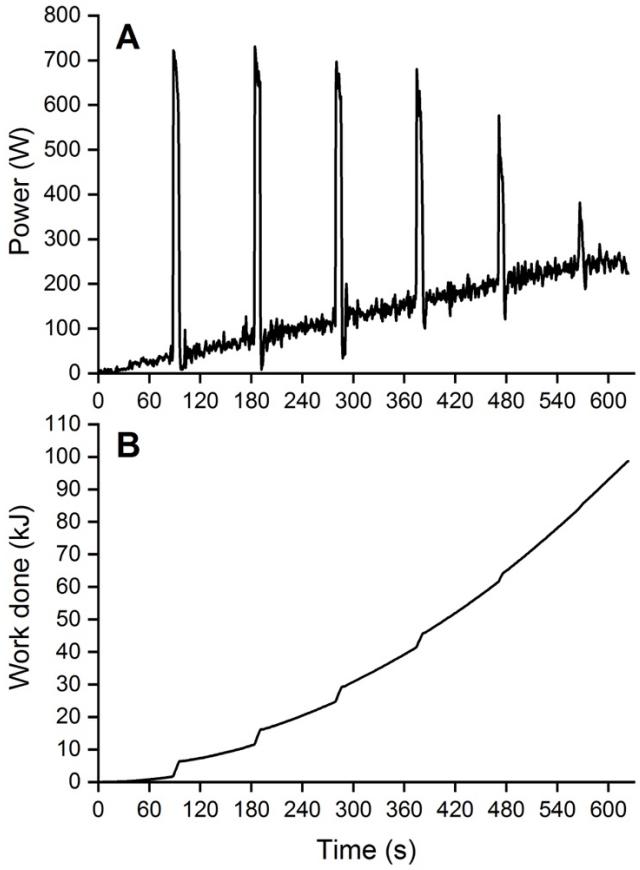

Figure 3.5 Work done during a ramp-incremental test with maximal voluntary isokinetic power measured every 90 s (RI-MVIP). A: Individual example of pedal-by-pedal stroke power during RI-MVIP plotted against time. B: Integration of graph A showing work done during RI-MVIP.

3.2.5 Statistics

Before any statistical tests were conducted, data were checked for normality using Shapiro-Wilk tests. Characteristics of the ramp-incremental protocols were compared using paired *t*-tests. Changes in MVIP and RMS-EMG over time during RI-MVIP were analysed using one-way repeated measures ANOVA. Where significant effects were identified, Bonferroni post-hoc tests were used to locate differences. Statistical significance was set at $p < 0.05$. Data are presented as means ± SD.

3.4 Results

3.4.1 Ramp-incremental exercise responses

The estimated LT was 1.91 ± 0.27 L·min^{-1} (50 ± 4% $\dot{V}O_{2peak}$). $\dot{V}O_{2peak}$ from RI and RI-MVIP protocols were not different ($p = 0.27$; Table 3.1). Peak ramp-incremental work rate (WR_{peak}) and time to intolerance (T_{lim}) were greater in RI compared to RI-MVIP (Table 3.1; $p < 0.05$). However, despite the longer T_{lim}, the addition of the MVIP measures during RI-MVIP meant that work done was 5.0 ± 5.1% greater in RI-MVIP compared to RI (RI-MVIP vs. RI; 104.4 ± 16.4 vs. 99.9 ± 17.5 kJ; $p = 0.01$).

Table 3.1 Characteristics of RI and RI-MVIP protocols.

Parameter	RI	RI-MVIP
WR_{peak} (W)	311 ± 27	285 ± 23*
T_{lim} (s)	697 ± 64	636 ± 54*
LT ($L \cdot min^{-1}$)	1.91 ± 0.27	
$\dot{V}O_{2peak}$ ($L \cdot min^{-1}$)	3.77 ± 0.53	3.86 ± 0.4
$\dot{V}O_{2peak}$ ($ml \cdot min^{-1} \cdot kg^{-1}$)	52 ± 8	53 ± 6
$\dot{V}CO_{2peak}$ ($L \cdot min^{-1}$)	4.56 ± 0.59	4.54 ± 0.50
RER_{peak}	1.21 ± 0.06	1.19 ± 0.04
$\dot{V}_{Epeak}$ ($L \cdot min^{-1}$)	158 ± 30	164 ± 28
HR_{peak} (bpm)	179 ± 10	181 ± 9

Values are mean ± SD. *n* = 10 for both protocols. LT = Lactate threshold; RER_{peak} = peak respiratory exchange ratio; T_{lim} = time to the limit of tolerance; $\dot{V}_{Epeak}$ = peak ventilation; $\dot{V}CO_{2peak}$ = peak carbon dioxide output; $\dot{V}O_{2peak}$ = peak oxygen uptake; WR_{peak} = peak work rate. All parameters were compared using paired *t*-tests. *significantly different to RI.

3.4.2 Exercise-induced fatigue in RI and RI-MVIP

All MVIP measurements were constrained at 80 rpm (80.4 ± 0.31 $rev \cdot min^{-1}$). MVIP at baseline was not different between ramp-incremental protocols (p = 0.86; Figure 3.6) and did not differ within individuals between test visits (test re-test variability = 2.9%). MVIP at the limit of tolerance (LoT MVIP) was also not different between protocols (Figure 3.6; RI vs. RI-MVIP: 358 ± 96 vs. 389 ± 111; p = 0.53). Further, the decline in MVIP from baseline to the limit of tolerance was not different in RI and RI-MVIP (RI vs. RI-MVIP: 501 ± 115 vs. 461 ± 133; p = 0.48), thus both protocols induced the same magnitude of exercise-induced fatigue.

In the RI protocol, MVIP at the limit of tolerance was not different to WR_{peak} (measured at flywheel; WR_{peak}: 311 ± 27 W; LoT MVIP: 358 ± 96 W; p = 0.16; Figure 3.6). Thus,

there was no reserve in power at the limit of tolerance in the RI protocol. However, because WR_{peak} was lower in the RI-MVIP protocol, MVIP at the limit of tolerance was greater than WR_{peak} (WR_{peak}: 285 ± 23 W; LoT MVIP: 388 ± 113 W; p = 0.01; Figure 3.6). The difference between WR_{peak} and LoT MVIP in RI-MVIP was only greater than the individual upper limit of natural fluctuation in crank power output in 4 out of 10 participants (Figure 3.7), suggesting a physiologically significant power reserve was only present in these 4 individuals. Peak RMS-EMG activity measured at intolerance during LoT MVIP was not different between protocols (RI vs. RI-MVIP: 69 ± 15 vs. 73 ± 14%$_{max}$; p = 0.48).

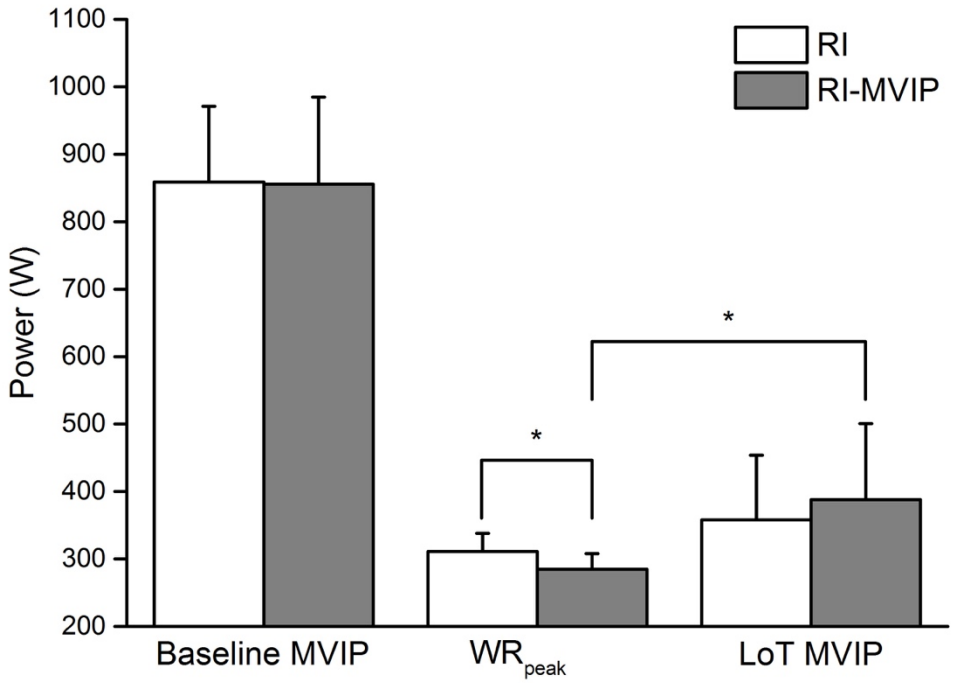

Figure 3.6 Maximum voluntary isokinetic power at baseline (Baseline MVIP), peak work rate (WR_{peak}) and isokinetic power at the limit of tolerance (LoT MVIP). *indicates significant difference between measurements.

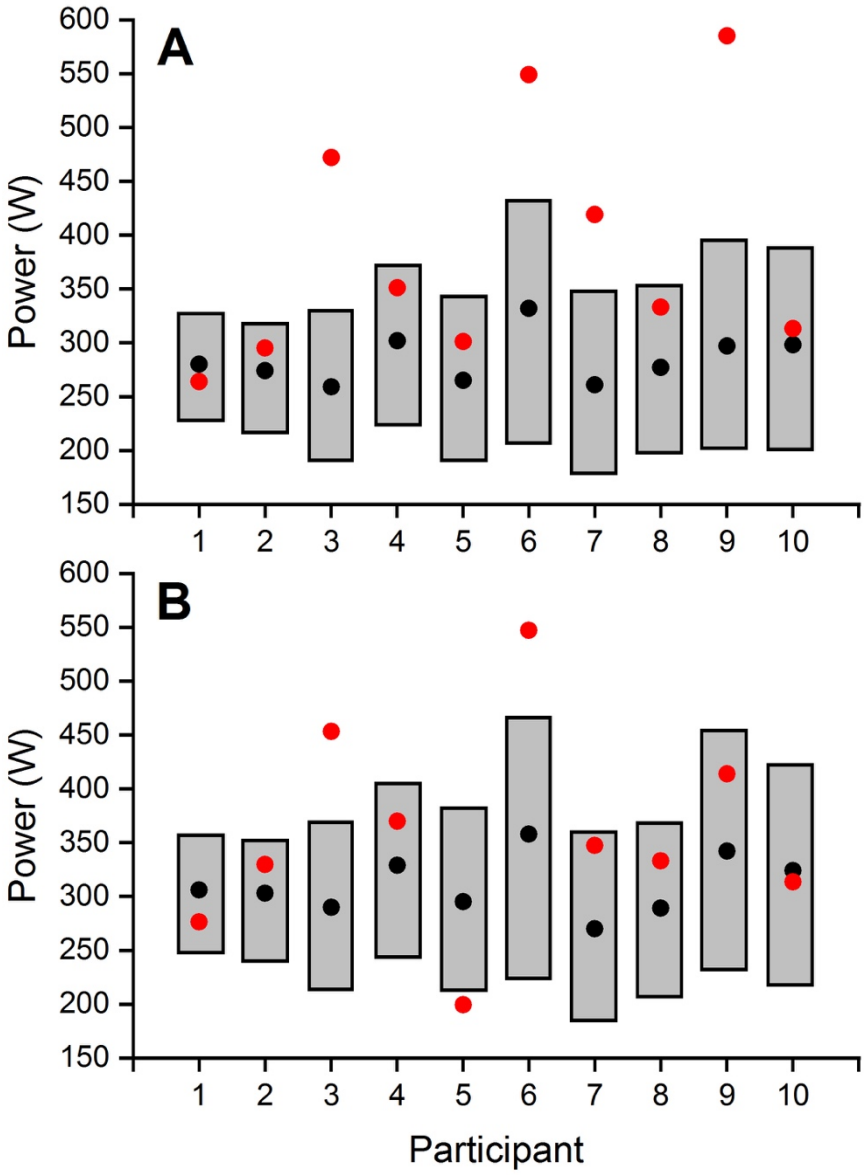

Figure 3.7 Natural fluctuation in pedal-by-pedal stroke power for each participant in (A) RI-MVIP and (B) RI. Black circles (●) represent WR_{peak} and red circles represent MVIP at LoT (●). Grey box represents individual fluctuation in pedal-by-pedal stroke power output for each participant at WR_{peak}. A reserve in power at the limit of ramp-incremental exercise is present in participant 3, 6, 7 and 9 in RI-MVIP but only in participant 3 and 6 in RI.

3.4.3 Temporal characteristics of exercise-induced fatigue in RI-MVIP

There was no decrease in MVIP below the lactate threshold when compared to baseline in RI-MVIP (Figure 3.8; $p > 0.05$). The first MVIP after the lactate threshold (Post-LT 1) was also not different compared to baseline, despite a 7.7 ± 7.0% reduction in maximal power generation (Figure 3.8; $p = 0.82$). However, there was a subsequent progressive decrease in MVIP from Post-LT-1 to the limit of ramp-incremental exercise (Figure 3.8; $p < 0.05$). In contrast, the sum of RMS-EMG was only reduced in comparison to baseline at the limit of tolerance (Figure 3.9). Therefore, MVIP decreased before there was any reduction in muscle activation (RMS-EMG) during the RI-MVIP (Figure 3.10).

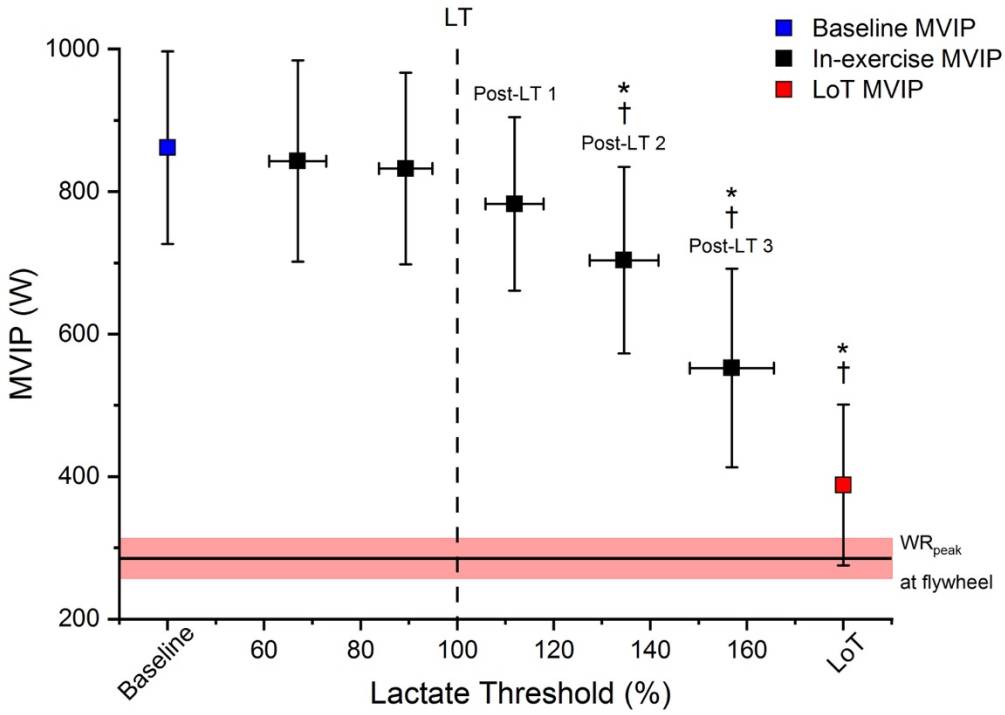

Figure 3.8 Mean (± SD) maximal voluntary isokinetic power (MVIP) during RI-MVIP. Also shown are the lactate threshold (LT; vertical dashed line) and RI-WR_{peak} (horizontal solid line, with the 95% prediction limits of the natural fluctuation in crank power represented by red box). * ($p < 0.05$) reduction in MVIP from baseline; † ($p < 0.05$) reduction in MVIP from previous MVIP. LoT = limit of tolerance.

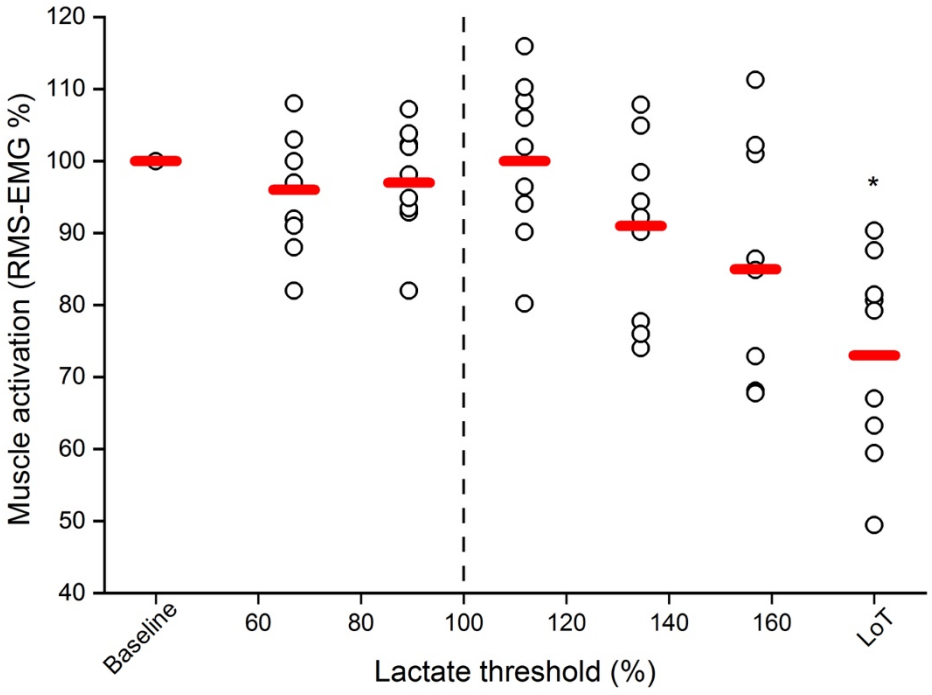

Figure 3.9 RMS-EMG during isokinetic cycling in RI-MVIP. Individual data presented (open circles) with mean (red lines). RMS-EMG expressed as % of baseline RMS-EMG. * (p < 0.05) reduction in RMS-EMG compared to baseline.

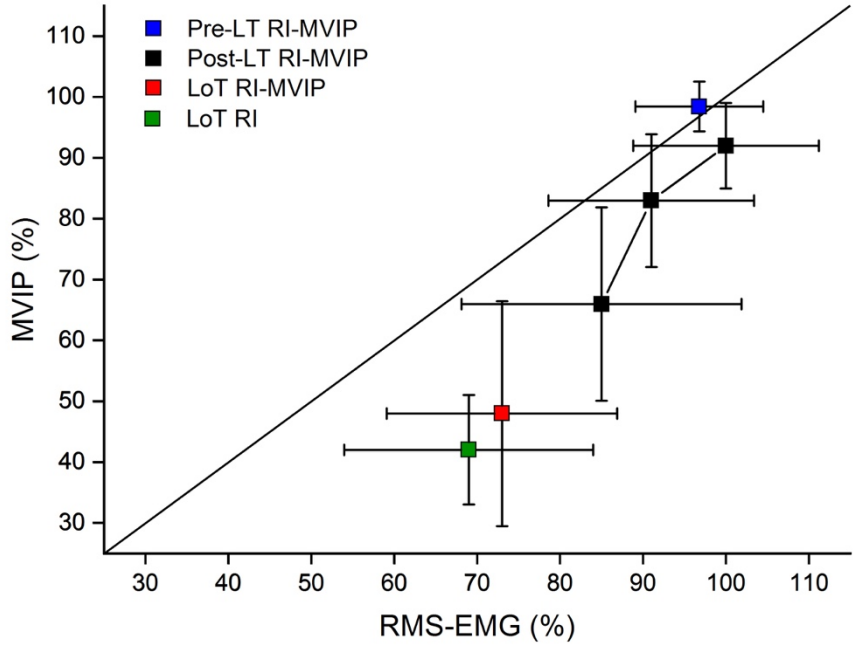

Figure 3.10 Relationship between MVIP and RMS-EMG during RI and RI-MVIP. MVIP and RMS-EMG expressed as % of baseline. Data presented as mean (± SD). Solid black line is line of identity.

3.6 Discussion

These data demonstrate for the first time that during ramp-incremental exercise, exercise-induced fatigue (measured via the reduction in MVIP) is only present after the lactate threshold has been exceeded. After the lactate threshold during RI exercise, exercise-induced fatigue increases in magnitude until MVIP intercepts with task demand to induce exercise intolerance once the neuromuscular limits for power production have been reached. Thus, the results of this study were consistent with our hypothesis and support the discrete responses seen during constant work rate exercise (Cannon et al. 2011), and the theory proposed by Ferguson et al. (2016) for incremental exercise. This study has also shown that muscle activation contributions to the reduction in MVIP occur after reductions due to muscle fatigue, suggesting peripheral mechanisms of fatigue are responsible for the initial reduction in MVIP observed above the lactate threshold in RI exercise.

3.6.1 Temporal characteristics of exercise-induced fatigue in RI-MVIP

RI exercise spans all intensity domains: moderate through to heavy then very-heavy intensity exercise (Whipp et al., 1981). The time course of exercise-induced fatigue seen in this study during RI exercise mirrors the profile of the intramuscular metabolite responses and muscle fatigue responses to discrete moderate, heavy and very-heavy intensity constant work rate exercise tests.

For moderate-intensity exercise the rapid attainment of a steady state negates any net contribution from anaerobic glycolysis to meet ATP demands of the task. Subsequently, for exercise within this domain, there is no metabolic acidosis, and metabolic perturbations are constrained below critical limits. Even when performed to intolerance, following a long period of moderate intensity exercise (~3-4 h), muscle phosphocreatine (PCr) remains at ~76% of the baseline value, whilst pH and blood lactate remain largely unchanged from resting values (Black et al., 2017,

Korzeniewski and Rossiter, 2020). The lack of fatigue-related metabolite accumulation during moderate-intensity exercise is then consistent with the absence of exercise-induced fatigue in this exercise intensity domain unless the exercise is performed for a prolonged period of time (Lepers et al., 2002). In line with this, when measuring MVIP, there is no decrease following 3 and 8 min of moderate intensity constant work rate cycling exercise (Cannon et al., 2011). Thus, the absence of a decline in MVIP below the lactate threshold during RI exercise in this study is consistent with the known voluntary (MVIP) fatigue response to moderate-intensity constant work rate exercise where muscle fatigue is absent (Cannon et al., 2011).

For exercise in the heavy-intensity domain a steady state in aerobic energy transfer can still be achieved; however, it can be delayed by up to 15 min (Barstow and Mole, 1991). Consequently, it is necessary for PCr breakdown and glycolysis to make substantial contributions to the energy transfer during heavy-intensity exercise, until this $\dot{V}O_2$ steady state can be achieved, with the greatest rate of contribution at the start of the exercise. Although stabilised over time, this results in a sustained elevation in inorganic phosphate and adenosine diphosphate that is significantly greater than the increases seen in moderate-intensity exercise, as well as a metabolic acidosis (Wasserman et al., 1986, Jones et al., 2008). The concentration of inorganic phosphate within the heavy-intensity domain has been proposed to exceed a ‘critical’ value that triggers a cascade of fatigue-related events that induce exercise-induced fatigue (Korzeniewski and Rossiter, 2020). Consequently, the time course of this disruption in homeostasis parallels the dynamics of exercise-induced fatigue during heavy-intensity exercise. Several authors have described a rapid onset of fatigue at the start of heavy-intensity exercise followed by the maintenance of peak torque (Cannon et al., 2011, Sargeant and Dolan, 1987). Indeed, there was a 10% reduction in MVIP after 3 min of heavy-intensity constant work rate cycle exercise that was maintained until exercise termination at 8 min (Cannon et al., 2011). The

presence of exercise-induced fatigue in this intensity domain is pronounced; 1 hour of heavy-intensity intermittent isometric quadriceps contractions resulted in a ~65-70% decline in maximal voluntary contraction from its pre-exercise value (Burnley et al., 2012). In line with non-volitional muscle fatigue and MVIP responses to heavy-intensity constant work rate exercise, a reduction in MVIP was identified after the lactate threshold in RI exercise. Although the first MVIP after the lactate threshold (i.e. Post-LT 1) was not different from baseline, despite a 7.7 ± 7.0% reduction in power, this change was similar to the 10% reduction in MVIP reported after 3 and 8 min of heavy-intensity constant work rate exercise (Cannon et al., 2011). In the present study, the absence of a statistical reduction is likely a consequence of performing MVIP assessments every 90 s, rather than at a specific $\dot{V}O_2$. This meant that post-LT 1 was performed somewhere between 0-90 s after the lactate threshold, and therefore measurement of Post-LT 1 ranged from 102-120% of the lactate threshold (mean ± SD: 112 ± 6%), and likely with a variable fatigue between participants. Nevertheless, the subsequent reduction in post-LT 2 compared to baseline MVIP, still demonstrates exercise-induced fatigue only occurs above the lactate threshold in RI exercise.

Within the very-heavy intensity domain a steady state cannot be achieved, and the rate of ATP resynthesise continues to rise over time (Cannon et al., 2014, Poole et al., 1988). Subsequently, this domain is associated with a progressive loss of muscle metabolic homeostasis with time (Jones et al., 2008). Indeed, the greatest reductions in PCr and greatest increases in inorganic phosphate and hydrogen ions, are reported during very-heavy intensity exercise (Black et al., 2017, Jones et al., 2008). Elevations in inorganic phosphate and hydrogen ions reduce power generation by disrupting cross-bridge cycling and reducing myofibrillar Ca^{2+} sensitivity (Fitts, 2008). The latter is particularly important because fatigue is associated with a reduction in the size of Ca^{2+} transients (Fitts, 2008). In addition to the effects of inorganic

phosphate and hydrogen ions, a reduction in intracellular potassium that occurs more profoundly in very-heavy intensity exercise than heavy intensity exercise, plays an important role in the fatigue cascade by compromising plasma membrane excitability (Black et al., 2017, Clausen and Nielsen, 2007). In accordance with the increase in exercise-related fatigue metabolites in very-heavy intensity exercise (compared to heavy), this domain is associated with greater exercise-induced fatigue. This is supported by the ~6-26 $N \cdot m \cdot min^{-1}$ greater rate of decline in maximal voluntary contraction per min during very-heavy versus heavy-intensity intermittent quadriceps contractions (Burnley et al., 2012). The same fatigue response has been demonstrated in dynamic whole-body exercise, following 8 min of heavy and very-heavy intensity constant work rate cycling, the latter resulted in an additional ~8% reduction in MVIP (Cannon et al., 2011). The progressive reduction in MVIP from Post-LT 1 to the limit of RI exercise conforms with MVIP responses to very-heavy intensity constant work rate exercise where a greater reduction in MVIP is seen during very-heavy than heavy-intensity exercise (Cannon et al., 2011).

The parallels between exercise-induced fatigue during RI exercise and known intramuscular metabolic responses to moderate, heavy and very-heavy constant work rate exercise, supports that a close link exists between metabolite accumulation and fatigue development, reflected in the reduction in MVIP.

3.6.2 Temporal characteristics of muscle activation during RI-MVIP

Exercise intolerance during dynamic whole-body RI exercise is complex and is likely explained by a multitude of interacting mechanisms. In the present study, a progressive decline in MVIP occurred from Post-LT 1 to the limit of tolerance; however, there was no reduction in RMS-EMG until the limit of tolerance. This response suggests distinct kinetics of ‘muscle fatigue’ and ‘activation fatigue’, with muscle fatigue occurring first during RI exercise and activation fatigue appearing later

toward task failure. In line with this finding, using external stimulation techniques, Decorte et al. (2012) reported that peripheral fatigue develops early in high-intensity constant work rate exercise and central fatigue is associated with task failure. A reduction in voluntary muscle activation was also only seen in the last quarter (after ~180 s) of knee extensor exercise prior to task failure at 243 ± 69 s, whereas maximum voluntary contractions and contractions evoked by electrical peripheral nerve stimulation fell progressively within ~60 s of exercise onset as a consequence of peripheral fatigue (Gruet et al., 2014).

The dynamics of muscle fatigue and subsequent activation fatigue during RI exercise may be underpinned by feedback from group III/IV muscle afferents. The rate of exercise-induced fatigue development during exercise can be altered by changes in arterial oxygen content or work rate, changing time to task failure. However, irrespective of these changes, at the point of task failure, a similar intramuscular metabolic perturbation and level of peripheral fatigue is present; often referred to as the 'critical threshold' (Amann et al., 2006, Amann and Dempsey, 2008, Gagnon et al., 2009, Burnley et al., 2010). During dynamic exercise, group III/IV muscle afferents provide feedback to the central nervous system pertaining the mechanical strain and metabolic state of the working locomotor muscles (Rotto and Kaufman, 1988, Mitchell et al., 1983). During fatiguing cycle exercise, neural feedback from group III/IV muscle afferents depresses the excitability of motor cortical cells that causes a reduction in central motor drive (Sidhu et al., 2017). In turn, voluntary muscle activation is attenuated, potentially compromising exercise performance, to regulate the degree of peripheral fatigue and protect the homeostasis of the organism (i.e. stop it surpassing the critical threshold; Amann, 2011, Amann and Dempsey, 2008). This is supported by studies that have blocked the effects of group III/IV muscle afferents, via pharmacological intervention (intrathecally administrated fentanyl), during high-intensity constant work rate exercise and shown an increase in central

motor drive and peripheral fatigue at task failure (Amann et al., 2011, Amann et al., 2009). Thus, the development of activation fatigue occurs in response to muscle fatigue.

At the limit of RI exercise, exercise-induced fatigue was consequent to muscle and activation fatigue (Figure 3.10). Thus, central mechanisms of fatigue relating to muscle activation and peripheral mechanisms of fatigue combine to reduce MVIP, usually to the point that task power cannot be exceeded (i.e. no power reserve), resulting in intolerance. However, the specific mechanism through which this integration occurs to induce task failure remains unknown. In line with previous studies, the reduction in muscle power production was proportionally greater than the reduction in muscle activation at the limit of RI exercise (i.e. greater reduction in MVIP for the given reduction in RMS-EMG; Figure 3.10). This finding indicates that exercise-induced fatigue at the limit of RI exercise was primarily due to peripheral mechanisms of fatigue rather than central mechanisms of fatigue relating to muscle activation.

3.6.3 MVIP at limit of RI and RI-MVIP exercise tests

At the limit of RI exercise, MVIP was not different from task power. This suggests that exercise intolerance occurred because individuals were unable to generate the power that the task demanded due to neuromuscular fatigue. This finding is in agreement with several previous studies that have measured MVIP at the limit of a standard RI exercise test in healthy individuals and shown that there is either no power reserve or a small (~ 10%) power reserve (Ferguson et al., 2016, Coelho et al., 2015, Cannon et al., 2016). Conversely, at the limit of RI-MVIP exercise, MVIP was greater than task power. However, further analysis found that MVIP at the limit of tolerance was only greater than task power by a magnitude that exceeded the natural fluctuation in pedal-by-pedal stroke power expected at the limit of RI exercise

in 4 participants. Thus, a physiologically significant power reserve was only present in 4/10 participants (Figure 3.6). In contrast, in the RI protocol, where there was no difference between task power and MVIP at the limit of tolerance, 2/10 participants demonstrated a physiologically significant power reserve. Importantly, there was no difference in $\dot{V}O_{2peak}$ or any other cardiorespiratory parameter at intolerance (e.g. HR_{peak}, $\dot{V}_{Epeak}$, $\dot{V}CO_{2peak}$) between the RI and RI-MVIP exercise test, showing participants provided a maximal effort during both exercise protocols. The presence of a power reserve suggests the perceptual and physiological limits of these individuals were briefly uncoupled during RI-MVIP, permitting a brief (~6 s) increase in power generation that exceeded the task demand at intolerance. It is possible that the additional isokinetic efforts in RI-MVIP increased mechanical strain and the accumulation of intramuscular fatigue metabolites, particularly if fast twitch (type II) fibres were recruited that are less oxidatively efficient and more fatigable, thus increasing the magnitude of metabolic disturbance (Grassi et al., 2015). Although speculative, this may have caused an increase in group III/IV muscle afferent feedback and perceived exertion for a given level of neuromuscular fatigue. In small muscle mass exercise, the blockage of group III/IV muscle afferent feedback can reduce the rate of perceived exertion at task failure by 50-60% (Broxterman et al., 2018, Broxterman et al., 2017). If an increase in the perception of effort occurred during the RI-MVIP protocol due to increased afferent feedback it may result in task failure occurring at a lower level of neuromuscular fatigue, and therefore, the presence of a power reserve at the limit of tolerance. This is supported by a lower level of peripheral fatigue being measured at the limit of RI exercise in individuals with a power reserve (single leg isokinetic dynamometer power) compared to those without a power reserve (Hodgson et al., 2018).

Swisher et al. (2019) measured MVIP at the limit of RI exercise using an almost identical protocol (MVIP was measured at 70 not 80 rpm) and found a greater reserve

in power generation (Swisher et al. vs. RI-MVIP in current study: 47 ± 31 vs. 36 ± 37% of WR_{peak}). Other authors have observed large significant power reserves (Morales-Alamo et al., 2015, Marcora and Staiano, 2010); however, these large power reserves are thought to be the result of the methodology rather than the underlying physiology. Morales-Alamo et al. (2015) assessed power generation using isokinetic cycling with power measured every 2° of angular rotation (i.e. the same method as the current study) but reported instantaneous peak power (i.e. highest 2° measurement of power), whereas Marcora and Staiano (2010) failed to control contraction velocity during the maximal power generation protocol, confounding these results. Thus, evidence suggests that there is no reserve in power at the limit of RI exercise in healthy individuals.

3.6.4 Exercise tolerance in RI and RI-MVIP exercise tests

Time to the limit of tolerance was greater in the RI than RI-MVIP protocol by 61 ± 24 s. However, the magnitude of exercise-induced fatigue at limit of RI exercise was not different between protocols; the ~56% reduction in MVIP at the limit of RI exercise in this study is similar to the ~45-50% reduction observed in previous studies (Ferguson et al., 2016, Coelho et al., 2015, Swisher et al., 2019, Davies et al., 2021).

This suggests that the rate of exercise-induced fatigue development was greater in the RI-MVIP than RI protocol as the same reduction in MVIP that was reached by 697 ± 64 s in RI was reached by 636 ± 54 s in RI-MVIP. It is likely that the additional work required during isokinetic efforts in the RI-MVIP protocol accelerated the development of exercise-induced fatigue, compromising time to intolerance. The metabolic consequence of maximal isokinetic efforts performed during moderate-intensity RI exercise (i.e. Pre-LT 1 and Pre-LT 2) is likely to have been very minor, with those performed in the heavy-intensity domain also having a minimal effect. This is because these exercise intensity domains are below the ‘critical power’ threshold;

the highest sustainable metabolic rate that is associated with a constant level of $\dot{V}O_2$ and metabolic (e.g. muscle and blood acid-base status) variables (Poole et al., 2016, Jones et al., 2019). As such, exercise in these domains should theoretically be associated with an 'oxidative metabolic reserve' that can be used for recovery processes, such as the replenishment of high-energy phosphates and clearance of H^+ (Jones and Vanhatalo, 2017). However, above critical power, in the very-heavy intensity domain, when the metabolic rate is no longer sustainable and $\dot{V}O_2$ and lactate increase inexorably until $\dot{V}O_{2peak}$ and the limit of tolerance are attained, recovery of high-energy phosphates is not possible. This is supported by Coats et al. (2003); after performing high-intensity constant work rate exercise that resulted in intolerance in 360 s, 6 participants were instructed to continue cycling for as long as possible (for a maximum of 20 min) at a work rate that was reduced to either 80% lactate threshold, 90% critical power or 110% critical power. When work rate was reduced to 80% lactate threshold all participants were able to cycle for 20 min; however, only 2 participants cycled for 20 min when work rate was reduced to 90% critical power with the remaining participants fatigued after ~10 min. Nonetheless, when power was reduced to 110% critical power participants were only able to tolerate an additional ~30 s of exercise. Thus, although inter-subject variability existed in time to intolerance at 90 and 110% critical power, this study demonstrates that recovery after very-heavy intensity exercise to intolerance only occurs at a work rate below critical power. In line with this, Chidnok et al. (2013) reported that single-leg knee-extension exercise to intolerance immediately followed by heavy-intensity exercise, permits the rapid recovery of PCr with 76% of baseline levels recovered in 10 min. However, when the same trial to intolerance was succeeded by very-heavy intensity exercise, muscle PCr was unable to recover and only reached ~37% of baseline in 10 min. In accordance, it is likely that the high-energy phosphates depleted during maximal isokinetic efforts performed above critical power in RI exercise is unrecoverable. Subsequently, maximal isokinetic efforts during RI

exercise reduce the finite energy store (specifically PCr) available to maintain RI exercise. In turn, whilst the same fatigue cascade likely occurs after energy stores have been depleted, this depletion occurs earlier in RI-MVIP than RI exercise because the store is essentially smaller due to the MVIP efforts, compromising time to intolerance. In support of this notion, the amount of work performed by participants during the MVIP measurements in RI-MVIP (20.4 ± 5.3 kJ) was not different to the work done during the extra time spent performing RI exercise in the standard RI compared to the RI-MVIP (16.8 ± 7.2 kJ; p = 0.325).

3.6.5 Future direction and limitations

The technique used to measure exercise-induced fatigue in this study relies on participants providing a maximal voluntary effort and is not independently verified by the application of an external stimulation technique. Thus, there is potential for MVIP data to be influenced by volitional effort. Non-volitional stimulation measures can be used to quantify the peripheral and central components of exercise induced fatigue; however, the application of these techniques instantaneously during dynamic whole-body exercise necessitates isometric contraction (Temesi et al., 2017, Doyle-Baker et al., 2018) rather than dynamic isokinetic contraction (the same contraction as the fatiguing task). This may confound findings as task specificity is a central aspect in the aetiology of fatigue (Bigland-Ritchie et al., 1995). Alternatively, participants dismount the ergometer for fatigue measurements to be made using external stimulation, but this introduces a time delay that may result in an underestimation of peripheral and central fatigue (Place et al., 2010). Furthermore, it would require many more study visits because each RI exercise test would have to be terminated following each fatigue measurement, substantially increasing participant burden. Although MVIP measurements depend on a maximal effort, the simplicity of the protocol means they can be integrated into whole-body exercise at any point, without inducing a time delay, providing an instantaneous measure of exercise-induced fatigue that represents the capacity of the individual to continue the task.

Whilst it is possible that volitional effort influenced MVIP measurements, the high reproducibility between each baseline MVIP before each test (test re-test variability = 2.9%) and MVIP measured before the lactate threshold (i.e. Pre-LT 1 and Pre-LT 2) in RI-MVIP (test re-test variability = 2.6%), suggests participants provided a maximal effort because it would be difficult to reproduce submaximal efforts to this level of precision. It is likely that familiarisation to MVIP efforts minimised variations between baseline MVIP measures. By nature, RI exercise tests are also predisposed to be influenced by volitional effort. However, the consistent cardiopulmonary values (e.g. $\dot{V}O_{2peak}$, HR_{peak}, $\dot{V}CO_{2peak}$) measured at intolerance in both tests suggest participants applied maximal efforts. Nevertheless, this protocol characteristic emphasises the importance of providing participants with strong verbal encouragement throughout RI exercise.

Surface EMG was used to provide a non-invasive indication of muscle activation. Unfortunately, this apparatus is unable to determine the origin of reduced muscle activation within the central nervous system, limiting insight into the mechanisms underpinning exercise-induced fatigue development during RI exercise. However, although external stimulation techniques can quantify peripheral and central components of exercise-induced fatigue, as previously discussed, these techniques cannot currently be implemented into dynamic whole-body exercise. Therefore, despite the drawbacks of EMG, this approach was chosen because it can be easily integrated into dynamic whole-body exercise.

This study has provided insight into the development of exercise-induced fatigue during a standard RI exercise test. However, the mechanisms of RI task failure in which $\dot{V}O_{2peak}$ is attained appear to depend on the incrementation rate (Davies et al.,

2021). For example, at the limit of RI exercise with a slow incrementation rate (10 $W.min^{-1}$) and subsequently longer test duration, the magnitude of exercise-induced fatigue (baseline MVIP vs. LoT MVIP) is significantly less compared to standard RI exercise. Moreover, a large reserve in power exists at the limit of intolerance of this RI with a slower incrementation rate that is absent during RI exercise tests with standard or faster incrementation rate (Davies et al., 2021). Currently, the development of exercise-induced fatigue during RI tests of varying incrementation rates is unknown. Characterising the development of exercise-induced fatigue during these RI protocols may further our understanding of the mechanisms underpinning exercise intolerance, permitting the design of interventions that target exercise intolerance.

3.6.6 Conclusions

This study aimed to characterise the development of exercise-induced fatigue (reduction in MVIP) during RI exercise. There was no reduction in MVIP below the lactate threshold consistent with known fatigue-related metabolite responses, and fatigue responses during moderate-intensity exercise. However, above the lactate threshold there was a progressive decline in MVIP until the limit of tolerance was attained, indicating a gradual increase in exercise-induced fatigue from the lactate threshold to the limit of tolerance. The time course of the decline in MVIP above the lactate threshold resembles that of fatigue-related metabolite accumulation during RI exercise, and thus, a close mechanistic link between the intramuscular environment and voluntary power generation. The absence of a decrease in RMS-EMG before the limit of RI exercise, suggests peripheral mechanisms of fatigue underpin the early reduction in MVIP. However, at the limit of RI exercise, central mechanisms relating to muscle activation integrate with peripheral mechanisms to contribute to the reduction in MVIP and RI exercise intolerance. The specific mechanism through which this integration occurs to induce task failure remains unknown.

Chapter 4 High-intensity interval training with blood flow restriction in chronic heart failure with reduced ejection fraction – feasibility and effect on endothelial progenitor cell number and $\dot{V}O_{2peak}$

4.1 Introduction

Heart failure with reduced ejection fraction (HFrEF) is a complex syndrome characterised by reduced exercise tolerance due to dyspnoea and fatigue in the presence of left ventricular systolic dysfunction (left ventricular ejection fraction <40%). Peak oxygen uptake ($\dot{V}O_{2peak}$) measured from an exercise test to intolerance is also reduced in HFrEF and is the strongest predictor of prognosis (Keteyian et al., 2016, Sarullo et al., 2010). $\dot{V}O_{2peak}$ in HFrEF is also used as the criterion for the Weber classification of heart failure severity.

Reduced $\dot{V}O_{2peak}$ in HFrEF is not solely the consequence of limited oxygen (O_2) delivery due to poor cardiac function and consequent reduction in maximum cardiac output; HFrEF is multi-system syndrome (Piepoli et al., 2010). In response to the index event that reduces cardiac function (specifically ejection fraction) a host of homeostatic mechanisms are triggered that aim to maintain cardiac output and blood pressure. Among the compensatory responses is an increase in the activation of the sympathetic nervous system and the renin-angiotensin-aldosterone pathway. The former maintains cardiac output by increasing heart rate and inducing peripheral vasoconstriction (increasing cardiac filling - preload), whilst the latter increases water and sodium retention and vasoconstriction in an effort to maintain blood pressure and tissue perfusion. At first these responses are compensatory; however, these responses are capacity limited, and when chronically activated result in adverse cardiac remodelling and maladaptations in the periphery that propagate disease progression and cause further reductions in $\dot{V}O_{2peak}$ (Zelis et al., 1988b).

In the peripheral vasculature, despite optimal HFrEF management incorporating pharmacological therapies that modulate the activation of neurohormonal pathways (e.g. beta-blockers and angiotensin converting enzyme inhibitors), there remains an imbalance between the production of reactive oxygen species and antioxidative enzymes, in addition to other pro-inflammatory changes, such as elevations in adhesion molecules, (VCAM-1 and ICAM-1), chemoattractants (MCP-1) and cytokines (TNF-α and IL-6; Bauersachs and Widder, 2008, Sharma et al., 2000, Andreassen et al., 1998). Together, these effects conflate to induce a state of endothelial dysfunction (Bauersachs and Widder, 2008). This dysfunction reduces the rate and magnitude of dilation in resistance vessels in response to the increase in shear stress that occurs following reactive hyperaemia, such as at the onset of exercise. This leads to an increased peripheral vascular resistance and impaired blood flow distribution during exercise in HFrEF (Sullivan et al., 1989, Poole et al., 2020). Subsequently, oxygen delivery to the working skeletal muscle is decreased, reducing microvascular O_2 partial pressure at any given $\dot{V}O_2$ and compromising skeletal muscle O_2 diffusing capacity (Wagner, 1996, Hirai et al., 2015, Poole et al., 2012). Figure 1.12 in section 1.13.2 depicts the convective and diffusive components of oxygen transfer that interact to determine $\dot{V}O_{2peak}$ and highlights that both these components are impaired in HFrEF. Thus, in addition to poor cardiac function, peripheral vascular dysfunction significantly contributes to reduced $\dot{V}O_{2peak}$ in HFrEF by impairing skeletal muscle O_2 delivery (Van Craenenbroeck and Conraads, 2013, Wagner, 1996, Hirai et al., 2015, Poole et al., 2012).

Maintaining vascular endothelial integrity and function depends on the dynamic balance between endothelial damage and endogenous repair mechanisms (Ross, 1993). Impaired O_2 delivery in HFrEF consequent to endothelial dysfunction, as described above, occurs when this balance is detrimentally altered, favouring vascular damage. Progenitor cells liberated from the bone marrow and identified in

the blood play an important role in endothelial repair and neovascularisation (Asahara et al., 1997, Rafii and Lyden, 2003, Rauscher Frederick et al., 2003). This heterogeneous population of cells includes hematopoietic $CD34^+$ expressing stem cells that have the capacity to differentiate into several phenotypes including hematopoietic and endothelial lineages and participate in vascular repair (Asahara et al., 1999). In addition, there is a rarer subset of $CD34^+$ cells that co-express vascular endothelial growth factor receptor 2 (KDR). The addition of this surface marker appears to derive a cell subset more enriched in endothelial specific progenitor cells (Fadini et al., 2012, Alaiti et al., 2010). In individuals with HFrEF the number of both circulating $CD34^+$ and $CD34^+/KDR^+$ progenitor cells are reduced (Samman Tahhan et al., 2017), suggesting an impaired endogenous repair capacity that is likely to affect the function of the endothelium by adversely altering the balance between endothelial damage and repair mechanisms (Samman Tahhan et al., 2017, Fritzenwanger et al., 2009, Valgimigli et al., 2004). The extent of the reduction in $CD34^+/KDR^+$ cells inversely correlate with HFrEF disease severity (assessed by NYHA classification), with more than a 3-fold reduction in circulating $CD34^+/KDR^+$ cells in patients with advanced symptoms (Samman Tahhan et al., 2017). This quantitative deficit in $CD34^+/KDR^+$ cells also correlate with adverse cardiovascular events and $CD34^+$ cell number independently predicts all-cause mortality in HFrEF, supporting the role of progenitor cells as disease biomarkers and a potential therapeutic target (Samman Tahhan et al., 2017, Koller et al., 2016, Werner et al., 2005, Schmidt-Lucke et al., 2005).

In healthy adults, acute exercise can induce a transient increase in the number of circulating progenitor cells, whilst exercise training can lead to an increase in the number of baseline circulating progenitor cells (Cubbon et al., 2010, Tsai et al., 2016, Laufs et al., 2005, Van Craenenbroeck et al., 2008b, Xia et al., 2012). Thus, both acute exercise and exercise training have a potent effect on progenitor cell

mobilisation in health. Elevations in shear stress during exercise, driven by increases in cardiac output, increase eNOS activity and NO production – the primary stimulus for exercise-induced progenitor cell mobilisation from the bone marrow into the peripheral blood (Heissig et al., 2002, Cubbon et al., 2010, Aicher et al., 2003). The normal increase in progenitor cell number in response to acute exercise seen in health appears to be severely attenuated in HFrEF potentially due to impaired progenitor cell mobilisation (Van Craenenbroeck et al., 2010a, Van Craenenbroeck et al., 2011); however, it is unknown whether this acute response to exercise can be restored by exercise training. Furthermore, although exercise training can lead to an increase the number of baseline $CD34^+$ and $CD34^+/KDR^+$ progenitor cells in HFrEF (Sandri et al., 2016, Mezzani et al., 2013), the optimal exercise strategy for increasing vascular endogenous repair capacity, exercise tolerance and $\dot{V}O_{2peak}$ remains unknown.

Exercise training can be difficult for individuals with HFrEF because symptoms of the disease, such as breathlessness and fatigue, occur even at low levels of physical activity (Conraads et al., 2012). Moreover, symptoms may limit the work that can be performed, and in doing so potentially restrict the physiological benefits that can be achieved from exercise training. High-intensity interval training (HIIT) is characterised by short periods of work at a relatively high work rate (cf. continuous) interspersed by periods of recovery, exercising at a low work rate or rest. A considerable body of evidence has supported the use of HIIT in HFrEF as an effective modality for improving both vascular function and $\dot{V}O_{2peak}$ to the same if not greater extent than traditional continuous moderate-intensity exercise training (Ramos et al., 2015, Elliott et al., 2015, Hannan et al., 2018, Wisløff et al., 2007). In part this is because HIIT mitigates disease symptoms; performing short periods of work separated by recovery bouts reduces the ventilatory response (cf. performing the same work rate of exercise continuously) and subsequent dyspnoea experienced by patients with chronic

diseases (Vogiatzis, 2011). Thus, HIIT allows individuals with chronic diseases to increase the time spent exercising at a given work rate (Vogiatzis et al., 2004). Indeed, using this approach chronic disease patients have been able to accumulate exercise at 120% of their WR_{peak} for up to 20 minutes (Porszasz et al., 2013), potentially increasing the adaptations and benefits gained from rehabilitation.

The physiological adaptations derived from HIIT may be improved further by combining HIIT with blood flow restriction (BFR). During HIIT with BFR, cuffs are inflated around the proximal portion of the exercising limb in exercise recovery periods, reducing arterial inflow and impairing venous outflow (Iida et al., 2005). In addition to reducing skeletal muscle oxygen tension, this increases the metabolic stress of the exercise because exercise-induced fatigue metabolite clearance is suppressed (Takano et al., 2005, Conceicao et al., 2018, Iida et al., 2007, Thomas et al., 2018). Subsequently, exercise with BFR is associated with greater phosphocreatine depletion, increased inorganic phosphate and lactate accumulation, and a lower intramuscular pH compared to the control condition (Suga et al., 2010, Suga et al., 2009). In healthy adults, the combination of HIIT and BFR has led to superior increases in $\dot{V}O_{2peak}$ and exercise tolerance compared to control training interventions without BFR (Abe et al., 2010, Taylor et al., 2016).

Exercise training with BFR may also lead to greater adaptations in the peripheral vasculature (Iida et al., 2011, Hunt et al., 2012, Patterson and Ferguson, 2010). Improvements in peak reactive hyperaemia and artery function before changes in artery structure have been observed following exercise training with BFR (Hunt et al., 2013). In addition to altered shear stress patterns, one potential mechanism for this is the increase in angiogenic factors, such as endothelial nitric oxide synthase and vascular endothelial growth factor (VEGF), reported after exercise with BFR

compared to matched exercise without BFR (Ferguson et al., 2018, Larkin et al., 2012). These angiogenic factors are also linked to the release of progenitor cells from the bone marrow into the peripheral blood (Asahara et al., 1999, Ceradini et al., 2004, Aicher et al., 2003). Thus, it is possible progenitor cells mobilised in response to exercise training with BFR contributed to these adaptations in the peripheral vasculature. However, the effect of aerobic exercise with BFR on hematopoietic and endothelial progenitor cell number is unknown.

Whilst the popularity of BFR exercise has increased greatly over the past decade, the combination of HIIT with BFR is yet to be investigated in HFrEF. Thus far, only low-load resistance exercise with BFR has been explored in this patient population (Groennebaek et al., 2019). Given the symptom limitation of HFrEF patients, any exercise strategy which could lead to superior adaptations from the same HIIT protocol warrants investigation. Therefore, the aim of this study was to investigate whether HIIT with BFR is feasible in HFrEF and determine whether 4 weeks of HIIT with BFR leads to greater improvements in vascular endogenous repair capacity (baseline $CD34^+$ and $CD34^+/KDR^+$ progenitor cell number), exercise tolerance and $\dot{V}O_{2peak}$ than HIIT alone. The progenitor cell response to a single bout of HIIT with BFR was also investigated pre- and post-training to determine whether this exercise strategy mobilises progenitor cells in HFrEF, or if this response is absence, whether chronic exposure to HIIT with BFR (i.e. exercise training) can restore this response.

4.2 Methods

4.2.1 Participants

17 patients (16 males and 1 female) with HFrEF were recruited from Leeds General Infirmary between March 2018 and February 2020. Participants were enrolled if they had NYHA Class I-III symptoms, a left ventricular ejection fraction ≤45% and were on optimally tolerated medical therapy with no change in medication or other invasive

cardiac procedures for at least 3 months. Participants were ineligible if they were unable to exercise or had a diagnosis of severe chronic obstructive pulmonary disease, active cancer, severe renal disease or primary pulmonary hypertension. Information on comorbidities, past medical history, medication, and NYHA functional class was collected. All participants provided written informed consent before entry into the study and the research protocol was approved by the local ethics committee and registered on clinicaltrails.gov (Blood Flow Restriction Training in Chronic Heart Failure: An Effective Training Strategy?; NCT03342833). It should be noted that an additional 6 participants (3 males and 3 females) were screened and performed a cardio-pulmonary exercise test but did not participate in the study for various reasons (acute decompensated heart failure, *n* = 1; claustrophobic from the mouthpiece, *n* = 1; knee pain whilst cycling, *n* = 1; sustained an injury outside the study, *n* = 2; withdrew from the study due to the time commitment; *n* = 1).

4.2.2 Study design

Participants were randomised 1:1 to either HIIT alone (HIIT) or HIIT with BFR (HIIT+BFR; Figure 4.1). Pre-training, and following 8 supervised exercise training sessions, participants completed a ramp-incremental cardiopulmonary exercise test. Following the initial training session that was used to familiarise participants with the allocated protocol, blood sampling for quantification of progenitor cells was performed before and 10 min after exercise cessation in the second and last training session. Blood was collected on 53/64 occasions; missing samples were consequent to venepuncture failure or a flow cytometer fault. Pulmonary gas exchange was also recorded throughout the duration of exercise at these visits to assess the intensity of exercise training (% $\dot{V}O_{2peak}$). Further, near-infrared spectroscopy (NIRS) was used to measure vastus lateralis muscle oxygenation during exercise in the second training session. In addition, measures of maximal voluntary isokinetic power (MVIP; maximum leg power) and self-reported health-related quality of life were assessed pre- and post-training. Quality of life was assessed using the Minnesota Living with

Heart Failure Questionnaire (MLHFQ; Rector, 1987). The score range for this questionnaire is 0-105 with higher scores indicating a worse health-related quality of life.

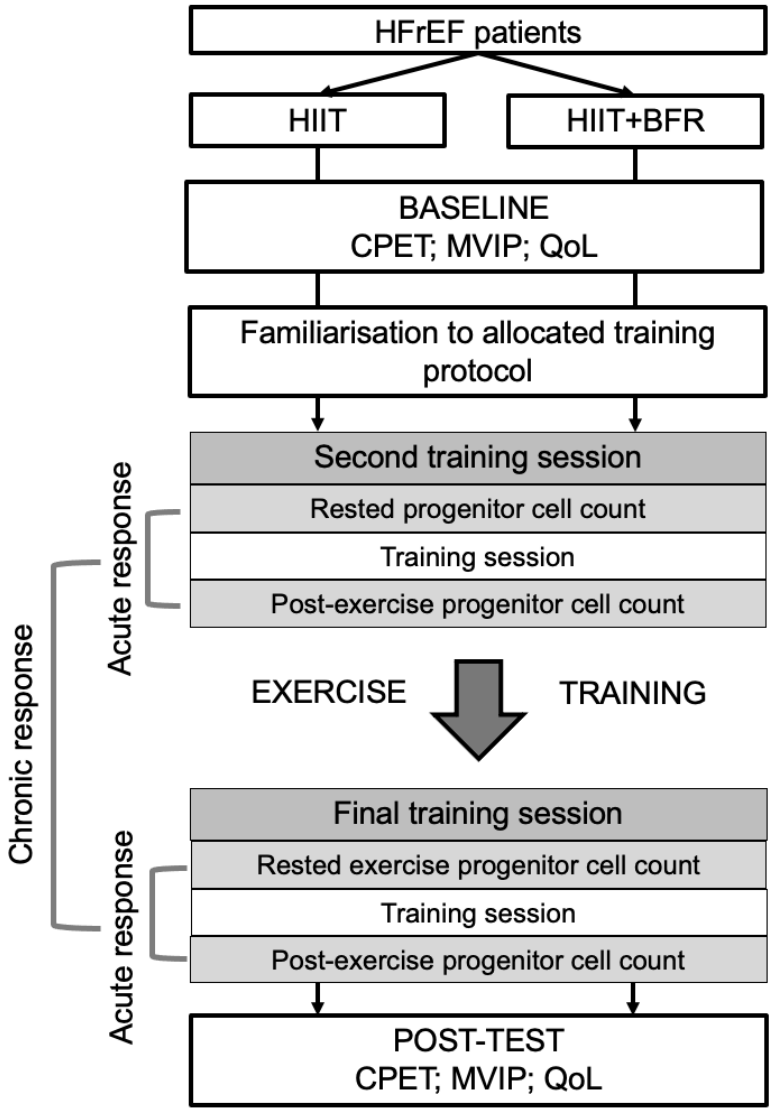

Figure 4.1 Study design. HFrEF patients were allocated to HIIT with BFR (HIIT+BFR) or HIIT without BFR (HIIT). At baseline and after 4 weeks of exercise training patients performed a cardiopulmonary exercise test (CPET) and maximal voluntary isokinetic power (MVIP) and quality of life (QoL) were assessed. At the second and final training session blood was sampled before and after exercise to enumerate $CD34^+$ and $CD34^+/KDR^+$ progenitor cells.

4.2.3 Equipment and measures

All exercise tests were performed on a computer-controlled, electromagnetically braked cycle ergometer (Excalibur Sport PFM, Lode, Groningen, The Netherlands). This ergometer allows for instantaneous switching between hyperbolic and isokinetic cycling modes and measurement of MVIP (Cannon et al., 2011). Isokinetic power is calculated as the product of force and angular velocity; strain gauges in the crank axis of each pedal measure force every 2 degree of angular rotation, whilst angular velocity is calculated from light sensors sampling in series. Further details on the cycle ergometer and MVIP measurements can be found in section 2.2 and 2.7.1.2.

Breath-by-breath pulmonary gas exchange was measured using a gas exchange analysis system (Cardio2, Medgraphics, Medical Graphics Corporation, St Paul, MN, USA). Prior to each experiment the system was calibrated. Details on the equipment used and calibration process can be found in section 2.3. Briefly, flow was calibrated using a 3 L syringe over a range of physiologically possible flow profiles and oxygen and carbon dioxide sensors were calibrated using gases of known concentrations (O_2: 12 and 21%; CO_2: 0 and 5%).

4.2.4 Cardiopulmonary exercise testing

Each participant performed a ramp-incremental exercise test (7 - 20 W min^{-1}) pre- and post-training to symptom limitation. Incrementation rate was selected based on the participants medical profile and any previous exercise test history, with the aim of achieving a test duration of ~8-12 min (Buchfuhrer et al., 1983). The same increment rate was used pre- and post-training to allow for appropriate comparisons between exercise tests. Breath-by-breath pulmonary gas exchange was measured throughout all exercise tests. For this, participants were asked to wear a facemask (covering both their nose and mouth) connected to the Medgraphics via the umbilical sample line. Participants were also attached to a 12 lead ECG (X12+, Mortara

Instrument UK Ltd, Stirling, UK) throughout the exercise test and recovery period to measure heart rate, and to monitor the participant. A cardiac physiologist was always present to monitor the participants ECG, discern any irregularities and dictate the appropriate response to any irregularities that occurred (for example, whether to immediately terminate the exercise and/or call a physician). Additional details on this exercise protocol and concomitant measurements can be found in section 2.3, 2.4 and 2.6.5.

4.2.5 Maximal voluntary isokinetic power

Prior to each cardiopulmonary exercise test, baseline MVIP was measured. For this, participants were asked to perform two short (~6 s) bouts of maximal effort isokinetic cycling at 70 rpm. The time between the two efforts was dictated by the participant and their recovery (return to resting heart rate) but was never less than 2 min.

4.2.6 Training intervention

Both groups performed the same HIIT protocol: five 2 min intervals at 80% work rate peak (calculated from cardiopulmonary exercise test) separated by 2 min recovery period (for schematic of exercise training session see Figure 4.2). During the recovery bout participants were given the option to rest or continue cycling at a low intensity (10 W). Participants in both groups wore 13 cm wide pneumatic cuffs (SC12^{TM} Straight Segmental Cuff, Hokanson Inc, WA, USA) connected to an aneroid sphygmomanometer (DS65 DuraShock Silver Series Sphygmomanometer, Welch Allyn Inc, NY, USA) on the proximal portion of each thigh. Immediately after each HIIT work bout cuffs were inflated manually by the researcher. Cuffs were inflated for the first 90 s of recovery to 100 mmHg for those in the HIIT+BFR group or 10 mmHg for those in the HIIT group. The cuff pressure used for the HIIT+BFR group (100 mmHg) was similar to the 110 mmHg used by Hunt et al. (2013), with this pressure causing approximately a 60% reduction in resting blood flow in the popliteal artery. The allocated cuff pressures remained constant throughout the training period. Both training groups completed 2 sessions per week for 4 weeks. After 2 weeks of exercise

training an additional exercise bout was added for progression (total bout number = 6). All sessions were separated by at least 24 h and were started and concluded with a 4-min warm-up and cool down at 10 W.

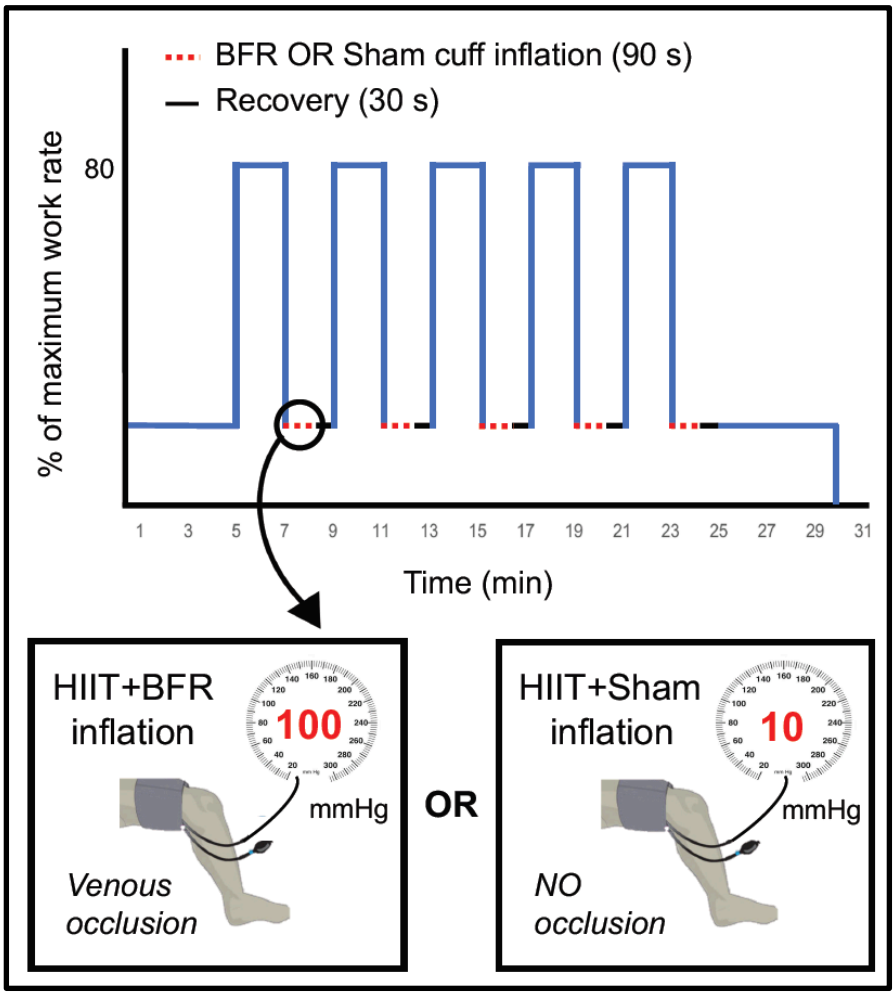

Figure 4.2 Schematic of HIIT with BFR (HIIT+BFR) and HIIT without BFR (HIIT) exercise training. Both groups performed the same HIIT protocol consisting of 2 min of exercise at 80% of work rate peak (calculated from cardiopulmonary exercise test) followed by 2 mins of recovery, repeated 5-6 times. For the first 90 s of recovery cuffs were inflated to the allocated pressure for HIIT+BFR (100 mmHg) and HIIT (10 mmHg).

4.2.7 Quantification of hematopoietic and endothelial progenitor cells

The number of progenitor cells ($CD34^+$ and $CD34^+/KDR^+$ cells) in venous blood was measured before and after exercise in the second and final exercise training session using flow cytometry, as previously described (section 2.9.2). Red blood cells were lysed using ammonium chloride solution. The remaining cells were washed and pre-treated with FcR blocker (Miltenyi Biotec, Bergisch Gladbach, Germany) before the following antibodies were added: KDR-APC (R&D Systems, Minneapolis, MN, USA), CD34-PE (Miltenyi Biotec) and CD3-FITC (Miltenyi Biotec). DAPI staining solution (Miltenyi Biotec) was added to sample tubes to allow exclusion of nonnucleated cells and debris. Negative controls included isotype controls, fluorescence minus one samples and unstained samples. At least one million total events were recorded on cytoFLEX S flow cytometer (Beckman Coulter, Indianapolis, IN, USA). The number of $CD34^+$ and $CD34^+/KDR^+$ cells were analysed using CytExpert software (Beckman Coulter) and presented as number of cells per 10^6 total events. Gating strategy for $CD34^+$ and $CD34^+/KDR^+$ cells is shown in section 2.9.2 (Figure 2.10). Briefly, live cells in the lymphocyte region were identified before cell doublets and $CD3^+$ cells were excluded. $CD34^+$ and $CD34^+/KDR^+$ cells were then identified and quantified in the $CD3^-$ population.

4.2.8 Muscle oxygenation

Oxygenation of the vastus lateralis muscle was measured throughout the second training session using a wireless, portable continuous wave, spatially resolved spectroscopy, NIRS device (PortaMon, Artinis, The Netherlands). This device was placed on the belly of the right vastus lateralis, secured on the skin with surgical tape, covered with an optically dense black cloth and wrapped with an elastic strap to occlude ambient light and minimise movement of the device during exercise. The NIRS device contained three light emitters that emit light at two wavelengths (760 and 850 nm) and a receiver. The emitters were located 30, 35 and 40 mm from the

receiver. This setup enabled the measurement of relative chromophore absorbance (oxygenated haemoglobin, deoxygenated haemoglobin and total haemoglobin) by spatially resolved spectroscopy. NIRS data were collected at a sampling frequency of 10 Hz. Tissue saturation index (TSI; %) was calculated as: (oxygenated haemoglobin)/(oxygenated haemoglobin + total haemoglobin) x 100. It is recognised that NIRS in unable to differentiate signals from haemoglobin and myoglobin, and therefore, results are considered as the combined O_2 saturation of both chromophores.

4.2.9 Data analysis

4.2.9.1 Pulmonary gas exchange

$\dot{V}O_2$ data collected during cardiopulmonary exercise tests was edited to remove occasional outliers (breaths which fall outside of 99% confidence limits (Lamarra et al., 1987, Rossiter et al., 2000). The lactate threshold (LT) was estimated using the v-slope method supported by standard ventilatory and pulmonary gas exchange criteria (Beaver et al., 1986b, Whipp et al., 1986) and $\dot{V}O_{2peak}$ was determined as the highest 12-breath mean recorded in the final ~20 s of the ramp-incremental test (Bowen et al., 2012).

Breath-by-breath $\dot{V}O_2$ data recorded during the second and last training session was analysed to calculate the peak of the oscillation in $\dot{V}O_2$ during training intervals. For each test, data was edited to exclude occasional outliers. The intermittent nature of the exercise training protocols precluded the application of 99% confidence limits. Thus, outliers were identified based on their characteristics (e.g. tidal volume and oxygen uptake) in relation to neighbouring breaths (Turner et al., 2006). Due to transient kinetics during the first work bout, this bout was also excluded from the analysis (Turner et al., 2006). Breath-by-breath data from each subsequent work bout was time aligned to the onset of exercise (i.e. time = 0-120 s). Breath-by-breath data

from all work bouts were then interpolated and averaged to increase signal: noise, resulting in a single mean $\dot{V}O_2$ trace for the work bout (Figure 4.3). A mean of the final 12 breaths during the work bout was calculated, with this peak of the $\dot{V}O_2$ response determining exercise intensity (Turner et al., 2006).

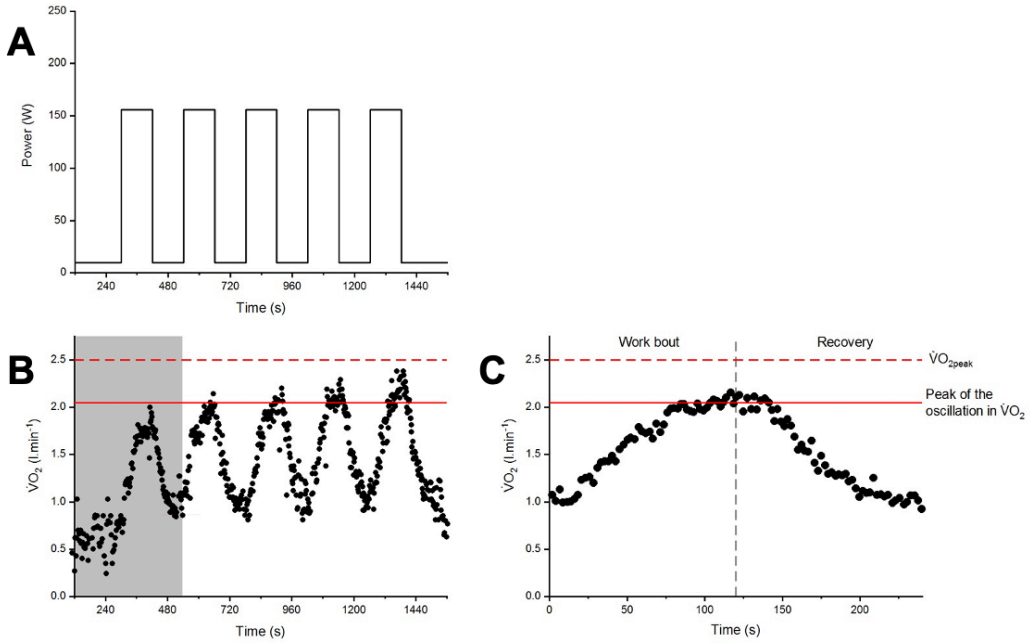

Figure 4.3 Representative participants HIIT protocol and corresponding $\dot{V}O_2$ responses for the whole protocol, and for the interpolated response. A: HIIT protocol: 5 x 2 min intervals at 80% ramp-incremental exercise WR_{peak}, separated by 2 min of recovery. B: $\dot{V}O_2$ response to training protocol. The first 2 min of exercise was removed (grey box) to exclude transient data. The four remaining work bouts were interpolated creating a single work bout shown in C. A mean $\dot{V}O_2$ of the final 12 breaths in this work bout was measured to determine the peak of the oscillation in $\dot{V}O_2$ (i.e. the training intensity).

4.2.9.2 Maximal voluntary isokinetic power

For each isokinetic effort, the isokinetic power of each pedal stroke was derived by summing the power measured at the left and right crank. MVIP was then calculated from the mean power of the first three pedal strokes of each isokinetic bout that were constrained at 70rpm. There was no difference between the two baseline MVIP

measurements (p > 0.05), therefore the highest of the two was used in further analysis. For additional details on the calculation of MVIP see section 2.7.1.2.

4.2.9.3 Quadriceps muscle oxygenation

Mean TSI measured in the final 30 s of unloaded pedalling was calculated to determine baseline TSI. To minimise the effect of baseline differences between participants, TSI values during exercise and recovery periods were calculated as changes (Δ) from baseline values. Due to transient kinetics, data from the first work bout and recovery period were excluded from analysis. The mean TSI was calculated for: the final 20 s of each work bout, cuff inflation and recovery period for each participant. A mean of these values was then taken to derive a single value of TSI at the end of exercise, cuff-inflation and recovery for each participant for the protocol before group means were calculated.

4.2.10 Statistics

Data are expressed as mean ± SD. Continuous variables were tested for normal distribution with the Shapiro-Wilk test. Baseline characteristics between exercise training groups were compared using unpaired *t*-test. Two-way repeated measures ANOVA with one within factor (time: pre-exercise vs. post-exercise or pre-training vs. post-training) and one between factor (intervention: HIIT+BFR vs. HIIT) was used to assess differences over time between groups. When significant interaction effects were observed, Bonferroni corrected post-hoc *t*-tests were performed to locate differences. Ordinal variables were compared using the Mann-Whitney U test or Wilcoxon signed-rank test. All tests were performed as two-sided with significance accepted at p < 0.05. All analyses were performed using IBM SPSS version 24 (SPSS Inc., Chicago, IL, USA).

4.3 Results

4.3.1 Participant characteristics

After random allocation, HIIT+BFR and HIIT groups included 8 and 9 participants, respectively. However, during training 1 participant from the HIIT group was withdrawn from the study after 7 training sessions due to surgery for another medical condition. Subsequently, 16 participants were included in the final analysis (HIIT+BFR: n = 8; HIIT: n = 8). Participant baseline characteristics and clinical data are shown in Table 4.1. $\dot{V}O_{2peak}$ was 16.5 ± 3.7 $ml \cdot min^{-1} \cdot kg^{-1}$ for HIIT+BFR and 16.1 ± 7.3 $ml \cdot min^{-1} \cdot kg^{-1}$ for HIIT, with no differences between groups at baseline (p = 0.89). Estimated LT was also not different between training groups at baseline (Table 4.2; p = 0.97).

Table 4.1 Baseline participant characteristics

Parameter	HIIT+BFR	HIIT
n	8	8
Age, y	71.8 ± 10.7	71.3 ± 11.9
BMI (kg/m^2)	26.9 ± 3.9	28.4 ± 3.8
Ischemic origin	2 (25)	5 (62.5)
Diabetes Mellitus	0 (0)	2 (25)
LVEF %	33 ± 8	34 ± 9
Atrial Fibrillation	6 (75)	5 (62.5)
NYHA Class		
I	1 (12.5)	2 (25)
II	6 (75)	3 (37.5)
III	1 (12.5)	3 (37.5)
Device therapy		
Pacemaker	0 (0)	1 (12.5)
ICD	0 (0)	1 (12.5)
CRT	1 (12.5)	2 (25)
CRT-D	1 (12.5)	0 (0)
Medical therapy		
Beta-blockers	8 (100)	8 (100)
ACE inhibitor/ARB	8 (100)	8 (100)
Diuretic	3 (37.5)	4 (50)
Digoxin	2 (50)	2 (50)
AA	4 (50)	2 (25)
Statin	3 (37.5)	6 (75)

Values are *n* (%) or mean ± SD. AA = aldosterone antagonist; ACE = angiotensin-converting enzyme; ARB = aldosterone receptor blocker; BFR = blood flow restriction; CRT = cardiac resynchronisation therapy; HIIT = high-intensity interval training; ICD = implantable cardioverter defibrillator; LVEF = left ventricular ejection fraction; NYHA = New York Heart Association.

4.3.2 Feasibility, adherence and intensity of exercise training

All participants tolerated with their allocated cuff pressure (HIIT+BFR: 100 mmHg; HIIT: 10 mmHg) and there were no adverse events relating to the addition of BFR to the HIIT protocol. Training compliance was 99% (1 participant missed a single training session). The work rate set on the cycle ergometer during training intervals (80% of ramp-incremental work rate peak) was not different between training groups at 87 ± 36 W for HIIT+BFR and 89 ± 50 W for HIIT (p = 0.92). The peak of the oscillation in $\dot{V}O_2$ during training bouts was not different between HIIT+BFR (1.19 ± 0.38 L.min^{-1}; 92 ± 15% baseline $\dot{V}O_{2peak}$) and HIIT groups (1.41 ± 0.82 L.min^{-1}; 98 ± 14% baseline $\dot{V}O_{2peak}$) in the second training session (p = 0.52) and was unchanged in the final training session with no differences between groups (HIIT+BFR: 1.22 ± 0.39 L.min^{-1}; 88 ± 15% baseline $\dot{V}O_{2peak}$; HIIT: 1.34 ± 0.81 L.min^{-1}; 93 ± 17% baseline $\dot{V}O_{2peak}$; time effect: p = 0.34; interaction: p = 0.95).

4.3.3 Quadriceps muscle oxygenation during HIIT+BFR and HIIT

At the end of the exercise bouts in the second training session, quadriceps muscle oxygenation (TSI; %) was not different between HIIT+BFR and HIIT groups (p = 0.85; Figure 4.4). There was an increase in quadriceps muscle oxygenation between end of exercise and end of cuff inflation in the HIIT group only (time effect: p = 0.04; interaction: p = 0.03; HIIT: p = 0.05; Figure 4.4). This suggests that the higher cuff pressure applied during HIIT+BFR prevented an increase in muscle oxygenation between end of exercise and end of cuff-inflation. Following cuff-release there was a reactive increase in muscle oxygenation during recovery in HIIT+BFR only (p = 0.31; Figure 4.4). At the end of recovery, there was no difference in quadriceps muscle oxygenation between training groups (p = 0.08).

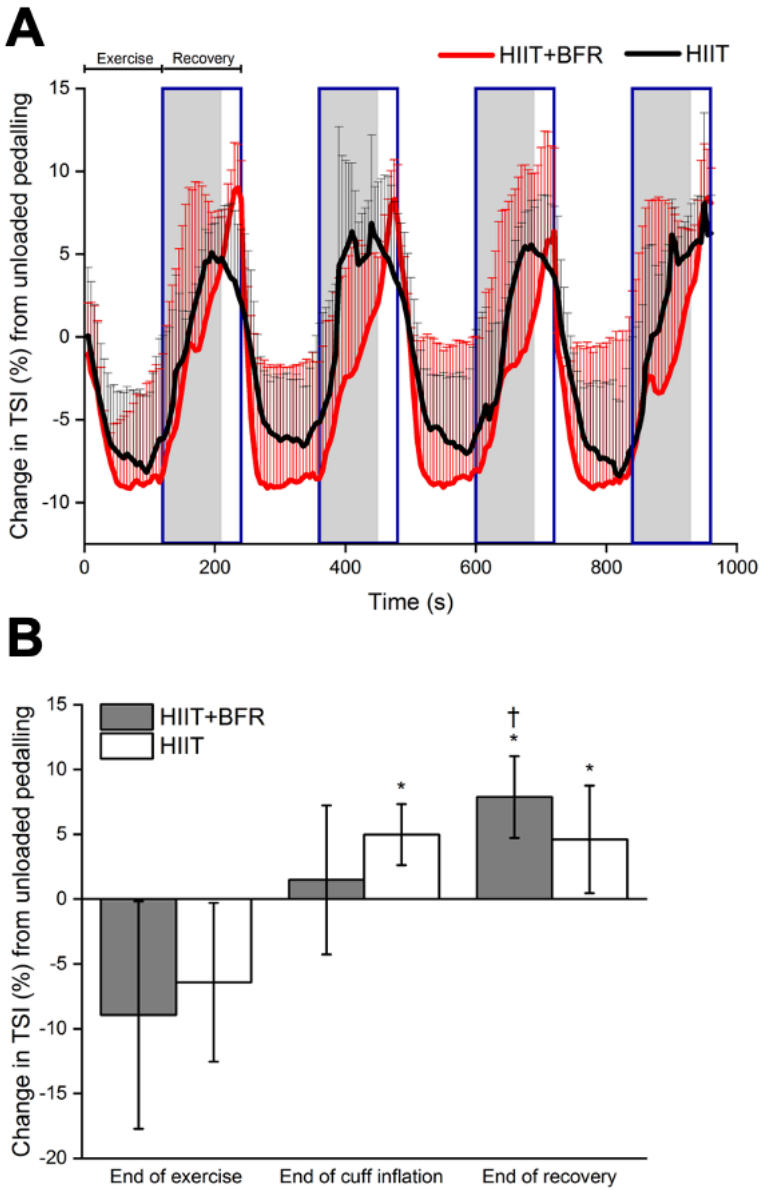

Figure 4.4 A: Quadriceps muscle oxygenation, assessed by tissue saturation index (TSI), during a single session of high-intensity interval training with BFR (HIIT+BFR; red line) and without BFR (HIIT; black line). Recovery bouts (blue open boxes) and cuff inflation periods (grey shading in blue open boxes) are shown. B: TSI at end of exercise, end of cuff inflation and end of recovery during HIIT+BFR and HIIT. Data are mean TSI for all bouts derived from the final 20 s of each exercise bout, cuff inflation and recovery period. *TSI greater than TSI at end of exercise bout; † increase in TSI from end of cuff inflation.

4.3.4 Pre-training: acute progenitor cell response to HIIT+BFR and HIIT

Pre-training, blood samples were drawn from 12 participants before and after the exercise session to assess the acute progenitor cell response (HIIT+BFR: $n = 6$; HIIT: $n = 6$). There was no difference in the number of $CD34^+$ and $CD34^+/KDR^+$ cells in HIIT+BFR and HIIT training groups before training, i.e. at baseline ($p > 0.05$). In addition, there was no main effect of time on $CD34^+$ progenitor cell number pre- to post exercise (HIIT+BFR: Pre = 2469 ± 1537; Post = 2343 ± 1362 /10^6 total events; HIIT: Pre = 2491 ± 1218; Post = 2408 ± 1137 /10^6 total events; time effect: $p = 0.71$; Figure 4.5). There was also no difference in the number of $CD34^+$ cells between groups pre- to post-exercise (interaction: $p = 0.94$). Similarly, the number of $CD34^+/KDR^+$ progenitor cells remained unchanged following a single session of HIIT+BFR and HIIT pre-training (HIIT+BFR: Pre = 78 ± 75; Post = 49 ± 27 /10^6 total events; HIIT: Pre = 66 ± 21; Post = 71 ± 41 /10^6 total events; time effect: $p = 0.40$; Figure 4.5), with no difference in $CD34^+/KDR^+$ cell number between groups pre- to post-exercise (interaction: $p = 0.23$).

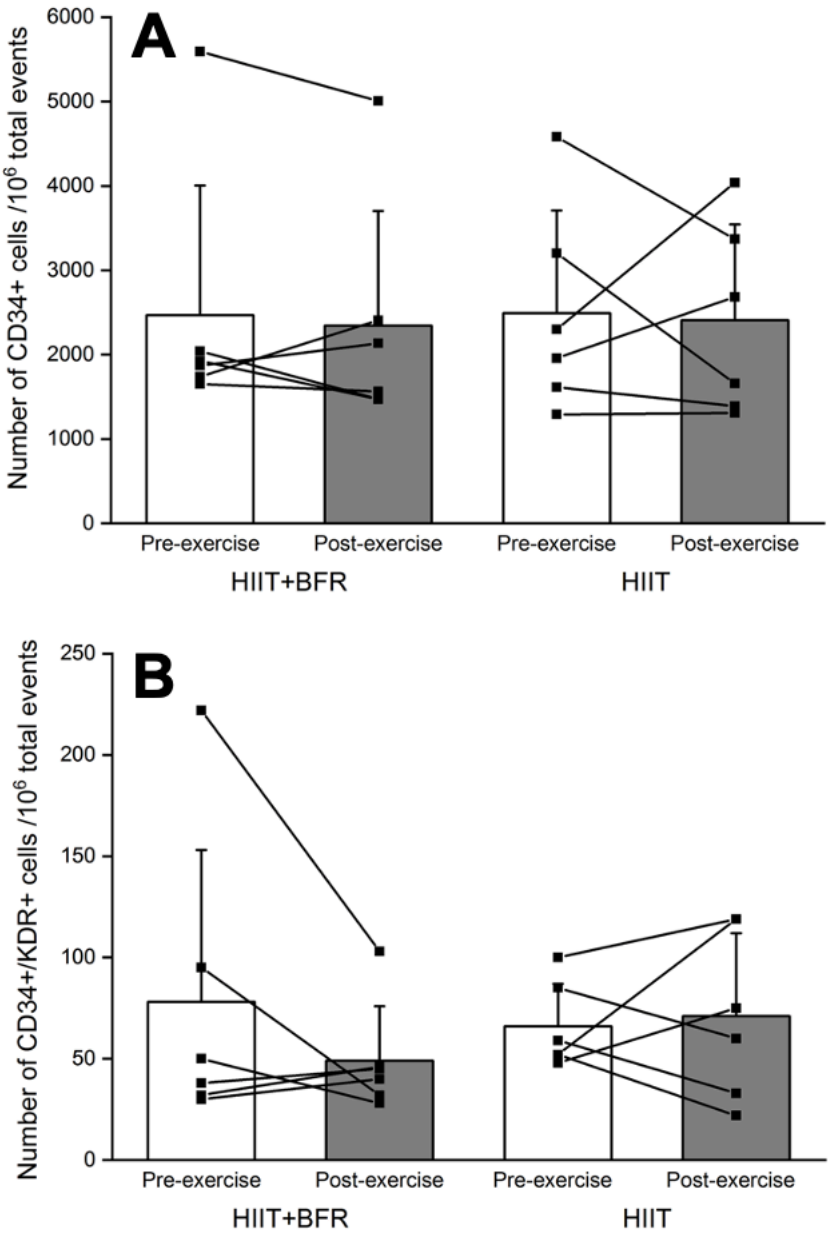

Figure 4.5 $CD34^+$ (A) and $CD34^+/KDR^+$ (B) progenitor cell responses to a single session of high-intensity interval training with BFR (HIIT+BFR) and without BFR (HIIT) before exercise training. The number of $CD34^+$ and $CD34^+/KDR^+$ cells remained unchanged following an acute bout of HIIT+BFR and HIIT pre-training (time effect: $p > 0.05$), with no differences between groups (interaction: $p > 0.05$). Values are mean ± SD for 12 participants (HIIT+BFR: $n = 6$; HIIT: $n = 6$).

4.3.5 Changes in exercise parameters after exercise training

There was a main effect of time on relative but not absolute $\dot{V}O_{2peak}$ pre- to post-training ($\dot{V}O_{2peak}$ ml·min^{-1}·kg^{-1}: time effect: $p = 0.04$; $\dot{V}O_{2peak}$ L·min^{-1}: time effect: $p = 0.06$; Figure 4.6); however, a significant interaction was present for both measures of $\dot{V}O_{2peak}$ (interaction: $p < 0.05$). Subsequently, differences over time within each group were explored using *post-hoc* paired-samples *t*-tests. This demonstrated no difference in either absolute or relative $\dot{V}O_{2peak}$ pre- to post-training in HIIT+BFR ($\dot{V}O_{2peak}$ L·min^{-1}: $p = 0.44$; $\dot{V}O_{2peak}$ ml·min^{-1}·kg^{-1}: $p = 0.54$), but an increase in absolute and relative $\dot{V}O_{2peak}$ pre- to post-training in HIIT ($\dot{V}O_{2peak}$ L·min^{-1}: $p = 0.01$; $\dot{V}O_{2peak}$ ml·min^{-1}·kg^{-1}: $p = 0.01$; Figure 4.6; Table 4.2).

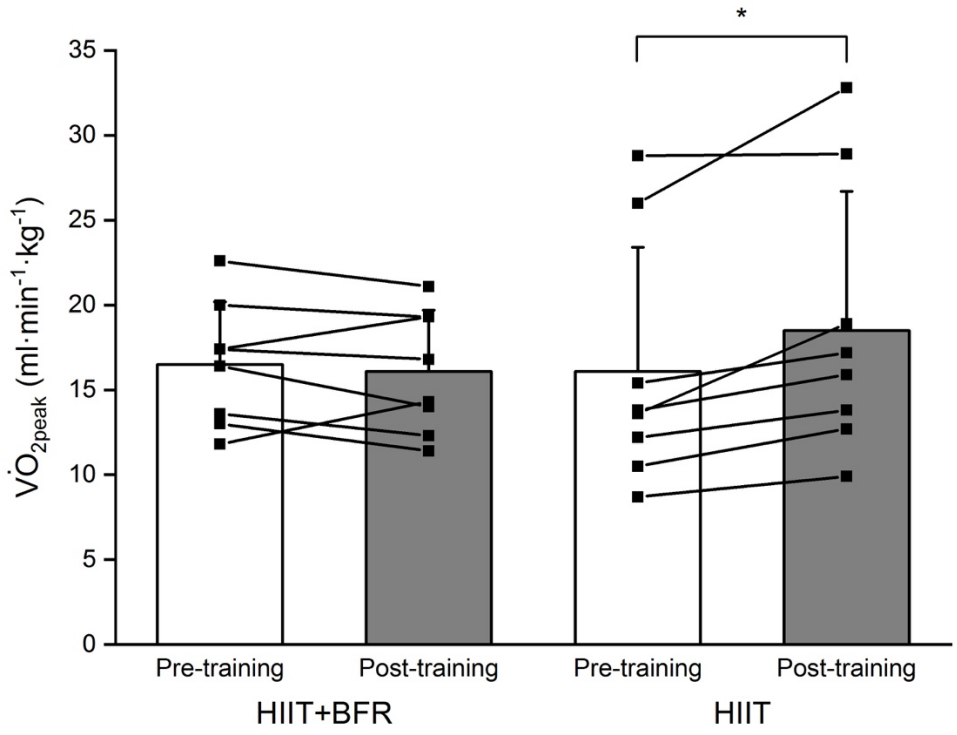

Figure 4.6 Ramp-incremental $\dot{V}O_{2peak}$ following high-intensity interval training with BFR (HIIT+BFR) and without BFR (HIIT). *Post-hoc analyses performed following a significant pre- to post-training time effect and interaction showed relative $\dot{V}O_{2peak}$ increased following HIIT ($p < 0.05$) but not HIIT+BFR ($p > 0.05$). Values are mean ± SD for 16 participants (HIIT+BFR: $n = 8$; HIIT: $n = 8$).

Estimated LT increased pre- to post-training (time effect: $p = 0.04$) with no difference between groups (interaction: $p > 0.05$; Table 4.2). However, ventilatory efficiency ($\dot{V}_E/\dot{V}CO_2$ slope and $\dot{V}_E/\dot{V}CO_2$ minimum) and peak oxygen pulse were unchanged with training (time effect: $p > 0.05$; Table 4.2). Ramp-incremental test duration and peak work rate (WR_{peak}) increased with training (time effect $p < 0.05$), with no difference in the magnitude of increase between HIIT+BFR and HIIT training groups (interaction: $p > 0.05$; Table 4.2, Figure 4.7). Maximal voluntary isokinetic power was unchanged with training (time effect: $p > 0.05$).

Table 4.2 Pulmonary gas exchange and power measurements

Parameter	HIIT+BFR		HIIT	
	Pre	Post	Pre	Post
$\dot{V}O_{2peak}$ ($L \cdot min^{-1}$)	1.39 ± 0.47	1.35 ± 0.42	1.33 ± 0.65	1.55 ± 0.74†
$\dot{V}O_{2peak}$ ($ml \cdot min^{-1} \cdot kg^{-1}$)	16.5 ± 3.7	16.1 ± 3.6	16.1 ± 7.3	18.8 ± 8.0†
$\dot{V}_E/\dot{V}CO_2$ slope	30 ± 4.9	31 ± 5.8	29 ± 5.7	30 ± 6.7
$\dot{V}_E/\dot{V}CO_2$ Minimum	31 ± 5.1	32 ± 5.2	29 ± 3.4	28 ± 3.5
RER_{peak}	1.18 ± 0.09	1.31 ± 0.20	1.28 ± 0.21	1.33 ± 0.20
HR_{peak} ($beats \cdot min^{-1}$)	130 ± 32	136 ± 22	114 ± 15	123 ± 17
Peak O_2 pulse ($ml \cdot beat^{-1}$)	12 ± 5.6	12 ± 5.0	13 ± 6.6	13 ± 4.6
LT ($L \cdot min^{-1}$)*	0.86 ± 0.32	0.94 ± 0.31	0.86 ± 0.37	0.99 ± 0.42
Exercise duration (s)*	483 ± 132	544 ± 110	499 ± 135	554 ± 143
WR_{peak} (W)*	108 ± 45	120 ± 45	111 ± 62	120 ± 62
MVIP (W)	260 ± 132	328 ± 157	303 ± 156	361 ± 184

Values are mean ± SD. n = 8 per group. HR_{peak} = Peak heart rate; LT = Lactate threshold; MVIP = Maximal voluntary isokinetic power; O_2 = Oxygen; RER_{peak} = Peak respiratory exchange ratio; $\dot{V}_E/\dot{V}CO_2$ = Minute ventilation to carbon dioxide output ratio; $\dot{V}O_{2peak}$ = Peak oxygen uptake; WR_{peak} = peak work rate from ramp-incremental exercise test.

***pre- to post training time effect from the two-way repeated measures ANOVA. † following a significant interaction, a significant pre-post training change within the HITT group (paired t-test).**

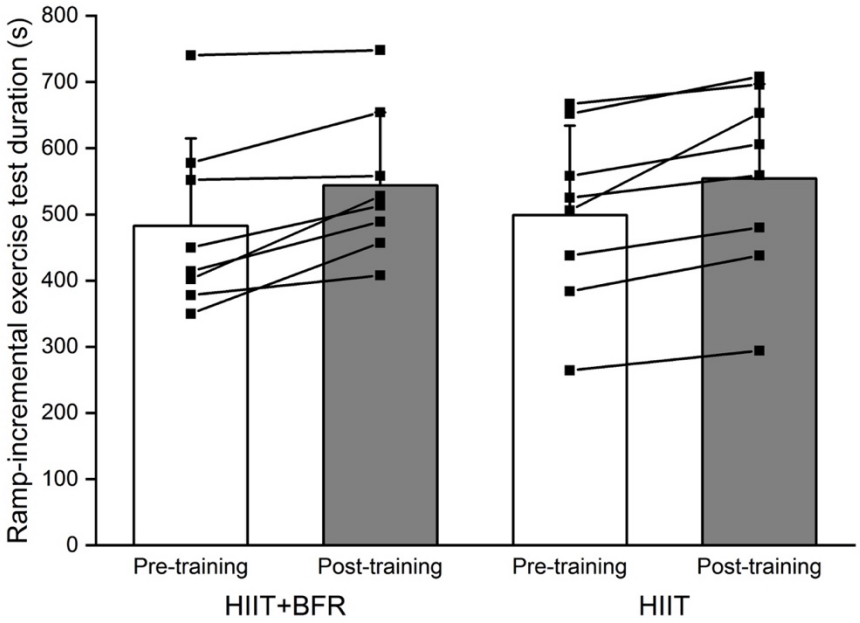

Figure 4.7 Ramp-incremental exercise time following high-intensity interval training with BFR (HIIT+BFR) and without BFR (HIIT). Ramp-incremental exercise time significantly increased after HIIT+BFR and HIIT (time effect: $p < 0.05$) with no difference between groups (interaction: $p > 0.05$). Values are mean ± SD for 16 participants (HIIT+BFR: $n = 8$; HIIT: $n = 8$).

4.3.6 Changes in baseline progenitor cell number following exercise training

Blood samples were drawn from 15 participants pre- and post-training (HIIT+BFR: $n = 7$; HIIT: $n = 8$) to determine the training response of HIIT+BFR and HIIT on baseline number of circulating progenitor cells. The number of $CD34^+$ cells did not change pre- to post-training in either group, with no difference between groups (HIIT+BFR: Pre = 2617 ± 1456; Post = 3303 ± 2259 /10^6 total events; HIIT: Pre = 2510 ± 1306; Post = 2660 ± 1339 /10^6 total events; time effect: $p = 0.34$; interaction effect: $p = 0.53$; Figure 4.8). Similarly, the number of $CD34^+/KDR^+$ progenitor cells remained unchanged with training in both groups, with no difference between groups (HIIT+BFR: Pre = 79 ± 68; Post = 111 ± 116 /10^6 total events; HIIT: Pre = 69 ± 30; Post = 63 ± 27 /10^6 total events; time effect: $p = 0.31$; interaction effect: $p = 0.14$; Figure 4.8).

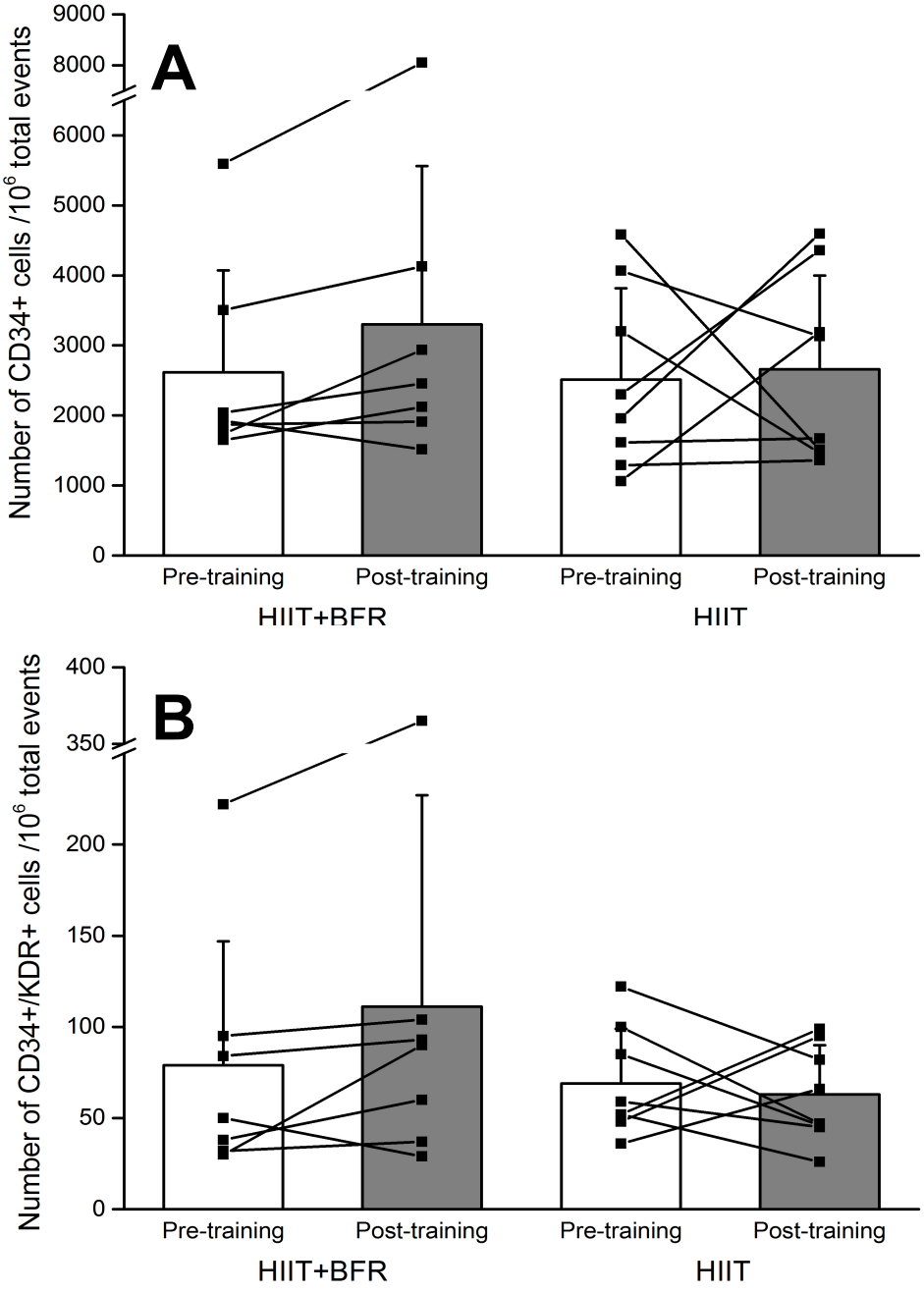

Figure 4.8 $CD34^+$ (A) and $CD34^+/KDR^+$ (B) progenitor cell response to high-intensity interval training with BFR (HIIT+BFR) and without BFR (HIIT). The number of $CD34^+$ and $CD34^+/KDR^+$ cells remained unchanged following HIIT+BFR and HIIT (time effect: $p > 0.05$) with no difference between groups (interaction: $p > 0.05$). Values are mean ± SD for 15 participants (HIIT+BFR: $n = 7$; HIIT: $n = 8$).

4.3.7 Quality of life

There was no difference in self-reported health-related quality of life between HIIT+BFR and HIIT at baseline (U = 27, p = 0.91). Questionnaire data was collected from all participants; however, data from one participant was excluded because scores were unduly influenced by an extraneous event (HIIT+BFR: n = 7; HIIT: n = 8). There were trends, with a large effect sizes (HIIT+BFR: r = 0.67; HIIT: r = 0.60) for quality of life to improve (score range = 0-105; higher scores indicate worse quality of life) pre- to post-training in HIIT+BFR (Pre = 31 ± 18; Post = 25 ± 20; p = 0.07) and HIIT (Pre = 33 ± 18; Post = 25 ± 20; p = 0.09; Figure 4.9). The absolute change in total score pre- to post-training was not different between groups (p = 0.49), indicating that both protocols had a similar effect on quality of life. Indeed, quality of life improved in 71% of HIIT+BFR participants and 75% of HIIT participants. Furthermore, total score reduced by ≥5 points (minimum clinically important difference) in the HIIT+BFR (n = 4) and HIIT (n = 5) groups.

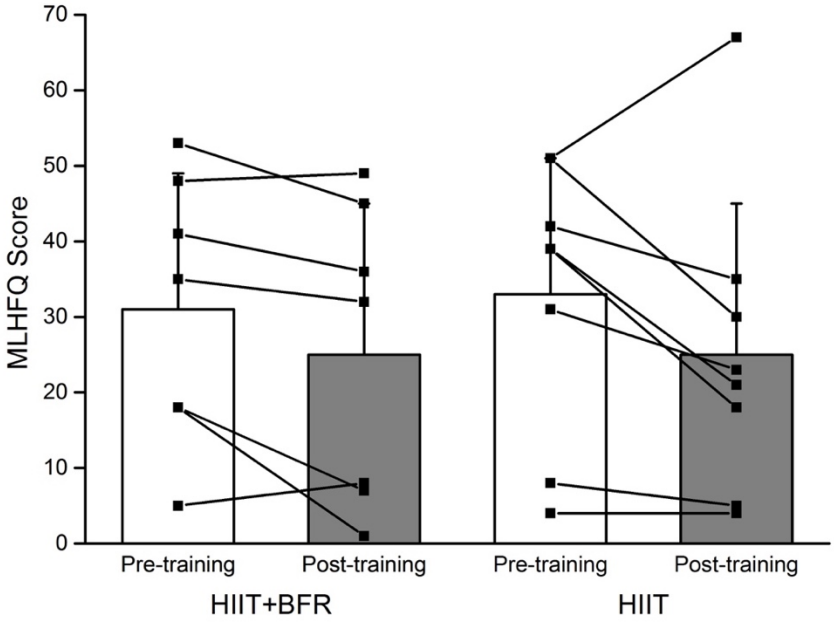

Figure 4.9 Self-reported health-related quality of life (assessed using the Minnesota Living with Heart Failure Questionnaire [MLHFQ]) after high-intensity interval training with blood flow restriction (HIIT+BFR) and without blood flow restriction (HIIT). There was a trend for quality of life to improve (MLHFQ score range is 0-105 and higher scores indicate worse quality of life) pre- to post-training in HIIT+BFR (r = 0.67; p = 0.07) and HIIT (r = 0.60; p = 0.09). Values are mean ± SD for 15 participants (HIIT+BFR: n = 7; HIIT: n = 8).

4.3.8 Post-training: acute progenitor cell response to HIIT+BFR and HIIT

Blood samples were collected from 11 participants before and after a single exercise session post-training (HIIT+BFR: *n* = 6; HIIT: *n* = 5). The number of $CD34^+$ and $CD34^+/KDR^+$ progenitor cells remained unchanged pre- to post-exercise (time effect = $p > 0.05$), with no differences between groups (interaction: $p > 0.05$; Figure 4.10). Thus, mirroring the pre-training response.

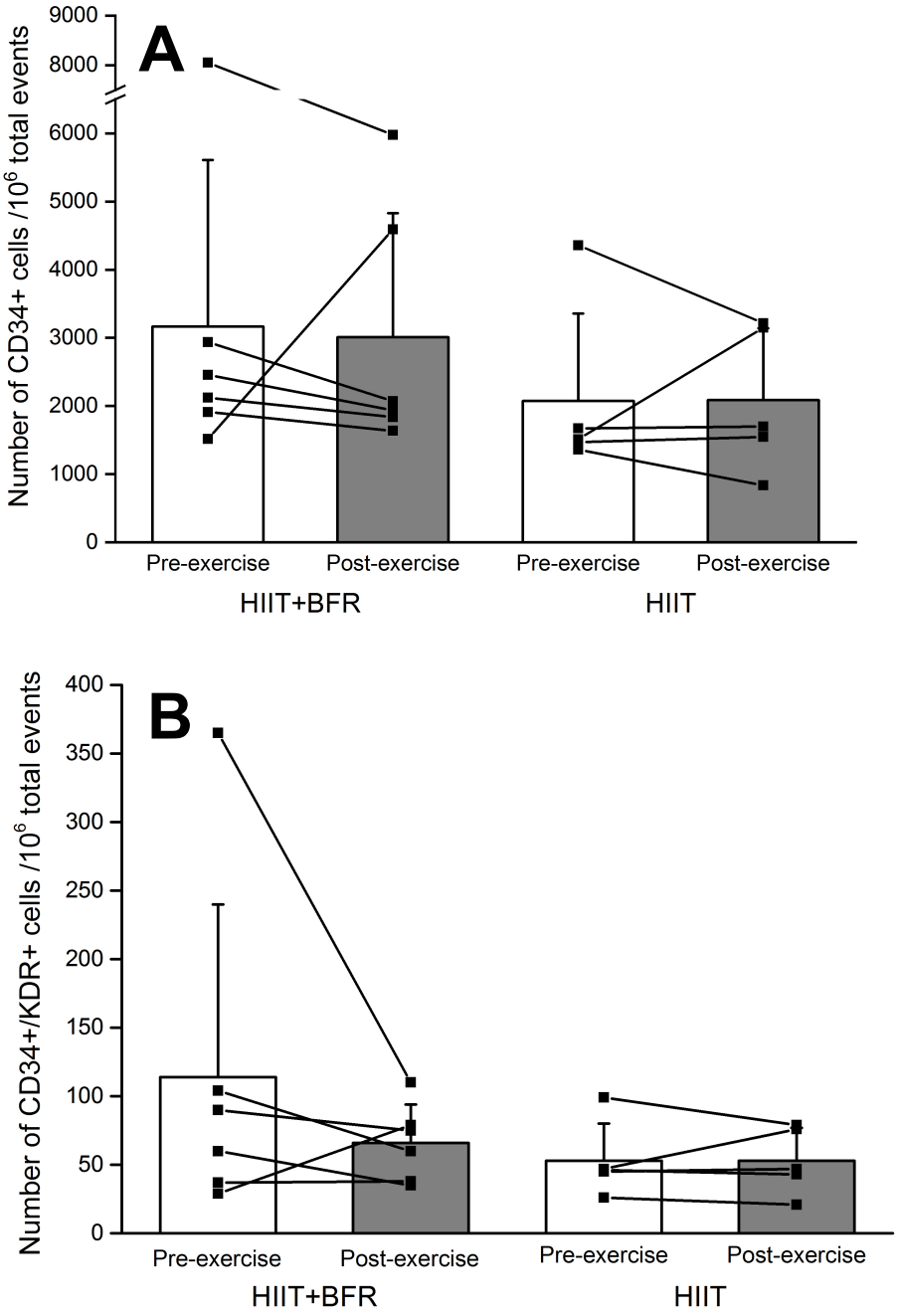

Figure 4.10 $CD34^+$ (A) and $CD34^+/KDR^+$ (B) progenitor cell response to a single session of high-intensity interval training with BFR (HIIT+BFR) and without BFR (HIIT) after exercise training. The number of $CD34^+$ and $CD34^+/KDR^+$ cells remained unchanged following an acute bout of HIIT+BFR and HIIT post-training (time effect: $p > 0.05$) with no difference between groups (interaction: $p > 0.05$). Values are mean ± SD for 11 participants (HIIT+BFR: $n = 6$; HIIT: $n = 5$).

4.4 Discussion

This study was the first to investigate the feasibility and effect of HIIT with BFR on progenitor cell number, $\dot{V}O_{2peak}$ and exercise tolerance in HFrEF. We found that HIIT with BFR is practicable and safe in HFrEF, with all participants able to adhere to the intervention, and there were no adverse events. However, the main finding of this study was that HIIT with or without BFR does not increase baseline $CD34^+$ or $CD34^+/KDR^+$ progenitor cell number in HFrEF. Furthermore, although HIIT does increase exercise tolerance (ramp-incremental exercise duration) and $\dot{V}O_{2peak}$ there is no additional benefit from adding BFR to the exercise protocol.

4.4.1 Effect of HIIT on progenitor cell number: the acute response

Prior work has shown that a single session of exercise can mobilise progenitor cells from the bone marrow into the peripheral blood to increase circulating cell number in healthy individuals (Yang et al., 2007, Van Craenenbroeck et al., 2008b), but that this response is severely attenuated in HFrEF (Van Craenenbroeck et al., 2010a, Van Craenenbroeck et al., 2011). Van Craenenbroeck and colleagues have consistently demonstrated no significant rise in $CD34^+/KDR^+$ number 10 min after a symptom-limited cardiopulmonary exercise test in HFrEF, despite elevations occurring in younger and older healthy controls (Van Craenenbroeck et al., 2011, Van Craenenbroeck et al., 2010a, Van Craenenbroeck et al., 2010b). The same protocol also results in no increase in circulating $CD34^+$ cell number in HFrEF in some (Van Craenenbroeck et al., 2010a, Van Craenenbroeck et al., 2010b), but not all (Van Craenenbroeck et al., 2011), studies. Further, additional samples collected by Van Craenenbroeck et al. (2011) between 30 min and 48 h after the cardiopulmonary exercise test showed no significant increase in progenitor cell number, ruling out a delayed response. In line with these results, no exercise-induced changes in $CD34^+$ and $CD34^+/KDR^+$ progenitor cell number were seen following a single HIIT session, both pre- and post-training. The lack of change in the progenitor cell response to

exercise pre- to post-training matches the response seen before and after 6 months of aerobic exercise training in HFrEF (3 times a week at 90% of heart rate at the respiratory compensation point; Van Craenenbroeck et al. (2010b).

Many authors have suggested that exercise-induced progenitor cell mobilisation in healthy participants is dependent on exercise intensity and duration (Ribeiro et al., 2017, Laufs et al., 2005). However, this study employed a high-intensity exercise strategy ($\dot{V}O_2$ 95 ± 14% of baseline $\dot{V}O_{2peak}$ during work intervals in second training session) with more time spent exercising at this high-intensity (10-12 min) than in previous investigations (Van Craenenbroeck et al., 2010b, Van Craenenbroeck et al., 2011, Van Craenenbroeck et al., 2010a). Thus, taken together, the present data, and those of others, suggest exercise-induced progenitor cell mobilisation is attenuated in HFrEF, and the training strategies employed here are unable to restore the response to exercise seen in health. Possible mechanisms underlying this response include poor nitric oxide bioavailability, consequent to a decline in maximum cardiac output decreasing in-exercise shear stress and nitric oxide production, or pro-inflammatory cytokines suppressing progenitor cell release from the bone marrow (Dufour et al., 2003, Valgimigli et al., 2004). However, resolution of the mechanism requires further investigation, which might reveal strategies to overcome this attenuated progenitor cell response in HFrEF.

4.4.2 Effect of HIIT+BFR on progenitor cell number: the acute response

This is the first study to investigate the progenitor cell response to an acute bout of exercise with BFR in HFrEF. In contrast to our hypothesis, the number of $CD34^+$ and $CD34^+/KDR^+$ progenitor cells remained unchanged following a single session of HIIT+BFR pre- and post-training. These results are comparable to a previous study showing no additional exercise-induced progenitor cell mobilisation following the addition of BFR to single leg knee extensor exercise in healthy individuals

(Montgomery et al., 2019). This result was surprising because exercise with BFR is associated with an increase in endothelial nitric oxide synthase activity (Ferguson et al., 2018), consequent to the shear stress stimulus elicited by reactive hyperaemia following cuff deflation. The vascular response to shear stress is determined by the magnitude of the stimulus and therefore the cuff pressure that is applied. A lower cuff pressure was used in this study compared to a previous study (100 mmHg vs. 110 mmHg; Ferguson et al., 2018) investigating the effect of exercise with BFR on angiogenic stimuli in healthy individuals. Thus, it is possible that if a higher cuff pressure was applied the reactive hyperaemia response and consequent nitric oxide production may have been greater, creating a greater stimulus for hematopoietic and endothelial progenitor cell mobilisation than HIIT alone. However, higher cuff pressures may compromise tolerability and clinical safety in HFrEF. Furthermore, a 10 mmHg increase in cuff pressure is unlikely to substantially influence the reactive hyperaemia response, as this is associated with only a further 10% increase in restricted blood flow (Hunt et al., 2016).

Progenitor cell mobilisation is commonly reported concomitantly with increases in VEGF, another angiogenic stimuli enhanced following exercise with BFR (Larkin et al., 2012). Indeed, a 5.2-fold increase in VEGF mRNA was observed 2 and 4 h after sprint interval training with 110 mmHg BFR (Ferguson et al., 2018). Although this response was reported in healthy individuals, previous work has demonstrated that the VEGF mRNA response to acute exercise is still intact in HFrEF and not different from healthy controls (Esposito et al., 2010a, Esposito et al., 2018). It is possible that HIIT+BFR significantly increased skeletal muscle VEGF mRNA abundance, resulting in an elevation in VEGF protein expression and subsequent increase in VEGF in the muscle interstitial fluid. However, due to the time course between VEGF mRNA and VEGF protein expression this may have occurred more than 4 h post-exercise. This study only assessed the immediate progenitor cell response to HIIT+BFR (10 min

post-exercise) and therefore a delayed increase in progenitor cell number cannot be ruled out. Thus, future studies are needed to assess the number of progenitor cells at several different time points after exercise with BFR.

Mechanistically, elevations in VEGF following exercise with BFR potentially result from shear stress driven increases in nitric oxide production promoting outflow of VEGF from the skeletal muscle (Benoit et al., 1999) or reductions in skeletal muscle oxygenation (Corvino et al., 2017) increasing the hypoxia-inducible factor 1 alpha and VEGF transcription. The lower cuff pressure that was used in this study (100 mmHg vs. 110 mmHg; Ferguson et al., 2018) may have resulted in an insufficient stimulus to increase VEGF expression but unfortunately this was not measured to allow for comparison.

4.4.3 Effect of exercise training on progenitor cell number

In contrast to the responses seen after 3 weeks to 6 months of high-intensity continuous exercise training in HFrEF (Sandri et al., 2016, Gatta et al., 2012, Van Craenenbroeck et al., 2010b), HIIT training did not increase $CD34^+$ and $CD34^+/KDR^+$ progenitor cell number in this study. Following 4 weeks of supervised aerobic exercise training, consisting of four 15-20 min cycle ergometry sessions each weekday at 60-70% of $\dot{V}O_{2peak}$, Sandri et al. (2016) demonstrated a 66 and 69% increase in $CD34^+/KDR^+$ number in younger and older HFrEF patients, respectively. Likewise, Gatta et al. (2012) reported an increase in $CD34^+/KDR^+$ cells from 5 ± 3 to 9 ± 6 cells/ml (~ 80%) after a 3-week training period involving calisthenics and 30 min of cycling at 75-85% HR_{max} twice daily on 6 days a week. However, the training volume used in these studies was much greater than the present study (5-6 x 2 min intervals at 80% ramp-incremental exercise WR_{peak} separated by 2 min of recovery, performed twice a week for 4 weeks). Thus, it is possible that an increase in $CD34^+/KDR^+$ number may have occurred if training frequency and the period of

exercise training increased, thus the dose. Nonetheless, additional training sessions require additional resources (e.g. staff time and use of training facilities), potentially compromising the feasibility of training programmes with >2 sessions per week in real-world rehabilitation settings.

Even with the addition of BFR, it appears that the HIIT protocol used in this study was insufficient for hematopoietic and endothelial progenitor cell mobilisation. It is tempting to speculate that the lack of progenitor cell response to HIIT+BFR (i.e. a greater stimulus for mobilisation) is consequent to impaired progenitor cell release from the bone marrow and not an insufficient stimulus for mobilisation. The primary stimulus for exercise-induced progenitor cell mobilisation is shear stress induced liberation of nitric oxide from vascular endothelial cells. Regular bouts of shear stress during training increase basal nitric oxide bioavailability and have an antioxidant effect on the vasculature (Green et al., 2004), leading to improved vascular health and a greater number of circulating progenitor cells. Given the prognostic role of progenitor cell counts and their association with reduced risk of cardiovascular events (Samman Tahhan et al., 2017, Schmidt-Lucke et al., 2005), future studies should endeavour to determine the factors involved in impaired progenitor cell release in HFrEF and the optimal exercise strategy (including intensity and volume) to increase progenitor cell number in HFrEF.

4.4.4 Effect of exercise training on $\dot{V}O_{2peak}$

A recent meta-analysis reported a mean increase in $\dot{V}O_{2peak}$ of 16% in HFrEF cohorts using HIIT (Gomes Neto et al., 2018), with individual studies showing improvements of between 4 and 46% (Dimopoulos et al., 2006, Roditis et al., 2007, Benda et al., 2015, Wisløff et al., 2007). In this study, $\dot{V}O_{2peak}$ (relative) increased by 18 ± 11% in the HIIT group (2.7 ± 2.2 $ml \cdot min^{-1} \cdot kg^{-1}$), surpassing the mean response to HIIT. Considering every 6% increase in $\dot{V}O_{2peak}$, when adjusted for other significant

predictors, is associated with a 5% lower risk of all-cause mortality (Swank et al., 2012), this improvement in $\dot{V}O_{2peak}$ in the HIIT group is likely to convey a positive effect on prognosis. Differences in the characteristics of the HIIT protocol (e.g. frequency, intensity and duration) may contribute to the magnitude of change seen with training. In comparison to other HIIT protocols that have led to much greater increases in $\dot{V}O_{2peak}$, training frequency and overall training duration was less in the current study, likely dampening the stimulus for adaptation.

In contrast to the HIIT group, there was no change in relative or absolute $\dot{V}O_{2peak}$ pre- to post-training in the HIIT+BFR group. The HIIT+BFR protocol utilised in this study was employed to increase the stimuli for progenitor cell mobilisation (e.g. BFR increases shear stress and angiogenic signalling; Mouser et al., 2017, Ferguson et al., 2018). However, the lack of change in progenitor cell number pre- to post-training suggests that the stimulus provided was insufficient to positively influence vascular endogenous repair capacity and thus most likely vascular health. In the absence of vascular adaptations, it is unlikely that blood flow (i.e. oxygen delivery) to the working skeletal muscle increased following HIIT+BFR, and thus, no increase in $\dot{V}O_{2peak}$ occurred via this mechanism.

Subsequently, the results of this study contrast with previous findings that have demonstrated greater increases in $\dot{V}O_{2peak}$ and exercise duration following exercise training with BFR in young healthy participants (Abe et al., 2010). Two studies investigating the effect of sprint interval training with BFR on $\dot{V}O_{2peak}$ in trained individuals reported a 4.5 and 5.9% increase, with no change reported after the same exercise without BFR (Taylor et al., 2016, Mitchell et al., 2019). Superior improvements in $\dot{V}O_{2peak}$ have also been seen following the addition of BFR to lower

intensity cycle exercise (40% $\dot{V}O_{2peak}$); however, cuffs were inflated for the entire training session (~18 min) in this study (Abe et al., 2010).

Although the determinants of $\dot{V}O_{2peak}$ are complex, changes in $\dot{V}O_{2peak}$ following exercise with BFR have previously been attributed to central cardiovascular adaptations. Specifically, during exercise with BFR the cardiovascular system is subjected to additional stress and the induction of the exercise pressor reflex. Once elicited this reflex causes an increase in heart rate and mean arterial blood pressure (responses seen during exercise with BFR; Iida et al., 2007, Thomas et al., 2018), resulting in an increase in cardiac work. Repetitive exposure to this acute response during exercise training with BFR may drive cardiac adaptations, specifically elevations in stroke volume; following 2 weeks of walk training with BFR, stroke volume increased by 21.4% (Park et al., 2010). In turn increases in cardiac output, driven by elevations in stroke volume, may increase oxygen delivery to the working muscle and thus $\dot{V}O_{2peak}$ (Renzi et al., 2010). However, it is noteworthy that the cuff pressure used in these studies (120-210 mmHg) was considerable higher than the 100 mmHg used in this study (Abe et al., 2010, Taylor et al., 2016, Mitchell et al., 2019). Therefore, it is possible that the cuff pressure used in this study did not induce greater cardiovascular strain than HIIT alone, and thus, there was no change in convective O_2 delivery and no increase in $\dot{V}O_{2peak}$.

Exercise training with BFR may also drive changes in the periphery, given the increased metabolic stress that this novel technique induces. However, mitochondrial protein content and skeletal muscle capillarisation appear to be unchanged following even extreme sprint interval training with BFR (120 mmHg), despite increases in $\dot{V}O_{2peak}$ being observed (Mitchell et al., 2019). Subsequently, further work is needed

to investigate the mechanisms underpinning changes in $\dot{V}O_{2peak}$ with BFR exercise training.

4.4.5 Effect of exercise training on exercise tolerance

Despite an increase in $\dot{V}O_{2peak}$ only being observed in the HIIT group, time to intolerance and WR_{peak} increased in both HIIT+BFR and HIIT training groups with no difference between groups. Whilst indicating that no additional advantage is conferred with regards to time to intolerance by combining HIIT with BFR, this suggests that different mechanisms may underpin the increase in exercise tolerance observed in both groups.

The increase in $\dot{V}O_{2peak}$ observed in the HIIT group, reflecting an increase in the capacity for aerobic ATP regeneration, likely underpins the increase in exercise tolerance in this training group. However, in addition to this LT increased in both groups. Therefore, it is probable that in part exercise tolerance increased in both groups because LT increased pre- to post-training, delaying the necessity to supplement aerobic mechanisms of energy provision with less efficient anaerobic mechanisms. Several other mechanisms may have contributed to this improvement in exercise tolerance. For example, HIIT+BFR and HIIT may have speeded $\dot{V}O_2$ kinetics (Corvino et al., 2019, Roditis et al., 2007, Mezzani et al., 2013), reducing the anaerobic contribution to energy provision during the initial minutes of ramp-incremental exercise, thus preserving anaerobic energy stores for utilisation later in the exercise test and potentially contributing to the increase in LT. We demonstrated a 12 ± 9 and 9 ± 4 W increase in WR_{peak} pre- to post-training in HIIT+BFR and HIIT, respectively; this is comparable to the 11 W increase that accompanied a 19% increase in mean response time in individuals with HFrEF following 3 months of moderate-intensity continuous exercise training (Mezzani et al., 2013). Although it was beyond the scope of the current study to measure $\dot{V}O_2$ kinetics as this would

have required additional study visits to complete a set of constant work rate exercise tests (Whipp and Rossiter, 2005), mean response time was estimated from the time between the lag of the $\dot{V}O_2$ response at the beginning of the ramp-incremental exercise test to the linear increase in $\dot{V}O_2$. Using this approach, estimated mean response time was not different between groups at baseline ($p > 0.05$) but was faster pre- to post-training by 9 ± 12 and 5 ± 7 s in the HIIT+BFR and HIIT group, respectively (time effect: $p = 0.01$; interaction effect: $p = 0.42$). Thus, indicating that HIIT and HIIT+BFR may have speeded $\dot{V}O_2$ kinetics in HFrEF; however, to confirm this requires further investigation.

Alternatively, it is plausible that HIIT+BFR and HIIT may have induced an increase in anaerobic capacity (maximal amount of ATP regeneration that is obtainable from anaerobic metabolism) that may have contributed to the improvement in exercise tolerance. Maximal accumulated oxygen deficit is often considered as a practical quantitative expression of anaerobic capacity (Medbø and Burgers, 1990). Normally, this parameter is determined from the difference in accumulated O_2 uptake and calculated O_2 demand during a short (2-3 min) maximal constant work rate exercise test.

However, an estimation of the anaerobic contribution to overall energy provision during the ramp-incremental exercise test pre- and post-training was derived in the current study by determining the difference between the total amount of external work done (i.e. total ATP demand) during the test and the work generated from aerobic metabolism (Pouilly and Busso, 2008). The latter was calculated based on the assumption that aerobic power (i.e. $\dot{V}O_2$) progresses as a linear function during ramp-incremental exercise following a delay due to the limb-lung transit time and muscle $\dot{V}O_2$ kinetics (i.e. mean response time; Figure 4.11).

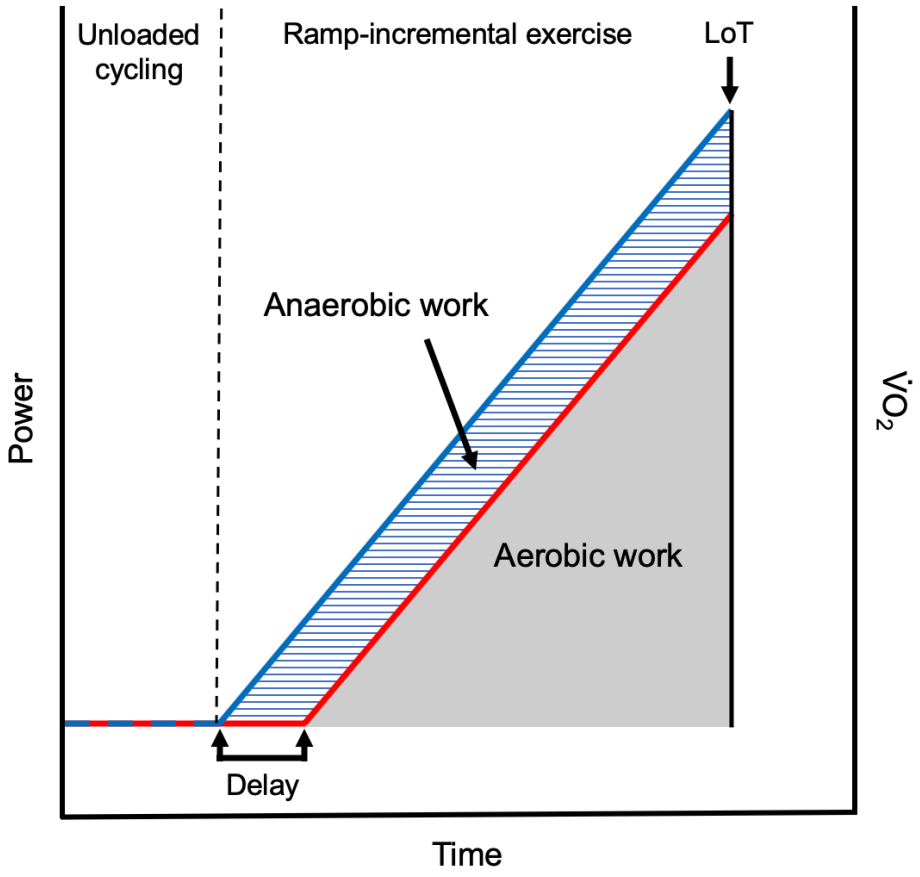

Figure 4.11 Schematic of the aerobic and anaerobic contributions to overall energy provision during ramp-incremental exercise to the limit of tolerance (LoT). External work (blue line) increases instantaneously at the onset of ramp-incremental exercise but there is a lag in the $\dot{V}O_2$ response (red line) due to the kinetics of the $\dot{V}O_2$ response. The difference between total external work and aerobic work provides an estimate of the anaerobic contribution to total energy production.

Prior to training, the anaerobic contribution to overall energy production during ramp-incremental exercise to intolerance was not different between training groups (p > 0.05) and there was no time effect pre- to post-training (p > 0.05). There was a trend with a large effect size for an interaction effect (p = 0.06; η^2 = 0.25), indicating a cross over effect. However, there were no differences over time within each group when explored using *post-hoc* paired-samples *t*-tests, despite a 64 ± 104% increase in the anaerobic contribution to overall energy production in the HIIT+BFR group

(HIIT+BFR: Pre = 1.44 ± 1.12; Post = 2.08 ± 1.15 $L \cdot min^{-1}$; HIIT: Pre = 1.55 ± 0.99; Post = 1.19 ± 0.73 $L \cdot min^{-1}$). Thus, although statistically insignificant, these results suggest that the addition of BFR to HIIT may increase anaerobic capacity more than HIIT alone. Nevertheless, whilst this proposition supports previous BFR research documenting an increase in anaerobic capacity post-training in healthy individuals (Park et al., 2010), it cannot be confirmed in HFrEF following HIIT with BFR using the information available from this study.

4.4.6 Effect of exercise training on quality of life

Health-related quality of life in HFrEF has been demonstrated to improve after a period of HIIT in several (van Tol et al., 2006, Chrysohoou et al., 2013) but not all previous investigations (Benda et al., 2015). In the current study, there was a trend for quality of life to increase with training, but this was not affected by training group. Indeed, HIIT with BFR improved MLHFQ score by 5.7 points, whilst HIIT improved MLHFQ score by 7.8 points. This is of clinical relevance as both of these improvements exceed the minimal clinically important difference (≥ 5 points; Rector et al., 1987) which is associated with reduced risk of hospitalisation and mortality in patients with severe HFrEF (Moser et al., 2009). The magnitude of improvement (reduction) in MLHFQ score in this study is also comparable to the 2014 Cochrane meta-analysis (mean difference of -7.1 points; Taylor et al., 2014). Subsequently, this study supports the use of HIIT as an intervention that can positively affect quality of life in HFrEF.

4.4.7 Limitations

There are limitations to this study that must be considered. Firstly, the degree of restricted blood flow may have differed between participants. In this study, a standard cuff pressure of 100 mmHg was used for all participants in the intervention group. However, the extent of BFR is influenced by several factors, including blood pressure, thigh circumference and limb composition (Loenneke et al., 2012, Hunt et al., 2016). Subsequently, it is likely that the degree of restricted blood flow was inconsistent

between participants and may have affected the magnitude of any adaptations. Secondly, although this study suggests that HIIT with BFR is feasible in individuals with HFrEF the results of this study cannot be translated to higher cuff pressures (>100 mmHg) that may be needed to induce the superior physiological adaptations observed following aerobic exercise with BFR. Only patients classified as NYHA class I-III were included in this study and therefore the results may not apply to patients with more severe HFrEF. While circadian swings in progenitor cell number were controlled by sampling blood at the same time pre- and post-training, blood was collected from participants in an unfasted state and several dietary components, such as flavonoids and flavanols, can influence progenitor cell number (Heiss et al., 2010, Buitrago-Lopez et al., 2011, Kim et al., 2006). Pharmacological therapies, such as statins, can also affect circulating progenitor cell number. However, medication remained unchanged before (>3 months) and throughout the intervention period. In addition, blood was only sampled 10 min after exercise to evaluate the acute progenitor cell response to a single bout of HIIT with and without BFR. Subsequently, a delayed progenitor cell response cannot be excluded. Finally, the addition of flow mediated dilation to assess vascular function in this study may have provided further insight on the effect of HIIT with BFR on vascular health in HFrEF.

4.4.8 Conclusion

In summary, despite the feasibility of HIIT with BFR in individuals with HFrEF, the addition of BFR does not further improve the effectiveness of this training intervention, and therefore is not an advantageous addition to HFrEF training programmes.

Chapter 5 The acute and chronic effects of novel intensity-matched interval exercise on vascular health and function

5.1 Foreword

This experimental chapter was impacted by the COVID-19 pandemic. The aim of this study was to investigate the effect of a novel 6-week exercise training intervention on capacity for vascular endogenous repair, endothelial function, exercise tolerance and $\dot{V}O_{2peak}$ in young and older adults. However, in response to the COVID-19 pandemic, the University of Leeds closed for an extended period of time and restrictions were placed on human research upon reopening. Therefore, data collection for this study ended prematurely in March 2020 and, to date, it has not been possible to re-start testing. As a result, this study still assessed the acute and chronic response to the novel exercise training intervention, but it was not possible to collect data from older individuals and data were collected from a reduced number of young individuals. The characterisation data (e.g. $\dot{V}O_{2peak}$ and exercise tolerance data) presented in this chapter were collected as part of a joint project in collaboration with Matt Chadwick. However, this chapter has specific aims and data to investigate the effects of novel intensity-matched interval exercise on vascular health and function.

5.2 Introduction

Cardiovascular disease is a major cause of mortality in the UK, responsible for almost 30% of all deaths (British Heart Foundation, 2021). Endothelial dysfunction is a key mediator in the development of atherosclerosis that precedes clinical symptoms and diagnosis of cardiovascular disease (Kobayashi et al., 2004, Juonala et al., 2004, Davignon and Ganz, 2004). Systemic endothelial dysfunction can be identified as a reduction in endothelial-dependent vasodilation assessed by flow-mediated dilation (FMD; Harris et al., 2010, Thijssen et al., 2019). FMD is a significant predictor of cardiovascular events in older individuals, even after adjustment for traditional risk factors (Yeboah et al., 2007). Furthermore, in those with a cardiovascular disease

diagnosis, such as atherosclerosis, hypertension and coronary artery disease, FMD correlates with disease severity and is strongly predictive of future cardiovascular events (Xu et al., 2014, Matsuzawa et al., 2015, Shechter et al., 2014, Ras et al., 2013, Neunteufl et al., 1997).

Endothelial dysfunction occurs when there is an imbalance between endothelial damage and endogenous repair mechanisms, favouring the former (Davignon and Ganz, 2004). Subsequently, increasing vascular endogenous repair capacity, assessed by the number of circulating progenitor cells, may preserve or even improve vascular endothelial integrity and function. These progenitor cells include hematopoietic progenitor cells ($CD34^+$) and endothelial progenitor cells ($CD34^+/KDR^+$) that contribute to vascular repair by binding to the activated endothelium and differentiating into endothelial cells or by secreting factors that promote the proliferation and migration of existing endothelial cells near the site of damage (Rehman et al., 2003, Leone et al., 2009, Urbich and Dimmeler, 2004, Lenk et al., 2011). Ageing and cardiovascular disease are independently associated with a reduction in the number of circulating hematopoietic and endothelial progenitor cells, with lower progenitor cell counts independently predictive of cardiovascular events and mortality (Werner et al., 2005, Schmidt-Lucke et al., 2005, Thijssen et al., 2006, Ross et al., 2018, Samman Tahhan et al., 2017). However, a single session of aerobic exercise can induce a transient increase in hematopoietic and endothelial progenitor cell number, whilst exercise training can lead to a sustained increase in baseline hematopoietic and endothelial progenitor cell number (Krüger et al., 2015, Xia et al., 2012, Tsai et al., 2016, Van Craenenbroeck et al., 2008b). A single session of aerobic exercise can also illicit an immediate increase or decrease in endothelial function (FMD), with decreases typically associated with high-intensity exercise (Dawson et al., 2013, Birk et al., 2013). However, exercise training is typically associated with increases in baseline endothelial function (Ramos et al., 2015,

Tinken et al., 2008, Green et al., 2004). Thus, exercise training represents a pragmatic therapy to increase vascular endogenous repair capacity and vascular function and reduce the risk of cardiovascular disease.

The “traditional” approach to aerobic training is to prescribe constant work rate exercise to increase vascular endothelial function (Tinken et al., 2008, Birk et al., 2012). However, interval exercise training characterised by periods of work interspersed by periods of recovery, has been shown to induce comparable, and at times superior, increases in endothelial function and exercise tolerance than constant work rate exercise training (Rakobowchuk et al., 2008, Harris et al., 2014, Boff et al., 2019, Sawyer et al., 2016, Conraads et al., 2015, Moholdt et al., 2009, Wisløff et al., 2007). Performing Interval exercise training can also increase vascular endogenous repair capacity and induce greater feelings of perceived enjoyment compared to constant work rate exercise (Bartlett et al., 2011, Tsai et al., 2016). In turn, this increase in enjoyment during interval exercise may lead to increased exercise adherence (Bartlett et al., 2011). However, the diversity between the interval protocols described in the literature makes it difficult to isolate the most important contributor for improving vascular endogenous repair capacity and endothelial function, limiting our understanding of how to personalise exercise therapy to maximise impact.

Vascular adaptations to exercise programmes may be impacted by: (1) the intensity of the exercise session. This is typically greater in interval protocols than constant work rate protocols, increasing the peak shear rate attained during each interval exercise bout; (2) the work:recovery durations. During interval exercise the length of the work and recovery periods affect the pattern of shear (peak and magnitude of oscillatory swings) and overall volume of shear accumulated during the exercise,

making interval exercise distinct from constant work rate exercise; (3) the work rate. This also tends to be greater in interval exercise than constant work rate exercise and may have intramuscular effects that also influence the systemic vasculature. These factors may independently, or interdependently influence vascular adaptations to interval training. Therefore, the relative importance of each variable in driving the adaptive response to interval exercise is unknown.

The nature of interval exercise dissociates the work rate from the metabolic stress (intensity) of the exercise, with the magnitude of the dissociation dependent on the work:recovery ratio. The greatest dissociation between exercise intensity and the work rate of the exercise occurs when work bouts are short (e.g. 10 s; Turner et al., 2006, Davies et al., 2017). Therefore, when the work:recovery durations are very short (e.g. 10:10 s) it is possible for both the intensity of the exercise, and the systemic shear stress pattern of interval exercise to be matched to that of constant work rate exercise to isolate whether there is any specific role of the higher work rate in mediating the adaptations seen with interval exercise. Critically, this protocol also maximises the volume of shear stress that can be accumulated using an interval protocol that is intensity-matched by maintaining the same peak shear rate throughout the exercise protocol as constant work rate exercise. This is achieved by eliminating the on-off oscillations in shear rate that are often a characteristic of interval exercise. By maximising the volume of shear stress and time at peak shear, this interval protocol may be the optimum training regimen for inducing vascular adaptations for a given exercise intensity and duration in individuals with a preference for interval exercise.

Arterial inflow is closely related to muscle contraction-relaxation duty cycles: during muscle contraction, intramuscular pressure is increased, causing mechanical

compression of the local vasculature and a transient reduction in blood flow. During the muscle relaxation phase, intramuscular pressure is low and arterial inflow is unrestricted (Barcroft and Dornhorst, 1949, Walløe and Wesche, 1988, Kagaya and Ogita, 1992, Robergs et al., 1997). As the force of the contraction increases, intramuscular pressure increases linearly (Sadamoto et al., 1983, Parker et al., 1984, Aratow et al., 1993). Thus, interval exercise with a higher work rate is likely to result in greater compression of the intramuscular vasculature and a greater reduction in arterial inflow during muscle contraction than interval exercise with a lower work rate. In turn, this reduction in blood flow may increase the degree of intermittent hypoxia that is experienced, leading to an increase in HIF-1α and VEGF; angiogenic factors that stimulate exercise-induced progenitor cell mobilisation from the bone marrow (Asahara et al., 1999, Ceradini et al., 2004, Volaklis et al., 2013, Aicher et al., 2003). Chronic exposure to this stimulus via exercise training may then lead to a greater increase in vascular endogenous repair capacity. In addition, the microvasculature in the working skeletal muscle may be exposed to an increase in shear stress during muscle contraction and an increase in reactive hyperaemia during muscle relaxation during interval exercise with a high work rate. This may increase NO production during acute interval exercise, leading to greater improvements in endothelial function with exercise training (Higashi and Yoshizumi, 2004). However, the isolated effect of a greater work rate during a single bout of interval exercise and exercise training on vascular endogenous repair capacity and systemic vascular function remains unknown.

Understanding how the characteristics of interval exercise (e.g. work rate, work:recovery ratio and exercise intensity) interact to influence acute and chronic vascular adaptations is vital for designing effective training strategies that improve vascular endogenous repair capacity and endothelial function. Therefore, the

purpose of this study was to investigate whether high-intensity interval exercise training (HIIT) with a high work rate and short work:recovery bouts (intended to minimise oscillations in shear rate and maximise the volume of shear rate accumulated), induces a greater increase in vascular endogenous repair capacity and endothelial function than intensity, shear rate and volume matched constant work rate exercise training. Thus, isolating the effect of a work rate that allows the greatest recruitment of skeletal muscle on vascular adaptations. The vascular response to a single session of HIIT with a high work rate was also examined pre- and post-training to determine the acute effect of this exercise strategy on vascular endogenous repair capacity and endothelial function and whether this acute response is influenced by exercise training.

5.3 Methods

5.3.1 Participants and ethical approval

The original intention was to recruit 25 young (<35 y) and 25 older (>60 y) individuals; however, due to the impact of COVID-19, 5 male and 7 female habitually active young individuals volunteered to participant in this study. All participants were screened prior to any exercise testing using a Health and Physical Activity Status Questionnaire to ensure that it was safe for them to undertake maximal exercise. Individuals were excluded if they had a history of cardiovascular disease, respiratory or musculoskeletal disease, an active medical condition (e.g. diabetes, asthma or uncontrolled hypertension), family history of sudden cardiac death, recent illness (within 2 weeks) or any contradiction to cycle exercise. All participants provided written informed consent before taking part in the study. This study and all of the procedures involved was approved by The Biological Sciences Faculty Research Ethics Committee.

5.3.2 Study design

Participants were randomised to perform 6 weeks of HIIT with a high work rate or intensity-matched constant work rate exercise training (Figure 5.1). Before and after 6 weeks of exercise training, participants completed a ramp-incremental exercise test and a constant work rate exercise test. During the 6 weeks of exercise training, participants attended the laboratory on two separate occasions each week (i.e. a total of 12 training sessions) to perform their allocated training protocol under researcher supervision.

The first and last exercise training sessions were used to determine the acute and chronic effect of the HIIT and constant work rate exercise protocols on vascular endogenous repair capacity and endothelial function, assessed by circulating hematopoietic and endothelial progenitor cell number and FMD, respectively. Blood was drawn before and 10 min post-exercise to measure hematopoietic and endothelial progenitor cell number using flow cytometry (Van Craenenbroeck et al., 2011). FMD was assessed before and 15 min post-exercise to measure endothelial function. Pulmonary gas exchange was also recorded during these visits to confirm that oxygen uptake ($\dot{V}O_2$) matched that of the target $\dot{V}O_2$ for the session (i.e. 40%Δ, see below for details).

All exercise tests were separated by >48 h and all training sessions were separated by >24 h. Prior to all exercise tests participants were asked to refrain from caffeine (4 h), alcohol and strenuous exercise (24 h). In addition to these requirements, participants were also instructed to arrive in a fasted state (>8 h) to the first and last training session when blood samples for hematopoietic and endothelial progenitor cell counts were drawn and endothelial function was measured. For all repeated visits (e.g. first and last training session and pre- and post-training exercise tests)

participants were asked to attend each visit at a similar time of day (± 2 h) to minimise the effect of external influences on outcome variables (Jones et al., 2010). The final exercise training session was performed >48 h after the penultimate training session to ensure post-training hematopoietic and endothelial progenitor cell counts were not influenced by a previous exercise bout.

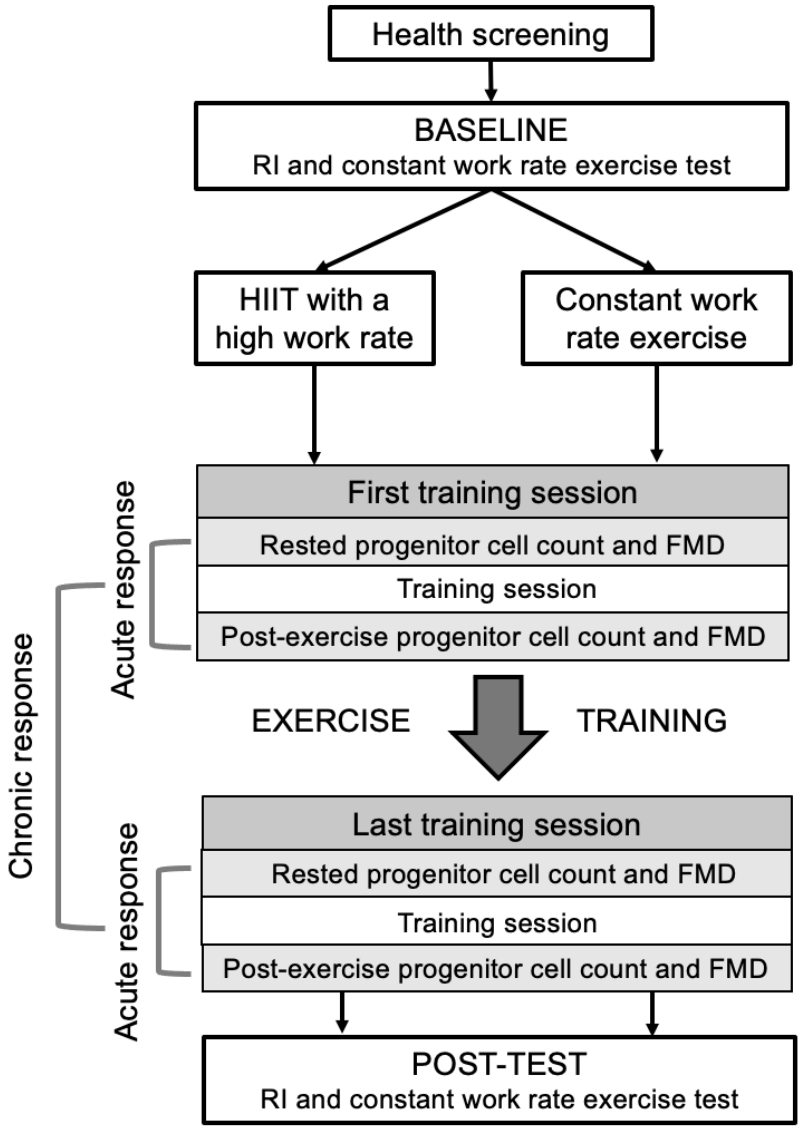

Figure 5.1 Study design. Participants were randomised to high-intensity interval exercise training (HIIT) with a high work rate or intensity-matched constant work rate exercise training. Before and after 6 weeks of exercise training participants performed a ramp-incremental (RI) and constant work rate exercise test. At the first and final training session blood was sampled before and after exercise to enumerate hematopoietic ($CD45^{dim}/CD34^{+}$) and endothelial ($CD45^{dim}/CD34^{+}/KDR^{+}$) progenitor cells. Brachial artery endothelial function was also assessed at these training sessions using flow-mediated dilation (FMD).

5.3.3 Exercise protocols

All exercise protocols were performed on a computer-controlled, electromagnetically braked cycle ergometer (Excalibur Sport PFM, Lode, Groningen, The Netherlands). Respired gases were measured using a breath-by-breath gas exchange system (Ultima Cardio$_2$, Medgraphics, Medical Graphics Corporation, St Paul, MN, USA) throughout exercise tests and the first and last training session. For this, participants breathed through a mouthpiece (whilst wearing a nose clip) attached to a preVent® flow sensor and an umbilical sample line that measured flow and transported the respired gases to the analysis system. The system was calibrated directly before each use as previously described in section 2.3.1. Participants were also attached to a 12 lead ECG (X12+, Mortara Instrument UK Ltd, Stirling, UK) throughout exercise and recovery periods when gas exchange was measured to monitor the participant and measure heart rate. Additional details on the cycle ergometer and breath-by-breath gas exchange system can be found in section 2.2 and 2.3.

Exercise tests

5.3.4.1 Ramp-incremental exercise test

After 2 min of seated rest on the ergometer and >4 min cycling at 20 W, work rate increased linearly with time. The incrementation rate was 20 and 25 W min^{-1} for female and male participants, respectively. Participants were instructed to cycle for as long as possible until the limit of tolerance was attained, determined as the point at which participants could no longer maintain a cadence above 50 rpm despite strong verbal encouragement. After the limit of tolerance was attained all participants completed >6 min cool down at 20 W. This test was used to determine the lactate threshold (LT), $\dot{V}O_{2peak}$ and WR_{peak}.

5.3.4.2 Constant work rate exercise test

All participants performed a constant work rate exercise test pre- and post-training to the limit of tolerance to measure time to intolerance. Following the same rest (2 min) and warm-up (>4 min at 20 W) phases as the ramp-incremental exercise test,

flywheel power increased instantaneously (1000 $W \cdot s^{-1}$) to a power that was equal to: ramp-incremental WR_{peak} – (2 x ramp incremental rate). This equation was used as it calculates a supra-critical power work rate that induces exercise intolerance in ~6 min (van der Vaart et al., 2014). Participants were instructed to cycle for as long as possible until the limit of tolerance was attained, again defined as the point at which participants could no longer maintain a cadence above 50 rpm despite strong verbal encouragement. In line with the ramp-incremental exercise test, this exercise protocol also concluded with >6 min cool down at 20 W.

5.3.4 Exercise training intervention

After completion of a >4 min warm up on the ergometer at 20 W participants performed their allocated training protocol. Work rate (W) for the HIIT and constant work rate exercise protocols were predicted using a modified version of a computational model of circulation and gas exchange dynamics designed at the University of Leeds by Dr Al Benson (Benson et al., 2013) to induce a mean $\dot{V}O_2$ during the exercise session that was 40%Δ; where Δ is the difference between $\dot{V}O_2$ at LT and $\dot{V}O_{2peak}$. For the constant work rate exercise protocol, work rate instantaneously increased on the cycle ergometer, and participants cycled at this work rate for 30 min (Figure 5.2). Individuals performing the HIIT protocol performed repeated 15:15 s work:recovery bouts until work done was equal to the work that would have been done if the participant performed the constant work rate protocol (Figure 5.2). Thus, the HIIT and constant work rate protocols were controlled for total work and mean $\dot{V}O_2$ but were differentiated by work rate. Recovery bouts during the HIIT protocol were active with participants cycling at 20 W (Figure 5.2). Both protocols were followed by a >6 min cool down at 20 W. Heart rate was measured during the first and last training session using a 12 lead ECG (X12+, Mortara Instrument UK Ltd, Stirling, UK). In the remainder of the sessions, participants wore a heart rate monitor belt (Polar H10, Polar Electro, Kempele, Finland) to measure heart rate. After 2 and 4 weeks of training, work rate was increased by 5% in both groups. However, during

the final training session work rate was returned to the work rate used in the first training session to determine any changes in the response to the exercise protocols pre- to post-training.

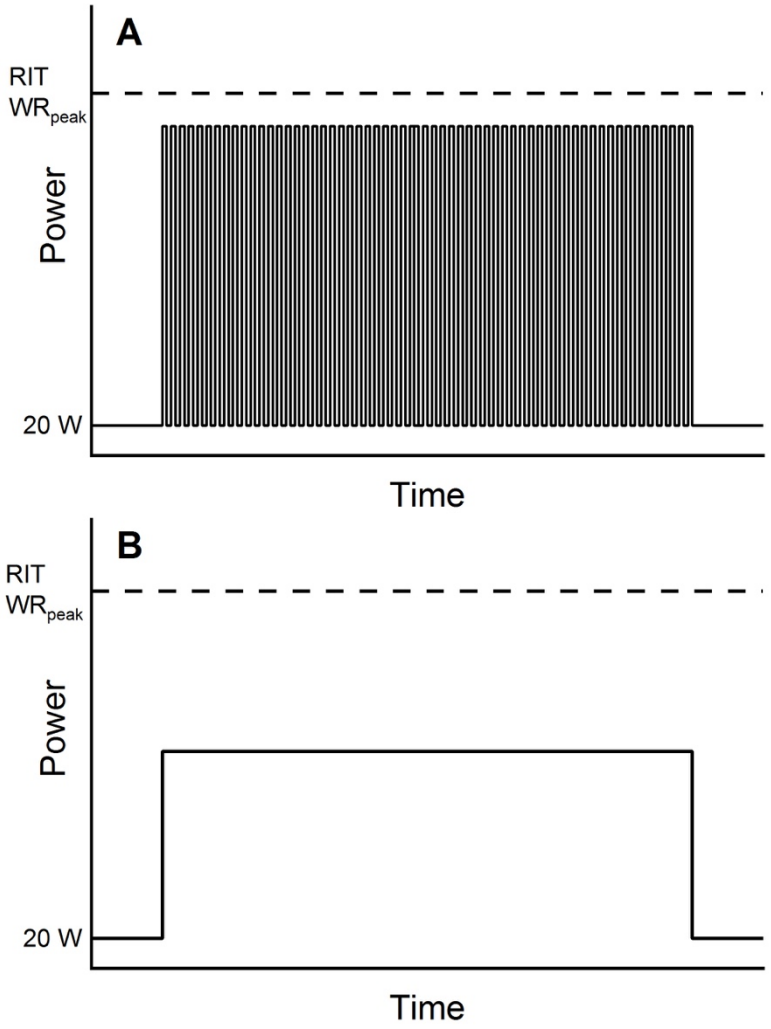

Figure 5.2 Schematic of the high-intensity interval training (HIIT) with a high work rate and intensity-matched constant work rate exercise training protocol used in this study: A. HIIT exercise protocol, consisting of 15:15 s work:recovery. B. Constant work rate exercise protocol. Both protocols were preceded by a >4 min warm-up and concluded with >6 min cool down both at 20 W. Despite the difference in work rate, protocols were intensity-matched.

5.3.5 Vascular measures

5.3.5.1 Quantification of progenitor cells

Peripheral blood was drawn into EDTA coated vacutainers (BD Biosciences, San Jose, CA, USA) to enumerate the number of circulating hematopoietic ($CD45^{dim}/CD34^{+}$) and endothelial ($CD45^{dim}/CD34^{+}/KDR^{+}$) progenitor cells. The protocol used to quantify the circulating hematopoietic and endothelial progenitor cells is described in detail in section 2.9.3. Progenitor cell data was obtained using a CytoFLEX S flow cytometer (Beckman Coulter, Indianapolis, IN, USA) and analysed using CytExpert software (Beckman Coulter). Gates were set using single controls and fluorescence minus one control tubes. The sequential gating strategy used to quantify $CD45^{dim}/CD34^{+}$ and $CD45^{dim}/CD34^{+}/KDR^{+}$ cells is shown in section 2.9.3 (Figure 2.11). First, debris, dead cells and cell doublets were excluded. A primary gate was then set on mononuclear cells in an SSC-A vs. FSC-A density plot. Next, $CD45^{dim}$ events were gated on a SSC-A vs. CD45-PE-Cy7 dot plot. $CD45^{dim}$ events that were $CD34^{+}$ were then identified and gated on a CD34-PE vs. SSC-A dot plot. Finally, $CD45^{dim}/CD34^{+}/KDR^{+}$ events were gated on a KDR-APC vs. SSC-A dot plot and quantified. More than 1 million events were recorded for each tube and presented as number of cells per 10^{6} mononuclear cells.

5.3.5.2 Assessment of endothelial function

Endothelial function was assessed non-invasively using FMD in accordance with previous guidelines (Thijssen et al., 2019, Thijssen et al., 2011a). Following >10 min semi-recumbent rest, baseline images of the brachial artery of the left upper limb and blood flow velocity measurements were obtained using high-resolution ultrasound (Vivid E9, GE Healthcare, Milwaukee, WI, USA). Probe position was recorded to ensure that the same section of artery was imaged in all subsequent scans. A cuff placed distal to the ultrasound probe was inflated to induce a 5 min period of forearm ischaemia. Images of the brachial artery and blood flow velocity were recorded 30 s

before cuff release until 150 s after cuff release (see section 2.10.1 for additional details).

5.3.6 Data analysis

5.3.6.1 Pulmonary gas exchange

Breath-by-breath data collected throughout ramp-incremental and constant work rate exercise tests was edited to remove errant breaths due to coughing and swallowing (breaths that fall outside 99% prediction limits; Lamarra et al., 1987). LT was estimated non-invasively using standard ventilatory and pulmonary gas exchange criteria (Whipp et al., 1986). Cardiopulmonary variables (e.g. $\dot{V}O_{2peak}$ and HR_{peak}) were determined as previously described (section 2.7.2).

Breath-by-breath $\dot{V}O_2$ data recorded during the first and final training session was analysed to assess exercise intensity. In line with $\dot{V}O_2$ data collected during the ramp-incremental and constant work rate exercise tests, each data set was initially edited using 99% prediction bands to exclude errant breaths. The $\dot{V}O_2$ data was then sorted into 5 min time-bins, resulting in 6 and 5 bins for the HIIT and constant work rate exercise protocol, respectively. The first bin (i.e. mean $\dot{V}O_2$ for 0-5 min) was excluded from further analysis due to the transient response at the start of exercise. A mean $\dot{V}O_2$ was calculated for the remaining time-bins and compared to 40%Δ values to ensure that the target $\dot{V}O_2$ was attained.

5.3.6.2 Flow-mediated dilation

The diameter of the brachial artery at rest and peak diameter induced by hyperaemia consequent to cuff deflation was determined using automated edge detection software (Brachial Analyzer for Research® Software, Medical Imaging Applications LLC, Coralville, Iowa, USA). Using these values absolute and relative FMD were calculated. Blood flow after cuff deflation was also analysed using the same software package to measure peak hyperaemia, peak shear rate and area under the curve (60

and 90 s post-cuff deflation). Finally, the time between cuff deflation and peak diameter was calculated using the times recorded on the ultrasound image frames. Further information on the FMD analysis can be found in section 2.10.2 and 2.10.3.

5.3.7 Statistics

Data were assessed for normal distribution using the Kolmogorov–Smirnov test. Significant variables were considered skewed, and log transformed where possible. If log transformation was not possible, non-parametric tests were employed. Baseline data were compared for group differences using unpaired *t*-test. Two-way repeated measures ANOVA with one within factor (time: pre-exercise vs. post-exercise or pre-training vs. post-training) and one between factor (intervention: HIIT vs. constant work rate exercise) was used to assess differences over time between groups. When a significant interaction was noted, Bonferroni corrected post-hoc *t*-tests were performed to locate differences. Due to the impact of COVID-19 on the number of datum collected, the standardised effect size (i.e. Cohen's *d*) was calculated to determine the magnitude of effect of time and group on outcome variables (Morris, 2008, Faraone, 2008). For the interaction effect size, an effect size of zero means that HIIT and constant work rate exercise protocols have equivalent effects. An effect size greater than zero indicates the degree that HIIT is more efficacious than constant work rate exercise, and effect sizes less than zero indicate the degree that HIIT is less efficacious than constant work rate exercise (Morris, 2008). All tests were performed as two-sided with significance accepted at $p < 0.05$. All values are presented as means ± SD. Analyses were performed using IBM SPSS version 24 (SPSS Inc., Chicago, IL, USA).

5.4 Results

5.4.1 Participant characteristics

Following random allocation, the HIIT and constant work rate exercise groups included 7 and 5 participants, respectively. However, during training 1 female participant from the HIIT group withdrew from the study following 5 training sessions. Subsequently, 11 participants were included in the final analysis (HIIT: $n = 6$; constant work rate: $n = 5$). Due to COVID-19, pulmonary gas-exchange data was not collected from 2 participants (HIIT: $n = 1$; constant work rate: $n = 1$) during their post-training constant work rate exercise test and these participants did not perform a post-training ramp-incremental exercise test. Ultrasound images were of insufficient quality on 2 occasions preventing measurement of FMD and/or blood flow, and were therefore excluded from the results. Progenitor cell numbers were also not counted on 3 occasions due to venepuncture failure or a flow cytometer fault. Participant characteristics are displayed in Table 5.1; there were no differences in these characteristics between HIIT and constant work rate exercise training groups at baseline ($p > 0.05$). There was also no difference in $\dot{V}O_{2peak}$ in the ramp-incremental and constant work rate exercise test in both groups at baseline (HIIT: $p = 0.86$; constant work rate: $p = 0.49$), confirming that $\dot{V}O_{2max}$ was achieved in both groups (Rossiter et al., 2005).

Table 5.1 Participant characteristics

Parameter	HIIT	Constant work rate	*p*
n	6	5	
Age (y)	26 ± 5	27 ± 2	0.49
Sex			
Male	2 (33)	3 (60)	
Female	4 (67)	2 (40)	
Weight (kg)	67.6 ± 8.7	66.2 ± 14	0.84
Height (cm)	169 ± 5.4	171 ± 5.7	0.40
BMI (kg/m^2)	23.6 ± 3.6	22.4 ± 3.8	0.61
RI $\dot{V}O_{2peak}$ ($L \cdot min^{-1}$)	2.90 ± 0.71	2.92 ± 0.73	0.42
RI $\dot{V}O_{2peak}$ ($ml \cdot min^{-1} \cdot kg^{-1}$)	42.5 ± 9.2	47.6 ± 8.5	0.22
LT ($L \cdot min^{-1}$)	1.54 ± 0.31	1.54 ± 0.26	0.83
Constant WR exercise test duration (s)	314 ± 27	308 ± 23	0.72
Constant WR exercise test $\dot{V}O_{2peak}$ ($L \cdot min^{-1}$)	2.83 ± 0.76	2.95 ± 0.80	0.88
Constant WR exercise test $\dot{V}O_{2peak}$ ($ml \cdot min^{-1} \cdot kg^{-1}$)	41.6 ± 10.6	48.7 ± 7.9	0.17

Values are *n* (%) or mean ± SD for 11 participants (HIIT: *n* = 6; Constant work rate: *n* = 5) except absolute and relative $\dot{V}O_{2peak}$ measured in the constant work rate exercise test. These values are for 9 participants (HIIT: *n* = 5; Constant work rate: *n* = 4) due to COVID-19 restrictions on gas exchange equipment. BMI = body mass index. LT = lactate threshold; RI = ramp-incremental exercise test. $\dot{V}O_{2peak}$ = peak oxygen uptake. WR = work rate.

5.4.2 Adherence and intensity of exercise training

There was an 98% adherence to the training sessions (2 training sessions were missed in the HIIT group). Protocol duration was 2121 ± 54 and 1800 ± 0 s for HIIT and constant work rate groups, respectively. Pre-training, 40%Δ ($L \cdot min^{-1}$) was not different between HIIT (1.97 ± 0.47 $L \cdot min^{-1}$) and constant work rate training groups (2.29 ± 0.58 $L \cdot min^{-1}$; $p = 0.36$). The work rate set on the cycle ergometer to evoke 40%Δ was greater during the exercise bouts in the HIIT protocol (work bout: 219 ±

49 W) than during the constant work rate protocol (146 ± 35 W) at baseline (p = 0.02). $\dot{V}O_2$ measured throughout the exercise session was always within 200 ml (breath-by-breath noise) of the target $\dot{V}O_2$ (i.e. 40%Δ). Mean HR measured during the final 5 min of exercise was not different between training groups pre-training (HIIT: 184 ± 11 bpm; constant work rate: 174 ± 9 bpm; p = 0.21).

Mean $\dot{V}O_2$ measured in the final 5 min of exercise remained unchanged following exercise training, with no differences between groups (time effect: p = 0.65; interaction: p = 0.10). Mean HR measured in the final 5 min of exercise decreased pre- to post-training (HIIT: pre = 186 ± 13; post = 172 ± 13; constant work rate: pre = 174 ± 9; post = 170 ± 4; time effect: p = 0.02). However, the effect of exercise training on mean HR in the final 5 min of exercise was not different between groups (interaction: p = 0.23).

5.4.3 Changes in exercise test parameters in response to exercise training

Both absolute and relative $\dot{V}O_{2peak}$ increased with training, with no differences between groups ($\dot{V}O_{2peak}$ $L \cdot min^{-1}$: time effect: p = 0.01, ES = 0.38; interaction: p = 0.24, ES = 0.16; $\dot{V}O_{2peak}$ $ml \cdot min^{-1} \cdot kg^{-1}$: time effect: p = 0.01, ES = 0.46; interaction: p = 0.20; ES = 0.20; Table 5.2). Ramp-incremental exercise test duration and work rate peak (WR_{peak}) also increased pre- to post-training, with no differences between training groups (ramp-incremental test duration: time effect: p = 0.01, ES = 0.59; interaction: p = 0.12, ES = 0.38; WR_{peak}: time effect: p = 0.01, ES = 0.38; interaction: p = 0.23, ES = 0.22; Table 5.2). Estimated LT increased pre- to post-training (time effect: p = 0.01, ES = 0.58). However, the effect of the training differed between groups (interaction: p = 0.03; ES = 0.74; Table 5.2); there was no difference in estimated LT following constant work rate exercise training (p = 0.45) but a 17 ± 12% increase after HIIT with a high work rate (p = 0.01).

Table 5.2 Pulmonary gas exchange responses to ramp-incremental exercise before and after exercise training

Parameter	HIIT		Constant work rate	
	Pre-training	Post-training	Pre-training	Post-training
RI $\dot{V}O_{2peak}$ ($L \cdot min^{-1}$)*	2.90 ± 0.71	3.20 ± 0.74	2.92 ± 0.73	3.11 ± 0.71
RI $\dot{V}O_{2peak}$ ($ml \cdot min^{-1} \cdot kg^{-1}$)*	42.5 ± 9.2	47.4 ± 9.3	47.6 ± 8.5	50.7 ± 7.8
RI WR_{peak} (W)*	242 ± 56	267 ± 63	252 ± 52	265 ± 61
RI duration (s)*	601 ± 95	669 ± 103	615 ± 94	649 ± 102
LT ($L \cdot min^{-1}$)*	1.54 ± 0.31	1.79 ± 0.27†	1.54 ± 0.26	1.59 ± 0.29
HR_{peak} ($beats \cdot min^{-1}$)	195 ± 8	193 ± 4	188 ± 7	187 ± 4
$\Delta\dot{V}O_2$ / ΔWR ($ml \cdot min^{-1} \cdot W^{-1}$)	11.1 ± 1.1	10.8 ± 1.5	10.3 ± 1.4	10.8 ± 1.3

Values are mean ± SD for 9 participants (HIIT: *n* = 5; constant work rate: *n* = 4). HR_{peak} = Peak heart rate; LT = Lactate threshold; RI = Ramp-incremental exercise test; $\dot{V}O_2$ = oxygen uptake; $\dot{V}O_{2peak}$ = Peak oxygen uptake; WR = work rate; WR_{peak} = Ramp-incremental exercise test peak work rate.

***Pre- to post training time effect from the two-way repeated measures ANOVA. † Following a significant interaction, a significant pre-post training change within the HIIT group (paired t-test).**

Constant work rate exercise test duration increased pre- to post-training (HIIT: Pre = 314 ± 27; Post = 585 ± 135 s; constant work rate: pre = 308 ± 23; post = 533 ± 139 s; time effect: p = 0.01, ES = 10.25; Figure 5.3). Although a large effect size was present, there was no difference in the magnitude of change between training groups (interaction: p = 0.61; ES = 1.89; Figure 5.3).

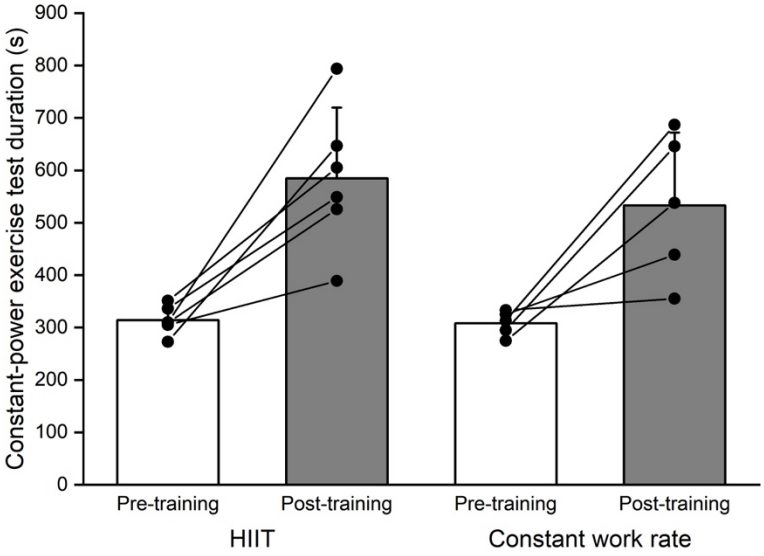

Figure 5.3 Constant work rate exercise test duration following high-intensity interval training (HIIT) with a high work rate and intensity-matched constant work rate exercise training. Time to intolerance significantly increased pre- to post-training (time effect: *p* = 0.01), with no difference between groups (interaction: *p* = 0.61). Values are mean ± SD for 11 participants (HIIT: *n* = 6; constant work rate: *n* = 5).

5.4.4 Progenitor cell responses to exercise training

Pre-exercise session blood samples were drawn from 11 participants pre- and post-training (HIIT: *n* = 6; constant work rate: *n* = 5) to determine the response to training on $CD45^{dim}/CD34^{+}$ and $CD45^{dim}/CD34^{+}/KDR^{+}$ number. There was no difference in $CD45^{dim}/CD34^{+}$ or $CD45^{dim}/CD34^{+}/KDR^{+}$ cell number in HIIT and constant work rate training groups before the first exercise session (i.e. at baseline; $p > 0.05$).

Pre- to post-training there was no difference in $CD45^{dim}/CD34^{+}$ (HIIT: pre = 726 ± 220; post = 740 ± 212; constant work rate: pre = 1117 ± 442; post = 1155 ± 502; time effect: $p = 0.79$; ES = 0.07) or $CD45^{dim}/CD34^{+}/KDR^{+}$ number (HIIT: pre = 91 ± 85; post = 92 ± 94; constant work rate: pre = 73 ± 31; post = 95 ± 75; time effect: $p = 0.70$; ES = 0.13), with no differences between training groups ($CD45^{dim}/CD34^{+}$: interaction: $p = 0.90$; ES = -0.06; $CD45^{dim}/CD34^{+}/KDR$: interaction: $p = 0.72$; ES = -

0.32). In other words, there was no exercise training-induced effect on vascular endogenous repair capacity.

5.4.5 Progenitor cell responses to acute exercise

Blood samples were drawn from 10 participants before and after the first exercise session (HIIT: *n* = 6; constant work rate: *n* = 4). $CD45^{dim}/CD34^{+}$ and $CD45^{dim}/CD34^{+}/KDR^{+}$ cell number did not change following a single exercise session, pre-training ($CD45^{dim}/CD34^{+}$: time effect: *p* = 0.44, ES = -0.35; $CD45^{dim}/CD34^{+}/KDR^{+}$: time effect: *p* = 0.22, ES = -0.50; Figure 5.4 and 5.5). The impact of the exercise session on both cell subsets did not differ between groups ($CD45^{dim}/CD34^{+}$: interaction: *p* = 0.41, ES = -062; $CD45^{dim}/CD34^{+}/KDR^{+}$: interaction: *p* = 0.58, ES = -0.39; Figure 5.4 and 5.5).

Blood samples were also drawn from 10 participants before and after the final exercise session (HIIT: *n* = 5; constant work rate: *n* = 5). Post-training, the number of $CD45^{dim}/CD34^{+}$ cells increased pre- to post-exercise (time effect: *p* = 0.04, ES = 0.82); however, there was no difference in the magnitude of change between training groups despite the large effect size (interaction: *p* = 0.08, ES = -1.30; Figure 5.4). The number of $CD45^{dim}/CD34^{+}/KDR^{+}$ cells remained unchanged after a single session of exercise post-training (time effect: *p* = 0.81, ES = 0.07), with no difference in $CD45^{dim}/CD34^{+}/KDR^{+}$ cell number between groups pre- to post-exercise (interaction: *p* = 0.60, ES = -0.31; Figure 5.5).

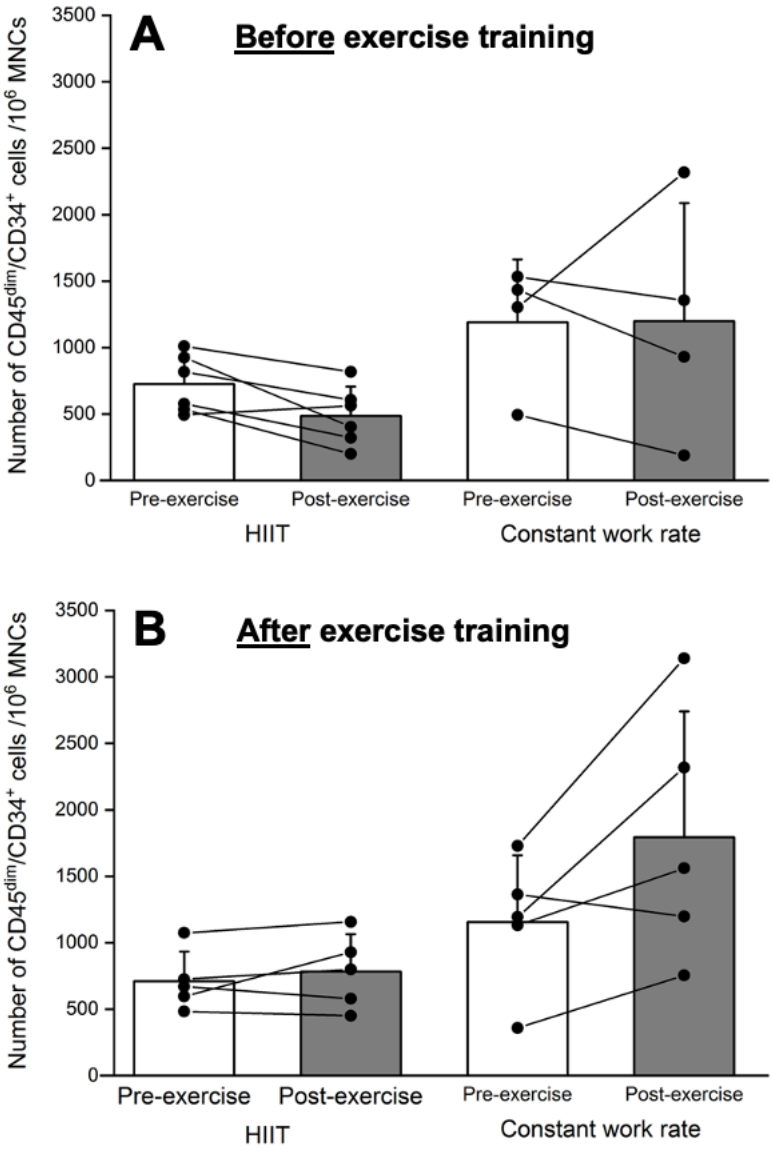

Figure 5.4 Hematopoietic progenitor cell ($CD45^{dim}/CD34^{+}$) response to a single session of high-intensity interval training (HIIT) with a high work rate and intensity-matched constant work rate exercise, before (A) and after (B) exercise training. $CD45^{dim}/CD34^{+}$ number increased pre- to post-exercise after exercise training only (time effect: $p = 0.04$) with no differences between training groups (interaction: $p = 0.08$). Values are mean ± SD for 10 participants. MNCs = mononuclear cells.

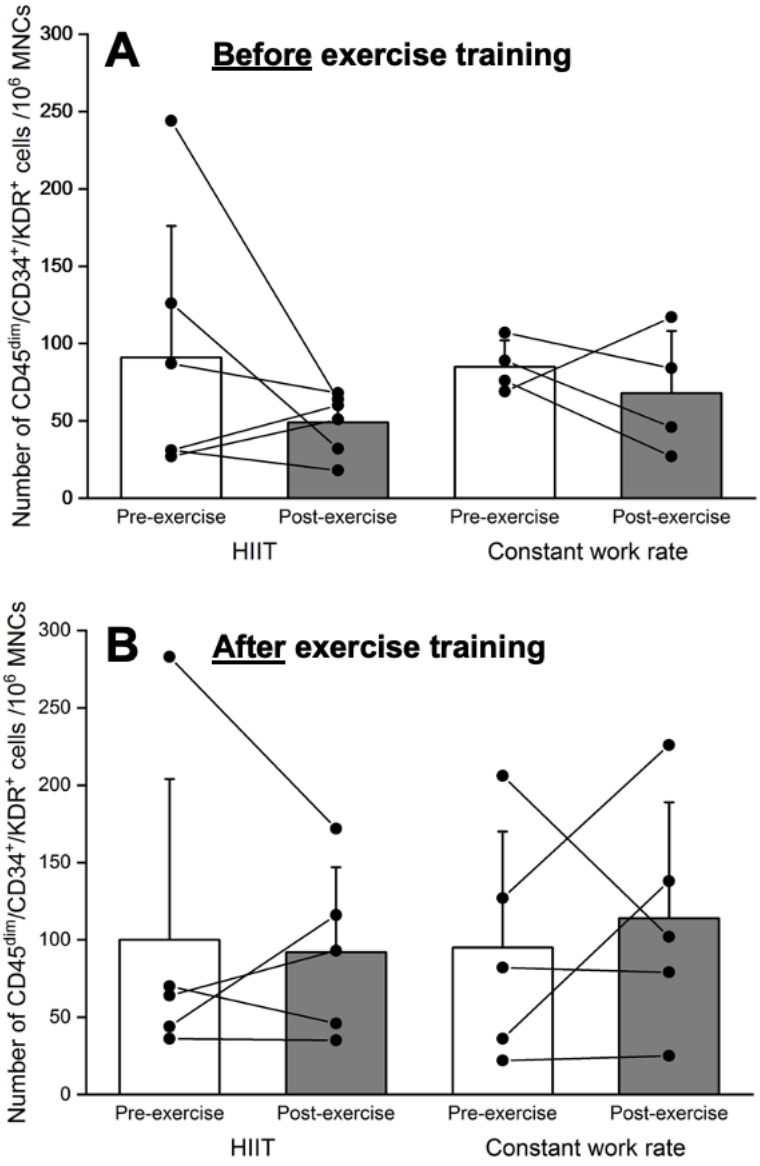

Figure 5.5 Endothelial progenitor cell ($CD45^{dim}/CD34^{+}/KDR^{+}$) response to a single session of high-intensity interval training (HIIT) with a high work rate and intensity-matched constant work rate exercise, before (A) and after (B) exercise training. The number of $CD45^{dim}/CD34^{+}/KDR^{+}$ cells remained unchanged following an acute bout of HIIT and constant work rate exercise before and after exercise training (time effect: $p > 0.05$), with no differences between groups (interaction: $p > 0.05$). Values are mean ± SD for 10 participants. MNCs = mononuclear cells.

5.4.6 Brachial artery FMD response to exercise training

There was no difference in baseline brachial artery diameter (p = 0.13), peak diameter (p = 0.06), time to peak diameter (p = 0.61), peak hyperaemia (p = 0.49), peak shear (p = 0.95), AUC_{60} (p = 0.67), AUC_{90} (p = 0.75) and reactive hyperaemia (p = 0.75) between HIIT and constant work rate exercise training groups at baseline (Table 5.3). However absolute FMD (p = 0.01) and relative FMD (p = 0.02) were greater in constant work rate group compared to HIIT group at baseline (Table 5.3).

There was no change in baseline or peak brachial artery diameter pre- to post-training (baseline diameter: time effect: p = 0.59, ES = 0.04; interaction: p = 0.56, ES = 0.08; peak diameter: time effect: p = 0.57, ES = 0.05; interaction: p = 0.24, ES = 0.16; Table 5.3). Brachial artery function (absolute and relative FMD) also remained unchanged with training, with no differences between groups (absolute FMD: time effect: p = 0.83, ES = 0.02; interaction: p = 0.26, ES = 0.26; relative FMD: time effect: p = 0.99, ES = 0.01; interaction: p = 0.28, ES = 0.36; Table 5.3). In addition, shear stimulus (peak hyperaemia, peak shear rate, AUC_{60} and AUC_{90}) and reactive hyperaemia were not influenced by exercise training (time effect: $p > 0.05$; interaction: $p > 0.05$; Table 5.3).

5.4.7 Brachial artery FMD response to acute exercise

Pre-training, baseline and peak brachial diameter did not change pre- to post-exercise (baseline diameter: time effect: p = 0.36, ES = 0.05; interaction: p = 0.80, ES = -0.03; peak diameter: time effect: p = 0.59, ES = 0.03; interaction: p = 0.10, ES = 0.17; Table 5.3). Similarly, both measures of endothelial function (absolute and relative FMD) also remained unchanged pre- to post-exercise, with no differences between HIIT and constant work rate exercise groups (absolute FMD: time effect: p = 0.43, ES = -0.21; interaction: p = 0.18, ES = 0.16; relative FMD: time effect: p = 0.34, ES = -0.27; interaction: p = 0.46, ES = 0.45; Table 5.3). The shear stimulus (i.e.

peak hyperaemia, peak shear rate, AUC_{60}, and AUC_{90}) was also not different pre- to post-exercise (time effect: $p > 0.05$; interaction: $p > 0.05$; Table 5.3). Time to peak diameter and reactive hyperaemia increased pre- to post-exercise (time effect: $p < 0.05$); however, the magnitude of change was not different between groups for either parameter (interaction: $p > 0.05$; time to peak diameter: ES = -0.62; reactive hyperaemia: ES = -0.13; Table 5.3).

Post-training, there was no pre- to post-exercise change in resting brachial artery diameter or peak brachial artery diameter (baseline diameter: time effect: $p = 0.97$, ES = 0.00; interaction: $p = 0.90$, ES = -0.01; peak diameter: time effect: $p = 0.67$, ES = 0.03; interaction: $p = 0.62$, ES = 0.08; Table 5.3). Further, absolute and relative FMD remained unchanged pre- to post-exercise, with no differences between groups (absolute FMD: time effect: $p = 0.62$, ES = 0.23; interaction: $p = 0.51$, ES = 0.52; relative FMD: time effect: $p = 0.45$, ES = 0.34; interaction: $p = 0.45$, ES = 0.68; Table 5.3). Time to peak diameter increased pre- to post-exercise (time effect: $p = 0.02$, ES = 0.99) with no difference in the magnitude of change between training groups (interaction: $p = 0.62$; ES = -0.12). The shear stimulus and reactive hyperaemia were not different pre- to post-exercise (time effect: $p > 0.05$; interaction: $p > 0.05$; ES < 0.30; Table 5.3). Thus, with the exception of reactive hyperaemia remaining unchanged pre- to post-exercise, the FMD response to HIIT and constant work rate exercise post-training mirrored the pre-training response, evidencing no acute change in endothelial function following the exercise bout, regardless of protocol.

Table 5.3 Parameters of endothelial function assessed using flow-mediated dilation before and after exercise both pre- and post-training

Parameter	HIIT				Constant work rate exercise training			
	Pre-training		Post-training		Pre-training		Post-training	
	Pre-exercise	Post-exercise	Pre-exercise	Post-exercise	Pre-exercise	Post-exercise	Pre-exercise	Post-exercise
Baseline diameter (mm)	3.58 ± 0.52	3.61 ± 0.50	3.66 ± 0.48	3.65 ± 0.41	3.95 ± 0.73	3.99 ± 0.83	3.95 ± 0.84	3.95 ± 0.91
Peak diameter (mm)	3.77 ± 0.53	3.85 ± 0.58	3.88 ± 0.49	3.91 ± 0.28	4.31 ± 0.73	4.27 ± 0.71	4.29 ± 0.88	4.29 ± 0.90
Time to peak diameter (s)*†	37 ± 4	48 ± 14	37 ± 10	45 ± 6	33 ± 4	47 ± 11	32 ± 10	42 ± 11
Absolute FMD (mm)	0.19 ± 0.04	0.20 ± 0.09	0.23 ± 0.06	0.26 ± 0.19	0.36 ± 0.11	0.28 ± 0.13	0.34 ± 0.11	0.33 ± 0.07
Relative FMD (%)	5.2 ± 1.4	4.4 ± 3.8	6.3 ± 2.0	7.6 ± 6.2	9.3 ± 3.4	7.7 ± 4.6	8.7 ± 2.8	8.7 ± 2.5
Peak Hyperaemia ($cm \cdot s^{-1}$)	81.2 ± 29.8	87.0 ± 16.6	104.3 ± 30.1	92.9 ± 16.2	89.6 ± 40.7	98.4 ± 41.3	103.4 ± 44.7	104.5 ± 37.6
Peak Shear Rate (s^{-1})	1902 ± 826	1946 ± 411	1973 ± 428	2088 ± 355	1831 ± 741	1999 ± 795	2135 ± 828	2161 ± 706
AUC_{60} (a.u.)	59915 ± 27942	52602 ± 11603	71273 ± 11848	57626 ± 9188	59142 ± 38709	55407 ± 30624	65399 ± 41694	59624 ± 31521
AUC_{90} (a.u.)	71673 ± 32603	66464 ± 20163	84467 ± 14094	73574 ± 16815	68904 ± 43464	70110 ± 41419	81661 ± 58158	73997 ± 41516
Reactive hyperaemia ($cm \cdot s^{-1}$)*	3945 ± 1778	5233 ± 2732	4837 ± 1387	5648 ± 2429	3811 ± 2027	5547 ± 3129	4598 ± 3126	5735 ± 3730

Values are mean ± SD for 11 participants (HIIT: *n* = 4; Constant work rate: *n* = 5). AUC = area under shear rate curve. * Time effect pre- to post-exercise, pre-training. † Time effect pre-to post-exercise, post-training.

5.5. Discussion

The major novel finding of this study is that chronic exposure to HIIT with a high work rate does not alter vascular endogenous repair capacity or endothelial function in young healthy adults. These variables also remained unchanged following chronic exposure to intensity, shear rate and volume matched constant work rate exercise with a lower work rate, suggesting that the high work rate during HIIT confers no additional benefit to any vascular adaptations when shear rate volume and peak shear rate stimulus are matched to that of constant work rate exercise. However, both training strategies effectively increase $\dot{V}O_{2peak}$ and exercise tolerance, although an absence of a change in vascular function in either training group suggests these changes are not vascularly mediated.

5.5.1 Effect of exercise training on $\dot{V}O_{2peak}$ and exercise tolerance

Both training strategies in this study induced an increase in $\dot{V}O_{2peak}$ (HIIT: 4.9 ± 0.3; constant work rate: 3.1 ± 3.0 $ml \cdot min^{-1} \cdot kg^{-1}$). These increases are similar to the meta-analysed effect of HIIT (5.5 $ml \cdot min^{-1} \cdot kg^{-1}$) and constant work rate exercise (4.9 $ml \cdot min^{-1} \cdot kg^{-1}$) training on $\dot{V}O_{2peak}$ in young health adults, when compared with non-exercise controls (Milanović et al., 2015). HIIT with a high work rate did not induce a superior increase in $\dot{V}O_{2peak}$ in this study, suggesting other variables, such as exercise intensity and work done, may be more important than the independent effects of work rate for inducing improvements in $\dot{V}O_{2peak}$ in young healthy adults.

Exercise tolerance (constant work rate exercise test duration) also increased pre- to post-training in this study. The magnitude of change was not statistically different between training groups; however, the increase was 13% (~46 s) greater in the HIIT group compared to the constant work rate exercise training group and a large effect size was present (interaction effect: $p = 0.03$; ES = 1.89). Given the low sample size in this study, these results may suggest that HIIT with a high work rate is more

effective at increasing exercise tolerance than intensity-matched constant work rate exercise but a future study with a larger cohort is needed to confirm this.

The improvements in $\dot{V}O_{2peak}$ and exercise tolerance in this study are not consequent to improvements in vascular endogenous repair capacity or endothelial function increasing convective O_2 delivery. The high work rate during the HIIT protocol may have been efficacious for driving adaptations in the skeletal muscle and increasing muscle oxidative capacity (i.e. O_2 utilisation), a factor that can limit exercise tolerance in young healthy individuals (Cardús et al., 1998). However, further work is needed to investigate the mechanisms underpinning changes in $\dot{V}O_{2peak}$ after HIIT with a high work rate and intensity-matched constant work rate exercise training.

Since $\dot{V}O_{2peak}$ is the strongest predictor of morbidity and mortality (Myers et al., 2002), individuals with reduced $\dot{V}O_{2peak}$ (e.g. older individuals and those with cardiovascular disease) may benefit from being prescribed either of the exercise training strategies used in this study. Nevertheless, additional studies are needed to determine whether the results of this study are reproduced in older adults and clinical populations, and whether any additional advantage is conveyed by the high work rate.

5.5.2 Effect of exercise training on progenitor cell numbers

Hematopoietic and endothelial progenitor cells are involved in vascular repair processes, promoting the preservation of vascular endothelial integrity and function. To our knowledge this was the first study to investigate whether a high work rate during exercise *per se* affects circulating hematopoietic and endothelial progenitor cell numbers. There were no increases in baseline hematopoietic ($CD45^{dim}/CD34^{+}$) or endothelial progenitor cell ($CD45^{dim}/CD34^{+}/KDR^{+}$) number pre- to post-training. Although some studies have shown that exercise training can increase baseline circulating hematopoietic and endothelial progenitor cell number (Xia et al., 2012,

Tsai et al., 2016), others have found no effect. For example, Rakobowchuk et al. (2012) reported no change in circulating $CD34^+$ or $CD34^+/KDR^+$ cells after 6 weeks (3 sessions per week) of moderate and heavy intensity interval exercise cycle training in young healthy adults. Harris et al. (2014) also reported no increase in $CD45^{dim}/CD34^+$ number after 4 weeks (3 sessions per week) of sprint interval training and work matched continuous sprint training in young healthy females. The majority of the studies demonstrating an increase in hematopoietic and endothelial progenitor cell number pre- to post-exercise training have been in older individuals or patient populations (Xia et al., 2012, Sandri et al., 2016, Sarto et al., 2007, Laufs et al., 2004). Thus, the lack of hematopoietic and endothelial progenitor cell response to exercise training in this study may be due to the population that was investigated; young healthy adults who already possess a 'normal' endogenous repair capacity. It is possible that vascular endogenous repair capacity is fixed in young healthy individuals and cannot be augmented to a 'supranormal' level with exercise training.

5.5.3 Effect of acute exercise on progenitor cell numbers

It was hypothesised that HIIT with a higher work rate may increase the degree of transient hypoxia during muscle contraction, leading to a greater increase in circulating angiogenic factors (e.g. VEGF, HIF-1α and SDF-1α) than intensity-matched constant work rate exercise. Previous studies have demonstrated a positive relationship between circulating angiogenic factors and progenitor cell mobilisation (Ribeiro et al., 2017, Yamaguchi et al., 2003, Hattori et al., 2001). However, in this study, a single session of HIIT with a high work rate did not increase $CD45^{dim}/CD34^+$ or $CD45^{dim}/CD34^+/KDR^+$ number pre-training. Thus, the stimulus induced by HIIT with a high work rate was insufficient to increase progenitor cell counts and work rate does not play an important independent role in stimulating exercise-induced progenitor cell mobilisation in young healthy adults. The lack of progenitor response to exercise pre-training may also explain the absent training response.

Despite the absence of a statistical difference, pre-training a single session of exercise decreased $CD45^{dim}/CD34^{+}$ and $CD45^{dim}/CD34^{+}/KDR^{+}$ cell counts in 8/10 and 7/10 participants, respectively. This magnitude of change is more than the absolute difference for within day reproducibility ($CD45^{dim}/CD34^{+}$: 60 cells; $CD45^{dim}/CD34^{+}/KDR^{+}$: 13 cells; see section 2.9.4). In contrast, post-training, $CD45^{dim}/CD34^{+}$ and $CD45^{dim}/CD34^{+}/KDR^{+}$ number only decreased pre- to post-exercise in 2/10 and 3/10 participants, respectively. Despite the small sample size in this study, this may suggest that a single session of HIIT with a high work rate and/or intensity-matched constant work rate exercise, reduces hematopoietic and endothelial progenitor cell number before but not after exercise training. As such, there may have been a positive effect of training that reduced the magnitude of the post-exercise reduction in hematopoietic and endothelial progenitor cells, with this effect not different between training protocols. However, to confirm this requires further investigation.

While a reduction in hematopoietic and endothelial progenitor cell number was not hypothesised, it is not without precedent. $CD34^{+}/CD45^{dim}$ and $CD31^{+}/CD34^{+}/CD45^{dim}$ number decreased by ~28 and ~34%, respectively, following 30 min of constant work rate exercise at 60% of peak power output (Sapp et al., 2019). A 21% reduction in $CD31^{+}/CD34^{+}/CD45^{dim}$ was also seen after 30 min of HIIT (3 mins at 85% peak power output separated by 6 min at 40% peak power output; Sapp et al., 2019). These reductions are similar to the 22 ± 43 decrease in $CD45^{dim}/CD34^{+}$ cells but greater than the 9 ± 68% decrease in $CD45^{dim}/CD34^{+}/KDR^{+}$ cells seen pre- to post-exercise before exercise training in this study. Circulating progenitor cells home to sites of vascular damage and adhere to the activated vasculature before secreting multiple cytokines and growth factors that aid vascular repair (Rehman et al., 2003, Gnecchi et al., 2008). Therefore, a possible explanation for the suggested reduction is recruitment to the vessel wall in response to exercise-induced damage to the

endothelial layer (Adams, 2018). After exercise training, this damage response may have been reduced/absent due to the lower relative intensity of the exercise session and/or an increased antioxidative capacity (Powers and Jackson, 2008).

Although the number of $CD45^{dim}/CD34^{+}/KDR^{+}$ cells remained unchanged throughout this study, a single session of exercise increased $CD45^{dim}/CD34^{+}$ number after exercise training. Thus, there is heterogeneity in exercise-induced mobilisation between progenitor cell subsets. In line with this observation, Krüger et al. (2015) reported an increase in circulating $CD45^{dim}/CD34^{+}$ cell number but no change in $CD45^{dim}/CD34^{+}/KDR^{+}$ cell number in healthy males after they cycled at 80% $\dot{V}O_{2peak}$ to intolerance (average cycling time: 43 ± 5 min). The mechanisms underpinning this exercise-induced increase in $CD45^{dim}/CD34^{+}$ cells post-training is unclear. Present data suggests it may be a training effect. However, a similar increase in $CD45^{dim}/CD34^{+}$ cells was seen after a maximal cycle ergometer exercise test in sedentary and trained young individuals (Thijssen et al., 2006). Therefore, additional studies are needed to understand factors that affect the mobilisation of specific progenitor cell subsets.

The increase in $CD45^{dim}/CD34^{+}$ cells seen pre- to post-exercise after exercise training was not statistically different between groups; however, a large negative effect size was present (interaction: $p = 0.08$, ES = -1.30). This suggests that HIIT with a high work rate may be less efficacious than constant work rate exercise at increasing $CD45^{dim}/CD34^{+}$ number pre- to post-exercise, post-training. Due to the small sample size of this study, this effect size was explored using post-hoc t-tests and showed a 62 ± 49% increase in $CD45^{dim}/CD34^{+}$ number pre- to post-exercise after constant work rate exercise only (HIIT: $p = 0.73$; Constant-work rate; $p = 0.01$). The current study benefited from closely matching the work done, intensity and therefore, volume

of shear stress, of the exercise protocols, whilst utilising different work rates, ruling out these variables as potential drivers for the increase in $CD45^{dim}/CD34^{+}$ cells seen following constant work rate exercise but not HIIT exercise post-training. Further work is needed to explore the mechanisms underpinning exercise-induced progenitor cell mobilisation as this has implications on the development of effective exercise strategies that target vascular endogenous repair capacity.

5.5.4 Effect of exercise training on brachial artery function

Exercise training did not affect brachial artery FMD in this study. This finding was unexpected, although no change in FMD has been seen previously in animal and human exercise training studies (Rakobowchuk et al., 2012, Padilla et al., 2010, Green et al., 2004). Of note, Rakobowchuk et al. (2012) also reported no change in brachial artery endothelial function following 6 weeks of heavy-intensity interval exercise training in young healthy adults. The timings of the post-training assessments in this study may have contributed to the lack of change in FMD pre- to post-training. Previous studies have shown increases in brachial and popliteal artery FMD within 2 weeks of exercise training before FMD values then returned to near baseline following 6-8 weeks of exercise training (Tinken et al., 2008, Hunt et al., 2013). Also, endothelial function was assessed in the brachial artery in this study, rather than in a conduit artery that delivers O_2 to the contracting skeletal muscles during cycle exercise (e.g. femoral or popliteal artery). FMD responses obtained from the brachial artery are important because they provide a non-invasive measure of vascular function that can be used to predict cardiovascular disease risk (Green et al., 2011, Inaba et al., 2010); however, brachial artery FMD measurements do not represent a systemic index of endothelial function, and therefore, cannot be extrapolated to other vascular beds (Thijssen et al., 2011b). Thus, it is possible that adaptations occurred in the femoral and/or popliteal arteries. Nevertheless, the lack of change in brachial artery FMD after HIIT with a high work rate suggests that work

rate is not an important independent factor for driving improvements in FMD with interval exercise training.

In order to investigate the independent effects of work rate during HIIT on vascular adaptations, the interval protocol employed in this study utilised a short work:recovery ratio (15: 15 s). This allowed for the greatest disassociation between exercise intensity and the work rate of the exercise. This work:recovery ratio also minimised the oscillations in shear stress that typically occur during interval exercise. Interval exercise is typically associated with greater oscillatory shear stress than intensity- and duration-matched constant work rate exercise due to the repeated transitions between 'work' and 'recovery' during the protocol increasing the volume of retrograde shear stress (Lyall et al., 2019). Acute exposure to oscillatory shear stress (20-30 min) is associated with an increase in the production of reactive oxygen species, endothelin-1 and adhesion molecules, and decreases in endothelial nitric oxide synthase expression, resulting in endothelial damage and impaired endothelial function (Jenkins et al., 2013, Laughlin et al., 2008, Rakobowchuk et al., 2013). However, chronic exposure to this stimulus (i.e. exercise training) may provide the foundation for greater long-term adaptive responses to exercise (i.e. a greater increase in endothelial function). The lack of adaptive response in this study may suggests that significant oscillations in shear stress may be needed for interval exercise to induce vascular adaptations. Thus, future work should investigate the independent effect of oscillatory shear stress patterns on training-induced vascular adaptations.

In addition, exercise intensity appears to play a key role in mediating vascular adaptations. Increases in exercise intensity are associated with increases in heart rate and cardiac output (i.e. blood flow) that elevate peripheral vascular shear stress

and NO production, promoting increases in endothelium-dependent vasodilation. Indeed, a 10% increase in exercise intensity (% $\dot{V}O_{2peak}$) is associated with a 1% improvement in endothelial function when assessed using FMD (Ashor et al., 2015). The metabolic strain (exercise intensity) of interval exercise is typically greater than in the control group performing constant work rate exercise, resulting in a higher peak shear during interval exercise bouts than during constant work rate exercise (Boff et al., 2019, Sawyer et al., 2016, Ramos et al., 2015). However, the protocols used in this study were intensity-matched ($\dot{V}O_2$ measured in the last 5 min of exercise was 80 ± 9 vs. 78 ± 2 % $\dot{V}O_{2peak}$ for HIIT and constant work rate protocols, respectively). The interval protocol used in this study maximises the volume of shear stress that can be accumulated using an interval protocol that is intensity-matched by maintaining the same peak shear rate throughout the exercise protocol as constant work rate exercise. However, the peak shear rate achieved in this protocol is less than the peak shear rate attained during traditional interval protocols with a higher exercise intensity (Sawyer et al., 2016, O'Brien et al., 2020, Molmen-Hansen et al., 2012, Schjerve et al., 2008). Therefore, the lack of vascular adaptation following interval exercise training in this study may suggest that a greater peak shear, consequent to a greater exercise intensity, may be needed to induce a greater adaptive response than that seen following constant work rate exercise training. Nevertheless, the protocol used in this study was in the heavy-intensity domain; therefore, additional increases in exercise intensity may reduce the tolerable duration of the exercise if the same work:recovery duration is used or necessitate a greater work:recovery ratio, with the consequence of reducing the volume of shear stress that is accumulated in a given time period. In addition, this increase in exercise intensity may result in the interval protocol being experienced as unpleasant, deterring participation. Therefore, if higher intensities are needed to induce vascular adaptations from interval exercise, alternative strategies that are equally effective but do not require such a high exercise intensity may be more favourable.

5.5.5 Effect of acute exercise on brachial artery function

We did not observe significant changes in brachial artery FMD in response to a single session of HIIT or intensity-matched constant work rate exercise, pre-training or post-training. Previous studies examining the acute effect of aerobic exercise on brachial artery FMD have shown various responses. Some studies demonstrate an immediate increase in FMD post-exercise (Tyldum et al., 2009, Zhu et al., 2010, Harvey et al., 2005, Harris et al., 2008, Tinken et al., 2009), whilst others show no change (Sapp et al., 2019) or an immediate decrease in endothelial function that returns back to or above baseline ~1-2 h post-exercise (Dawson et al., 2013, Birk et al., 2013, Hwang et al., 2012). Exercise intensity is deemed to be an important factor in determining the FMD response to acute exercise, with higher exercise intensities associated with impaired endothelial function post-exercise (Dawson et al., 2013, Birk et al., 2013). For example, Birk et al. (2013) reported a significant decline in FMD following 30 min of cycling at 70 and 85% HR_{max} but not after 30 min of cycling 50% HR_{max}. In the aforementioned study, resistance (i.e. work rate) was adjusted on the cycle ergometer to alter exercise intensity (Birk et al., 2013). The current study altered work rate, whilst tightly controlling for the effect of exercise intensity on FMD and reported no change in FMD pre- to post-exercise. Thus, suggesting that work rate does not play a dominant independent role in determining the FMD response to acute exercise. Instead, evidence would suggest that vascular adaptations are more likely to be independently affected by exercise intensity.

5.5.6 Limitations

The current study is not without limitations. First, COVID-19 resulted in a reduced sample size, impairing the ability to detect changes between the exercise protocols. The acute effect of HIIT with a high work rate and intensity-matched constant work rate exercise on progenitor cell counts was only assessed immediately after exercise (10 min post-exercise). Therefore a delayed increase, or even decrease, in hematopoietic and/or endothelial progenitor cell number cannot be ruled out. Other

studies have reported significant increases in $CD45^{dim}/CD34^{+}/KDR^{+}$ cells 2 and 3 hours after resistance exercise (Ross et al., 2014, Krüger et al., 2015). Therefore, in the future, progenitor cell numbers should be assessed at additional time points after HIIT with a high work rate to rule out the possibility of a delayed response. Quantifying rare cell events using flow cytometry is a technical challenge. In this study cells were expressed as cells/10^6 mononuclear cells. This method does not account for the potential effect of exercise on peripheral blood mononuclear cell count, potentially influencing study results. In addition, exercise training was performed for 6 weeks, resulting in menstrual cycle differences between pre- and post-training assessments. Some studies have reported variations in endothelium-dependent vasodilation during the menstrual cycle (Williams et al., 2001, Hashimoto et al., 1995). Shill et al. (2016) also reported variations in progenitor cell counts during the menstrual cycle; however, $CD45^{dim}/CD34^{+}$ and $CD45^{dim}/CD34^{+}/KDR^{+}$ cells were not included in this analysis.

5.5.7 Conclusion

In summary, HIIT with a high work rate does not increase vascular endogenous repair capacity or endothelial function in young health adults. Thus, indicating that work rate is not an important independent driver for vascular adaptations. A greater peak shear stress during interval exercise bouts and/or large oscillations in shear stress may be required during interval exercise to induce vascular adaptations in this population. Nevertheless, both protocols increase $\dot{V}O_{2peak}$ and exercise tolerance.

Chapter 6 Conclusions and future considerations

Exercise strategies that effectively overcome exercise limitations to increase exercise tolerance are likely to improve health-related quality of life, provide morbidity and mortality protection in all adults, and reduce hospitalisation readmissions in those with chronic disease. However, to maximise the efficacy of exercise therapy, interventions that are specific to the individual and their exercise limitation(s) must be established. Currently, the mechanisms underpinning exercise intolerance are poorly understood, which is a key step that limits this process. Therefore, the first aim of this thesis was to explore the mechanisms underpinning exercise intolerance during ramp-incremental (RI) exercise.

In characterising the development of exercise-induced fatigue during RI exercise, Chapter 3 demonstrated that this response during RI exercise in health is consistent with known intramuscular metabolite responses and muscle fatigue responses to discrete moderate, heavy and very-heavy intensity constant work rate exercise (Cannon et al., 2011, Rossiter et al., 2002, Black et al., 2017). Furthermore, this study demonstrated that 'muscle fatigue' develops before 'activation fatigue', proxy markers of peripheral and central fatigue, respectively, during dynamic whole-body exercise. However, this may not always be the case. The mechanisms that limit RI exercise appear to be different in chronic disease. Individuals with chronic obstructive pulmonary disease appear not to be limited by the power producing capacity of the neuromuscular system at the limit of RI exercise, evidenced by their ability to generate a power that is ~160% greater than WR_{peak} at RI exercise intolerance (Cannon et al., 2016). In addition, the mechanisms of RI intolerance may be different, and also variable between individuals with a chronic disease (e.g. preliminary data in HFrEF; Ferguson et al., 2019).

Therefore, it may be interesting to explore the characterisation of exercise-induced fatigue during RI exercise in clinical populations, to understand how exercise-induced fatigue develops and limits RI exercise in patient populations. This approach may enable comparisons to be made, for example, between the ratio of 'muscle fatigue' and 'activation fatigue' during RI exercise in health and disease. It is possible that 'activation fatigue' may be seen prior to intolerance in chronic disease (contrasting the response seen in healthy individuals in Chapter 3) due to the pathophysiology of the conditions inducing a mismatch between the perception of effort and physiological capacity. Whilst speculative, the information from this approach, in combination with other approaches, such as cardiopulmonary exercise testing with invasive monitoring that permits steps in the O_2 transport and utilisation cascade to be assessed (Houstis et al., 2018), might enable exercise limitations to be identified, and therefore be of clinical significance. This may afford diagnostic, as well as prognostic information to be derived from cardiopulmonary exercise tests. Although significantly more work is needed to understand the clinical significance of the exercise limitations and how these limitations can be targeted with exercise therapy, this information may inform exercise prescription. Alternatively, this approach may be employed to assess pre- and post-training changes in the mechanisms of exercise intolerance to understand how exercise strategies influence the mechanisms of intolerance. Re-assessing exercise limitations also affords the opportunity to re-optimise exercise training to target current limitations at any given time in the disease process.

Any factor that impairs O_2 delivery and/or utilisation (i.e. lowers $\dot{V}O_{2peak}$) is likely to limit exercise tolerance. The peripheral vasculature plays a central role in O_2 delivery as it determines blood flow (i.e. O_2 delivery) to the working skeletal muscle during exercise. Ageing and the onset and development of chronic disease, specifically HFrEF, compromise endothelial function, impairing O_2 transport and $\dot{V}O_{2peak}$ during dynamic whole-body exercise. Highlighting the significance of this, superficial femoral

artery FMD correlates with exercise tolerance in HFrEF (Hundley et al., 2007). Independent to the effect that peripheral vascular function has on exercise intolerance, peripheral vascular dysfunction plays an important pathophysiological role in the development of atherosclerosis and cardiovascular disease. Several studies have shown that FMD is inversely associated with future cardiovascular events and cardiovascular disease severity (Yeboah et al., 2007, Ras et al., 2013, Neunteufl et al., 1997, Shechter et al., 2009, Xu et al., 2014). Similarly, hematopoietic and endothelial progenitor cell counts are markers of cardiovascular disease risk and correlate with HFrEF disease severity (assessed by NYHA classification; Samman Tahhan et al., 2017, Werner et al., 2005, Schmidt-Lucke et al., 2005). Ultimately, if vascular endothelial function can be preserved, or even improved, convective O_2 transport, and therefore, exercise tolerance may be preserved, and cardiovascular disease progression attenuated.

Exercise training can increase vascular endogenous repair capacity and endothelial function in health and disease (Boff et al., 2019, Conraads et al., 2015, Wisløff et al., 2007, Sandri et al., 2016, Tsai et al., 2016, Tinken et al., 2008). High-intensity interval training (HIIT) has emerged as an effective alternative exercise strategy to exercise guidelines promoting constant work rate exercise training. Compared to moderate intensity constant work rate exercise training, HIIT induces equivalent if not superior increases in vascular endothelial function (Boff et al., 2019, Sawyer et al., 2016, Wisløff et al., 2007, Ramos et al., 2015). In addition, HIIT may be a more enjoyable and time-efficient training strategy (Gillen and Gibala, 2014). However, it is unknown whether the effectiveness of HIIT can be improved by optimising the HIIT protocol that is used. Increasing the effectiveness of HIIT has the potential to augment the increase in health-related quality of life and decrease the risk of death and need for clinical interventions that are associated with exercise training.

This thesis assessed the effectiveness of HIIT with blood flow restriction (BFR) on vascular endogenous repair capacity and exercise tolerance in HFrEF (Chapter 4). This study demonstrated that HIIT with BFR is feasible in HFrEF; however, the addition of BFR to HIIT does not lead to a greater increase in exercise tolerance than HIIT alone. Further, this exercise strategy does not increase vascular endogenous repair capacity. Therefore, HIIT with BFR is not an advantageous addition to HFrEF training programmes. Although the addition of BFR to HIIT did not increase the effectiveness of exercise training in HFrEF, it does not mean that alternative strategies cannot augment the vascular adaptations induced by exercise training. Nevertheless, identifying new approaches requires research.

A key barrier to optimising exercise strategies is understanding the drivers for specific adaptations. There are many training variables (e.g. exercise intensity, work rate, work:recovery duration) that may independently, or interdependently influence the physiological adaptations induced by HIIT. The independent effect that each of these variables has on vascular endothelial function must be understood to determine the optimal HIIT stimulus for increasing vascular function. In Chapter 5, both HIIT with a high work and intensity-matched constant work rate exercise did not increase vascular endogenous repair capacity or endothelial function. Therefore, this thesis suggests that work rate does not play an important independent role in inducing vascular adaptations. Although this finding informs exercise prescription, the primary drivers for inducing vascular adaptations remain unknown, preventing the development of targeted therapies.

Subsequently, further research is required that continues the systematic approach applied in this thesis to identify the factors responsible for driving vascular

adaptations. The HIIT protocol used in Chapter 5 employed short work:recovery durations (15:15 s) to minimise oscillations in shear stress during exercise. The lack of vascular adaptation induced by HIIT in Chapter 5 may suggest that oscillations in shear stress, evoked by greater work:recovery durations, are needed to induce vascular adaptations. Therefore, a logical next step may be to investigate the independent role of the other variables of shear in inducing vascular adaptations (e.g. oscillatory shear, shear rate volume and peak shear rate), whilst tightly controlling exercise intensity and work done. Introducing greater oscillations in shear stress during HIIT reduces the volume of shear stress that is accumulated during a fixed exercise duration. This may need to be considered if shear volume is an important independent factor for driving vascular adaptations, especially in the context of cardiac rehabilitation sessions where session duration is fixed. The interdependent nature of the variables that may influence vascular adaptations induced by HIIT highlights the complexity of determining the optimal exercise prescription.

A considerable amount of work is still needed to understand exercise limitations and determine the optimal exercise strategy for improving vascular endogenous repair capacity and peripheral vascular function in health and disease. Nevertheless, this thesis sets precedence on the systematic approach that is needed to understand the independent effect of training variables on peripheral vascular function, taking an important step forward in the pursuit of personalised exercise prescription.

References

ABE, T., FUJITA, S., NAKAJIMA, T., SAKAMAKI, M., OZAKI, H., OGASAWARA, R., SUGAYA, M., KUDO, M., KURANO, M., YASUDA, T., SATO, Y., OHSHIMA, H., MUKAI, C. & ISHII, N. 2010. Effects of Low-Intensity Cycle Training with Restricted Leg Blood Flow on Thigh Muscle Volume and VO2MAX in Young Men. *J Sports Sci Med,* 9**,** 452-8.

ADAIR, T. H. 2005. Growth regulation of the vascular system: an emerging role for adenosine. *American Journal of Physiology-Regulatory, Integrative and Comparative Physiology,* 289**,** R283-R296.

ADAMS, V. 2018. CrossTalk proposal: Acute exercise elicits damage to the endothelial layer of systemic blood vessels in healthy individuals. *The Journal of physiology,* 596**,** 537-539.

ADAMS, V., LINKE, A., BREUCKMANN, F., LEINEWEBER, K., ERBS, S., KRÄNKEL, N., BRÖCKER-PREUSS, M., WOITEK, F., ERBEL, R., HEUSCH, G., HAMBRECHT, R., SCHULER, G. & MÖHLENKAMP, S. 2008. Circulating progenitor cells decrease immediately after marathon race in advanced-age marathon runners. *Eur J Cardiovasc Prev Rehabil,* 15**,** 602-7.

AICHER, A., HEESCHEN, C., MILDNER-RIHM, C., URBICH, C., IHLING, C., TECHNAU-IHLING, K., ZEIHER, A. M. & DIMMELER, S. 2003. Essential role of endothelial nitric oxide synthase for mobilization of stem and progenitor cells. *Nat Med,* 9**,** 1370-6.

ALAITI, M. A., ISHIKAWA, M. & COSTA, M. A. 2010. Bone marrow and circulating stem/progenitor cells for regenerative cardiovascular therapy. *Translational Research,* 156**,** 112-129.

ALDERTON, W. K., COOPER, C. E. & KNOWLES, R. G. 2001. Nitric oxide synthases: structure, function and inhibition. *Biochemical Journal,* 357**,** 593-615.

ALLEN, D. G., LAMB, G. D. & WESTERBLAD, H. 2008. Skeletal Muscle Fatigue: Cellular Mechanisms. *Physiological Reviews,* 88**,** 287-332.

AMANN, M. 2011. Central and Peripheral Fatigue: Interaction during Cycling Exercise in Humans. *Medicine & Science in Sports & Exercise,* 43.

AMANN, M., BLAIN, G. M., PROCTOR, L. T., SEBRANEK, J. J., PEGELOW, D. F. & DEMPSEY, J. A. 2011. Implications of group III and IV muscle afferents for high-intensity endurance exercise performance in humans. *J Physiol,* 589**,** 5299-309.

AMANN, M. & DEMPSEY, J. A. 2008. Locomotor muscle fatigue modifies central motor drive in healthy humans and imposes a limitation to exercise performance. *The Journal of physiology,* 586**,** 161-173.

AMANN, M., ELDRIDGE, M. W., LOVERING, A. T., STICKLAND, M. K., PEGELOW, D. F. & DEMPSEY, J. A. 2006. Arterial oxygenation influences central motor output and exercise performance via effects on peripheral locomotor muscle fatigue in humans. *The Journal of physiology,* 575**,** 937-952.

AMANN, M., PROCTOR, L. T., SEBRANEK, J. J., PEGELOW, D. F. & DEMPSEY, J. A. 2009. Opioid-mediated muscle afferents inhibit central motor drive and limit peripheral muscle fatigue development in humans. *J Physiol,* 587**,** 271-83.

AMELN, H., GUSTAFSSON, T., SUNDBERG, C. J., OKAMOTO, K., JANSSON, E., POELLINGER, L. & MAKINO, Y. 2005. Physiological activation of hypoxia inducible factor-1 in human skeletal muscle. *Faseb j,* 19**,** 1009-11.

ANDREASSEN, A. K., NORDØY, I., SIMONSEN, S., UELAND, T., MÜLLER, F., FRØLAND, S. S., GULLESTAD, L. & AUKRUST, P. 1998. Levels of circulating adhesion molecules in congestive heart failure and after heart transplantation. *Am J Cardiol,* 81**,** 604-8.

ARATOW, M., BALLARD, R. E., CRENSHAW, A. G., STYF, J., WATENPAUGH, D. E., KAHAN, N. J. & HARGENS, A. R. 1993. Intramuscular pressure and electromyography as indexes of force during isokinetic exercise. *J Appl Physiol (1985),* 74**,** 2634-40.

ARENA, R. & HUMPHREY, R. 2002. Comparison of ventilatory expired gas parameters used to predict hospitalization in patients with heart failure. *Am Heart J,* 143**,** 427-32.

ARENA, R., MYERS, J., ABELLA, J., PEBERDY, M. A., BENSIMHON, D., CHASE, P. & GUAZZI, M. 2007. Development of a ventilatory classification system in patients with heart failure. *Circulation,* 115**,** 2410-7.

ARENA, R., MYERS, J., ASLAM, S. S., VARUGHESE, E. B. & PEBERDY, M. A. 2004. Peak VO2 and VE/VCO2 slope in patients with heart failure: a prognostic comparison. *Am Heart J,* 147**,** 354-60.

ASAHARA, T., MUROHARA, T., SULLIVAN, A., SILVER, M., VAN DER ZEE, R., LI, T., WITZENBICHLER, B., SCHATTEMAN, G. & ISNER, J. M. 1997. Isolation of Putative Progenitor Endothelial Cells for Angiogenesis. *Science,* 275**,** 964-966.

ASAHARA, T., TAKAHASHI, T., MASUDA, H., KALKA, C., CHEN, D., IWAGURO, H., INAI, Y., SILVER, M. & ISNER, J. M. 1999. VEGF contributes to postnatal neovascularization by mobilizing bone marrow-derived endothelial progenitor cells. *Embo j,* 18**,** 3964-72.

ASHOR, A. W., LARA, J., SIERVO, M., CELIS-MORALES, C., OGGIONI, C., JAKOVLJEVIC, D. G. & MATHERS, J. C. 2015. Exercise Modalities and Endothelial Function: A Systematic Review and Dose–Response Meta-Analysis of Randomized Controlled Trials. *Sports Medicine,* 45**,** 279-296.

AYAJIKI, K., KINDERMANN, M., HECKER, M., FLEMING, I. & BUSSE, R. 1996. Intracellular pH and Tyrosine Phosphorylation but Not Calcium Determine Shear Stress–Induced Nitric Oxide Production in Native Endothelial Cells. *Circulation Research,* 78**,** 750-758.

BAGHER, P. & SEGAL, S. S. 2011. Regulation of blood flow in the microcirculation: role of conducted vasodilation. *Acta Physiol (Oxf),* 202**,** 271-84.

BALLINGER, S. W., PATTERSON, C., YAN, C. N., DOAN, R., BUROW, D. L., YOUNG, C. G., YAKES, F. M., VAN HOUTEN, B., BALLINGER, C. A., FREEMAN, B. A. & RUNGE, M. S. 2000. Hydrogen peroxide- and peroxynitrite-induced mitochondrial DNA damage and dysfunction in vascular endothelial and smooth muscle cells. *Circ Res,* 86**,** 960-6.

BANK, A. J., LEE, P. C. & KUBO, S. H. 2000. Endothelial dysfunction in patients with heart failure: relationship to disease severity. *J Card Fail,* 6**,** 29-36.

BARCROFT, H. & DORNHORST, A. 1949. The blood flow through the human calf during rhythmic exercise. *The Journal of physiology,* 109**,** 402-411.

BARILI, A., CORRALO, V. D. S., CARDOSO, A. M., MÂNICA, A., BONADIMAN, B., BAGATINI, M. D., DA SILVA-GRIGOLETTO, M. E., DE OLIVEIRA, G. G. & DE SÁ, C. A. 2018. Acute responses of hemodynamic and oxidative stress parameters to aerobic exercise with blood flow restriction in hypertensive elderly women. *Mol Biol Rep,* 45**,** 1099-1109.

BARSTOW, T. J. & MOLE, P. A. 1991. Linear and nonlinear characteristics of oxygen uptake kinetics during heavy exercise. *Journal of Applied Physiology,* 71**,** 2099-2106.

BARTLETT, J. D., CLOSE, G. L., MACLAREN, D. P., GREGSON, W., DRUST, B. & MORTON, J. P. 2011. High-intensity interval running is perceived to be more enjoyable than moderate-intensity continuous exercise: implications for exercise adherence. *J Sports Sci,* 29**,** 547-53.

BARTON, M., COSENTINO, F., BRANDES, R. P., MOREAU, P., SHAW, S. & LÜSCHER, T. F. 1997. Anatomic heterogeneity of vascular aging: role of nitric oxide and endothelin. *Hypertension,* 30**,** 817-24.

BAUERSACHS, J. & WIDDER, J. D. 2008. Endothelial dysfunction in heart failure. *Pharmacol Rep,* 60**,** 119-26.

BEAVER, W. L., WASSERMAN, K. & WHIPP, B. J. 1986a. Bicarbonate buffering of lactic acid generated during exercise. *Journal of Applied Physiology,* 60**,** 472-478.

BEAVER, W. L., WASSERMAN, K. & WHIPP, B. J. 1986b. A new method for detecting anaerobic threshold by gas exchange. *J Appl Physiol (1985),* 60**,** 2020-7.

BEELEN, A. & SARGEANT, A. J. 1991. Effect of fatigue on maximal power output at different contraction velocities in humans. *J Appl Physiol (1985),* 71**,** 2332-7.

BENDA, N. M., SEEGER, J. P., STEVENS, G. G., HIJMANS-KERSTEN, B. T., VAN DIJK, A. P., BELLERSEN, L., LAMFERS, E. J., HOPMAN, M. T. & THIJSSEN, D. H. 2015. Effects of High-Intensity Interval Training versus Continuous Training on Physical Fitness, Cardiovascular Function and Quality of Life in Heart Failure Patients. *PLoS One,* 10**,** e0141256.

BENJAMIN, I. J. & SCHNEIDER, M. D. 2005. Learning from failure: congestive heart failure in the postgenomic age. *The Journal of Clinical Investigation,* 115**,** 495-499.

BENOIT, H., JORDAN, M., WAGNER, H. & WAGNER, P. D. 1999. Effect of NO, vasodilator prostaglandins, and adenosine on skeletal muscle angiogenic growth factor gene expression. *J Appl Physiol (1985),* 86**,** 1513-8.

BENSON, A. P., GRASSI, B. & ROSSITER, H. B. 2013. A validated model of oxygen uptake and circulatory dynamic interactions at exercise onset in humans. *Journal of Applied Physiology,* 115**,** 743-755.

BEREZIN, A. E. & KREMZER, A. A. 2014. Circulating endothelial progenitor cells as markers for severity of ischemic chronic heart failure. *J Card Fail,* 20**,** 438-47.

BETIK, A. C., LUCKHAM, V. B. & HUGHSON, R. L. 2004. Flow-mediated dilation in human brachial artery after different circulatory occlusion

conditions. *American Journal of Physiology-Heart and Circulatory Physiology,* 286**,** H442-H448.

BIGLAND-RITCHIE, B., RICE, C. L., GARLAND, S. J. & WALSH, M. L. 1995. Task-Dependent Factors in Fatigue of Human Voluntary Contractions. *In:* GANDEVIA, S. C., ENOKA, R. M., MCCOMAS, A. J., STUART, D. G., THOMAS, C. K. & PIERCE, P. A. (eds.) *Fatigue: Neural and Muscular Mechanisms.* Boston, MA: Springer US.

BIGLAND-RITCHIE, B. & WOODS, J. J. 1984. Changes in muscle contractile properties and neural control during human muscular fatigue. *Muscle Nerve,* 7**,** 691-9.

BIRK, G. K., DAWSON, E. A., ATKINSON, C., HAYNES, A., CABLE, N. T., THIJSSEN, D. H. & GREEN, D. J. 2012. Brachial artery adaptation to lower limb exercise training: role of shear stress. *J Appl Physiol (1985),* 112**,** 1653-8.

BIRK, G. K., DAWSON, E. A., BATTERHAM, A. M., ATKINSON, G., CABLE, T., THIJSSEN, D. H. & GREEN, D. J. 2013. Effects of exercise intensity on flow mediated dilation in healthy humans. *Int J Sports Med,* 34**,** 409-14.

BLACK, M. A., CABLE, N. T., THIJSSEN, D. H. & GREEN, D. J. 2009. Impact of age, sex, and exercise on brachial artery flow-mediated dilatation. *Am J Physiol Heart Circ Physiol,* 297**,** H1109-16.

BLACK, M. I., JONES, A. M., BLACKWELL, J. R., BAILEY, S. J., WYLIE, L. J., MCDONAGH, S. T. J., THOMPSON, C., KELLY, J., SUMNERS, P., MILEVA, K. N., BOWTELL, J. L. & VANHATALO, A. 2017. Muscle metabolic and neuromuscular determinants of fatigue during cycling in different exercise intensity domains. *Journal of Applied Physiology,* 122**,** 446-459.

BOFF, W., DA SILVA, A. M., FARINHA, J. B., RODRIGUES-KRAUSE, J., REISCHAK-OLIVEIRA, A., TSCHIEDEL, B., PUÑALES, M. & BERTOLUCI, M. C. 2019. Superior Effects of High-Intensity Interval vs. Moderate-Intensity Continuous Training on Endothelial Function and Cardiorespiratory Fitness in Patients With Type 1 Diabetes: A Randomized Controlled Trial. *Frontiers in Physiology,* 10.

BONETTI, P. O., LERMAN, L. O. & LERMAN, A. 2003. Endothelial Dysfunction. *Arteriosclerosis, Thrombosis, and Vascular Biology,* 23**,** 168-175.

BONSIGNORE, M. R., MORICI, G., RICCIONI, R., HUERTAS, A., PETRUCCI, E., VECA, M., MARIANI, G., BONANNO, A., CHIMENTI, L., GIOIA, M., PALANGE, P. & TESTA, U. 2010. Hemopoietic and angiogenetic progenitors in healthy athletes: different responses to endurance and maximal exercise. *J Appl Physiol (1985),* 109**,** 60-7.

BONSIGNORE, M. R., MORICI, G., SANTORO, A., PAGANO, M., CASCIO, L., BONANNO, A., ABATE, P., MIRABELLA, F., PROFITA, M., INSALACO, G., GIOIA, M., VIGNOLA, A. M., MAJOLINO, I., TESTA, U. & HOGG, J. C. 2002. Circulating hematopoietic progenitor cells in runners. *J Appl Physiol (1985),* 93**,** 1691-7.

BOWEN, T. S., CANNON, D. T., BEGG, G., BALIGA, V., WITTE, K. K. & ROSSITER, H. B. 2012. A novel cardiopulmonary exercise test protocol and criterion to determine maximal oxygen uptake in chronic heart failure. *Journal of applied physiology (Bethesda, Md. : 1985),* 113**,** 451-458.

BRANDES, R. P., FLEMING, I. & BUSSE, R. 2005. Endothelial aging. *Cardiovascular research,* 66**,** 286-294.

BRAUNWALD, E. 2015. The war against heart failure: the Lancet lecture. *Lancet,* 385**,** 812-24.

BRAUNWALD, E. & BRISTOW, M. R. 2000. Congestive heart failure: fifty years of progress. *Circulation,* 102**,** Iv14-23.

BRITISH HEART FOUNDATION. 2021. *UK Factsheet January 2021* [Online]. Available: https://www.bhf.org.uk/ [Accessed 4th March 2021].

BROXTERMAN, R. M., HUREAU, T. J., LAYEC, G., MORGAN, D. E., BLEDSOE, A. D., JESSOP, J. E., AMANN, M. & RICHARDSON, R. S. 2018. Influence of group III/IV muscle afferents on small muscle mass exercise performance: a bioenergetics perspective. *The Journal of physiology,* 596**,** 2301-2314.

BROXTERMAN, R. M., LAYEC, G., HUREAU, T. J., MORGAN, D. E., BLEDSOE, A. D., JESSOP, J. E., AMANN, M. & RICHARDSON, R. S. 2017. Bioenergetics and ATP Synthesis during Exercise: Role of Group III/IV Muscle Afferents. *Med Sci Sports Exerc,* 49**,** 2404-2413.

BRUNO, R. M., GHIADONI, L., SERAVALLE, G., DELL'ORO, R., TADDEI, S. & GRASSI, G. 2012. Sympathetic regulation of vascular function in health and disease. *Frontiers in physiology,* 3**,** 284-284.

BUCHFUHRER, M. J., HANSEN, J. E., ROBINSON, T. E., SUE, D. Y., WASSERMAN, K. & WHIPP, B. J. 1983. Optimizing the exercise protocol for cardiopulmonary assessment. *J Appl Physiol Respir Environ Exerc Physiol,* 55**,** 1558-64.

BUITRAGO-LOPEZ, A., SANDERSON, J., JOHNSON, L., WARNAKULA, S., WOOD, A., DI ANGELANTONIO, E. & FRANCO, O. H. 2011. Chocolate consumption and cardiometabolic disorders: systematic review and meta-analysis. *BMJ (Clinical research ed.),* 343**,** d4488-d4488.

BUONO, M. J., KRIPPES, T., KOLKHORST, F. W., WILLIAMS, A. T. & CABRALES, P. 2016. Increases in core temperature counterbalance effects of haemoconcentration on blood viscosity during prolonged exercise in the heat. *Experimental physiology,* 101**,** 332-342.

BURGOYNE, J. R. & EATON, P. 2010. Oxidant sensing by protein kinases a and g enables integration of cell redox state with phosphoregulation. *Sensors (Basel, Switzerland),* 10**,** 2731-2751.

BURNLEY, M., VANHATALO, A., FULFORD, J. & JONES, A. M. 2010. Similar metabolic perturbations during all-out and constant force exhaustive exercise in humans: a (31)P magnetic resonance spectroscopy study. *Exp Physiol,* 95**,** 798-807.

BURNLEY, M., VANHATALO, A. & JONES, A. M. 2012. Distinct profiles of neuromuscular fatigue during muscle contractions below and above the critical torque in humans. *Journal of Applied Physiology,* 113**,** 215-223.

BURSI, F., WESTON, S. A., REDFIELD, M. M., JACOBSEN, S. J., PAKHOMOV, S., NKOMO, V. T., MEVERDEN, R. A. & ROGER, V. L. 2006. Systolic and Diastolic Heart Failure in the Community. *JAMA,* 296**,** 2209-2216.

CAI, H. & HARRISON, D. G. 2000. Endothelial Dysfunction in Cardiovascular Diseases: The Role of Oxidant Stress. *Circulation Research,* 87**,** 840-844.

CAIRNS, S. P., KNICKER, A. J., THOMPSON, M. W. & SJØGAARD, G. 2005. Evaluation of models used to study neuromuscular fatigue. *Exerc Sport Sci Rev,* 33**,** 9-16.

CANNON, D. T., BIMSON, W. E., HAMPSON, S. A., BOWEN, T. S., MURGATROYD, S. R., MARWOOD, S., KEMP, G. J. & ROSSITER, H. B. 2014. Skeletal muscle ATP turnover by 31P magnetic resonance spectroscopy during moderate and heavy bilateral knee extension. *The Journal of physiology,* 592**,** 5287-5300.

CANNON, D. T., COELHO, A. C., CAO, R., CHENG, A., PORSZASZ, J., CASABURI, R. & ROSSITER, H. B. 2016. Skeletal muscle power and fatigue at the tolerable limit of ramp-incremental exercise in COPD. *Journal of Applied Physiology,* 121**,** 1365-1373.

CANNON, D. T., WHITE, A. C., ANDRIANO, M. F., KOLKHORST, F. W. & ROSSITER, H. B. 2011. Skeletal muscle fatigue precedes the slow component of oxygen uptake kinetics during exercise in humans. *J Physiol,* 589**,** 727-39.

CAO, L., LI, L., YANG, H. & YIN, H. 2010. Overexpression of P-selectin glycoprotein ligand-1 enhances adhesive properties of endothelial progenitor cells through Syk activation. *Acta Biochim Biophys Sin,* 42**,** 507-514.

CARDÚS, J., MARRADES, R. M., ROCA, J., BARBERÀ, J. A., DIAZ, O., MASCLANS, J. R., RODRIGUEZ-ROISIN, R. & WAGNER, P. D. 1998. Effects of F(I)O2 on leg VO2 during cycle ergometry in sedentary subjects. *Med Sci Sports Exerc,* 30**,** 697-703.

CARVALHO, V. O., RUIZ, M. A., BOCCHI, E. A., CARVALHO, V. O. & GUIMARÃES, G. V. 2009. Correlation between CD34+ and exercise capacity, functional class, quality of life and norepinephrine in heart failure patients. *Cardiol J,* 16**,** 426-31.

CASEY, D. P. & JOYNER, M. J. 2012. Compensatory vasodilatation during hypoxic exercise: mechanisms responsible for matching oxygen supply to demand. *The Journal of physiology,* 590**,** 6321-6326.

CAU, S. B., CARNEIRO, F. S. & TOSTES, R. C. 2012. Differential modulation of nitric oxide synthases in aging: therapeutic opportunities. *Front Physiol,* 3**,** 218.

CELERMAJER, D. S., SORENSEN, K. E., GOOCH, V. M., SPIEGELHALTER, D. J., MILLER, O. I., SULLIVAN, I. D., LLOYD, J. K. & DEANFIELD, J. E. 1992. Non-invasive detection of endothelial dysfunction in children and adults at risk of atherosclerosis. *Lancet (London, England),* 340**,** 1111-1115.

CELERMAJER, D. S., SORENSEN, K. E., SPIEGELHALTER, D. J., GEORGAKOPOULOS, D., ROBINSON, J. & DEANFIELD, J. E. 1994. Aging is associated with endothelial dysfunction in healthy men years before the age-related decline in women. *Journal of the American College of Cardiology,* 24**,** 471-476.

CENCIONI, C., SPALLOTTA, F., MAI, A., MARTELLI, F., FARSETTI, A., ZEIHER, A. M. & GAETANO, C. 2015. Sirtuin function in aging heart and vessels. *J Mol Cell Cardiol,* 83**,** 55-61.

CENTNER, C., ZDZIEBLIK, D., DRESSLER, P., FINK, B., GOLLHOFER, A. & KÖNIG, D. 2018. Acute effects of blood flow restriction on exercise-induced free radical production in young and healthy subjects. *Free Radical Research,* 52**,** 446-454.

CERADINI, D. J., KULKARNI, A. R., CALLAGHAN, M. J., TEPPER, O. M., BASTIDAS, N., KLEINMAN, M. E., CAPLA, J. M., GALIANO, R. D., LEVINE, J. P. & GURTNER, G. C. 2004. Progenitor cell trafficking is regulated by hypoxic gradients through HIF-1 induction of SDF-1. *Nat Med,* 10**,** 858-64.

CHAVAKIS, E., AICHER, A., HEESCHEN, C., SASAKI, K.-I., KAISER, R., EL MAKHFI, N., URBICH, C., PETERS, T., SCHARFFETTER-KOCHANEK, K., ZEIHER, A. M., CHAVAKIS, T. & DIMMELER, S. 2005. Role of beta2-integrins for homing and neovascularization capacity of endothelial progenitor cells. *The Journal of experimental medicine,* 201**,** 63-72.

CHENG, C., TEMPEL, D., HAPEREN, R. V., BAAN, A. V. D., GROSVELD, F., DAEMEN, M. J. A. P., KRAMS, R. & CROM, R. D. 2006. Atherosclerotic Lesion Size and Vulnerability Are Determined by Patterns of Fluid Shear Stress. *Circulation,* 113**,** 2744-2753.

CHENG, C., VAN HAPEREN, R., DE WAARD, M., VAN DAMME, L. C., TEMPEL, D., HANEMAAIJER, L., VAN CAPPELLEN, G. W., BOS, J., SLAGER, C. J. & DUNCKER, D. J. 2005. Shear stress affects the intracellular distribution of eNOS: direct demonstration by a novel in vivo technique. *Blood,* 106**,** 3691-3698.

CHIDNOK, W., FULFORD, J., BAILEY, S. J., DIMENNA, F. J., SKIBA, P. F., VANHATALO, A. & JONES, A. M. 2013. Muscle metabolic determinants of exercise tolerance following exhaustion: relationship to the "critical power". *J Appl Physiol (1985),* 115**,** 243-50.

CHIU, J.-J. & CHIEN, S. 2011. Effects of Disturbed Flow on Vascular Endothelium: Pathophysiological Basis and Clinical Perspectives. *Physiological Reviews,* 91**,** 327-387.

CHRISTIANSEN, D., EIBYE, K., HOSTRUP, M. & BANGSBO, J. 2020. Training with blood flow restriction increases femoral artery diameter and thigh oxygen delivery during knee-extensor exercise in recreationally trained men. *J Physiol,* 598**,** 2337-2353.

CHRISTIANSEN, D., EIBYE, K. H., HOSTRUP, M. & BANGSBO, J. 2019a. Blood flow-restricted training enhances thigh glucose uptake during exercise and muscle antioxidant function in humans. *Metabolism,* 98**,** 1-15.

CHRISTIANSEN, D., EIBYE, K. H., RASMUSSEN, V., VOLDBYE, H. M., THOMASSEN, M., NYBERG, M., GUNNARSSON, T. G. P., SKOVGAARD, C., LINDSKROG, M. S., BISHOP, D. J., HOSTRUP, M. & BANGSBO, J. 2019b. Cycling with blood flow restriction improves performance and muscle K(+) regulation and alters the effect of anti-oxidant infusion in humans. *J Physiol,* 597**,** 2421-2444.

CHRISTIANSEN, D., MURPHY, R. M., BANGSBO, J., STATHIS, C. G. & BISHOP, D. J. 2018. Increased FXYD1 and PGC-1α mRNA after blood flow-restricted running is related to fibre type-specific AMPK signalling and oxidative stress in human muscle. *Acta physiologica (Oxford, England),* 223**,** e13045-e13045.

CHRYSOHOOU, C., TSITSINAKIS, G., VOGIATZIS, I., CHEROUVEIM, E., ANTONIOU, C., TSIANTILAS, A., TSIACHRIS, D., DIMOPOULOS, D., PANAGIOTAKOS, D. B., PITSAVOS, C., KOULOURIS, N. G. & STEFANADIS, C. 2013. High intensity, interval exercise improves

quality of life of patients with chronic heart failure: a randomized controlled trial. *QJM: An International Journal of Medicine,* 107**,** 25-32.

CLANTON, T. L. 2007. Hypoxia-induced reactive oxygen species formation in skeletal muscle. *J Appl Physiol (1985),* 102**,** 2379-88.

CLARK, A. L., POOLE-WILSON, P. A. & COATS, A. J. 1992. Relation between ventilation and carbon dioxide production in patients with chronic heart failure. *J Am Coll Cardiol,* 20**,** 1326-32.

CLARK, A. L., VOLTERRANI, M., SWAN, J. W. & COATS, A. J. S. 1995. Ventilation-perfusion matching in chronic heart failure. *International Journal of Cardiology,* 48**,** 259-270.

CLARKSON, P., MONTGOMERY, H. E., MULLEN, M. J., DONALD, A. E., POWE, A. J., BULL, T., JUBB, M., WORLD, M. & DEANFIELD, J. E. 1999. Exercise training enhances endothelial function in young men. *Journal of the American College of Cardiology,* 33**,** 1379-1385.

CLAUSEN, J. P. 1976. Circulatory adjustments to dynamic exercise and effect of physical training in normal subjects and in patients with coronary artery disease. *Prog Cardiovasc Dis,* 18**,** 459-95.

CLAUSEN, T. & NIELSEN, O. B. 2007. Potassium, Na+,K+-pumps and fatigue in rat muscle. *J Physiol,* 584**,** 295-304.

COATS, E. M., ROSSITER, H. B., DAY, J. R., MIURA, A., FUKUBA, Y. & WHIPP, B. J. 2003. Intensity-dependent tolerance to exercise after attaining V̇o2 max in humans. *Journal of Applied Physiology,* 95**,** 483-490.

COELHO, A. C., CANNON, D. T., CAO, R., PORSZASZ, J., CASABURI, R., KNORST, M. M. & ROSSITER, H. B. 2015. Instantaneous quantification of skeletal muscle activation, power production, and fatigue during cycle ergometry. *J Appl Physiol (1985),* 118**,** 646-54.

COMINI, L., BACHETTI, T., GAIA, G., PASINI, E., AGNOLETTI, L., PEPI, P., CECONI, C., CURELLO, S. & FERRARI, R. 1996. Aorta and skeletal muscle NO synthase expression in experimental heart failure. *J Mol Cell Cardiol,* 28**,** 2241-8.

CONCEICAO, M. S., GASPARI, A. F., RAMKRAPES, A. P. B., JUNIOR, E. M. M., BERTUZZI, R., CAVAGLIERI, C. R. & CHACON-MIKAHIL, M. P. T. 2018. Anaerobic metabolism induces greater total energy expenditure during exercise with blood flow restriction. *PLoS One,* 13**,** e0194776.

CONRAADS, V. M., DEATON, C., PIOTROWICZ, E., SANTAULARIA, N., TIERNEY, S., PIEPOLI, M. F., PIESKE, B., SCHMID, J.-P., DICKSTEIN, K., PONIKOWSKI, P. P. & JAARSMA, T. 2012. Adherence of heart failure patients to exercise: barriers and possible solutions. *European Journal of Heart Failure,* 14**,** 451-458.

CONRAADS, V. M., PATTYN, N., DE MAEYER, C., BECKERS, P. J., COECKELBERGHS, E., CORNELISSEN, V. A., DENOLLET, J., FREDERIX, G., GOETSCHALCKX, K., HOYMANS, V. Y., POSSEMIERS, N., SCHEPERS, D., SHIVALKAR, B., VOIGT, J. U., VAN CRAENENBROECK, E. M. & VANHEES, L. 2015. Aerobic interval training and continuous training equally improve aerobic exercise capacity in patients with coronary artery disease: the SAINTEX-CAD study. *Int J Cardiol,* 179**,** 203-10.

CONRAADS, V. M., VAN CRAENENBROECK, E. M., DE MAEYER, C., VAN BERENDONCKS, A. M., BECKERS, P. J. & VRINTS, C. J. 2013.

Unraveling new mechanisms of exercise intolerance in chronic heart failure: role of exercise training. *Heart Fail Rev,* 18**,** 65-77.

CORVINO, R. B., OLIVEIRA, M. F. M., DENADAI, B. S., ROSSITER, H. B. & CAPUTO, F. 2019. Speeding of oxygen uptake kinetics is not different following low-intensity blood-flow-restricted and high-intensity interval training. *Experimental Physiology,* 104**,** 1858-1867.

CORVINO, R. B., ROSSITER, H. B., LOCH, T., MARTINS, J. C. & CAPUTO, F. 2017. Physiological responses to interval endurance exercise at different levels of blood flow restriction. *Eur J Appl Physiol,* 117**,** 39-52.

COSTES, F., AGRESTI, A., COURT-FORTUNE, I., ROCHE, F., VERGNON, J. M. & BARTHÉLÉMY, J. C. 2003. Noninvasive ventilation during exercise training improves exercise tolerance in patients with chronic obstructive pulmonary disease. *J Cardiopulm Rehabil,* 23**,** 307-13.

CREDEUR, D. P., HOLLIS, B. C. & WELSCH, M. A. 2010. Effects of handgrip training with venous restriction on brachial artery vasodilation. *Med Sci Sports Exerc,* 42**,** 1296-302.

CROSS, T. J., KIM, C.-H., JOHNSON, B. D. & LALANDE, S. 2020. The interactions between respiratory and cardiovascular systems in systolic heart failure. *Journal of Applied Physiology,* 128**,** 214-224.

CUBBON, R. M., MURGATROYD, S. R., FERGUSON, C., BOWEN, T. S., RAKOBOWCHUK, M., BALIGA, V., CANNON, D., RAJWANI, A., ABBAS, A., KAHN, M., BIRCH, K. M., PORTER, K. E., WHEATCROFT, S. B., ROSSITER, H. B. & KEARNEY, M. T. 2010. Human Exercise-Induced Circulating Progenitor Cell Mobilization Is Nitric Oxide-Dependent and Is Blunted in South Asian Men. *Arteriosclerosis, Thrombosis, and Vascular Biology,* 30**,** 878-884.

DA SILVA, C. G., SPECHT, A., WEGIEL, B., FERRAN, C. & KACZMAREK, E. 2009. Mechanism of purinergic activation of endothelial nitric oxide synthase in endothelial cells. *Circulation,* 119**,** 871-9.

DAVIES, M. J., BENSON, A. P., CANNON, D. T., MARWOOD, S., KEMP, G. J., ROSSITER, H. B. & FERGUSON, C. 2017. Dissociating external power from intramuscular exercise intensity during intermittent bilateral knee-extension in humans. *The Journal of physiology,* 595**,** 6673-6686.

DAVIES, M. J., LYALL, G. K., BENSON, A. P., CANNON, D. T., BIRCH, K. M., ROSSITER, H. B. & FERGUSON, C. 2021. Power Reserve at Intolerance in Ramp-Incremental Exercise Is Dependent on Incrementation Rate. *Medicine & Science in Sports & Exercise,* Publish Ahead of Print.

DAVIGNON, J. & GANZ, P. 2004. Role of Endothelial Dysfunction in Atherosclerosis. *Circulation,* 109**,** III-27-III-32.

DAWSON, E. A., GREEN, D. J., CABLE, N. T. & THIJSSEN, D. H. J. 2013. Effects of acute exercise on flow-mediated dilatation in healthy humans. *Journal of Applied Physiology,* 115**,** 1589-1598.

DAWSON, E. A., WHYTE, G. P., BLACK, M. A., JONES, H., HOPKINS, N., OXBOROUGH, D., GAZE, D., SHAVE, R. E., WILSON, M. & GEORGE, K. P. 2008. Changes in vascular and cardiac function after prolonged strenuous exercise in humans. *Journal of Applied Physiology,* 105**,** 1562-1568.

DE MEYER, T., RIETZSCHEL, E. R., DE BUYZERE, M. L., VAN CRIEKINGE, W. & BEKAERT, S. 2011. Telomere length and cardiovascular aging: The means to the ends? *Ageing Research Reviews,* 10**,** 297-303.

DE OLIVEIRA, M. F. M., CAPUTO, F., CORVINO, R. B. & DENADAI, B. S. 2016. Short-term low-intensity blood flow restricted interval training improves both aerobic fitness and muscle strength. *Scandinavian Journal of Medicine & Science in Sports,* 26**,** 1017-1025.

DECORTE, N., LAFAIX, P. A., MILLET, G. Y., WUYAM, B. & VERGES, S. 2012. Central and peripheral fatigue kinetics during exhaustive constant-load cycling. *Scand J Med Sci Sports,* 22**,** 381-91.

DELP, M. D., BEHNKE, B. J., SPIER, S. A., WU, G. & MULLER-DELP, J. M. 2008. Ageing diminishes endothelium-dependent vasodilatation and tetrahydrobiopterin content in rat skeletal muscle arterioles. *The Journal of Physiology,* 586**,** 1161-1168.

DIMMELER, S., FLEMING, I., FISSLTHALER, B., HERMANN, C., BUSSE, R. & ZEIHER, A. M. 1999. Activation of nitric oxide synthase in endothelial cells by Akt-dependent phosphorylation. *Nature,* 399**,** 601-605.

DIMOPOULOS, S., ANASTASIOU-NANA, M., SAKELLARIOU, D., DRAKOS, S., KAPSIMALAKOU, S., MAROULIDIS, G., RODITIS, P., PAPAZACHOU, O., VOGIATZIS, I., ROUSSOS, C. & NANAS, S. 2006. Effects of exercise rehabilitation program on heart rate recovery in patients with chronic heart failure. *Eur J Cardiovasc Prev Rehabil,* 13**,** 67-73.

DIXON, L. J., MORGAN, D. R., HUGHES, S. M., MCGRATH, L. T., EL-SHERBEENY, N. A., PLUMB, R. D., DEVINE, A., LEAHEY, W., JOHNSTON, G. D. & MCVEIGH, G. E. 2003. Functional Consequences of Endothelial Nitric Oxide Synthase Uncoupling in Congestive Cardiac Failure. *Circulation,* 107**,** 1725-1728.

DONATO, A. J., GANO, L. B., ESKURZA, I., SILVER, A. E., GATES, P. E., JABLONSKI, K. & SEALS, D. R. 2009. Vascular endothelial dysfunction with aging: endothelin-1 and endothelial nitric oxide synthase. *Am J Physiol Heart Circ Physiol,* 297**,** H425-32.

DONATO, A. J., MACHIN, D. R. & LESNIEWSKI, L. A. 2018. Mechanisms of Dysfunction in the Aging Vasculature and Role in Age-Related Disease. *Circ Res,* 123**,** 825-848.

DONATO, A. J., MAGERKO, K. A., LAWSON, B. R., DURRANT, J. R., LESNIEWSKI, L. A. & SEALS, D. R. 2011. SIRT-1 and vascular endothelial dysfunction with ageing in mice and humans. *The Journal of physiology,* 589**,** 4545-4554.

DOSHI, S. N., NAKA, K. K., PAYNE, N., JONES, C. J., ASHTON, M., LEWIS, M. J. & GOODFELLOW, J. 2001. Flow-mediated dilatation following wrist and upper arm occlusion in humans: the contribution of nitric oxide. *Clinical science,* 101**,** 629-635.

DOYLE-BAKER, D., TEMESI, J., MEDYSKY, M. E., HOLASH, R. J. & MILLET, G. Y. 2018. An Innovative Ergometer to Measure Neuromuscular Fatigue Immediately after Cycling. *Med Sci Sports Exerc,* 50**,** 375-387.

DREXLER, H. 1998. Hypertension, heart failure, and endothelial function. *American Journal of Cardiology,* 82**,** 20S-22S.

DREXLER, H., HAYOZ, D., MÜNZEL, T., HORNIG, B., JUST, H., BRUNNER, H. R. & ZELIS, R. 1992a. Endothelial function in chronic congestive heart failure. *American Journal of Cardiology,* 69**,** 1596-1601.

DREXLER, H., HAYOZ, D., MÜNZEL, T., JUST, H., ZELIS, R. & BRUNNER, H. R. 1993. Endothelial function in congestive heart failure. *American Heart Journal,* 126**,** 761-764.

DREXLER, H., RIEDE, U., MÜNZEL, T., KÖNIG, H., FUNKE, E. & JUST, H. 1992b. Alterations of skeletal muscle in chronic heart failure. *Circulation,* 85**,** 1751-1759.

DUFOUR, C., CORCIONE, A., SVAHN, J., HAUPT, R., POGGI, V., BÉKA'SSY, A. N., SCIMÈ, R., PISTORIO, A. & PISTOIA, V. 2003. TNF-alpha and IFN-gamma are overexpressed in the bone marrow of Fanconi anemia patients and TNF-alpha suppresses erythropoiesis in vitro. *Blood,* 102**,** 2053-9.

DYSON, K. S., SHOEMAKER, J. K. & HUGHSON, R. L. 2006. Effect of acute sympathetic nervous system activation on flow-mediated dilation of brachial artery. *American Journal of Physiology-Heart and Circulatory Physiology,* 290**,** H1446-H1453.

EGGINTON, S. 2008. Invited review: activity-induced angiogenesis. *Pflügers Archiv - European Journal of Physiology,* 457**,** 963.

ELEUTERI, E., MEZZANI, A., DI STEFANO, A., VALLESE, D., GNEMMI, I., DELLE DONNE, L., TADDEO, A., DELLA BELLA, S. & GIANNUZZI, P. 2013. Aerobic training and angiogenesis activation in patients with stable chronic heart failure: a preliminary report. *Biomarkers,* 18**,** 418-424.

ELLINGSEN, Ø., HALLE, M., CONRAADS, V., STØYLEN, A., DALEN, H., DELAGARDELLE, C., LARSEN, A.-I., HOLE, T., MEZZANI, A., CRAENENBROECK, E. M. V., VIDEM, V., BECKERS, P., CHRISTLE, J. W., WINZER, E., MANGNER, N., WOITEK, F., HÖLLRIEGEL, R., PRESSLER, A., MONK-HANSEN, T., SNOER, M., FEIEREISEN, P., VALBORGLAND, T., KJEKSHUS, J., HAMBRECHT, R., GIELEN, S., KARLSEN, T., PRESCOTT, E. & LINKE, A. 2017. High-Intensity Interval Training in Patients With Heart Failure With Reduced Ejection Fraction. *Circulation,* 135**,** 839-849.

ELLIOTT, A. D., RAJOPADHYAYA, K., BENTLEY, D. J., BELTRAME, J. F. & AROMATARIS, E. C. 2015. Interval training versus continuous exercise in patients with coronary artery disease: a meta-analysis. *Heart Lung Circ,* 24**,** 149-57.

ELMER, S. J., AMANN, M., MCDANIEL, J., MARTIN, D. T. & MARTIN, J. C. 2013. Fatigue is specific to working muscles: no cross-over with single-leg cycling in trained cyclists. *European journal of applied physiology,* 113**,** 479-488.

EMTNER, M., PORSZASZ, J., BURNS, M., SOMFAY, A. & CASABURI, R. 2003. Benefits of Supplemental Oxygen in Exercise Training in Nonhypoxemic Chronic Obstructive Pulmonary Disease Patients. *American Journal of Respiratory and Critical Care Medicine,* 168**,** 1034-1042.

ERBS, S., HÖLLRIEGEL, R., LINKE, A., BECK, E. B., ADAMS, V., GIELEN, S., MÖBIUS-WINKLER, S., SANDRI, M., KRÄNKEL, N., HAMBRECHT, R. & SCHULER, G. 2010. Exercise training in patients with advanced chronic heart failure (NYHA IIIb) promotes restoration of peripheral vasomotor function, induction of endogenous regeneration, and improvement of left ventricular function. *Circ Heart Fail,* 3**,** 486-94.

ERICSON, M. O., BRATT, A., NISELL, R., ARBORELIUS, U. P. & EKHOLM, J. 1986. Power output and work in different muscle groups during ergometer cycling. *Eur J Appl Physiol Occup Physiol,* 55**,** 229-35.

ESPOSITO, F., MATHIEU-COSTELLO, O., ENTIN, P. L., WAGNER, P. D. & RICHARDSON, R. S. 2010a. The skeletal muscle VEGF mRNA response to acute exercise in patients with chronic heart failure. *Growth Factors,* 28**,** 139-47.

ESPOSITO, F., MATHIEU-COSTELLO, O., SHABETAI, R., WAGNER, P. D. & RICHARDSON, R. S. 2010b. Limited maximal exercise capacity in patients with chronic heart failure: partitioning the contributors. *J Am Coll Cardiol,* 55**,** 1945-54.

ESPOSITO, F., MATHIEU-COSTELLO, O., WAGNER, P. D. & RICHARDSON, R. S. 2018. Acute and chronic exercise in patients with heart failure with reduced ejection fraction: evidence of structural and functional plasticity and intact angiogenic signalling in skeletal muscle. *The Journal of physiology,* 596**,** 5149-5161.

EVANS, C., VANCE, S. & BROWN, M. 2010. Short-term resistance training with blood flow restriction enhances microvascular filtration capacity of human calf muscles. *J Sports Sci,* 28**,** 999-1007.

FADINI, G. P., CORACINA, A., BAESSO, I., AGOSTINI, C., TIENGO, A., AVOGARO, A. & DE KREUTZENBERG, S. V. 2006. Peripheral blood CD34+KDR+ endothelial progenitor cells are determinants of subclinical atherosclerosis in a middle-aged general population. *Stroke,* 37**,** 2277-82.

FADINI, G. P., LOSORDO, D. & DIMMELER, S. 2012. Critical reevaluation of endothelial progenitor cell phenotypes for therapeutic and diagnostic use. *Circulation research,* 110**,** 624-637.

FAILURE, M.-A. G. G. I. C. H. 2012. The survival of patients with heart failure with preserved or reduced left ventricular ejection fraction: an individual patient data meta-analysis. *Eur Heart J,* 33**,** 1750-7.

FARAONE, S. V. 2008. Interpreting estimates of treatment effects: implications for managed care. *Pharmacy and Therapeutics,* 33**,** 700.

FEIL, C. & AUGUSTIN, H. G. 1998. Endothelial cells differentially express functional CXC-chemokine receptor-4 (CXCR-4/fusin) under the control of autocrine activity and exogenous cytokines. *Biochem Biophys Res Commun,* 247**,** 38-45.

FERGUSON, C., DAVIES, M. J., GARNHAM, J. O., GIERULA, J., PATON, M. F., ROSSITER, H. B. & WITTE, K. K. 2019. Dichotomy In The Mechanism Of Ramp-incremental Exercise Intolerance In Chronic Heart Failure: 1095 Board #329 May 29 3:30 PM - 5:00 PM. *Medicine & Science in Sports & Exercise,* 51.

FERGUSON, C., WYLDE, L. A., BENSON, A. P., CANNON, D. T. & ROSSITER, H. B. 2016. No reserve in isokinetic cycling power at intolerance during ramp incremental exercise in endurance-trained men. *J Appl Physiol (1985),* 120**,** 70-7.

FERGUSON, R. A., HUNT, J. E. A., LEWIS, M. P., MARTIN, N. R. W., PLAYER, D. J., STANGIER, C., TAYLOR, C. W. & TURNER, M. C. 2018. The acute angiogenic signalling response to low-load resistance exercise with blood flow restriction. *Eur J Sport Sci,* 18**,** 397-406.

FITSCHEN, P. J., KISTLER, B. M., JEONG, J. H., CHUNG, H. R., WU, P. T., WALSH, M. J. & WILUND, K. R. 2014. Perceptual effects and efficacy

of intermittent or continuous blood flow restriction resistance training. *Clin Physiol Funct Imaging,* 34**,** 356-63.

FITTS, R. H. 2008. The cross-bridge cycle and skeletal muscle fatigue. *J Appl Physiol (1985),* 104**,** 551-8.

FÖRSTERMANN, U. & MÜNZEL, T. 2006. Endothelial Nitric Oxide Synthase in Vascular Disease. *Circulation,* 113**,** 1708-1714.

FRANCIOSA, J. A., PARK, M. & LEVINE, T. B. 1981. Lack of correlation between exercise capacity and indexes of resting left ventricular performance in heart failure. *Am J Cardiol,* 47**,** 33-9.

FRANZONI, F., GHIADONI, L., GALETTA, F., PLANTINGA, Y., LUBRANO, V., HUANG, Y., SALVETTI, G., REGOLI, F., TADDEI, S. & SANTORO, G. 2005. Physical activity, plasma antioxidant capacity, and endothelium-dependent vasodilation in young and older men. *American journal of hypertension,* 18**,** 510-516.

FRITZENWANGER, M., LORENZ, F., JUNG, C., FABRIS, M., THUDE, H., BARZ, D. & FIGULLA, H. R. 2009. Differential number of CD34+, CD133+ and CD34+/CD133+ cells in peripheral blood of patients with congestive heart failure. *Eur J Med Res,* 14**,** 113-7.

FROYD, C., MILLET, G. Y. & NOAKES, T. D. 2013. The development of peripheral fatigue and short-term recovery during self-paced high-intensity exercise. *J Physiol,* 591**,** 1339-46.

GAGNON, P., SAEY, D., VIVODTZEV, I., LAVIOLETTE, L., MAINGUY, V., MILOT, J., PROVENCHER, S. & MALTAIS, F. 2009. Impact of preinduced quadriceps fatigue on exercise response in chronic obstructive pulmonary disease and healthy subjects. *Journal of Applied Physiology,* 107**,** 832-840.

GALE, C. P., CATTLE, B., WOOLSTON, A., BAXTER, P., WEST, T., SIMMS, A., BLAXILL, J., GREENWOOD, D., FOX, K. & WEST, R. 2011. Resolving inequalities in care? Reduced mortality in the elderly after acute coronary syndromes. The Myocardial Ischaemia National Audit Project 2003–2010. *European heart journal***,** ehr381.

GANDEVIA, S. C. 2001. Spinal and Supraspinal Factors in Human Muscle Fatigue. *Physiological Reviews,* 81**,** 1725-1789.

GATES, P. E., BOUCHER, M. L., SILVER, A. E., MONAHAN, K. D. & SEALS, D. R. 2007. Impaired flow-mediated dilation with age is not explained by L-arginine bioavailability or endothelial asymmetric dimethylarginine protein expression. *Journal of Applied Physiology,* 102**,** 63-71.

GATTA, L., ARMANI, A., IELLAMO, F., CONSOLI, C., MOLINARI, F., CAMINITI, G., VOLTERRANI, M. & ROSANO, G. M. 2012. Effects of a short-term exercise training on serum factors involved in ventricular remodelling in chronic heart failure patients. *Int J Cardiol,* 155**,** 409-13.

GERBER, Y., WESTON, S. A., BERARDI, C., MCNALLAN, S. M., JIANG, R., REDFIELD, M. M. & ROGER, V. L. 2013. Contemporary trends in heart failure with reduced and preserved ejection fraction after myocardial infarction: a community study. *American journal of epidemiology,* 178**,** 1272-1280.

GIANNATTASIO, C., ACHILLI, F., GRAPPIOLO, A., FAILLA, M., MELES, E., GENTILE, G., CALCHERA, I., CAPRA, A., BAGLIVO, J., VINCENZI, A., SALA, L. & MANCIA, G. 2001. Radial artery flow-mediated dilatation in heart failure patients: effects of pharmacological and nonpharmacological treatment. *Hypertension,* 38**,** 1451-5.

GIBALA, M. J. & LITTLE, J. P. 2020. Physiological basis of brief vigorous exercise to improve health. *The Journal of Physiology,* 598**,** 61-69.

GIEBEL, B., CORBEIL, D., BECKMANN, J., HÖHN, J., FREUND, D., GIESEN, K., FISCHER, J., KÖGLER, G. & WERNET, P. 2004. Segregation of lipid raft markers including CD133 in polarized human hematopoietic stem and progenitor cells. *Blood,* 104**,** 2332-8.

GIELEN, S., ADAMS, V., MÖBIUS-WINKLER, S., LINKE, A., ERBS, S., YU, J., KEMPF, W., SCHUBERT, A., SCHULER, G. & HAMBRECHT, R. 2003. Anti-inflammatory effects of exercise training in the skeletal muscle of patients with chronic heart failure. *J Am Coll Cardiol,* 42**,** 861-8.

GILLEN, J. B. & GIBALA, M. J. 2014. Is high-intensity interval training a time-efficient exercise strategy to improve health and fitness? *Appl Physiol Nutr Metab,* 39**,** 409-12.

GLIEMANN, L., VESTERGAARD HANSEN, C., RYTTER, N. & HELLSTEN, Y. 2019. Regulation of skeletal muscle blood flow during exercise. *Current Opinion in Physiology,* 10**,** 146-155.

GNECCHI, M., ZHANG, Z., NI, A. & DZAU, V. J. 2008. Paracrine Mechanisms in Adult Stem Cell Signaling and Therapy. *Circulation Research,* 103**,** 1204-1219.

GOLDENBERG, I., KUTYIFA, V., KLEIN, H. U., CANNOM, D. S., BROWN, M. W., DAN, A., DAUBERT, J. P., ESTES, N. A. M., FOSTER, E., GREENBERG, H., KAUTZNER, J., KLEMPFNER, R., KUNISS, M., MERKELY, B., PFEFFER, M. A., QUESADA, A., VISKIN, S., MCNITT, S., POLONSKY, B., GHANEM, A., SOLOMON, S. D., WILBER, D., ZAREBA, W. & MOSS, A. J. 2014. Survival with Cardiac-Resynchronization Therapy in Mild Heart Failure. *New England Journal of Medicine,* 370**,** 1694-1701.

GOMES NETO, M., DURÃES, A. R., CONCEIÇÃO, L. S. R., SAQUETTO, M. B., ELLINGSEN, Ø. & CARVALHO, V. O. 2018. High intensity interval training versus moderate intensity continuous training on exercise capacity and quality of life in patients with heart failure with reduced ejection fraction: A systematic review and meta-analysis. *International Journal of Cardiology,* 261**,** 134-141.

GOMEZ-CABRERA, M.-C., DOMENECH, E. & VIÑA, J. 2008. Moderate exercise is an antioxidant: Upregulation of antioxidant genes by training. *Free Radical Biology and Medicine,* 44**,** 126-131.

GORI, T., GROTTI, S., DRAGONI, S., LISI, M., DI STOLFO, G., SONNATI, S., FINESCHI, M. & PARKER, J. D. 2010. Assessment of vascular function: flow-mediated constriction complements the information of flow-mediated dilatation. *Heart,* 96**,** 141-7.

GOUNDER, S. S., KANNAN, S., DEVADOSS, D., MILLER, C. J., WHITEHEAD, K. J., ODELBERG, S. J., FIRPO, M. A., PAINE, R., 3RD, HOIDAL, J. R., ABEL, E. D. & RAJASEKARAN, N. S. 2012. Impaired transcriptional activity of Nrf2 in age-related myocardial oxidative stress is reversible by moderate exercise training. *PLoS One,* 7**,** e45697.

GRASSI, B., ROSSITER, H. B. & ZOLADZ, J. A. 2015. Skeletal muscle fatigue and decreased efficiency: two sides of the same coin? *Exerc Sport Sci Rev,* 43**,** 75-83.

GREEN, D. J., BILSBOROUGH, W., NAYLOR, L. H., REED, C., WRIGHT, J., O'DRISCOLL, G. & WALSH, J. H. 2005. Comparison of forearm blood

flow responses to incremental handgrip and cycle ergometer exercise: relative contribution of nitric oxide. *The Journal of Physiology,* 562**,** 617-628.

GREEN, D. J., JONES, H., THIJSSEN, D., CABLE, N. T. & ATKINSON, G. 2011. Flow-mediated dilation and cardiovascular event prediction: does nitric oxide matter? *Hypertension,* 57**,** 363-9.

GREEN, D. J., MAIORANA, A., O'DRISCOLL, G. & TAYLOR, R. 2004. Effect of exercise training on endothelium-derived nitric oxide function in humans. *The Journal of physiology,* 561**,** 1-25.

GREEN, D. J., O'DRISCOLL, G., JOYNER, M. J. & CABLE, N. T. 2008. Exercise and cardiovascular risk reduction: time to update the rationale for exercise? *Journal of applied physiology (Bethesda, Md. : 1985),* 105**,** 766-768.

GROENNEBAEK, T., SIELJACKS, P., NIELSEN, R., PRYDS, K., JESPERSEN, N. R., WANG, J., CARLSEN, C. R., SCHMIDT, M. R., DE PAOLI, F. V., MILLER, B. F., VISSING, K. & BØTKER, H. E. 2019. Effect of Blood Flow Restricted Resistance Exercise and Remote Ischemic Conditioning on Functional Capacity and Myocellular Adaptations in Patients With Heart Failure. *Circ Heart Fail,* 12**,** e006427.

GRUET, M., TEMESI, J., RUPP, T., LEVY, P., VERGES, S. & MILLET, G. Y. 2014. Dynamics of corticospinal changes during and after high-intensity quadriceps exercise. *Experimental Physiology,* 99**,** 1053-1064.

GUAZZI, M., MYERS, J. & ARENA, R. 2005. Cardiopulmonary exercise testing in the clinical and prognostic assessment of diastolic heart failure. *J Am Coll Cardiol,* 46**,** 1883-90.

GUNDERMANN, D. M., FRY, C. S., DICKINSON, J. M., WALKER, D. K., TIMMERMAN, K. L., DRUMMOND, M. J., VOLPI, E. & RASMUSSEN, B. B. 2012. Reactive hyperemia is not responsible for stimulating muscle protein synthesis following blood flow restriction exercise. *J Appl Physiol (1985),* 112**,** 1520-8.

HAGEN, T. M. 2003. Oxidative stress, redox imbalance, and the aging process. *Antioxid Redox Signal,* 5**,** 503-6.

HAJAR, R. 2016. Framingham Contribution to Cardiovascular Disease. *Heart views : the official journal of the Gulf Heart Association,* 17**,** 78-81.

HAMBRECHT, R., ADAMS, V., ERBS, S., LINKE, A., KRÄNKEL, N., SHU, Y., BAITHER, Y., GIELEN, S., THIELE, H., GUMMERT, J. F., MOHR, F. W. & SCHULER, G. 2003. Regular physical activity improves endothelial function in patients with coronary artery disease by increasing phosphorylation of endothelial nitric oxide synthase. *Circulation,* 107**,** 3152-8.

HANNAN, A. L., HING, W., SIMAS, V., CLIMSTEIN, M., COOMBES, J. S., JAYASINGHE, R., BYRNES, J. & FURNESS, J. 2018. High-intensity interval training versus moderate-intensity continuous training within cardiac rehabilitation: a systematic review and meta-analysis. *Open Access J Sports Med,* 9**,** 1-17.

HANSEN, J. E., CASABURI, R., COOPER, D. M. & WASSERMAN, K. 1988. Oxygen uptake as related to work rate increment during cycle ergometer exercise. *European journal of applied physiology and occupational physiology,* 57**,** 140-145.

HANSEN, J. E., SUE, D. Y., OREN, A. & WASSERMAN, K. 1987. Relation of oxygen uptake to work rate in normal men and men with circulatory disorders. *The American Journal of Cardiology,* 59**,** 669-674.

HANSSON, G. K. & LIBBY, P. 2006. The immune response in atherosclerosis: a double-edged sword. *Nature reviews immunology,* 6**,** 508-519.

HARMS, C. A., BABCOCK, M. A., MCCLARAN, S. R., PEGELOW, D. F., NICKELE, G. A., NELSON, W. B. & DEMPSEY, J. A. 1997. Respiratory muscle work compromises leg blood flow during maximal exercise. *Journal of Applied Physiology,* 82**,** 1573-1583.

HARRIS, E., RAKOBOWCHUK, M. & BIRCH, K. M. 2014. Sprint Interval and Sprint Continuous Training Increases Circulating CD34+ Cells and Cardio-Respiratory Fitness in Young Healthy Women. *PLOS ONE,* 9**,** e108720.

HARRIS, R. A., NISHIYAMA, S. K., WRAY, D. W. & RICHARDSON, R. S. 2010. Ultrasound assessment of flow-mediated dilation. *Hypertension,* 55**,** 1075-85.

HARRIS, R. A., PADILLA, J., HANLON, K. P., RINK, L. D. & WALLACE, J. P. 2008. The flow-mediated dilation response to acute exercise in overweight active and inactive men. *Obesity,* 16**,** 578-584.

HARVEY, P. J., PICTON, P. E., SU, W. S., MORRIS, B. L., NOTARIUS, C. F. & FLORAS, J. S. 2005. Exercise as an alternative to oral estrogen for amelioration of endothelial dysfunction in postmenopausal women. *American heart journal,* 149**,** 291-297.

HASHIMOTO, M., AKISHITA, M., ETO, M., ISHIKAWA, M., KOZAKI, K., TOBA, K., SAGARA, Y., TAKETANI, Y., ORIMO, H. & OUCHI, Y. 1995. Modulation of endothelium-dependent flow-mediated dilatation of the brachial artery by sex and menstrual cycle. *Circulation,* 92**,** 3431-5.

HATTORI, K., HEISSIG, B., TASHIRO, K., HONJO, T., TATENO, M., SHIEH, J.-H., HACKETT, N. R., QUITORIANO, M. S., CRYSTAL, R. G. & RAFII, S. 2001. Plasma elevation of stromal cell–derived factor-1 induces mobilization of mature and immature hematopoietic progenitor and stem cells. *Blood, The Journal of the American Society of Hematology,* 97**,** 3354-3360.

HAYNES, M. P., SINHA, D., RUSSELL, K. S., COLLINGE, M., FULTON, D., MORALES-RUIZ, M., SESSA, W. C. & BENDER, J. R. 2000. Membrane estrogen receptor engagement activates endothelial nitric oxide synthase via the PI3-kinase–Akt pathway in human endothelial cells. *Circulation research,* 87**,** 677-682.

HEESCHEN, C., LEHMANN, R., HONOLD, J., ASSMUS, B., AICHER, A., WALTER, D. H., MARTIN, H., ZEIHER, A. M. & DIMMELER, S. 2004. Profoundly reduced neovascularization capacity of bone marrow mononuclear cells derived from patients with chronic ischemic heart disease. *Circulation,* 109**,** 1615-22.

HEISS, C., JAHN, S., TAYLOR, M., REAL, W. M., ANGELI, F. S., WONG, M. L., AMABILE, N., PRASAD, M., RASSAF, T., OTTAVIANI, J. I., MIHARDJA, S., KEEN, C. L., SPRINGER, M. L., BOYLE, A., GROSSMAN, W., GLANTZ, S. A., SCHROETER, H. & YEGHIAZARIANS, Y. 2010. Improvement of endothelial function with dietary flavanols is associated with mobilization of circulating angiogenic cells in patients with coronary artery disease. *J Am Coll Cardiol,* 56**,** 218-24.

HEISS, C., KEYMEL, S., NIESLER, U., ZIEMANN, J., KELM, M. & KALKA, C. 2005. Impaired progenitor cell activity in age-related endothelial dysfunction. *J Am Coll Cardiol,* 45**,** 1441-8.

HEISSIG, B., HATTORI, K., DIAS, S., FRIEDRICH, M., FERRIS, B., HACKETT, N. R., CRYSTAL, R. G., BESMER, P., LYDEN, D. & MOORE, M. A. 2002. Recruitment of stem and progenitor cells from the bone marrow niche requires MMP-9 mediated release of kit-ligand. *Cell,* 109**,** 625-637.

HIGASHI, Y. & YOSHIZUMI, M. 2004. Exercise and endothelial function: role of endothelium-derived nitric oxide and oxidative stress in healthy subjects and hypertensive patients. *Pharmacol Ther,* 102**,** 87-96.

HIRAI, D. M., MUSCH, T. I. & POOLE, D. C. 2015. Exercise training in chronic heart failure: improving skeletal muscle O2 transport and utilization. *American Journal of Physiology-Heart and Circulatory Physiology,* 309**,** H1419-H1439.

HITOSUGI, M., KAWATO, H., NAGAI, T., OGAWA, Y., NIWA, M., IIDA, N., YUFU, T. & TOKUDOME, S. 2004. Changes in Blood Viscosity with Heavy and Light Exercise. *Medicine, Science and the Law,* 44**,** 197-200.

HODGSON, M. D., KEIR, D. A., COPITHORNE, D. B., RICE, C. L. & KOWALCHUK, J. M. 2018. Power reserve following ramp-incremental cycling to exhaustion: implications for muscle fatigue and function. *Journal of Applied Physiology,* 125**,** 304-312.

HØIER, B., OLSEN, K., NYBERG, M., BANGSBO, J. & HELLSTEN, Y. 2010. Contraction-induced secretion of VEGF from skeletal muscle cells is mediated by adenosine. *American Journal of Physiology-Heart and Circulatory Physiology,* 299**,** H857-H862.

HOUSTIS, N. E., EISMAN, A. S., PAPPAGIANOPOULOS, P. P., WOOSTER, L., BAILEY, C. S., WAGNER, P. D. & LEWIS, G. D. 2018. Exercise Intolerance in Heart Failure With Preserved Ejection Fraction: Diagnosing and Ranking Its Causes Using Personalized O(2) Pathway Analysis. *Circulation,* 137**,** 148-161.

HU, X., TANG, M., FISHER, A. B., OLASHAW, N. & ZUCKERMAN, K. S. 1999. TNF-alpha-induced growth suppression of CD34+ myeloid leukemic cell lines signals through TNF receptor type I and is associated with NF-kappa B activation. *J Immunol,* 163**,** 3106-15.

HUBERT, L., DARBOUSSET, R., PANICOT-DUBOIS, L., ROBERT, S., SABATIER, F., FALLAGUE, K., DIGNAT-GEORGE, F. & DUBOIS, C. 2014. Neutrophils recruit and activate human endothelial colony-forming cells at the site of vessel injury via P-selectin glycoprotein ligand-1 and L-selectin. *Journal of Thrombosis and Haemostasis,* 12**,** 1170-1181.

HUDLICKA, O. & BROWN, M. D. 2009. Adaptation of skeletal muscle microvasculature to increased or decreased blood flow: role of shear stress, nitric oxide and vascular endothelial growth factor. *J Vasc Res,* 46**,** 504-12.

HUNDLEY, W. G., BAYRAM, E., HAMILTON, C. A., HAMILTON, E. A., MORGAN, T. M., DARTY, S. N., STEWART, K. P., LINK, K. M., HERRINGTON, D. M. & KITZMAN, D. W. 2007. Leg flow-mediated arterial dilation in elderly patients with heart failure and normal left

ventricular ejection fraction. *American Journal of Physiology-Heart and Circulatory Physiology,* 292**,** H1427-H1434.

HUNT, J. E. A., GALEA, D., TUFFT, G., BUNCE, D. & FERGUSON, R. A. 2013. Time course of regional vascular adaptations to low load resistance training with blood flow restriction. *Journal of Applied Physiology,* 115**,** 403-411.

HUNT, J. E. A., STODART, C. & FERGUSON, R. A. 2016. The influence of participant characteristics on the relationship between cuff pressure and level of blood flow restriction. *European journal of applied physiology,* 116**,** 1421-1432.

HUNT, J. E. A., WALTON, L. A. & FERGUSON, R. A. 2012. Brachial artery modifications to blood flow-restricted handgrip training and detraining. *Journal of Applied Physiology,* 112**,** 956-961.

HWANG, I.-C., KIM, K.-H., CHOI, W.-S., KIM, H.-J., IM, M.-S., KIM, Y.-J., KIM, S.-H., KIM, M.-A., SOHN, D.-W. & ZO, J.-H. 2012. Impact of acute exercise on brachial artery flow-mediated dilatation in young healthy people. *Cardiovascular ultrasound,* 10**,** 1-12.

IIDA, H., KURANO, M., TAKANO, H., KUBOTA, N., MORITA, T., MEGURO, K., SATO, Y., ABE, T., YAMAZAKI, Y., UNO, K., TAKENAKA, K., HIROSE, K. & NAKAJIMA, T. 2007. Hemodynamic and neurohumoral responses to the restriction of femoral blood flow by KAATSU in healthy subjects. *Eur J Appl Physiol,* 100**,** 275-85.

IIDA, H., NAKAJIMA, T., KURANO, M., YASUDA, T., SAKAMAKI, M., SATO, Y., YAMASOBA, T. & ABE, T. 2011. Effects of walking with blood flow restriction on limb venous compliance in elderly subjects. *Clin Physiol Funct Imaging,* 31**,** 472-6.

IIDA, H., TAKANO, H., MEGURO, K., ASADA, K., OONUMA, H., MORITA, T., KURANO, M., SAKAGAMI, F., UNO, K., HIROSE, K., NAGATA, T., TAKENAKA, K., SUZUKI, J., HIRATA, Y., FURUICHI, T., ETO, F., NAGAI, R., SATO, Y. & NAKAJIMA, T. 2005. Hemodynamic and autonomic nervous responses to the restriction of femoral blood flow by KAATSU. *International Journal of KAATSU Training Research,* 1**,** 57-64.

INABA, Y., CHEN, J. A. & BERGMANN, S. R. 2010. Prediction of future cardiovascular outcomes by flow-mediated vasodilatation of brachial artery: a meta-analysis. *Int J Cardiovasc Imaging,* 26**,** 631-40.

IVERSEN, P. O., WOLDBAEK, P. R., TØNNESSEN, T. & CHRISTENSEN, G. 2002. Decreased hematopoiesis in bone marrow of mice with congestive heart failure. *Am J Physiol Regul Integr Comp Physiol,* 282**,** R166-72.

IWAKURA, A., LUEDEMANN, C., SHASTRY, S., HANLEY, A., KEARNEY, M., AIKAWA, R., ISNER, J. M., ASAHARA, T. & LOSORDO, D. W. 2003. Estrogen-mediated, endothelial nitric oxide synthase-dependent mobilization of bone marrow-derived endothelial progenitor cells contributes to reendothelialization after arterial injury. *Circulation,* 108**,** 3115-21.

JENKINS, N. T., PADILLA, J., BOYLE, L. J., CREDEUR, D. P., LAUGHLIN, M. H. & FADEL, P. J. 2013. Disturbed blood flow acutely induces activation and apoptosis of the human vascular endothelium. *Hypertension,* 61**,** 615-21.

JOHNSON, P. C. 2008. Overview of the Microcirculation. *In:* TUMA, R. F., DURÁN, W. N. & LEY, K. (eds.) *Microcirculation (Second Edition).* San Diego: Academic Press.

JONES, A. M., BURNLEY, M., BLACK, M. I., POOLE, D. C. & VANHATALO, A. 2019. The maximal metabolic steady state: redefining the 'gold standard'. *Physiological Reports,* 7**,** e14098.

JONES, A. M. & VANHATALO, A. 2017. The 'Critical Power' Concept: Applications to Sports Performance with a Focus on Intermittent High-Intensity Exercise. *Sports medicine (Auckland, N.Z.),* 47**,** 65-78.

JONES, A. M., WILKERSON, D. P., DIMENNA, F., FULFORD, J. & POOLE, D. C. 2008. Muscle metabolic responses to exercise above and below the "critical power" assessed using 31P-MRS. *Am J Physiol Regul Integr Comp Physiol,* 294**,** R585-93.

JONES, H., GREEN, D. J., GEORGE, K. & ATKINSON, G. 2010. Intermittent exercise abolishes the diurnal variation in endothelial-dependent flow-mediated dilation in humans. *American Journal of Physiology-Regulatory, Integrative and Comparative Physiology,* 298**,** R427-R432.

JOSHI, S., MAHONEY, S., JAHAN, J., PITTS, L., HACKNEY, K. J. & JARAJAPU, Y. P. 2020. Blood flow restriction exercise stimulates mobilization of hematopoietic stem/progenitor cells and increases the circulating ACE2 levels in healthy adults. *Journal of Applied Physiology,* 128**,** 1423-1431.

JOYNER, M. J. & CASEY, D. P. 2015. Regulation of increased blood flow (hyperemia) to muscles during exercise: a hierarchy of competing physiological needs. *Physiological reviews,* 95**,** 549-601.

JOYNER, M. J. & GREEN, D. J. 2009. Exercise protects the cardiovascular system: effects beyond traditional risk factors. *The Journal of Physiology,* 587**,** 5551-5558.

JUONALA, M., VIIKARI, J. S. A., LAITINEN, T., MARNIEMI, J., HELENIUS, H., RÖNNEMAA, T. & RAITAKARI, O. T. 2004. Interrelations Between Brachial Endothelial Function and Carotid Intima-Media Thickness in Young Adults. *Circulation,* 110**,** 2918-2923.

KACIN, A., ROSENBLATT, B., ŽARGI, T. G. & BISWAS, A. 2015. Safety considerations with blood flow restricted resistance training. *Annales Kinesiologiae,* 6**,** 3-26.

KAGAYA, A. & OGITA, F. 1992. Blood flow during muscle contraction and relaxation in rhythmic exercise at different intensities. *The Annals of physiological anthropology,* 11**,** 251-256.

KAIJSER, L., SUNDBERG, C. J., EIKEN, O., NYGREN, A., ESBJÖRNSSON, M., SYLVÉN, C. & JANSSON, E. 1990. Muscle oxidative capacity and work performance after training under local leg ischemia. *J Appl Physiol (1985),* 69**,** 785-7.

KATAYAMA, Y., BATTISTA, M., KAO, W.-M., HIDALGO, A., PEIRED, A. J., THOMAS, S. A. & FRENETTE, P. S. 2006. Signals from the Sympathetic Nervous System Regulate Hematopoietic Stem Cell Egress from Bone Marrow. *Cell,* 124**,** 407-421.

KATZ, S. D., KHAN, T., ZEBALLOS, G. A., MATHEW, L., POTHARLANKA, P., KNECHT, M. & WHELAN, J. 1999. Decreased activity of the L-arginine-nitric oxide metabolic pathway in patients with congestive heart failure. *Circulation,* 99**,** 2113-7.

KATZ, S. D., KRUM, H., KHAN, T. & KNECHT, M. 1996. Exercise-induced vasodilation in forearm circulation of normal subjects and patients with congestive heart failure: Role of endothelium-derived nitric oxide. *Journal of the American College of Cardiology,* 28**,** 585-590.

KERAMIDAS, M. E., KOUNALAKIS, S. N. & GELADAS, N. D. 2012. The effect of interval training combined with thigh cuffs pressure on maximal and submaximal exercise performance. *Clinical physiology and functional imaging,* 32**,** 205-213.

KETEYIAN, S. J., PATEL, M., KRAUS, W. E., BRAWNER, C. A., MCCONNELL, T. R., PIÑA, I. L., LEIFER, E. S., FLEG, J. L., BLACKBURN, G., FONAROW, G. C., CHASE, P. J., PINER, L., VEST, M., O'CONNOR, C. M., EHRMAN, J. K., WALSH, M. N., EWALD, G., BENSIMHON, D. & RUSSELL, S. D. 2016. Variables Measured During Cardiopulmonary Exercise Testing as Predictors of Mortality in Chronic Systolic Heart Failure. *Journal of the American College of Cardiology,* 67**,** 780-789.

KIM, D., SINGH, H., LOENNEKE, J. P., THIEBAUD, R. S., FAHS, C. A., ROSSOW, L. M., YOUNG, K., SEO, D. I., BEMBEN, D. A. & BEMBEN, M. G. 2016. Comparative Effects of Vigorous-Intensity and Low-Intensity Blood Flow Restricted Cycle Training and Detraining on Muscle Mass, Strength, and Aerobic Capacity. *J Strength Cond Res,* 30**,** 1453-61.

KIM, W., JEONG, M. H., CHO, S. H., YUN, J. H., CHAE, H. J., AHN, Y. K., LEE, M. C., CHENG, X., KONDO, T., MUROHARA, T. & KANG, J. C. 2006. Effect of green tea consumption on endothelial function and circulating endothelial progenitor cells in chronic smokers. *Circ J,* 70**,** 1052-7.

KIMURA, M., UEDA, K., GOTO, C., JITSUIKI, D., NISHIOKA, K., UMEMURA, T., NOMA, K., YOSHIZUMI, M., CHAYAMA, K. & HIGASHI, Y. 2007. Repetition of Ischemic Preconditioning Augments Endothelium-Dependent Vasodilation in Humans. *Arteriosclerosis, Thrombosis, and Vascular Biology,* 27**,** 1403-1410.

KINDIG, C. A., MUSCH, T. I., BASARABA, R. J. & POOLE, D. C. 1999. Impaired capillary hemodynamics in skeletal muscle of rats in chronic heart failure. *Journal of Applied Physiology,* 87**,** 652-660.

KOBAYASHI, K., AKISHITA, M., YU, W., HASHIMOTO, M., OHNI, M. & TOBA, K. 2004. Interrelationship between non-invasive measurements of atherosclerosis: flow-mediated dilation of brachial artery, carotid intima-media thickness and pulse wave velocity. *Atherosclerosis,* 173**,** 13-8.

KODAMA, S., SAITO, K., TANAKA, S., MAKI, M., YACHI, Y., ASUMI, M., SUGAWARA, A., TOTSUKA, K., SHIMANO, H., OHASHI, Y., YAMADA, N. & SONE, H. 2009. Cardiorespiratory fitness as a quantitative predictor of all-cause mortality and cardiovascular events in healthy men and women: a meta-analysis. *JAMA,* 301**,** 2024-35.

KOJDA, G. & HAMBRECHT, R. 2005. Molecular mechanisms of vascular adaptations to exercise. Physical activity as an effective antioxidant therapy? *Cardiovasc Res,* 67**,** 187-97.

KOLLER, L., HOHENSINNER, P., SULZGRUBER, P., BLUM, S., MAURER, G., WOJTA, J., HULSMANN, M. & NIESSNER, A. 2016. Prognostic

relevance of circulating endothelial progenitor cells in patients with chronic heart failure. *Thromb Haemost,* 116**,** 309-16.

KORTHUIS, R. J. Skeletal muscle circulation. Colloquium Series on Integrated Systems Physiology: From Molecule to Function, 2011. Morgan & Claypool Life Sciences, 1-144.

KORZENIEWSKI, B. & ROSSITER, H. B. 2020. Exceeding a "critical" muscle P(i): implications for [Formula: see text] and metabolite slow components, muscle fatigue and the power-duration relationship. *Eur J Appl Physiol,* 120**,** 1609-1619.

KOUREK, C., KARATZANOS, E., PSARRA, K., NTALIANIS, A., MITSIOU, G., DELIS, D., LINARDATOU, V., PITTARAS, T., VASILEIADIS, I., DIMOPOULOS, S. & NANAS, S. 2020. Endothelial progenitor cells mobilization after maximal exercise in patients with chronic heart failure. *Hellenic Journal of Cardiology*.

KRÜGER, K., PILAT, C., SCHILD, M., LINDNER, N., FRECH, T., MUDERS, K. & MOOREN, F. 2015. Progenitor cell mobilization after exercise is related to systemic levels of G-CSF and muscle damage. *Scandinavian journal of medicine & science in sports,* 25**,** e283-e291.

KRUGER, R. L., ABOODARDA, S. J., JAIMES, L. M., SAMOZINO, P. & MILLET, G. Y. 2019. Cycling Performed on an Innovative Ergometer at Different Intensities-Durations in Men: Neuromuscular Fatigue and Recovery Kinetics. *Appl Physiol Nutr Metab*.

KUBO, S. H., RECTOR, T. S., BANK, A. J., WILLIAMS, R. E. & HEIFETZ, S. M. 1991. Endothelium-dependent vasodilation is attenuated in patients with heart failure. *Circulation,* 84**,** 1589-96.

LAMARRA, N., WHIPP, B. J., WARD, S. A. & WASSERMAN, K. 1987. Effect of interbreath fluctuations on characterizing exercise gas exchange kinetics. *J Appl Physiol (1985),* 62**,** 2003-12.

LANDMESSER, U., ENGBERDING, N., BAHLMANN, F. H., SCHAEFER, A., WIENCKE, A., HEINEKE, A., SPIEKERMANN, S., HILFIKER-KLEINER, D., TEMPLIN, C., KOTLARZ, D., MUELLER, M., FUCHS, M., HORNIG, B., HALLER, H. & DREXLER, H. 2004. Statin-induced improvement of endothelial progenitor cell mobilization, myocardial neovascularization, left ventricular function, and survival after experimental myocardial infarction requires endothelial nitric oxide synthase. *Circulation,* 110**,** 1933-9.

LANDMESSER, U., SPIEKERMANN, S., DIKALOV, S., TATGE, H., WILKE, R., KOHLER, C., HARRISON, D. G., HORNIG, B. & DREXLER, H. 2002. Vascular Oxidative Stress and Endothelial Dysfunction in Patients With Chronic Heart Failure. *Circulation,* 106**,** 3073-3078.

LANSFORD, K. A., SHILL, D. D., DICKS, A. B., MARSHBURN, M. P., SOUTHERN, W. M. & JENKINS, N. T. 2016. Effect of acute exercise on circulating angiogenic cell and microparticle populations. *Exp Physiol,* 101**,** 155-67.

LAPIDOT, T. & PETIT, I. 2002. Current understanding of stem cell mobilization: the roles of chemokines, proteolytic enzymes, adhesion molecules, cytokines, and stromal cells. *Exp Hematol,* 30**,** 973-81.

LARKIN, K. A., MACNEIL, R. G., DIRAIN, M., SANDESARA, B., MANINI, T. M. & BUFORD, T. W. 2012. Blood flow restriction enhances post-resistance exercise angiogenic gene expression. *Med Sci Sports Exerc,* 44**,** 2077-83.

LAUFS, U., URHAUSEN, A., WERNER, N., SCHARHAG, J., HEITZ, A., KISSNER, G., BÖHM, M., KINDERMANN, W. & NICKENIG, G. 2005. Running exercise of different duration and intensity: effect on endothelial progenitor cells in healthy subjects. *European journal of cardiovascular prevention and rehabilitation,* 12**,** 407-414.

LAUFS, U., WERNER, N., LINK, A., ENDRES, M., WASSMANN, S., JÜRGENS, K., MICHE, E., BÖHM, M. & NICKENIG, G. 2004. Physical Training Increases Endothelial Progenitor Cells, Inhibits Neointima Formation, and Enhances Angiogenesis. *Circulation,* 109**,** 220-226.

LAUGHLIN, M. H., NEWCOMER, S. C. & BENDER, S. B. 2008. Importance of hemodynamic forces as signals for exercise-induced changes in endothelial cell phenotype. *J Appl Physiol (1985),* 104**,** 588-600.

LEICK, L., HELLSTEN, Y., FENTZ, J., LYNGBY, S. S., WOJTASZEWSKI, J. F. P., HIDALGO, J. & PILEGAARD, H. 2009. PGC-1α mediates exercise-induced skeletal muscle VEGF expression in mice. *American Journal of Physiology-Endocrinology and Metabolism,* 297**,** E92-E103.

LENK, K., UHLEMANN, M., SCHULER, G. & ADAMS, V. 2011. Role of endothelial progenitor cells in the beneficial effects of physical exercise on atherosclerosis and coronary artery disease. *Journal of Applied Physiology,* 111**,** 321-328.

LEONE, A. M., VALGIMIGLI, M., GIANNICO, M. B., ZACCONE, V., PERFETTI, M., D'AMARIO, D., REBUZZI, A. G. & CREA, F. 2009. From bone marrow to the arterial wall: the ongoing tale of endothelial progenitor cells. *European heart journal,* 30**,** 890-899.

LEPERS, R., MAFFIULETTI, N. A., ROCHETTE, L., BRUGNIAUX, J. & MILLET, G. Y. 2002. Neuromuscular fatigue during a long-duration cycling exercise. *J Appl Physiol (1985),* 92**,** 1487-93.

LERMAN, A. & ZEIHER, A. M. 2005. Endothelial Function. *Circulation,* 111**,** 363-368.

LEVICK, J. R. 2012. *An Introduction to Cardiovascular Physiology 5E*, Hodder Education.

LIN, R.-Z., MORENO-LUNA, R., LI, D., JAMINET, S.-C., GREENE, A. K. & MELERO-MARTIN, J. M. 2014. Human endothelial colony-forming cells serve as trophic mediators for mesenchymal stem cell engraftment via paracrine signaling. *Proceedings of the National Academy of Sciences,* 111**,** 10137-10142.

LOCKARD, M. M., WITKOWSKI, S., JENKINS, N. T., SPANGENBURG, E. E., OBISESAN, T. O. & HAGBERG, J. M. 2010. Thrombin and exercise similarly influence expression of cell cycle genes in cultured putative endothelial progenitor cells. *Journal of applied physiology (Bethesda, Md. : 1985),* 108**,** 1682-1690.

LOENNEKE, J. P., FAHS, C. A., ROSSOW, L. M., SHERK, V. D., THIEBAUD, R. S., ABE, T., BEMBEN, D. A. & BEMBEN, M. G. 2012. Effects of cuff width on arterial occlusion: implications for blood flow restricted exercise. *Eur J Appl Physiol,* 112**,** 2903-12.

LUSIS, A. J. 2000. Atherosclerosis. *Nature,* 407**,** 233-241.

LYALL, G. K., DAVIES, M. J., FERGUSON, C., PORTER, K. E. & BIRCH, K. M. 2019. In-exercise vascular shear rate during acute continuous and interval exercise: impact on endothelial function and miR-21. *Journal of Applied Physiology,* 127**,** 1754-1762.

MACINNIS, M. J. & GIBALA, M. J. 2017. Physiological adaptations to interval training and the role of exercise intensity. *The Journal of Physiology,* 595**,** 2915-2930.

MAJESKY, M. W., DONG, X. R., HOGLUND, V., MAHONEY, W. M. & DAUM, G. 2011. The Adventitia. *Arteriosclerosis, Thrombosis, and Vascular Biology,* 31**,** 1530-1539.

MANCINI, D. M., WALTER, G., REICHEK, N., LENKINSKI, R., MCCULLY, K. K., MULLEN, J. L. & WILSON, J. R. 1992. Contribution of skeletal muscle atrophy to exercise intolerance and altered muscle metabolism in heart failure. *Circulation,* 85**,** 1364-73.

MANINI, T. M. & CLARK, B. C. 2009. Blood flow restricted exercise and skeletal muscle health. *Exerc Sport Sci Rev,* 37**,** 78-85.

MARCORA, S. M. & STAIANO, W. 2010. The limit to exercise tolerance in humans: mind over muscle? *Eur J Appl Physiol,* 109**,** 763-70.

MARTI, C. N., GHEORGHIADE, M., KALOGEROPOULOS, A. P., GEORGIOPOULOU, V. V., QUYYUMI, A. A. & BUTLER, J. 2012. Endothelial Dysfunction, Arterial Stiffness, and Heart Failure. *Journal of the American College of Cardiology,* 60**,** 1455-1469.

MATSUZAWA, Y., KWON, T. G., LENNON, R. J., LERMAN, L. O. & LERMAN, A. 2015. Prognostic Value of Flow-Mediated Vasodilation in Brachial Artery and Fingertip Artery for Cardiovascular Events: A Systematic Review and Meta-Analysis. *J Am Heart Assoc,* 4.

MCMURRAY, J. J. & STEWART, S. 2000. Epidemiology, aetiology, and prognosis of heart failure. *Heart,* 83**,** 596-602.

MEDBØ, J. I. & BURGERS, S. 1990. Effect of training on the anaerobic capacity. *Med Sci Sports Exerc,* 22**,** 501-7.

MEDINA, R. J., BARBER, C. L., SABATIER, F., DIGNAT-GEORGE, F., MELERO-MARTIN, J. M., KHOSROTEHRANI, K., OHNEDA, O., RANDI, A. M., CHAN, J. K. Y., YAMAGUCHI, T., VAN HINSBERGH, V. W. M., YODER, M. C. & STITT, A. W. 2017. Endothelial Progenitors: A Consensus Statement on Nomenclature. *Stem Cells Transl Med,* 6**,** 1316-1320.

METTAUER, B., LAMPERT, E., PETITJEAN, P., BOGUI, P., EPAILLY, E., SCHNEDECKER, B., GENY, B., EISENMANN, B., HABEREY, P. & LONSDORFER, J. 1996. Persistent exercise intolerance following cardiac transplantation despite normal oxygen transport. *Int J Sports Med,* 17**,** 277-86.

MEZZANI, A., GRASSI, B., JONES, A. M., GIORDANO, A., CORRA, U., PORCELLI, S., DELLA BELLA, S., TADDEO, A. & GIANNUZZI, P. 2013. Speeding of pulmonary VO2 on-kinetics by light-to-moderate-intensity aerobic exercise training in chronic heart failure: clinical and pathophysiological correlates. *Int J Cardiol,* 167**,** 2189-95.

MHEID, I. A., CORRIGAN, F., SHIRAZI, F., VELEDAR, E., LI, Q., ALEXANDER, W. R., TAYLOR, W. R., WALLER, E. K. & QUYYUMI, A. A. 2014. Circadian Variation in Vascular Function and Regenerative Capacity in Healthy Humans. *Journal of the American Heart Association,* 3**,** e000845.

MICHELL, B., GRIFFITHS, J., MITCHELHILL, K., RODRIGUEZ-CRESPO, I., TIGANIS, T., BOZINOVSKI, S., DE MONTELLANO, P. O., KEMP, B. & PEARSON, R. 1999. The Akt kinase signals directly to endothelial nitric oxide synthase. *Current biology,* 9**,** 845-S1.

MICHOWITZ, Y., GOLDSTEIN, E., WEXLER, D., SHEPS, D., KEREN, G. & GEORGE, J. 2007. Circulating endothelial progenitor cells and clinical outcome in patients with congestive heart failure. *Heart,* 93**,** 1046-50.

MILANOVIĆ, Z., SPORIŠ, G. & WESTON, M. 2015. Effectiveness of High-Intensity Interval Training (HIT) and Continuous Endurance Training for VO2max Improvements: A Systematic Review and Meta-Analysis of Controlled Trials. *Sports Med,* 45**,** 1469-81.

MILLET, G. Y., MARTIN, V., MARTIN, A. & VERGÈS, S. 2011. Electrical stimulation for testing neuromuscular function: from sport to pathology. *European journal of applied physiology,* 111**,** 2489-2500.

MITCHELL, E. A., MARTIN, N. R. W., TURNER, M. C., TAYLOR, C. W. & FERGUSON, R. A. 2019. The combined effect of sprint interval training and blood flow restriction on critical power, capillary growth and mitochondrial proteins in trained cyclists. *Journal of Applied Physiology,* 0**,** null.

MITCHELL, J. H., KAUFMAN, M. P. & IWAMOTO, G. A. 1983. The exercise pressor reflex: its cardiovascular effects, afferent mechanisms, and central pathways. *Annu Rev Physiol,* 45**,** 229-42.

MÖBIUS-WINKLER, S., HILBERG, T., MENZEL, K., GOLLA, E., BURMAN, A., SCHULER, G. & ADAMS, V. 2009. Time-dependent mobilization of circulating progenitor cells during strenuous exercise in healthy individuals. *J Appl Physiol (1985),* 107**,** 1943-50.

MOHOLDT, T. T., AMUNDSEN, B. H., RUSTAD, L. A., WAHBA, A., LØVØ, K. T., GULLIKSTAD, L. R., BYE, A., SKOGVOLL, E., WISLØFF, U. & SLØRDAHL, S. A. 2009. Aerobic interval training versus continuous moderate exercise after coronary artery bypass surgery: a randomized study of cardiovascular effects and quality of life. *Am Heart J,* 158**,** 1031-7.

MOHRI, M., EGASHIRA, K., TAGAWA, T., KUGA, T., TAGAWA, H., HARASAWA, Y., SHIMOKAWA, H. & TAKESHITA, A. 1997. Basal Release of Nitric Oxide Is Decreased in the Coronary Circulation in Patients With Heart Failure. *Hypertension,* 30**,** 50-56.

MOLMEN-HANSEN, H. E., STOLEN, T., TJONNA, A. E., AAMOT, I. L., EKEBERG, I. S., TYLDUM, G. A., WISLOFF, U., INGUL, C. B. & STOYLEN, A. 2012. Aerobic interval training reduces blood pressure and improves myocardial function in hypertensive patients. *Eur J Prev Cardiol,* 19**,** 151-60.

MONTERO, D., PIERCE, G. L., STEHOUWER, C. D., PADILLA, J. & THIJSSEN, D. H. 2015. The impact of age on vascular smooth muscle function in humans. *J Hypertens,* 33**,** 445-53; discussion 453.

MONTGOMERY, R., PATERSON, A., WILLIAMSON, C., FLORIDA-JAMES, G. & ROSS, M. D. 2019. Blood Flow Restriction Exercise Attenuates the Exercise-Induced Endothelial Progenitor Cell Response in Healthy, Young Men. *Front Physiol,* 10**,** 447.

MORA, S., COOK, N., BURING, J. E., RIDKER, P. M. & LEE, I. M. 2007. Physical activity and reduced risk of cardiovascular events: potential mediating mechanisms. *Circulation,* 116**,** 2110-8.

MORALES-ALAMO, D., LOSA-REYNA, J., TORRES-PERALTA, R., MARTIN-RINCON, M., PEREZ-VALERA, M., CURTELIN, D., PONCE-GONZÁLEZ, J. G., SANTANA, A. & CALBET, J. A. L. 2015. What limits

performance during whole-body incremental exercise to exhaustion in humans? *The Journal of Physiology,* 593**,** 4631-4648.

MORICI, G., ZANGLA, D., SANTORO, A., PELOSI, E., PETRUCCI, E., GIOIA, M., BONANNO, A., PROFITA, M., BELLIA, V., TESTA, U. & BONSIGNORE, M. R. 2005. Supramaximal exercise mobilizes hematopoietic progenitors and reticulocytes in athletes. *Am J Physiol Regul Integr Comp Physiol,* 289**,** R1496-503.

MORRIS, S. B. 2008. Estimating effect sizes from pretest-posttest-control group designs. *Organizational research methods,* 11**,** 364-386.

MORTENSEN, S. P., DAMSGAARD, R., DAWSON, E. A., SECHER, N. H. & GONZÁLEZ-ALONSO, J. 2008. Restrictions in systemic and locomotor skeletal muscle perfusion, oxygen supply and VO2 during high-intensity whole-body exercise in humans. *The Journal of physiology,* 586**,** 2621-2635.

MORTENSEN, S. P., GONZÁLEZ-ALONSO, J., DAMSGAARD, R., SALTIN, B. & HELLSTEN, Y. 2007. Inhibition of nitric oxide and prostaglandins, but not endothelial-derived hyperpolarizing factors, reduces blood flow and aerobic energy turnover in the exercising human leg. *J Physiol,* 581**,** 853-61.

MOSER, D. K., YAMOKOSKI, L., SUN, J. L., CONWAY, G. A., HARTMAN, K. A., GRAZIANO, J. A., BINANAY, C. & STEVENSON, L. W. 2009. Improvement in Health-related Quality of Life After Hospitalization Predicts Event-free Survival in Patients With Advanced Heart Failure. *Journal of Cardiac Failure,* 15**,** 763-769.

MOUSER, J. G., ADE, C. J., BLACK, C. D., BEMBEN, D. A. & BEMBEN, M. G. 2018. Brachial blood flow under relative levels of blood flow restriction is decreased in a nonlinear fashion. *Clin Physiol Funct Imaging,* 38**,** 425-430.

MOUSER, J. G., DANKEL, S. J., JESSEE, M. B., MATTOCKS, K. T., BUCKNER, S. L., COUNTS, B. R. & LOENNEKE, J. P. 2017. A tale of three cuffs: the hemodynamics of blood flow restriction. *Eur J Appl Physiol,* 117**,** 1493-1499.

MUTHUSAMY, V. R., KANNAN, S., SADHAASIVAM, K., GOUNDER, S. S., DAVIDSON, C. J., BOEHEME, C., HOIDAL, J. R., WANG, L. & RAJASEKARAN, N. S. 2012. Acute exercise stress activates Nrf2/ARE signaling and promotes antioxidant mechanisms in the myocardium. *Free Radical Biology and Medicine,* 52**,** 366-376.

MYERS, J., ARENA, R., OLIVEIRA, R. B., BENSIMHON, D., HSU, L., CHASE, P., GUAZZI, M., BRUBAKER, P., MOORE, B., KITZMAN, D. & PEBERDY, M. A. 2009. The lowest VE/VCO2 ratio during exercise as a predictor of outcomes in patients with heart failure. *J Card Fail,* 15**,** 756-62.

MYERS, J., PRAKASH, M., FROELICHER, V., DO, D., PARTINGTON, S. & ATWOOD, J. E. 2002. Exercise capacity and mortality among men referred for exercise testing. *N Engl J Med,* 346**,** 793-801.

NEUNTEUFL, T., KATZENSCHLAGER, R., HASSAN, A., KLAAR, U., SCHWARZACHER, S., GLOGAR, D., BAUER, P. & WEIDINGER, F. 1997. Systemic endothelial dysfunction is related to the extent and severity of coronary artery disease. *Atherosclerosis,* 129**,** 111-8.

NEWMAN, A. B., SIMONSICK, E. M., NAYDECK, B. L., BOUDREAU, R. M., KRITCHEVSKY, S. B., NEVITT, M. C., PAHOR, M., SATTERFIELD,

S., BRACH, J. S., STUDENSKI, S. A. & HARRIS, T. B. 2006. Association of long-distance corridor walk performance with mortality, cardiovascular disease, mobility limitation, and disability. *Jama,* 295**,** 2018-26.

NIEMIRO, G. M., ALLEN, J. M., MAILING, L. J., KHAN, N. A., HOLSCHER, H. D., WOODS, J. A. & DE LISIO, M. 2018. Effects of endurance exercise training on inflammatory circulating progenitor cell content in lean and obese adults. *J Physiol,* 596**,** 2811-2822.

NIEMIRO, G. M., PAREL, J., BEALS, J., VAN VLIET, S., PALUSKA, S. A., MOORE, D. R., BURD, N. A. & DE LISIO, M. 2017. Kinetics of circulating progenitor cell mobilization during submaximal exercise. *J Appl Physiol (1985),* 122**,** 675-682.

NOLLET, E., HOYMANS, V. Y., RODRIGUS, I. R., DE BOCK, D., DOM, M., VANASSCHE, B., VAN HOOF, V. O. M., COOLS, N., VAN ACKEREN, K., WOUTERS, K., VERMEULEN, K., VRINTS, C. J. & VAN CRAENENBROECK, E. M. 2016. Bone Marrow-Derived Progenitor Cells Are Functionally Impaired in Ischemic Heart Disease. *Journal of cardiovascular translational research,* 9**,** 266-278.

NYBERG, M., MORTENSEN, S. P., THANING, P., SALTIN, B. & HELLSTEN, Y. 2010. Interstitial and Plasma Adenosine Stimulate Nitric Oxide and Prostacyclin Formation in Human Skeletal Muscle. *Hypertension,* 56**,** 1102-1108.

O'BRIEN, M. W., JOHNS, J. A., ROBINSON, S. A., BUNGAY, A., MEKARY, S. & KIMMERLY, D. S. 2020. Impact of High-Intensity Interval Training, Moderate-Intensity Continuous Training, and Resistance Training on Endothelial Function in Older Adults. *Med Sci Sports Exerc,* 52**,** 1057-1067.

O'CARROLL, L., WARDROP, B., MURPHY, R. P., ROSS, M. D. & HARRISON, M. 2019. Circulating angiogenic cell response to sprint interval and continuous exercise. *Eur J Appl Physiol,* 119**,** 743-752.

OLIVEIRA, R. B., MYERS, J., ARAÚJO, C. G. S., ARENA, R., MANDIC, S., BENSIMHON, D., ABELLA, J., CHASE, P., GUAZZI, M., BRUBAKER, P., MOORE, B., KITZMAN, D. & PEBERDY, M. A. 2009. Does peak oxygen pulse complement peak oxygen uptake in risk stratifying patients with heart failure? *The American journal of cardiology,* 104**,** 554-558.

OLSON, T. P., JOYNER, M. J., DIETZ, N. M., EISENACH, J. H., CURRY, T. B. & JOHNSON, B. D. 2010. Effects of respiratory muscle work on blood flow distribution during exercise in heart failure. *The Journal of physiology,* 588**,** 2487-2501.

OZCELIK, O., WARD, S. A. & WHIPP, B. J. 1999. Effect of altered body CO2 stores on pulmonary gas exchange dynamics during incremental exercise in humans. *Exp Physiol,* 84**,** 999-1011.

PACKER, M., COATS, A. J. S., FOWLER, M. B., KATUS, H. A., KRUM, H., MOHACSI, P., ROULEAU, J. L., TENDERA, M., CASTAIGNE, A., ROECKER, E. B., SCHULTZ, M. K., STAIGER, C., CURTIN, E. L. & DEMETS, D. L. 2001. Effect of Carvedilol on Survival in Severe Chronic Heart Failure. *New England Journal of Medicine,* 344**,** 1651-1658.

PADILLA, J., NEWCOMER, S. C., SIMMONS, G. H., KREUTZER, K. V. & LAUGHLIN, M. H. 2010. Long-term exercise training does not alter brachial and femoral artery vasomotor function and endothelial

phenotype in healthy pigs. *Am J Physiol Heart Circ Physiol,* 299**,** H379-85.

PAIVA, F. M., VIANNA, L. C., FERNANDES, I. A., NÓBREGA, A. C. & LIMA, R. M. 2016. Effects of disturbed blood flow during exercise on endothelial function: a time course analysis. *Braz J Med Biol Res,* 49**,** e5100.

PALANGE, P., WARD, S. A., CARLSEN, K. H., CASABURI, R., GALLAGHER, C. G., GOSSELINK, R., O'DONNELL, D. E., PUENTE-MAESTU, L., SCHOLS, A. M., SINGH, S. & WHIPP, B. J. 2007. Recommendations on the use of exercise testing in clinical practice. *Eur Respir J,* 29**,** 185-209.

PARK, S., KIM, J. K., CHOI, H. M., KIM, H. G., BEEKLEY, M. D. & NHO, H. 2010. Increase in maximal oxygen uptake following 2-week walk training with blood flow occlusion in athletes. *Eur J Appl Physiol,* 109**,** 591-600.

PARKER, P., KÖRNER, L. & KADEFORS, R. 1984. Estimation of muscle force from intramuscular total pressure. *Medical and Biological Engineering and Computing,* 22**,** 453-457.

PATEL, A. R., KUVIN, J. T., PANDIAN, N. G., SMITH, J. J., UDELSON, J. E., MENDELSOHN, M. E., KONSTAM, M. A. & KARAS, R. H. 2001. Heart failure etiology affects peripheral vascular endothelial function after cardiac transplantation. *J Am Coll Cardiol,* 37**,** 195-200.

PATERSON, D. H., CUNNINGHAM, D. A., KOVAL, J. J. & ST CROIX, C. M. 1999. Aerobic fitness in a population of independently living men and women aged 55-86 years. *Med Sci Sports Exerc,* 31**,** 1813-20.

PATON, C. D., ADDIS, S. M. & TAYLOR, L.-A. 2017. The effects of muscle blood flow restriction during running training on measures of aerobic capacity and run time to exhaustion. *European Journal of Applied Physiology,* 117**,** 2579-2585.

PATTERSON, S. D. & FERGUSON, R. A. 2010. Increase in calf post-occlusive blood flow and strength following short-term resistance exercise training with blood flow restriction in young women. *Eur J Appl Physiol,* 108**,** 1025-33.

PAUL, J. D., POWELL, T. M., THOMPSON, M., BENJAMIN, M., RODRIGO, M., CARLOW, A., ANNAVAJJHALA, V., SHIVA, S., DEJAM, A., GLADWIN, M. T., MCCOY, J. P., ZALOS, G., PRESS, B., MURPHY, M., HILL, J. M., CSAKO, G., WACLAWIW, M. A. & CANNON, R. O., 3RD 2007. Endothelial progenitor cell mobilization and increased intravascular nitric oxide in patients undergoing cardiac rehabilitation. *J Cardiopulm Rehabil Prev,* 27**,** 65-73.

PEARSON, S. J. & HUSSAIN, S. R. 2015. A Review on the Mechanisms of Blood-Flow Restriction Resistance Training-Induced Muscle Hypertrophy. *Sports Medicine,* 45**,** 187-200.

PICKWORTH, K. K. 1992. Long-term dobutamine therapy for refractory congestive heart failure. *Clin Pharm,* 11**,** 618-24.

PIEPOLI, M. F., GUAZZI, M., BORIANI, G., CICOIRA, M., CORRÀ, U., DALLA LIBERA, L., EMDIN, M., MELE, D., PASSINO, C., VESCOVO, G., VIGORITO, C., VILLANI, G. Q. & AGOSTONI, P. 2010. Exercise intolerance in chronic heart failure: mechanisms and therapies. Part I. *Eur J Cardiovasc Prev Rehabil,* 17**,** 637-42.

PLACE, N., YAMADA, T., BRUTON, J. D. & WESTERBLAD, H. 2010. Muscle fatigue: from observations in humans to underlying mechanisms studied in intact single muscle fibres. *European Journal of Applied Physiology,* 110**,** 1-15.

POLKEY, M. I., KYROUSSIS, D., HAMNEGARD, C. H., MILLS, G. H., GREEN, M. & MOXHAM, J. 1996. Quadriceps strength and fatigue assessed by magnetic stimulation of the femoral nerve in man. *Muscle & Nerve,* 19**,** 549-555.

POOLE, D. C., BEHNKE, B. J. & MUSCH, T. I. 2020. The role of vascular function on exercise capacity in health and disease. *The Journal of Physiology,* n/a.

POOLE, D. C., BURNLEY, M., VANHATALO, A., ROSSITER, H. B. & JONES, A. M. 2016. Critical Power: An Important Fatigue Threshold in Exercise Physiology. *Medicine and science in sports and exercise,* 48**,** 2320-2334.

POOLE, D. C., HIRAI, D. M., COPP, S. W. & MUSCH, T. I. 2012. Muscle oxygen transport and utilization in heart failure: implications for exercise (in)tolerance. *Am J Physiol Heart Circ Physiol,* 302**,** H1050-63.

POOLE, D. C., RICHARDSON, R. S., HAYKOWSKY, M. J., HIRAI, D. M. & MUSCH, T. I. 2018. Exercise limitations in heart failure with reduced and preserved ejection fraction. *J Appl Physiol (1985),* 124**,** 208-224.

POOLE, D. C., WARD, S. A., GARDNER, G. W. & WHIPP, B. J. 1988. Metabolic and respiratory profile of the upper limit for prolonged exercise in man. *Ergonomics,* 31**,** 1265-79.

PORSZASZ, J., RAMBOD, M., VAN DER VAART, H., ROSSITER, H. B., MA, S., KILEDJIAN, R. & CASABURI, R. 2013. Sinusoidal high-intensity exercise does not elicit ventilatory limitation in chronic obstructive pulmonary disease. *Exp Physiol,* 98**,** 1102-14.

POUILLY, J. P. & BUSSO, T. 2008. Accumulated oxygen deficit during ramp exercise. *Int J Sports Med,* 29**,** 16-20.

POWERS, S. K. & JACKSON, M. J. 2008. Exercise-induced oxidative stress: cellular mechanisms and impact on muscle force production. *Physiol Rev,* 88**,** 1243-76.

RADOMSKI, M. W., PALMER, R. M. & MONCADA, S. 1990. An L-arginine/nitric oxide pathway present in human platelets regulates aggregation. *Proc Natl Acad Sci U S A,* 87**,** 5193-7.

RAFII, S. & LYDEN, D. 2003. Therapeutic stem and progenitor cell transplantation for organ vascularization and regeneration. *Nature Medicine,* 9**,** 702-712.

RAKOBOWCHUK, M., HARRIS, E., TAYLOR, A., BALIGA, V., CUBBON, R. M., ROSSITER, H. B. & BIRCH, K. M. 2012. Heavy and moderate interval exercise training alters low-flow-mediated constriction but does not increase circulating progenitor cells in healthy humans. *Exp Physiol,* 97**,** 375-85.

RAKOBOWCHUK, M., PARSLOE, E. R., GIBBINS, S. E., HARRIS, E. & BIRCH, K. M. 2013. Prolonged low flow reduces reactive hyperemia and augments low flow mediated constriction in the brachial artery independent of the menstrual cycle. *PLoS One,* 8**,** e55385.

RAKOBOWCHUK, M., TANGUAY, S., BURGOMASTER, K. A., HOWARTH, K. R., GIBALA, M. J. & MACDONALD, M. J. 2008. Sprint interval and

traditional endurance training induce similar improvements in peripheral arterial stiffness and flow-mediated dilation in healthy humans. *Am J Physiol Regul Integr Comp Physiol,* 295**,** R236-42.

RAMOS, J. S., DALLECK, L. C., TJONNA, A. E., BEETHAM, K. S. & COOMBES, J. S. 2015. The impact of high-intensity interval training versus moderate-intensity continuous training on vascular function: a systematic review and meta-analysis. *Sports Med,* 45**,** 679-92.

RAS, R. T., STREPPEL, M. T., DRAIJER, R. & ZOCK, P. L. 2013. Flow-mediated dilation and cardiovascular risk prediction: a systematic review with meta-analysis. *International journal of cardiology,* 168**,** 344-351.

RAUSCHER FREDERICK, M., GOLDSCHMIDT-CLERMONT PASCAL, J., DAVIS BRYCE, H., WANG, T., GREGG, D., RAMASWAMI, P., PIPPEN ANNE, M., ANNEX BRIAN, H., DONG, C. & TAYLOR DORIS, A. 2003. Aging, Progenitor Cell Exhaustion, and Atherosclerosis. *Circulation,* 108**,** 457-463.

RAYNER, M., PETERSEN, S., MOHER, M., WRIGHT, L. & LAMPE, F. 2001. Coronary heart disease statistics: morbidity supplement 2001 edition.

RÉCALDE, A., RICHART, A., GUÉRIN, C., COCHAIN, C., ZOUGGARI, Y., YIN, K. H. W., VILAR, J., DROUET, I., LÉVY, B., VAROQUAUX, O. & SILVESTRE, J.-S. 2012. Sympathetic Nervous System Regulates Bone Marrow–Derived Cell Egress Through Endothelial Nitric Oxide Synthase Activation. *Arteriosclerosis, Thrombosis, and Vascular Biology,* 32**,** 643-653.

RECTOR, T. 1987. Patient's self-assessment of their congestive heart failure: II. Content, reli-ability and validity of a new measure-The Minnesota Living with Heart Failure Questionnaire. *Heart failure,* 3**,** 198.

REHMAN, J., LI, J., ORSCHELL, C. M. & MARCH, K. L. 2003. Peripheral blood "endothelial progenitor cells" are derived from monocyte/macrophages and secrete angiogenic growth factors. *Circulation,* 107**,** 1164-9.

REMENSNYDER, J. P., MITCHELL, J. H. & SARNOFF, S. J. 1962. Functional sympatholysis during muscular activity. Observations on influence of carotid sinus on oxygen uptake. *Circ Res,* 11**,** 370-80.

RENZI, C. P., TANAKA, H. & SUGAWARA, J. 2010. Effects of leg blood flow restriction during walking on cardiovascular function. *Med Sci Sports Exerc,* 42**,** 726-32.

RIBEIRO, F., RIBEIRO, I. P., GONÇALVES, A. C., ALVES, A. J., MELO, E., FERNANDES, R., COSTA, R., SARMENTO-RIBEIRO, A. B., DUARTE, J. A., CARREIRA, I. M., WITKOWSKI, S. & OLIVEIRA, J. 2017. Effects of resistance exercise on endothelial progenitor cell mobilization in women. *Scientific Reports,* 7**,** 17880.

RICHARDSON, M. R. & YODER, M. C. 2011. Endothelial progenitor cells: quo vadis? *Journal of molecular and cellular cardiology,* 50**,** 266-272.

ROBERGS, R. A., ICENOGLE, M. V., HUDSON, T. L. & GREENE, E. R. 1997. Temporal inhomogeneity in brachial artery blood flow during forearm exercise. *Medicine and science in sports and exercise,* 29**,** 1021-1027.

RODITIS, P., DIMOPOULOS, S., SAKELLARIOU, D., SARAFOGLOU, S., KALDARA, E., VENETSANAKOS, J., VOGIATZIS, J., ANASTASIOU-NANA, M., ROUSSOS, C. & NANAS, S. 2007. The effects of exercise

training on the kinetics of oxygen uptake in patients with chronic heart failure. *Eur J Cardiovasc Prev Rehabil,* 14**,** 304-11.

ROSS, M. D., MALONE, E. M., SIMPSON, R., CRANSTON, I., INGRAM, L., WRIGHT, G. P., CHAMBERS, G. & FLORIDA-JAMES, G. 2018. Lower resting and exercise-induced circulating angiogenic progenitors and angiogenic T cells in older men. *Am J Physiol Heart Circ Physiol,* 314**,** H392-h402.

ROSS, M. D., WEKESA, A. L., PHELAN, J. P. & HARRISON, M. 2014. Resistance exercise increases endothelial progenitor cells and angiogenic factors. *Med Sci Sports Exerc,* 46**,** 16-23.

ROSS, R. 1993. The pathogenesis of atherosclerosis: a perspective for the 1990s. *Nature,* 362**,** 801-809.

ROSSITER, H. B., HOWE, F. A., WARD, S. A., KOWALCHUK, J. M., GRIFFITHS, J. R. & WHIPP, B. J. 2000. Intersample fluctuations in phosphocreatine concentration determined by 31P-magnetic resonance spectroscopy and parameter estimation of metabolic responses to exercise in humans. *The Journal of physiology,* 528 Pt 2**,** 359-369.

ROSSITER, H. B., WARD, S. A., HOWE, F. A., KOWALCHUK, J. M., GRIFFITHS, J. R. & WHIPP, B. J. 2002. Dynamics of intramuscular 31P-MRS P(i) peak splitting and the slow components of PCr and O2 uptake during exercise. *J Appl Physiol (1985),* 93**,** 2059-69.

ROSSMAN, M. J., VENTURELLI, M., MCDANIEL, J., AMANN, M. & RICHARDSON, R. S. 2012. Muscle mass and peripheral fatigue: a potential role for afferent feedback? *Acta physiologica (Oxford, England),* 206**,** 242-250.

ROTTO, D. M. & KAUFMAN, M. P. 1988. Effect of metabolic products of muscular contraction on discharge of group III and IV afferents. *J Appl Physiol (1985),* 64**,** 2306-13.

RUBIN, S. A., CHATTERJEE, K., PORTS, T. A., GELBERG, H. J., BRUNDAGE, B. H. & PARMLEY, W. W. 1979. Influence of short-term oral hydralazine therapy on exercise hemodynamics in patients with severe chronic heart failure. *Am J Cardiol,* 44**,** 1183-9.

RUDIC, R. D., SHESELY, E. G., MAEDA, N., SMITHIES, O., SEGAL, S. S. & SESSA, W. C. 1998. Direct evidence for the importance of endothelium-derived nitric oxide in vascular remodeling. *J Clin Invest,* 101**,** 731-6.

SACKS, C. A., JARCHO, J. A. & CURFMAN, G. D. 2014. Paradigm Shifts in Heart-Failure Therapy — A Timeline. *New England Journal of Medicine,* 371**,** 989-991.

SADAMOTO, T., BONDE-PETERSEN, F. & SUZUKI, Y. 1983. Skeletal muscle tension, flow, pressure, and EMG during sustained isometric contractions in humans. *Eur J Appl Physiol Occup Physiol,* 51**,** 395-408.

SAMMAN TAHHAN, A., HAMMADAH, M., SANDESARA, P. B., HAYEK, S. S., KALOGEROPOULOS, A. P., ALKHODER, A., MOHAMED KELLI, H., TOPEL, M., GHASEMZADEH, N., CHIVUKULA, K., KO, Y. A., AIDA, H., HESAROIEH, I., MAHAR, E., KIM, J. H., WILSON, P., SHAW, L., VACCARINO, V., WALLER, E. K. & QUYYUMI, A. A. 2017. Progenitor Cells and Clinical Outcomes in Patients With Heart Failure. *Circ Heart Fail,* 10.

SANDRI, M., VIEHMANN, M., ADAMS, V., RABALD, K., MANGNER, N., HÖLLRIEGEL, R., LURZ, P., ERBS, S., LINKE, A., KIRSCH, K., MÖBIUS-WINKLER, S., THIERY, J., TEUPSER, D., HAMBRECHT, R., SCHULER, G. & GIELEN, S. 2016. Chronic heart failure and aging - effects of exercise training on endothelial function and mechanisms of endothelial regeneration: Results from the Leipzig Exercise Intervention in Chronic heart failure and Aging (LEICA) study. *Eur J Prev Cardiol,* 23**,** 349-58.

SAPP, R. M., EVANS, W. S., EAGAN, L. E., CHESNEY, C. A., ZIETOWSKI, E. M., PRIOR, S. J., RANADIVE, S. M. & HAGBERG, J. M. 2019. The effects of moderate and high-intensity exercise on circulating markers of endothelial integrity and activation in young, healthy men. *Journal of Applied Physiology,* 127**,** 1245-1256.

SARELIUS, I. & POHL, U. 2010. Control of muscle blood flow during exercise: local factors and integrative mechanisms. *Acta physiologica (Oxford, England),* 199**,** 349-365.

SARGEANT, A. J. & DOLAN, P. 1987. Effect of prior exercise on maximal short-term power output in humans. *Journal of Applied Physiology,* 63**,** 1475-1480.

SARGEANT, A. J., HOINVILLE, E. & YOUNG, A. 1981. Maximum leg force and power output during short-term dynamic exercise. *J Appl Physiol Respir Environ Exerc Physiol,* 51**,** 1175-82.

SARTO, P., BALDUCCI, E., BALCONI, G., FIORDALISO, F., MERLO, L., TUZZATO, G., PAPPAGALLO, G. L., FRIGATO, N., ZANOCCO, A., FORESTIERI, C., AZZARELLO, G., MAZZUCCO, A., VALENTI, M. T., ALBORINO, F., NOVENTA, D., VINANTE, O., PASCOTTO, P., SARTORE, S., DEJANA, E. & LATINI, R. 2007. Effects of exercise training on endothelial progenitor cells in patients with chronic heart failure. *J Card Fail,* 13**,** 701-8.

SARULLO, F. M., FAZIO, G., BRUSCA, I., FASULLO, S., PATERNA, S., LICATA, P., NOVO, G., NOVO, S. & DI PASQUALE, P. 2010. Cardiopulmonary Exercise Testing in Patients with Chronic Heart Failure: Prognostic Comparison from Peak VO2 and VE/VCO2 Slope. *Open Cardiovasc Med J,* 4**,** 127-34.

SAWYER, B. J., TUCKER, W. J., BHAMMAR, D. M., RYDER, J. R., SWEAZEA, K. L. & GAESSER, G. A. 2016. Effects of high-intensity interval training and moderate-intensity continuous training on endothelial function and cardiometabolic risk markers in obese adults. *Journal of Applied Physiology,* 121**,** 279-288.

SCHJERVE, I. E., TYLDUM, G. A., TJØNNA, A. E., STØLEN, T., LOENNECHEN, J. P., HANSEN, H. E., HARAM, P. M., HEINRICH, G., BYE, A. & NAJJAR, S. M. 2008. Both aerobic endurance and strength training programmes improve cardiovascular health in obese adults. *Clinical science,* 115**,** 283-293.

SCHMIDT-LUCKE, C., FICHTLSCHERER, S., AICHER, A., TSCHÖPE, C., SCHULTHEISS, H.-P., ZEIHER, A. M. & DIMMELER, S. 2010. Quantification of Circulating Endothelial Progenitor Cells Using the Modified ISHAGE Protocol. *PLOS ONE,* 5**,** e13790.

SCHMIDT-LUCKE, C., RÖSSIG, L., FICHTLSCHERER, S., VASA, M., BRITTEN, M., KÄMPER, U., DIMMELER, S. & ZEIHER, A. M. 2005.

Reduced Number of Circulating Endothelial Progenitor Cells Predicts Future Cardiovascular Events. *Circulation,* 111**,** 2981-2987.

SCHRAGE, W. G., JOYNER, M. J. & DINENNO, F. A. 2004. Local inhibition of nitric oxide and prostaglandins independently reduces forearm exercise hyperaemia in humans. *The Journal of Physiology,* 557**,** 599-611.

SCHREUDER, T. H. A., GREEN, D. J., HOPMAN, M. T. E. & THIJSSEN, D. H. J. 2014. Acute impact of retrograde shear rate on brachial and superficial femoral artery flow-mediated dilation in humans. *Physiological reports,* 2**,** e00193-e00193.

SEALS, D. R., JABLONSKI, K. L. & DONATO, A. J. 2011. Aging and vascular endothelial function in humans. *Clin Sci (Lond),* 120**,** 357-75.

SHARMA, R., COATS, A. J. S. & ANKER, S. D. 2000. The role of inflammatory mediators in chronic heart failure: cytokines, nitric oxide, and endothelin-1. *International Journal of Cardiology,* 72**,** 175-186.

SHECHTER, M., MATETZKY, S., ARAD, M., FEINBERG, M. S. & FREIMARK, D. 2009. Vascular endothelial function predicts mortality risk in patients with advanced ischaemic chronic heart failure†. *European Journal of Heart Failure,* 11**,** 588-593.

SHECHTER, M., SHECHTER, A., KOREN-MORAG, N., FEINBERG, M. S. & HIERSCH, L. 2014. Usefulness of Brachial Artery Flow-Mediated Dilation to Predict Long-Term Cardiovascular Events in Subjects Without Heart Disease. *The American Journal of Cardiology,* 113**,** 162-167.

SHEN, L., GAO, Y., QIAN, J., SUN, A. & GE, J. 2011. A novel mechanism for endothelial progenitor cells homing: The SDF-1/CXCR4–Rac pathway may regulate endothelial progenitor cells homing through cellular polarization. *Medical Hypotheses,* 76**,** 256-258.

SHI, Q., RAFII, S., WU, M. H., WIJELATH, E. S., YU, C., ISHIDA, A., FUJITA, Y., KOTHARI, S., MOHLE, R., SAUVAGE, L. R., MOORE, M. A., STORB, R. F. & HAMMOND, W. P. 1998. Evidence for circulating bone marrow-derived endothelial cells. *Blood,* 92**,** 362-7.

SHILL, D. D., MARSHBURN, M. P., HEMPEL, H. K., LANSFORD, K. A. & JENKINS, N. T. 2016. Heterogeneous Circulating Angiogenic Cell Responses to Acute Maximal Exercise. *Medicine and science in sports and exercise,* 48**,** 2536-2543.

SHIMIZU, R., HOTTA, K., YAMAMOTO, S., MATSUMOTO, T., KAMIYA, K., KATO, M., HAMAZAKI, N., KAMEKAWA, D., AKIYAMA, A., KAMADA, Y., TANAKA, S. & MASUDA, T. 2016. Low-intensity resistance training with blood flow restriction improves vascular endothelial function and peripheral blood circulation in healthy elderly people. *Eur J Appl Physiol,* 116**,** 749-57.

SIDHU, S. K., WEAVIL, J. C., MANGUM, T. S., JESSOP, J. E., RICHARDSON, R. S., MORGAN, D. E. & AMANN, M. 2017. Group III/IV locomotor muscle afferents alter motor cortical and corticospinal excitability and promote central fatigue during cycling exercise. *Clinical neurophysiology : official journal of the International Federation of Clinical Neurophysiology,* 128**,** 44-55.

SINGH, N., PRASAD, S., SINGER, D. R. & MACALLISTER, R. J. 2002. Ageing is associated with impairment of nitric oxide and prostanoid dilator pathways in the human forearm. *Clin Sci (Lond),* 102**,** 595-600.

SINKLER, S. Y. & SEGAL, S. S. 2017. Rapid versus slow ascending vasodilatation: intercellular conduction versus flow-mediated signalling with tetanic versus rhythmic muscle contractions. *The Journal of Physiology,* 595**,** 7149-7165.

SMITH, C. J., SUN, D., HOEGLER, C., ROTH, B. S., ZHANG, X., ZHAO, G., XU, X. B., KOBARI, Y., PRITCHARD, K., JR., SESSA, W. C. & HINTZE, T. H. 1996. Reduced gene expression of vascular endothelial NO synthase and cyclooxygenase-1 in heart failure. *Circ Res,* 78**,** 58-64.

SOLAL, A. C., CHABERNAUD, J. M. & GOURGON, R. 1990. Comparison of oxygen uptake during bicycle exercise in patients with chronic heart failure and in normal subjects. *Journal of the American College of Cardiology,* 16**,** 80-85.

STEINER, S., NIESSNER, A., ZIEGLER, S., RICHTER, B., SEIDINGER, D., PLEINER, J., PENKA, M., WOLZT, M., HUBER, K., WOJTA, J., MINAR, E. & KOPP, C. W. 2005. Endurance training increases the number of endothelial progenitor cells in patients with cardiovascular risk and coronary artery disease. *Atherosclerosis,* 181**,** 305-310.

STEWART, S., JENKINS, A., BUCHAN, S., MCGUIRE, A., CAPEWELL, S. & MCMURRAY, J. J. 2002. The current cost of heart failure to the National Health Service in the UK. *Eur J Heart Fail,* 4**,** 361-71.

STICKLAND, M. K., MILLER, J. D., SMITH, C. A. & DEMPSEY, J. A. 2007. Carotid chemoreceptor modulation of regional blood flow distribution during exercise in health and chronic heart failure. *Circ Res,* 100**,** 1371-8.

SUGA, T., OKITA, K., MORITA, N., YOKOTA, T., HIRABAYASHI, K., HORIUCHI, M., TAKADA, S., OMOKAWA, M., KINUGAWA, S. & TSUTSUI, H. 2010. Dose effect on intramuscular metabolic stress during low-intensity resistance exercise with blood flow restriction. *J Appl Physiol (1985),* 108**,** 1563-7.

SUGA, T., OKITA, K., MORITA, N., YOKOTA, T., HIRABAYASHI, K., HORIUCHI, M., TAKADA, S., TAKAHASHI, T., OMOKAWA, M., KINUGAWA, S. & TSUTSUI, H. 2009. Intramuscular metabolism during low-intensity resistance exercise with blood flow restriction. *J Appl Physiol (1985),* 106**,** 1119-24.

SULLIVAN, M. J., KNIGHT, J. D., HIGGINBOTHAM, M. B. & COBB, F. R. 1989. Relation between central and peripheral hemodynamics during exercise in patients with chronic heart failure. Muscle blood flow is reduced with maintenance of arterial perfusion pressure. *Circulation,* 80**,** 769-81.

SUNDBERG, C. J. 1994. Exercise and training during graded leg ischaemia in healthy man with special reference to effects on skeletal muscle. *Acta physiologica Scandinavica. Supplementum,* 615**,** 1-50.

SUNDBERG, C. J., EIKEN, O., NYGREN, A. & KAIJSER, L. 1993. Effects of ischaemic training on local aerobic muscle performance in man. *Acta Physiol Scand,* 148**,** 13-9.

SWANK, A. M., HORTON, J., FLEG, J. L., FONAROW, G. C., KETEYIAN, S., GOLDBERG, L., WOLFEL, G., HANDBERG, E. M., BENSIMHON, D., ILLIOU, M. C., VEST, M., EWALD, G., BLACKBURN, G., LEIFER, E., COOPER, L. & KRAUS, W. E. 2012. Modest increase in peak VO2 is related to better clinical outcomes in chronic heart failure patients:

results from heart failure and a controlled trial to investigate outcomes of exercise training. *Circ Heart Fail,* 5**,** 579-85.

SWISHER, A. R., KOEHN, B., YONG, S., CUNHA, J., FERGUSON, C. & CANNON, D. T. 2019. Dynamics of Locomotor Fatigue during Supra-critical Power Exercise. *Med Sci Sports Exerc,* 51**,** 1720-1726.

TADDEI, S., GALETTA, F., VIRDIS, A., GHIADONI, L., SALVETTI, G., FRANZONI, F., GIUSTI, C. & SALVETTI, A. 2000. Physical activity prevents age-related impairment in nitric oxide availability in elderly athletes. *Circulation,* 101**,** 2896-901.

TAKANO, H., MORITA, T., IIDA, H., ASADA, K., KATO, M., UNO, K., HIROSE, K., MATSUMOTO, A., TAKENAKA, K., HIRATA, Y., ETO, F., NAGAI, R., SATO, Y. & NAKAJIMA, T. 2005. Hemodynamic and hormonal responses to a short-term low-intensity resistance exercise with the reduction of muscle blood flow. *Eur J Appl Physiol,* 95**,** 65-73.

TAKARADA, Y., TAKAZAWA, H., SATO, Y., TAKEBAYASHI, S., TANAKA, Y. & ISHII, N. 2000. Effects of resistance exercise combined with moderate vascular occlusion on muscular function in humans. *Journal of Applied Physiology,* 88**,** 2097-2106.

TASEV, D., KOOLWIJK, P. & VAN HINSBERGH, V. W. 2016. Therapeutic Potential of Human-Derived Endothelial Colony-Forming Cells in Animal Models. *Tissue Eng Part B Rev,* 22**,** 371-382.

TAYLOR, C. W., INGHAM, S. A. & FERGUSON, R. A. 2016. Acute and chronic effect of sprint interval training combined with postexercise blood-flow restriction in trained individuals. *Experimental physiology,* 101**,** 143-154.

TAYLOR, R. S., SAGAR, V. A., DAVIES, E. J., BRISCOE, S., COATS, A. J., DALAL, H., LOUGH, F., REES, K. & SINGH, S. 2014. Exercise-based rehabilitation for heart failure. *Cochrane Database Syst Rev,* 2014**,** Cd003331.

TEERLINK, J. R. 2005. Endothelins: pathophysiology and treatment implications in chronic heart failure. *Curr Heart Fail Rep,* 2**,** 191-7.

TEMESI, J., MATTIONI MATURANA, F., PEYRARD, A., PIUCCO, T., MURIAS, J. M. & MILLET, G. Y. 2017. The relationship between oxygen uptake kinetics and neuromuscular fatigue in high-intensity cycling exercise. *Eur J Appl Physiol,* 117**,** 969-978.

TEPPER, O. M., CAPLA, J. M., GALIANO, R. D., CERADINI, D. J., CALLAGHAN, M. J., KLEINMAN, M. E. & GURTNER, G. C. 2005. Adult vasculogenesis occurs through in situ recruitment, proliferation, and tubulization of circulating bone marrow-derived cells. *Blood,* 105**,** 1068-77.

THIJSSEN, D. H., BRUNO, R. M., VAN MIL, A. C., HOLDER, S. M., FAITA, F., GREYLING, A., ZOCK, P. L., TADDEI, S., DEANFIELD, J. E. & LUSCHER, T. 2019. Expert consensus and evidence-based recommendations for the assessment of flow-mediated dilation in humans. *European heart journal,* 40**,** 2534-2547.

THIJSSEN, D. H., DAWSON, E. A., BLACK, M. A., HOPMAN, M. T., CABLE, N. T. & GREEN, D. J. 2008. Heterogeneity in conduit artery function in humans: impact of arterial size. *Am J Physiol Heart Circ Physiol,* 295**,** H1927-34.

THIJSSEN, D. H., DAWSON, E. A., TINKEN, T. M., CABLE, N. T. & GREEN, D. J. 2009. Retrograde flow and shear rate acutely impair endothelial function in humans. *Hypertension,* 53**,** 986-992.

THIJSSEN, D. H., VOS, J. B., VERSEYDEN, C., VAN ZONNEVELD, A. J., SMITS, P., SWEEP, F. C., HOPMAN, M. T. & DE BOER, H. C. 2006. Haematopoietic stem cells and endothelial progenitor cells in healthy men: effect of aging and training. *Aging Cell,* 5**,** 495-503.

THIJSSEN, D. H. J., BLACK, M. A., PYKE, K. E., PADILLA, J., ATKINSON, G., HARRIS, R. A., PARKER, B., WIDLANSKY, M. E., TSCHAKOVSKY, M. E. & GREEN, D. J. 2011a. Assessment of flow-mediated dilation in humans: a methodological and physiological guideline. *American journal of physiology. Heart and circulatory physiology,* 300**,** H2-H12.

THIJSSEN, D. H. J., MAIORANA, A. J., O'DRISCOLL, G., CABLE, N. T., HOPMAN, M. T. E. & GREEN, D. J. 2010. Impact of inactivity and exercise on the vasculature in humans. *European Journal of Applied Physiology,* 108**,** 845-875.

THIJSSEN, D. H. J., ROWLEY, N., PADILLA, J., SIMMONS, G. H., LAUGHLIN, M. H., WHYTE, G., CABLE, N. T. & GREEN, D. J. 2011b. Relationship between upper and lower limb conduit artery vasodilator function in humans. *Journal of Applied Physiology,* 111**,** 244-250.

THOMAS, H. J., SCOTT, B. R. & PEIFFER, J. J. 2018. Acute physiological responses to low-intensity blood flow restriction cycling. *Journal of Science and Medicine in Sport*.

TINKEN, T. M., THIJSSEN, D. H., BLACK, M. A., CABLE, N. T. & GREEN, D. J. 2008. Time course of change in vasodilator function and capacity in response to exercise training in humans. *J Physiol,* 586**,** 5003-12.

TINKEN, T. M., THIJSSEN, D. H., HOPKINS, N., BLACK, M. A., DAWSON, E. A., MINSON, C. T., NEWCOMER, S. C., LAUGHLIN, M. H., CABLE, N. T. & GREEN, D. J. 2009. Impact of shear rate modulation on vascular function in humans. *Hypertension,* 54**,** 278-285.

TSAI, H. H., LIN, C. P., LIN, Y. H., HSU, C. C. & WANG, J. S. 2016. High-intensity Interval training enhances mobilization/functionality of endothelial progenitor cells and depressed shedding of vascular endothelial cells undergoing hypoxia. *Eur J Appl Physiol,* 116**,** 2375-2388.

TURNER, A. P., CATHCART, A. J., PARKER, M. E., BUTTERWORTH, C., WILSON, J. & WARD, S. A. 2006. Oxygen uptake and muscle desaturation kinetics during intermittent cycling. *Med Sci Sports Exerc,* 38**,** 492-503.

TYLDUM, G. A., SCHJERVE, I. E., TJØNNA, A. E., KIRKEBY-GARSTAD, I., STØLEN, T. O., RICHARDSON, R. S. & WISLØFF, U. 2009. Endothelial dysfunction induced by post-prandial lipemia: complete protection afforded by high-intensity aerobic interval exercise. *Journal of the American College of Cardiology,* 53**,** 200-206.

URBICH, C. & DIMMELER, S. 2004. Endothelial Progenitor Cells. *Circulation Research,* 95**,** 343-353.

URSPRUNG, W. & SMITH, J. D. The effects of blood flow restriction training on VO2max and 1.5 mile run performance. International Journal of Exercise Science: Conference Proceedings, 2017. 108.

VALGIMIGLI, M., RIGOLIN, G. M., FUCILI, A., PORTA, M. D., SOUKHOMOVSKAIA, O., MALAGUTTI, P., BUGLI, A. M., BRAGOTTI, L. Z., FRANCOLINI, G., MAURO, E., CASTOLDI, G. & FERRARI, R. 2004. CD34+ and endothelial progenitor cells in patients with various degrees of congestive heart failure. *Circulation,* 110**,** 1209-12.

VAN CRAENENBROECK, E. M., BECKERS, P. J., POSSEMIERS, N. M., WUYTS, K., FREDERIX, G., HOYMANS, V. Y., WUYTS, F., PAELINCK, B. P., VRINTS, C. J. & CONRAADS, V. M. 2010a. Exercise acutely reverses dysfunction of circulating angiogenic cells in chronic heart failure. *European heart journal,* 31**,** 1924-1934.

VAN CRAENENBROECK, E. M., BRUYNDONCKX, L., VAN BERCKELAER, C., HOYMANS, V. Y., VRINTS, C. J. & CONRAADS, V. M. 2011. The effect of acute exercise on endothelial progenitor cells is attenuated in chronic heart failure. *Eur J Appl Physiol,* 111**,** 2375-9.

VAN CRAENENBROECK, E. M. & CONRAADS, V. M. 2013. Mending injured endothelium in chronic heart failure: A new target for exercise training. *International Journal of Cardiology,* 166**,** 310-314.

VAN CRAENENBROECK, E. M., CONRAADS, V. M., VAN BOCKSTAELE, D. R., HAINE, S. E., VERMEULEN, K., VAN TENDELOO, V. F., VRINTS, C. J. & HOYMANS, V. Y. 2008a. Quantification of circulating endothelial progenitor cells: a methodological comparison of six flow cytometric approaches. *J Immunol Methods,* 332**,** 31-40.

VAN CRAENENBROECK, E. M., HOYMANS, V. Y., BECKERS, P. J., POSSEMIERS, N. M., WUYTS, K., PAELINCK, B. P., VRINTS, C. J. & CONRAADS, V. M. 2010b. Exercise training improves function of circulating angiogenic cells in patients with chronic heart failure. *Basic Research in Cardiology,* 105**,** 665-676.

VAN CRAENENBROECK, E. M., VRINTS, C. J., HAINE, S. E., VERMEULEN, K., GOOVAERTS, I., VAN TENDELOO, V. F., HOYMANS, V. Y. & CONRAADS, V. M. 2008b. A maximal exercise bout increases the number of circulating CD34+/KDR+ endothelial progenitor cells in healthy subjects. Relation with lipid profile. *J Appl Physiol (1985),* 104**,** 1006-13.

VAN DER LOO, B., LABUGGER, R., SKEPPER, J. N., BACHSCHMID, M., KILO, J., POWELL, J. M., PALACIOS-CALLENDER, M., ERUSALIMSKY, J. D., QUASCHNING, T., MALINSKI, T., GYGI, D., ULLRICH, V. & LÜSCHER, T. F. 2000. Enhanced peroxynitrite formation is associated with vascular aging. *The Journal of experimental medicine,* 192**,** 1731-1744.

VAN DER VAART, H., MURGATROYD, S. R., ROSSITER, H. B., CHEN, C., CASABURI, R. & PORSZASZ, J. 2014. Selecting constant work rates for endurance testing in COPD: the role of the power-duration relationship. *COPD: Journal of Chronic Obstructive Pulmonary Disease,* 11**,** 267-276.

VAN TOL, B. A., HUIJSMANS, R. J., KROON, D. W., SCHOTHORST, M. & KWAKKEL, G. 2006. Effects of exercise training on cardiac performance, exercise capacity and quality of life in patients with heart failure: a meta-analysis. *Eur J Heart Fail,* 8**,** 841-50.

VANHOUTTE, P. M. 1983. Adjustments in the peripheral circulation in chronic heart failure. *Eur Heart J,* 4 Suppl A**,** 67-83.

VANHOUTTE, P. M., SHIMOKAWA, H., FELETOU, M. & TANG, E. H. C. 2017. Endothelial dysfunction and vascular disease – a 30th anniversary update. *Acta Physiologica,* 219**,** 22-96.

VANHOUTTE, P. M., SHIMOKAWA, H., TANG, E. H. C. & FELETOU, M. 2009. Endothelial dysfunction and vascular disease. *Acta Physiologica,* 196**,** 193-222.

VASA, M., FICHTLSCHERER, S., AICHER, A., ADLER, K., URBICH, C., MARTIN, H., ZEIHER, A. M. & DIMMELER, S. 2001. Number and migratory activity of circulating endothelial progenitor cells inversely correlate with risk factors for coronary artery disease. *Circ Res,* 89**,** E1-7.

VITA, J. A. 2005. Endothelial function and clinical outcome. *Heart (British Cardiac Society),* 91**,** 1278-1279.

VOGIATZIS, I. 2011. Strategies of muscle training in very severe COPD patients. *European Respiratory Journal,* 38**,** 971-975.

VOGIATZIS, I., NANAS, S., KASTANAKIS, E., GEORGIADOU, O., PAPAZAHOU, O. & ROUSSOS, C. 2004. Dynamic hyperinflation and tolerance to interval exercise in patients with advanced COPD. *European Respiratory Journal,* 24**,** 385-390.

VOLAKLIS, K. A., TOKMAKIDIS, S. P. & HALLE, M. 2013. Acute and chronic effects of exercise on circulating endothelial progenitor cells in healthy and diseased patients. *Clinical Research in Cardiology,* 102**,** 249-257.

WAGNER, P. D. 1996. Determinants of maximal oxygen transport and utilization. *Annual review of physiology,* 58**,** 21-50.

WALLØE, L. & WESCHE, J. 1988. Time course and magnitude of blood flow changes in the human quadriceps muscles during and following rhythmic exercise. *The Journal of physiology,* 405**,** 257-273.

WASSERMAN, K., BEAVER, W. L. & WHIPP, B. J. 1986. Mechanisms and patterns of blood lactate increase during exercise in man. *Medicine & Science in Sports & Exercise,* 18**,** 344-352.

WASSERMAN, K., HANSEN, J., SUE, D. Y., STRINGER, W., SIETSEMA, K., SUN, X.-G. & WHIPP, B. J. 2011. *Principles of exercise testing and interpretation: Including pathophysiology and clinical applications: Fifth edition*.

WASSERMAN, K., ZHANG, Y.-Y., GITT, A., BELARDINELLI, R., KOIKE, A., LUBARSKY, L. & AGOSTONI, P. G. 1997. Lung Function and Exercise Gas Exchange in Chronic Heart Failure. *Circulation,* 96**,** 2221-2227.

WERNER, N., KOSIOL, S., SCHIEGL, T., AHLERS, P., WALENTA, K., LINK, A., BÖHM, M. & NICKENIG, G. 2005. Circulating endothelial progenitor cells and cardiovascular outcomes. *N Engl J Med,* 353**,** 999-1007.

WESTENBRINK, B. D., VOORS, A. A., DE BOER, R. A., SCHURINGA, J. J., KLINKENBERG, T., VAN DER HARST, P., VELLENGA, E., VAN VELDHUISEN, D. J. & VAN GILST, W. H. 2010. Bone marrow dysfunction in chronic heart failure patients. *European Journal of Heart Failure,* 12**,** 676-684.

WHIPP, B. & ROSSITER, H. 2005. The kinetics of oxygen uptake. Physiological inferences from parameters. *Oxygen uptake knetics in sport, exercise and medicine***,** 62-94.

WHIPP, B. J., DAVIS, J. A., TORRES, F. & WASSERMAN, K. 1981. A test to determine parameters of aerobic function during exercise. *J Appl Physiol Respir Environ Exerc Physiol,* 50**,** 217-21.

WHIPP, B. J. & WARD, S. A. 2009. Quantifying intervention-related improvements in exercise tolerance. *European Respiratory Journal,* 33**,** 1254-1260.

WHIPP, B. J., WARD, S. A. & WASSERMAN, K. 1986. Respiratory markers of the anaerobic threshold. *Adv Cardiol,* 35**,** 47-64.

WILLIAMS, M. R., WESTERMAN, R. A., KINGWELL, B. A., PAIGE, J., BLOMBERY, P. A., SUDHIR, K. & KOMESAROFF, P. A. 2001. Variations in endothelial function and arterial compliance during the menstrual cycle. *J Clin Endocrinol Metab,* 86**,** 5389-95.

WILLIAMS, T. J. & MCKENNA, M. J. 2012. Exercise limitation following transplantation. *Compr Physiol,* 2**,** 1937-79.

WISLØFF, U., STØYLEN, A., LOENNECHEN, J. P., BRUVOLD, M., ROGNMO, Ø., HARAM, P. M., TJØNNA, A. E., HELGERUD, J., SLØRDAHL, S. A., LEE, S. J., VIDEM, V., BYE, A., SMITH, G. L., NAJJAR, S. M., ELLINGSEN, Ø. & SKJÆRPE, T. 2007. Superior Cardiovascular Effect of Aerobic Interval Training Versus Moderate Continuous Training in Heart Failure Patients. *Circulation,* 115**,** 3086-3094.

WITTE, K. K. A., NIKITIN, N. P., DE SILVA, R., CLELAND, J. G. F. & CLARK, A. L. 2004. Exercise capacity and cardiac function assessed by tissue Doppler imaging in chronic heart failure. *Heart,* 90**,** 1144-1150.

WRAY, D. W., UBEROI, A., LAWRENSON, L. & RICHARDSON, R. S. 2006. Evidence of preserved endothelial function and vascular plasticity with age. *American Journal of Physiology-Heart and Circulatory Physiology,* 290**,** H1271-H1277.

WRIGHT, D. C., HAN, D. H., GARCIA-ROVES, P. M., GEIGER, P. C., JONES, T. E. & HOLLOSZY, J. O. 2007. Exercise-induced mitochondrial biogenesis begins before the increase in muscle PGC-1alpha expression. *J Biol Chem,* 282**,** 194-9.

XIA, W.-H., LI, J., SU, C., YANG, Z., CHEN, L., WU, F., ZHANG, Y.-Y., YU, B.-B., QIU, Y.-X., WANG, S.-M. & TAO, J. 2012. Physical exercise attenuates age-associated reduction in endothelium-reparative capacity of endothelial progenitor cells by increasing CXCR4/JAK-2 signaling in healthy men. *Aging Cell,* 11**,** 111-119.

XU, Y., ARORA, R. C., HIEBERT, B. M., LERNER, B., SZWAJCER, A., MCDONALD, K., RIGATTO, C., KOMENDA, P., SOOD, M. M. & TANGRI, N. 2014. Non-invasive endothelial function testing and the risk of adverse outcomes: a systematic review and meta-analysis. *Eur Heart J Cardiovasc Imaging,* 15**,** 736-46.

YAMAGUCHI, J., KUSANO, K. F., MASUO, O., KAWAMOTO, A., SILVER, M., MURASAWA, S., BOSCH-MARCE, M., MASUDA, H., LOSORDO, D. W., ISNER, J. M. & ASAHARA, T. 2003. Stromal cell-derived factor-1 effects on ex vivo expanded endothelial progenitor cell recruitment for ischemic neovascularization. *Circulation,* 107**,** 1322-8.

YANG, Z., WANG, J. M., CHEN, L., LUO, C. F., TANG, A. L. & TAO, J. 2007. Acute exercise-induced nitric oxide production contributes to upregulation of circulating endothelial progenitor cells in healthy subjects. *J Hum Hypertens,* 21**,** 452-60.

YANG, Z., XIA, W. H., SU, C., WU, F., ZHANG, Y. Y., XU, S. Y., LIU, X., ZHANG, X. Y., OU, Z. J., LAI, G. H., LIAO, X. X., JIN, Y. F. & TAO, J. 2013. Regular exercise-induced increased number and activity of

circulating endothelial progenitor cells attenuates age-related decline in arterial elasticity in healthy men. *Int J Cardiol,* 165**,** 247-54.

YEBOAH, J., CROUSE, J. R., HSU, F. C., BURKE, G. L. & HERRINGTON, D. M. 2007. Brachial flow-mediated dilation predicts incident cardiovascular events in older adults: the Cardiovascular Health Study. *Circulation,* 115**,** 2390-7.

ZAMPETAKI, A., KIRTON, J. P. & XU, Q. 2008. Vascular repair by endothelial progenitor cells. *Cardiovasc Res,* 78**,** 413-21.

ZELIS, R., FLAIM, S. F., LIEDTKE, A. J. & NELLIS, S. H. 1981. Cardiocirculatory dynamics in the normal and failing heart. *Annu Rev Physiol,* 43**,** 455-76.

ZELIS, R., SINOWAY, L., MUSCH, T. & DAVIS, D. 1988a. The peripheral distribution of cardiac output in heart failure. *Z Kardiol,* 77 Suppl 5**,** 61-5.

ZELIS, R., SINOWAY, L. I., MUSCH, T. I., DAVIS, D. & JUST, H. 1988b. Regional blood flow in congestive heart failure: Concept of compensatory mechanisms with short and long time constants. *The American Journal of Cardiology,* 62**,** 2E-8E.

ZHENG, G., QIU, P., XIA, R., LIN, H., YE, B., TAO, J. & CHEN, L. 2019. Effect of Aerobic Exercise on Inflammatory Markers in Healthy Middle-Aged and Older Adults: A Systematic Review and Meta-Analysis of Randomized Controlled Trials. *Front Aging Neurosci,* 11**,** 98.

ZHENG, H., FU, G., DAI, T. & HUANG, H. 2007. Migration of endothelial progenitor cells mediated by stromal cell-derived factor-1alpha/CXCR4 via PI3K/Akt/eNOS signal transduction pathway. *J Cardiovasc Pharmacol,* 50**,** 274-80.

ZHU, W., ZENG, J., YIN, J., ZHANG, F., WU, H., YAN, S. & WANG, S. 2010. Both flow-mediated vasodilation procedures and acute exercise improve endothelial function in obese young men. *European journal of applied physiology,* 108**,** 727-732.

ZIEGLER, T., BOUZOURÈNE, K., HARRISON, V. J., BRUNNER, H. R. & HAYOZ, D. 1998. Influence of oscillatory and unidirectional flow environments on the expression of endothelin and nitric oxide synthase in cultured endothelial cells. *Arterioscler Thromb Vasc Biol,* 18**,** 686-92.